

# Green Chemistry

Cutting-edge research for a greener sustainable future

[www.rsc.org/greenchem](http://www.rsc.org/greenchem)

Volume 10 | Number 11 | November 2008 | Pages 1121–1236

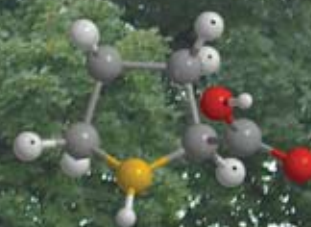
**Ball Mill**



**Microwave**



**Organocatalysis**



**Ultrasound**

ISSN 1463-9262

RSC Publishing

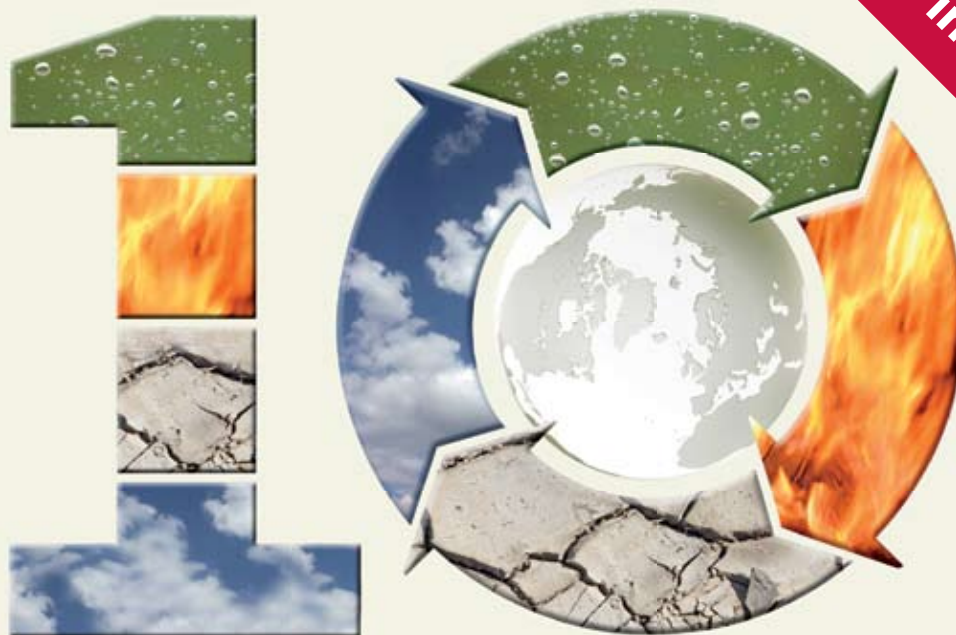
Bolm *et al.*  
Organocatalytic reactions

Han *et al.*  
Switching the basicity of ionic liquids



1463-9262(2008)10:11;1-D

Number 1  
in the field



# years of publishing!

## *Green Chemistry...*



- The most highly cited *Green Chemistry* journal, Impact factor = 4.836\*
- Fast publication, typically <90 days for full papers
- Full variety of research including reviews, communications, full papers and perspectives.

Celebrating 10 years of publishing, *Green Chemistry* offers the latest research that reduces the environmental impact of the chemical enterprise by developing alternative sustainable technologies, and provides a unique forum for the rapid publication of cutting-edge and innovative research for a greener, sustainable future

*...for a sustainable future!*

\* 2007 Thomson Scientific (ISI) Journal Citation Reports®



# Green Chemistry

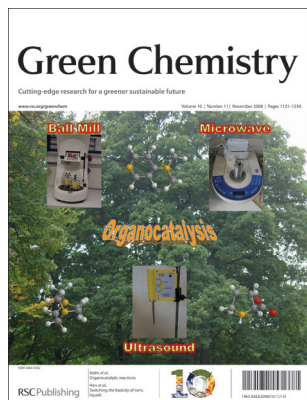
Cutting-edge research for a greener sustainable future

[www.rsc.org/greenchem](http://www.rsc.org/greenchem)

RSC Publishing is a not-for-profit publisher and a division of the Royal Society of Chemistry. Any surplus made is used to support charitable activities aimed at advancing the chemical sciences. Full details are available from [www.rsc.org](http://www.rsc.org)

## IN THIS ISSUE

ISSN 1463-9262 CODEN GRCHFJ 10(11) 1121–1236 (2008)



### Cover

See Bolm *et al.*, pp. 1131–1141. Organocatalytic processes can be improved by applying ball milling, microwave heating and ultrasound irradiation, which support conventional laboratory techniques.

Image reproduced with permission of Carsten Bolm from *Green Chem.*, 2008, **11**, 1131.

## CHEMICAL TECHNOLOGY

### T81

Drawing together research highlights and news from all RSC publications, *Chemical Technology* provides a 'snapshot' of the latest applications and technological aspects of research across the chemical sciences, showcasing newsworthy articles and significant scientific advances.

## Chemical Technology

November 2008/Volume 5/Issue 11

[www.rsc.org/chemicaltechnology](http://www.rsc.org/chemicaltechnology)

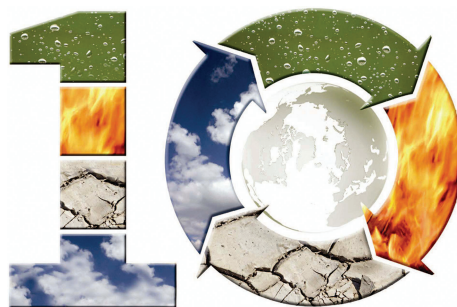
## EDITORIAL

### 1129

#### Chemical activation by mechanochemical mixing, microwave and ultrasonic irradiation

Rajender S. Varma\*

Rajender Varma discusses the new strategies that are being developed to make chemical processes cleaner.



## EDITORIAL STAFF

**Editor**

Sarah Ruthven

**Assistant editor**

Sarah Dixon

**Publishing assistant**

Ruth Bircham

**Team leader, serials production**

Stephen Wilkes

**Technical editor**

Edward Morgan

**Production administration coordinator**

Sonya Spring

**Administration assistants**Clare Davies, Donna Fordham, Kirsty Lunnon,  
Julie Thompson**Publisher**

Emma Wilson

Green Chemistry (print: ISSN 1463-9262; electronic: ISSN 1463-9270) is published 12 times a year by the Royal Society of Chemistry, Thomas Graham House, Science Park, Milton Road, Cambridge, UK CB4 0WF.

All orders, with cheques made payable to the Royal Society of Chemistry, should be sent to RSC Distribution Services, c/o Portland Customer Services, Commerce Way, Colchester, Essex, UK CO2 8HP. Tel +44 (0) 1206 226050; E-mail sales@rscdistribution.org

2008 Annual (print + electronic) subscription price: £947; US\$1799. 2008 Annual (electronic) subscription price: £852; US\$1695. Customers in Canada will be subject to a surcharge to cover GST. Customers in the EU subscribing to the electronic version only will be charged VAT.

If you take an institutional subscription to any RSC journal you are entitled to free, site-wide web access to that journal. You can arrange access via Internet Protocol (IP) address at [www.rsc.org/ip](http://www.rsc.org/ip). Customers should make payments by cheque in sterling payable on a UK clearing bank or in US dollars payable on a US clearing bank. Periodicals postage paid at Rahway, NJ, USA and at additional mailing offices. Airfreight and mailing in the USA by Mercury Airfreight International Ltd., 365 Blair Road, Avenel, NJ 07001, USA.

US Postmaster: send address changes to Green Chemistry, c/o Mercury Airfreight International Ltd., 365 Blair Road, Avenel, NJ 07001. All despatches outside the UK by Consolidated Airfreight.

PRINTED IN THE UK

**Advertisement sales:** Tel +44 (0) 1223 432246; Fax +44 (0) 1223 426017; E-mail [advertising@rsc.org](mailto:advertising@rsc.org)

# Green Chemistry

Cutting-edge research for a greener sustainable future

[www.rsc.org/greenchem](http://www.rsc.org/greenchem)

Green Chemistry focuses on cutting-edge research that attempts to reduce the environmental impact of the chemical enterprise by developing a technology base that is inherently non-toxic to living things and the environment.

## EDITORIAL BOARD

**Chair**

Professor Martyn Poliakoff  
Nottingham, UK

**Scientific Editor**

Professor Walter Leitner  
RWTH-Aachen, Germany

**Associate Editors**

Professor C. J. Li  
McGill University, Canada

**Members**

Professor Paul Anastas  
Yale University, USA  
Professor Joan Brennecke  
University of Notre Dame, USA  
Professor Mike Green  
Sasol, South Africa  
Professor Buxing Han  
Chinese Academy of Sciences,  
China

Dr Alexei Lapkin  
Bath University, UK  
Professor Steven Ley  
Cambridge, UK  
Dr Janet Scott  
Unilever, UK  
Professor Tom Welton  
Imperial College, UK

## ADVISORY BOARD

James Clark, York, UK  
Avelino Corma, Universidad  
Politécnica de Valencia, Spain  
Mark Harmer, DuPont Central  
R&D, USA  
Herbert Hugl, Lanxess Fine  
Chemicals, Germany  
Roshan Jachuck,  
Clarkson University, USA  
Makoto Misono, nite,  
Japan

Colin Raston,  
University of Western Australia,  
Australia  
Robin D. Rogers, Centre for Green  
Manufacturing, USA  
Kenneth Seddon, Queen's  
University, Belfast, UK  
Roger Sheldon, Delft University of  
Technology, The Netherlands  
Gary Sheldrake, Queen's  
University, Belfast, UK

Pietro Tundo, Università ca  
Foscari di Venezia, Italy

## INFORMATION FOR AUTHORS

Full details of how to submit material for publication in Green Chemistry are given in the Instructions for Authors (available from <http://www.rsc.org/authors>). Submissions should be sent via ReSource: <http://www.rsc.org/resource>.

Authors may reproduce/republish portions of their published contribution without seeking permission from the RSC, provided that any such republication is accompanied by an acknowledgement in the form: (Original citation) – Reproduced by permission of the Royal Society of Chemistry.

© The Royal Society of Chemistry 2008. Apart from fair dealing for the purposes of research or private study for non-commercial purposes, or criticism or review, as permitted under the Copyright, Designs and Patents Act 1988 and the Copyright and Related Rights Regulations 2003, this publication may only be reproduced, stored or transmitted, in any form or by any means, with the prior permission in writing of the Publishers or in the case of reprographic reproduction in accordance with the terms of licences issued by the Copyright Licensing Agency in the UK. US copyright law is applicable to users in the USA.

The Royal Society of Chemistry takes reasonable care in the preparation of this publication but does not accept liability for the consequences of any errors or omissions.

The paper used in this publication meets the requirements of ANSI/NISO Z39.48-1992 (Permanence of Paper).

Royal Society of Chemistry: Registered Charity No. 207890



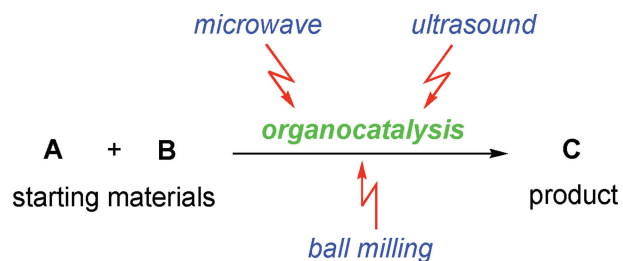
## CRITICAL REVIEW

1131

**Organocatalytic reactions: effects of ball milling, microwave and ultrasound irradiation**

Angelika Bruckmann, Anke Krebs and Carsten Bolm\*

An overview of the uses of ball milling, microwave and ultrasound irradiation in organocatalytic reactions.



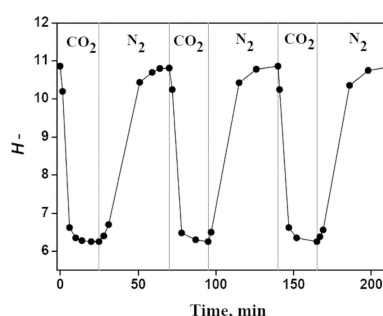
## COMMUNICATION

1142

**Switching the basicity of ionic liquids by CO<sub>2</sub>**

Wenjing Li, Zhaofu Zhang, Buxing Han,\* Suqin Hu, Jinliang Song, Ye Xie and Xiaosi Zhou

The basicity of several basic ionic liquids is studied quantitatively for the first time. The basicity of the ionic liquids can be switched repeatedly by bubbling CO<sub>2</sub> and N<sub>2</sub> through the solution alternately.



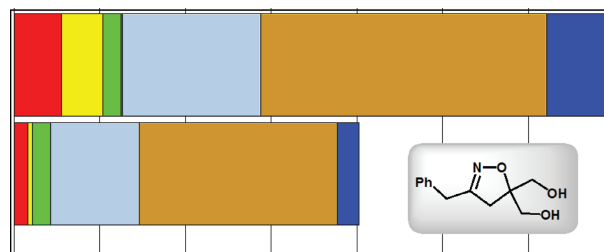
## PAPERS

1146

**Comparative assessment of an alternative route to (5-benzylfuran-3-yl)methanol (Elliott's alcohol), a key intermediate for the industrial production of resmethrins**

Goffredo Rosini, Valerio Borzatta, Claudio Paolucci and Paolo Righi\*

The details of a new alternative and greener route to a Resmethrin intermediate are reported. A quantitative comparative assessment of this new route over the best existing one is also reported.



1152

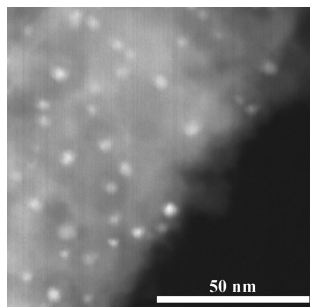
**Purity specification methods for ionic liquids**

Annegret Stark,\* Peter Behrend, Oliver Braun, Anja Müller, Johannes Ranke,\* Bernd Ondruschka and Bernd Jastorff

An array of various quantitative analytical methods for the determination of the purity has been developed and compiled to facilitate the specification of organic and inorganic starting materials, solvents, water and decomposition products in ionic liquids.



1162

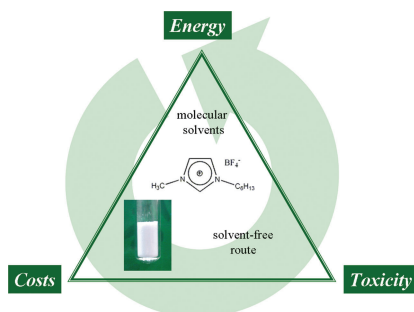


### The role of the support in achieving high selectivity in the direct formation of hydrogen peroxide

Edwin Ntainjua N., Jennifer K. Edwards, Albert F. Carley, Jose Antonio Lopez-Sanchez, Jacob A. Moulijn, Andrew A. Herzing, Christopher J. Kiely and Graham J. Hutchings\*

The selection of the support for the active Au–Pd nanoparticles is shown to be a major factor in designing selective catalysts for the direct synthesis of hydrogen peroxide.

1170

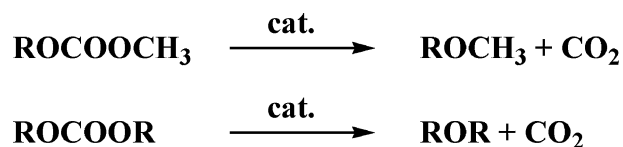


### Evaluating the greenness of alternative reaction media

Denise Reinhardt,\* Florian Ilgen, Dana Kralisch, Burkhard König and Günter Kreisel

The application of alternative reaction media (ionic liquids, carbohydrate–urea melts, solvent-free alternative) in a Diels–Alder reaction is evaluated and compared to conventional solvents with the help of an economic and ecological screening method in order to accentuate opportunities and challenges.

1182

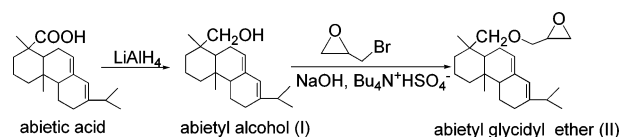


### Synthesis of dialkyl ethers by decarboxylation of dialkyl carbonates

Pietro Tundo,\* Fabio Aricò, Anthony E. Rosamilia and Sofia Memoli

The decarboxylation reaction of dialkyl carbonates to give their related ethers was investigated. The influence of several reaction parameters on the selectivity was studied. Symmetrical and dissymmetrical dialkyl ethers can be synthesised with yields up to 80%.

1190



### Synthesis of biobased epoxy and curing agents using rosin and the study of cure reactions

Honghua Wang, Bo Liu, Xiaoqing Liu, Jinwen Zhang\* and Ming Xian\*

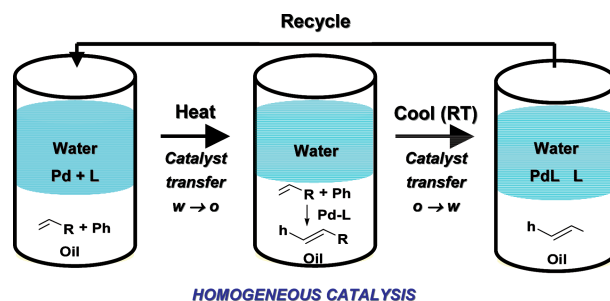
Abietyl glycidyl ether and methyl maleopimarate have been synthesized; the former representing rosin-based epoxies, and the latter representing rosin-based anhydride curing agents. Cure reactions were also studied.

1197

### Thermoregulated aqueous biphasic catalysis of Heck reactions using an amphiphilic dipyridyl-based ligand

Hicham Azoui, Krystyna Baczko, Stéphanie Cassel and Chantal Larpent\*

A neat water-based catalytic system for C–C coupling reactions that allows the product/catalyst separation by a simple variation of temperature without the need of organic solvent.

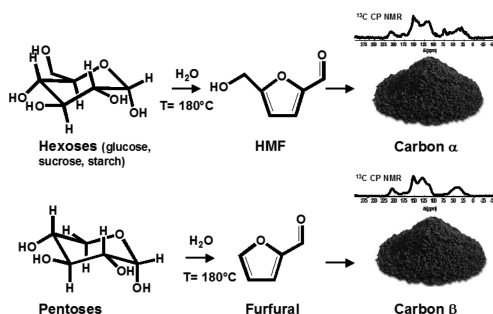


1204

### Hydrothermal carbon from biomass: a comparison of the local structure from poly- to monosaccharides and pentoses/hexoses

Maria-Magdalena Titirici, Markus Antonietti and Niki Baccile\*

Similarities and differences between hydrothermal carbon powders obtained from mono-, polysaccharides, both in their hexose and pentose forms, and their furan-like dehydration derivatives (HMF and furfural) are discussed.

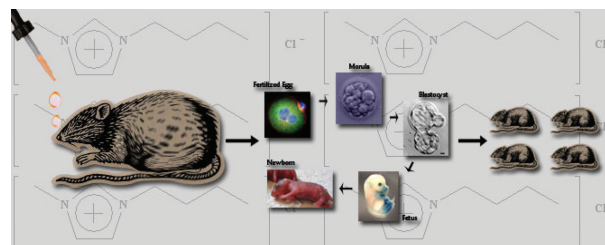


1213

### Developmental toxicity assessment of the ionic liquid 1-butyl-3-methylimidazolium chloride in CD-1 mice

Melissa M. Bailey, Megan B. Townsend, Peter L. Jernigan, John Sturdivant, Whitney L. Hough-Troutman, Jane F. Rasco, Richard P. Swatloski, Robin D. Rogers\* and Ronald D. Hood

Many toxicity studies have been performed on the commonly used ionic liquid, 1-butyl-3-methylimidazolium, yet none have determined the maternal or developmental toxicity.

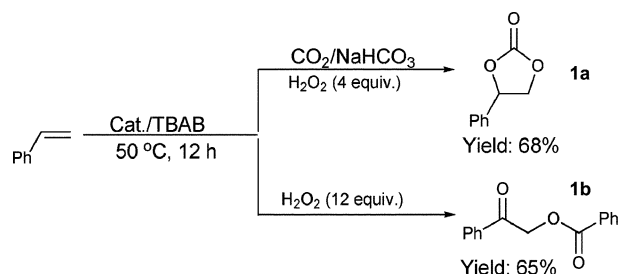


1218

### A CO<sub>2</sub>/H<sub>2</sub>O<sub>2</sub>-tunable reaction: direct conversion of styrene into styrene carbonate catalyzed by sodium phosphotungstate/*n*-Bu<sub>4</sub>NBr

Jing-Lun Wang, Jin-Quan Wang, Liang-Nian He,\* Xiao-Yong Dou and Fang Wu

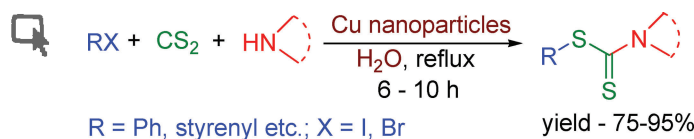
A facile synthesis of styrene carbonate was realized directly from styrene and CO<sub>2</sub> in an environmentally benign manner with an inorganic base as a “deprotonation reagent”, a recyclable catalyst system, and mild reaction conditions. Selective formation of carbonate **1a** and preferentially producing benzoate **1b** could be controlled by subtly tuning the quantities of CO<sub>2</sub> and H<sub>2</sub>O<sub>2</sub>.





## PAPERS

1224

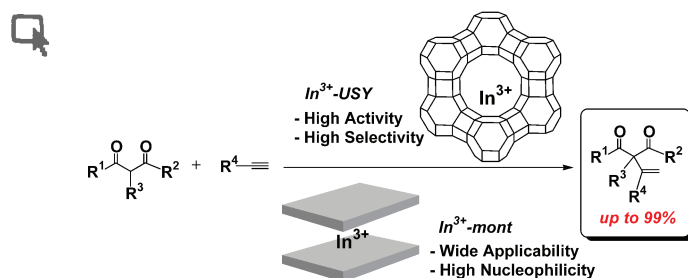


### One-pot copper nanoparticle-catalyzed synthesis of S-aryl- and S-vinyl dithiocarbamates in water: high diastereoselectivity achieved for vinyl dithiocarbamates

Sukalyan Bhadra, Amit Saha and Brindaban C. Ranu\*

Copper nanoparticles efficiently catalyze the three-component condensation of an amine, carbon disulfide and aryl iodide or styrenyl bromide in water to produce the corresponding S-aryl or S-styrenyl dithiocarbamates in high yields. High diastereoselectivities are achieved for styrenyl derivatives.

1231



### Recyclable indium catalysts for additions of 1,3-dicarbonyl compounds to unactivated alkynes affected by structure and acid strength of solid supports

Kiyotomi Kaneda,\* Ken Motokura, Nobuaki Nakagiri, Tomoo Mizugaki and Koichiro Jitsukawa

Indium species can be immobilized on solid acids by ion exchange, which increases their activity and enables the generation of the first recyclable heterogeneous indium catalysts for addition reactions of 1,3-dicarbonyl compounds to unactivated alkynes.

## AUTHOR INDEX

Antonietti, Markus, 1204  
 Aricò, Fabio, 1182  
 Azoui, Hicham, 1197  
 Baccile, Niki, 1204  
 Baczko, Krystyna, 1197  
 Bailey, Melissa M., 1213  
 Behrend, Peter, 1152  
 Bhadra, Sukalyan, 1224  
 Bolm, Carsten, 1131  
 Borzatta, Valerio, 1146  
 Braun, Oliver, 1152  
 Bruckmann, Angelika, 1131  
 Carley, Albert F., 1162  
 Cassel, Stéphanie, 1197  
 Dou, Xiao-Yong, 1218  
 Edwards, Jennifer K., 1162  
 Han, Buxing, 1142  
 He, Liang-Nian, 1218  
 Herzing, Andrew A., 1162

Hood, Ronald D., 1213  
 Hough-Troutman, Whitney L., 1213  
 Hu, Suqin, 1142  
 Hutchings, Graham J., 1162  
 Ilgen, Florian, 1170  
 Jastorff, Bernd, 1152  
 Jernigan, Peter L., 1213  
 Jitsukawa, Koichiro, 1231  
 Kaneda, Kiyotomi, 1231  
 Kiely, Christopher J., 1162  
 König, Burkhard, 1170  
 Kralisch, Dana, 1170  
 Krebs, Anke, 1131  
 Kreisel, Günter, 1170  
 Larpent, Chantal, 1197  
 Li, Wenjing, 1142  
 Liu, Bo, 1190  
 Liu, Xiaoqing, 1190

Lopez-Sanchez, Jose Antonio, 1162  
 Memoli, Sofia, 1182  
 Mizugaki, Tomoo, 1231  
 Motokura, Ken, 1231  
 Moulijn, Jacob A., 1162  
 Müller, Anja, 1152  
 Nakagiri, Nobuaki, 1231  
 Ntainjua N., Edwin, 1162  
 Ondruschka, Bernd, 1152  
 Paolucci, Claudio, 1146  
 Ranke, Johannes, 1152  
 Ranu, Brindaban C., 1224  
 Rasco, Jane F., 1213  
 Reinhardt, Denise, 1170  
 Righi, Paolo, 1146  
 Rogers, Robin D., 1213  
 Rosamilia, Anthony E., 1182  
 Rosini, Goffredo, 1146

Saha, Amit, 1224  
 Song, Jinliang, 1142  
 Stark, Annegret, 1152  
 Sturdivant, John, 1213  
 Swatloski, Richard P., 1213  
 Titirici, Maria-Magdalena, 1204  
 Townsend, Megan B., 1213  
 Tundo, Pietro, 1182  
 Varma, Rajender S., 1129  
 Wang, Honghua, 1190  
 Wang, Jin-Quan, 1218  
 Wang, Jing-Lun, 1218  
 Wu, Fang, 1218  
 Xian, Ming, 1190  
 Xie, Ye, 1142  
 Zhang, Jinwen, 1190  
 Zhang, Zhaofu, 1142  
 Zhou, Xiaosi, 1142

## FREE E-MAIL ALERTS AND RSS FEEDS

Contents lists in advance of publication are available on the web *via* [www.rsc.org/greenchem](http://www.rsc.org/greenchem) – or take advantage of our free e-mail alerting service ([www.rsc.org/ej\\_alert](http://www.rsc.org/ej_alert)) to receive notification each time a new list becomes available.

Try our RSS feeds for up-to-the-minute news of the latest research. By setting up RSS feeds, preferably using feed reader software, you can be alerted to the latest Advance Articles published on the RSC web site. Visit [www.rsc.org/publishing/technology/rss.asp](http://www.rsc.org/publishing/technology/rss.asp) for details.

## ADVANCE ARTICLES AND ELECTRONIC JOURNAL

Free site-wide access to Advance Articles and the electronic form of this journal is provided with a full-rate institutional subscription. See [www.rsc.org/ejs](http://www.rsc.org/ejs) for more information.

\* Indicates the author for correspondence: see article for details.

Electronic supplementary information (ESI) is available *via* the online article (see <http://www.rsc.org/esi> for general information about ESI).

# Chemical Technology

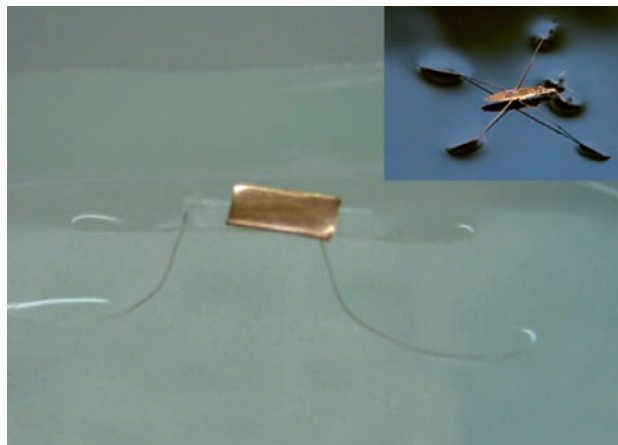
Polymer nanofibres imitate wetting behaviour of leaves, feathers and insects

## Like water off a duck's back

Scientists have made a range of structures that mimic water-repellant surfaces found in nature.

The team, led by Wei Pan at Tsinghua University, Beijing, China, developed a new electrospinning technique that aligns hydrophobic polymer nanofibres as they form from solution by collecting them on a thin silver wire. When they collected the fibres on to a flat surface instead of the wire, the fibres formed in a random arrangement.

Wu showed that the random arrangement of fibres resulted in a hydrophobic surface like that of the lotus leaf, on which water droplets can roll in all directions with equal ease, known as isotropic wetting. But he found that the aligned fibres formed a surface on which water droplets roll off preferentially in one direction. This behaviour, known as anisotropic wetting, is displayed by bamboo leaves, goose feathers and the legs of water strider insects, but it has never before been successfully mimicked by man.



'We believe we are the first team to realise surfaces with anisotropic wetting in two or three directions in large scale by nanofibres. And we also successfully made artificial water strider's legs with fibrils for the first time,' says Wu.

Wu's artificial water strider can float on the surface of a water bath while carrying a weight of one gram, 100 times heavier than the real insect. The supporting force

**The artificial water strider carries a weight 100 times heavier than the real insect (inset)**

**Reference**  
H Wu *et al*, *Soft Matter*, 2008, DOI: 10.1039/b805570j

achieved could be a new record, Wu says: 'It was more than 200 dynes per centimetre, which is higher than that of any previously reported man-made water strider.'

Wu says he believes the technology could have some exciting uses. 'It may find its application in microfluid control, non-wetting and self-cleaning surfaces, and also biologically inspired water strider robots, which could serve as a new type of aquatic vehicles,' he says.

Polymer expert Vladimir Tsukruk, from the Georgia Institute of Technology, Atlanta, US, is enthusiastic about the work. 'This is very intriguing research. This technology-friendly approach of creating a three dimensional surface with distributed anisotropic wettability looks appealing for applications such as sophisticated tissue engineering. Also, it could be useful for fluid separation processes and microfluidic arrays with distributed droplet motion control,' he comments.

*James Hodge*

## In this issue

### Lab-on-an-egg-beater

Scientists whip up a new centrifuge using a kitchen utensil

### Microcontainers hold cells captive

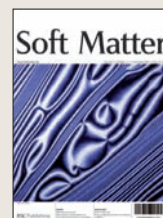
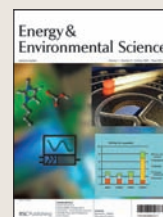
Porous containers provide a realistic three-dimensional environment for studying cells

### Interview: Finger on the pulse

Spiros Pergantis talks to May Copsey about metals in biology and in the environment

### Instant insight: Dendrimers in the spotlight

Seok-Ho Hwang, Charles Moorefield and George Newkome examine the use of dendrimers in organic light-emitting diodes



The latest applications and technological aspects of research across the chemical sciences

# Application highlights

PCR method allows fast detection of bacteria on rotting seafood

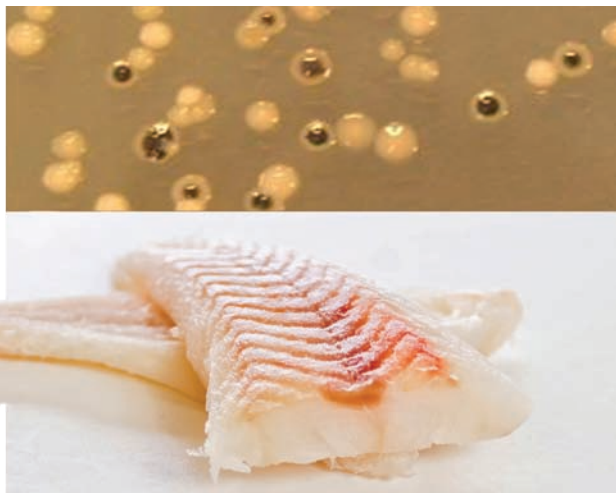
## How fresh is your fish?

Rapid and accurate detection of the bacteria that make fish go off is now possible, according to scientists in Iceland.

Eyjólfur Reynisson from Matis–Icelandic Food Research, Reykjavik, and colleagues, have developed a method that uses the polymerase chain reaction (PCR) to amplify, detect and quantify DNA sequences from *Pseudomonas* bacteria in fish.

*Pseudomonas* bacteria play an important role in seafood spoilage. They live on the surface, gills and in the gut of living fish. Soon after a fish dies, the bacteria invade the flesh and start to break it down. The bacteria grow and multiply, producing compounds responsible for the unpleasant fishy smell often associated with old seafood.

‘Real-time PCR detection technologies are fairly new in the scientific world in comparison to



conventional cultivation methods,’ says Reynisson. He explains that the new assay is much quicker than conventional detection methods and Paw Dalgaard, who studies microbial seafood spoilage at DTU

***Pseudomonas* bacteria (top) are responsible for the strong fishy smell of old seafood**

Aqua, Kongens Lyngby, Denmark, agrees. ‘The new real-time PCR method allows quantification of spoilage *Pseudomonas* in fish within about five hours compared to approximately 20 hours for the conductance assay, which was previously the fastest method,’ says Dalgaard.

This short detection time will provide the fish industry with an important tool for monitoring contamination by spoilage bacteria and for quality control, claims Reynisson. ‘Using this technique in combination with predictive microbiological models might provide a tool for predicting the remaining shelf life of the product in the future,’ he added.

Sarah Corcoran

### Reference

E Reynisson *et al*, *J. Environ. Monit.*, 2008, DOI: 10.1039/b806603e

A biofuel cell inspired by living organisms

## Sugar-powered electronics

Japanese scientists have made a biofuel cell that produces enough power to run an mp3 player or a remote controlled car.

Inspired by power generation in living organisms, Tsuyonobu Hatazawa, from the Sony Corporation, Kanagawa, and colleagues developed a bio-battery that generates electricity from glucose using enzymes as catalysts.

Typical biofuel cell consists of an anode and a cathode separated by a proton-conducting membrane. A renewable fuel, such as a sugar, is oxidised by microorganisms at the anode, generating electrons and protons. The protons migrate through the membrane to the cathode while the electrons are transferred to the cathode by an external circuit. The electrons and protons combine with oxygen at the cathode to form water.

Until now, the energy output



from biofuel cells has been too low for practical applications. Electron transfer in a biofuel cell can be slow so Hatazawa used a naphthoquinone derivative – known as an electron transfer mediator – to shuttle electrons between the electrodes and enzymes. This increased the current density – a measure of the rate of an electrochemical reaction

**The biofuel cell can power an mp3 player with a set of speakers**

### Reference

H Sakai *et al*, *Energy Environ. Sci.*, 2008, DOI: 10.1039/b809841g

– and increased the power output.

To increase the current density further, Hatazawa packed the mediator and enzymes on to a carbon-fibre anode. The large surface area and porosity of the electrode avoided disruption to glucose transport and maintained enzyme activity. They used a similar design to optimise the cathode so it supplied oxygen efficiently to the fuel cell.

When the researchers stacked four of the cells together, they achieved a power output of 100 milliwatts – enough to run an mp3 player with speakers or a small remote controlled car.

Adam Heller, an expert in bioelectrochemistry from the University of Texas at Austin, US, says the research ‘will give much needed impetus to the development of useful biofuel cells, after years of studies aimed at unachievable goals’.

Nicola Burton



## Scientists whip up new centrifuge using kitchen utensil

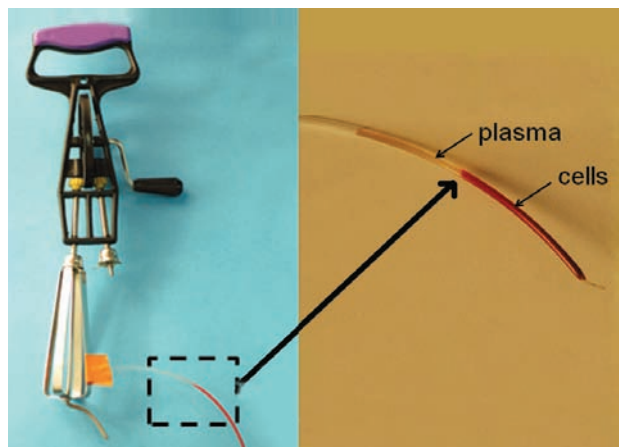
# Lab-on-an-egg-beater

A hand-powered egg beater can act as a centrifuge for separating plasma from blood, thanks to modifications made by US scientists.

George Whitesides and colleagues at Harvard University, Cambridge, carried out the work to enable point-of-care disease detection in developing countries.

Many immunoassays require plasma to diagnose disease. Typically, blood is transported to a lab where the plasma is separated by electrically-powered centrifuges and stored in refrigerators. But the equipment is expensive and difficult to move, which hinders its use in rural and developing communities where people cannot travel easily to health centres.

'The objective was to separate serum from blood using readily obtained materials in a resource-constrained environment,' explains



Whitesides. 'The work opens eyes to new possibilities.'

The cheap, portable and readily-available egg beater can be used at the point of care, meaning that health workers can diagnose illness

**The egg beater separates plasma from blood cells**

in remote areas. The technique also uses smaller volumes of blood than regular centrifuges.

'This technique is simple and works remarkably well,' says Doug Weibel, an expert in microbiology at the University of Wisconsin-Madison, US. 'This technique complements several other "simple solutions" that the Whitesides group has developed to tackle point-of-care diagnostics in resource-poor settings. The most striking thing about this collection of technologies is that they address a specific need or capability while carefully taking into consideration the limitations of the environment in which they will be operated.'

*Robin Forder*

#### Reference

A P Wong *et al*, *Lab Chip*, DOI: 10.1039/b809830c

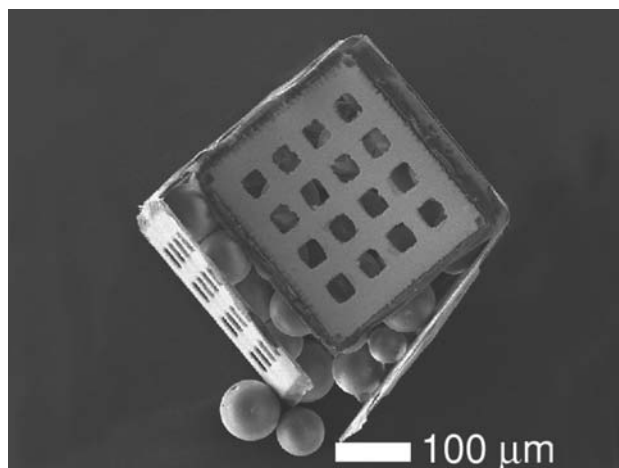
## Porous containers provide a realistic environment for studying cells

# Microcontainers hold cells captive

US scientists have made miniature containers that can catch and encapsulate cells.

Microwells in substrates are often used for studying cells but they can only be accessed from the top surface. David Gracias and colleagues from Johns Hopkins University, Baltimore, made 3D porous microcontainers that are accessible from all sides, meaning cells can interact more with surrounding media. 'Life is not 2D so these containers give a more realistic environment when studying biological systems,' explains Gracias.

Gracias' group made the containers from 2D cruciform templates, each with six faces joined by hinges made from metal and a polymer. They patterned the flat templates with pores using lithography. When they heated the template to 40°C, the polymer softened, causing the hinges to bend. The template folded together into a porous



cubic container, capturing inside any nearby objects, such as cells. 'We've shown that the process does not kill cells so it is compatible with live cells and organisms,' says Gracias.

The containers can load themselves with biological objects without the need for

**The porous template folds into a cube when heated, capturing nearby objects**

#### Reference

T G Leong *et al*, *Lab Chip*, 2008, 8, 1621 (DOI: 10.1039/b809098j)

microinjection or pipetting. This makes experiments that require slightly different conditions in each container easier and quicker, explains Gracias.

David Beebe, who engineers cellular scale systems at the University of Wisconsin, Madison, US, called the work 'a step forward over previous work by other scientists', adding that it 'extends the functionality and potential applications of engineered microcontainers'.

As well as studying cells and biological systems, Gracias says he hopes the containers could be used for drug delivery, envisaging that the pores could control how much drug is released from the container. The current containers are the right size for cells but if drugs and biologically active molecules are to be encapsulated in the future, Gracias says he will have to make the containers even smaller with very precise pores.

*Fay Riordan*

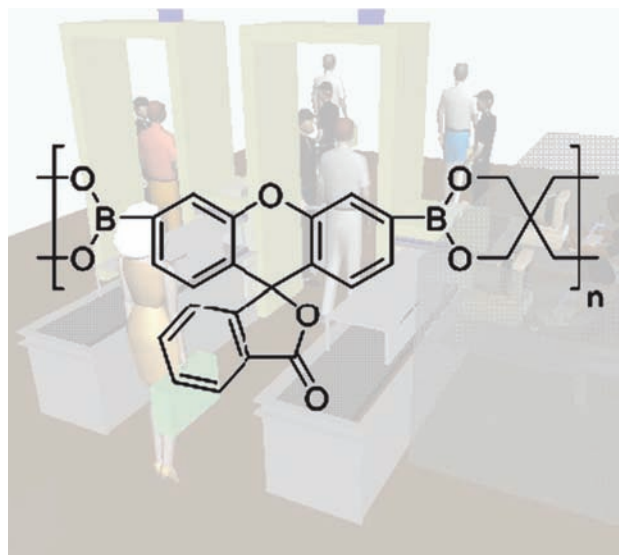
Boronate polymer offers rapid and sensitive explosive detection

## Fluorescent polymer detects peroxide

US scientists have developed an easy route to a polymer that can detect peroxide-based explosives.

Security teams need robust and portable explosive-detection devices to help prevent terrorist attacks. But peroxide-based explosives, such as triacetone triperoxide (TATP) and hexamethylene triperoxide diamine (HMTD), are challenging targets for detection because they lack aromatic or nitro groups. Jason Sanchez and William Trogler at the University of California, San Diego, US, have developed a new route to a boronate-based polymer that they say can rapidly detect low quantities of these explosives.

Trogler explains that the key to detecting TATP and HMTD is to detect the hydrogen peroxide they produce when they decompose. Current methods for detecting hydrogen peroxide typically involve liquid sampling, he says, which is not ideal for practical applications.



Sanchez and Trogler linked together molecules containing two boronate groups with a tetrahydroxy compound, in a process

**The boronate-based polymer could be used for airport security**

called double transesterification. Not only is this the first application of this reaction to the synthesis of stabilised boronate polymers, says Trogler, but the polymer product fluoresces within 30 seconds when exposed to hydrogen peroxide vapour at levels as low as 30 parts per million.

'This is an excellent piece of work and a nice addition to the toolbox of polymer chemists,' says Ben Zhong Tang, an expert in polymer science at the Hong Kong University of Science & Technology, China.

Trogler concludes that their polymer 'provides a robust low-cost alternative to current technology' for detecting hydrogen peroxide, something that Tang agrees 'will be of great importance for homeland security'.

David Barden

### Reference

J C Sanchez and W C Trogler, *J. Mater. Chem.*, 2008, DOI: 10.1039/b809674k

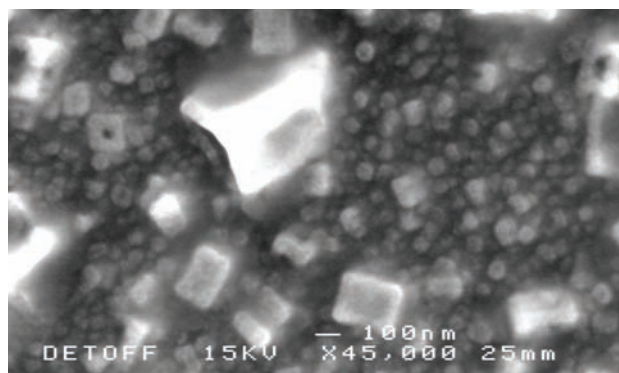
New precursors for key component of electronic circuits

## Toughening up thin films

UK scientists have made thin films that could help to make electronic devices faster and smaller.

Claire Carmalt's group at University College London, in collaboration with the manufacturing chemicals producer, SAFC Hitech in Bromborough, used chemical vapour deposition (CVD) to produce thin films of tungsten carbonitride from new precursor materials.

Today's society demands faster and higher capacity electronic devices such as computers, calculators and mobile phones. To improve these gadgets, their circuitry must be reduced in size. The barrier layer, which can be made from tungsten carbonitride, is a key component of electronic circuits. It prevents the circuit degrading by stopping copper diffusion from the circuit's wires into the semiconducting silicon



**Tungsten carbonitride films are made by chemical vapour deposition**

components. To reduce the circuit's size, this barrier layer must be made smaller and CVD can help by allowing scientists to deposit the layer over smaller areas.

Carmalt's group investigated a range of tungsten imido complexes to produce precursors with ideal thermal properties for CVD. They successfully tuned the

ligands surrounding the tungsten centre to optimise the thermal properties of the precursors to produce tungsten carbonitride thin films. The films produced by the team were uniform, adhesive, hard and resistant to scratching with a steel scalpel.

'By studying the thermal properties of the precursors, we get an idea of how they decompose and so what conditions we need to get film deposition,' says Carmalt. 'It also gives us an idea of their stability and hence what their shelf-life would be for potential industrial applications.'

George Koutsantonis, an expert in CVD from the University of Western Australia, Perth, comments that this work 'demonstrates the clear advantages that chemists have with their structured approach to materials synthesis'.  
Ruth Doherty

### Reference

S E Potts *et al.*, *Dalton Trans.*, 2008, DOI: 10.1039/b808650h

## Interview

# The flying chemist

*Spiros Pergantis talks to May Copsey about metals in biology and the environment, the future of metallomics and how he nearly became a pilot*



## Spiros Pergantis

**Spiros Pergantis is an associate professor in analytical chemistry at the University of Crete and a member of the *Journal of Analytical Atomic Spectrometry* Advisory Editorial board. His research involves the development and application of analytical methods for the detection and characterisation of metal-containing species in a variety of biological and environmental samples.**

### Why did you decide to become a chemist?

I come from a generation in Greece where many of our parents, because of the war, were not well educated. So it was important for them that we got a good education, and natural sciences were easy for me. I like experimental subjects. In high school, I wanted to figure out what chemistry was about so it became my first choice. For the first six months in university, I didn't like it very much because the practical labs weren't very inspiring. I almost took another option – to become an air force pilot. To become a pilot in Greece, you have to go into a military national academy. I had the marks but they needed an approval form. Luckily, my parents refused to sign it. I had to become more patient with chemistry and in my second year, I really started to appreciate it.

### When did you decide to specialise in analytical chemistry?

I went to the University of British Columbia in Vancouver and did my PhD with Professor William Cullen. That was a great experience. Bill Cullen is a synthetic inorganic chemist who had gone into analytical chemistry to study speciation in real samples, so I'm a bit of a mix. For some of the methods that we used, we had to isolate and purify milligram amounts of compounds from natural sources to get good NMR spectra. At that time, I thought: 'I'm never going to do this; it's too tedious.' So I started to get more involved with mass spectrometry to figure out how to perform these tasks with less purification and without requiring huge amounts.

### What's the most exciting research in your lab at the moment?

Apart from continuously trying to characterise novel arsenic, selenium and antimony species, we are now developing a novel hyphenated technique that involves coupling a nano-electrospray ion mobility spectrometer with an ICP-MS (inductively coupled plasma mass spectrometer). The idea behind this is that nanoparticles can be separated by size, ranging from three to 150 nanometres, using the ion mobility spectrometer. The element composition can then be determined in the ICP-MS. We do this because the sizes of biomolecules, like proteins and DNA, are within this range. We can now use this novel hyphenated technique to size biomolecules; however, we still

need to improve the system's overall sensitivity in order to be able to determine the metal or heteroatom content of the biomolecules. We can also use this system to investigate how metal species interact with biomolecules. Nano-electrospray is ideal for this as it does not tend to disrupt weak interactions, even non-covalent interactions. In this way we can probe the function of metal species. Our community has identified over 50 different compounds for arsenic and we are also finding many metabolites for antimony. However, we don't know what their functions are. Another interesting application would be to use electrospray to introduce viral particles into the gas phase. They contain metals in their proteins and we could possibly get fingerprints for these.

### Do you have any collaborations with other researchers?

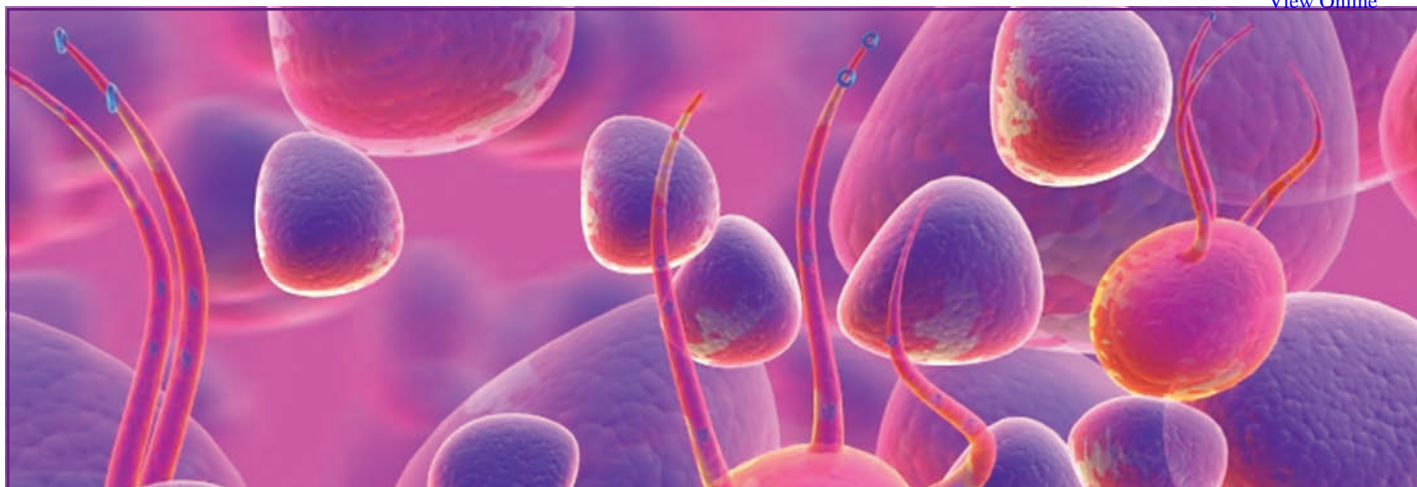
We collaborate with some medical groups on the metabolism of metal-containing drugs. We offer analytical tools to characterise the metabolites that are being produced and provide a better understanding of the mechanism of how the drug works. We also collaborate with biologists, environmental scientists and even materials chemists in some cases.

### How do you see the field of metallomics developing?

I think that we have a lot to learn by looking into the areas of metabolomics and proteomics. I think metallomics will be a complementary area, maybe not as big, but an essential part of the puzzle, so we have to be ready. We have to follow the huge developments that are being made in these areas and adapt them to metallomics. There's no reason that what can be done with organic compounds cannot be done with most inorganic, organometallic or metal containing biomolecules. There are many different communities and there are not enough bridges between them. The groups that have used both molecular mass spectrometry and atomic techniques have really made some amazing advances, which could never be made if you just stuck to the traditional atomic techniques. I think we are really making good progress as a result of this synergistic effect.

*The RSC is launching the new journal Metallomics in January 2009. For more information and free online access visit [www.rsc.org/metallomics](http://www.rsc.org/metallomics)*





*Integrative Biology* would like to congratulate the 2008 recipients of the

## Nobel Prize in Chemistry

The prize was awarded to Roger Y. Tsien, Osamu Shimomura and Martin Chalfie for outstanding contributions in chemistry for their work in the development of the gene marker green fluorescent protein (GFP).

"We are all immensely pleased that 2008 Nobel Prize winner Roger Tsien is an Editorial Board member for *Integrative Biology*; his work typifies the quality of material we are seeking in the development of biology through new tools and technologies."

Harp Minhas, managing editor of *Integrative Biology*

### Submit your work to *Integrative Biology*

Launching January 2009, *Integrative Biology* provides a unique venue for elucidating biological processes, mechanisms and phenomena through quantitative enabling technologies at the convergence of biology with physics, chemistry, engineering, imaging and informatics.

Submissions are welcomed via ReSource, our homepage for authors and referees. [www.rsc.org/resource](http://www.rsc.org/resource)



Professor Roger Y. Tsien, Editorial Board, *Integrative Biology*

Go online Today!

## Instant insight

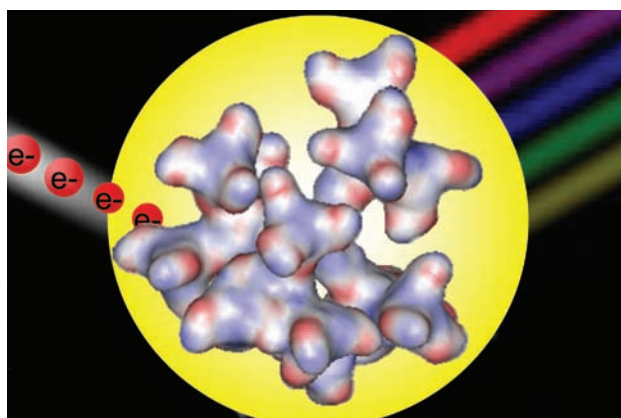
## Dendrimers in the spotlight

Seok-Ho Hwang, Charles Moorefield and George Newkome from the University of Akron, US, examine the use of dendrimers in organic light-emitting diodes

It has been projected that one billion US dollars in business will be generated during 2008 from the use of organic light-emitting diodes (OLEDs) in display devices. As a result, companies such as Samsung, Sony and LG are greatly interested in OLED technology. OLEDs possess a number of advantages over conventional, non-organic light-emitting diodes including higher luminous efficiency; faster response time; lower power consumption; lower cost; lighter weight; and higher brightness and contrast, which eliminates the necessity for backlighting. OLED displays can be built on large, rigid or flexible substrates and in a virtually unlimited choice of colours.

And so government agencies, industry and academia are carrying out intense research in an attempt to refine and control the electro-optical properties of OLEDs. The OLED field can be divided into three groups of electroluminescent host materials: small organic molecules, polymers and dendritic macromolecules. Dendritic chemistry – which helps to integrate classical small molecule property control with macromolecular material design and processability – is particularly promising in the field.

Dendritic architectures consist of a core, branch junctions and connectors and termini. Each dendritic component of an OLED can be best chosen to fulfill the required function. For example, the use of a conjugated polymeric core can define the emitted colour; the branching moieties can be designed to aid charge transport to or from the core; or the surface groups can be matched to the processing



properties (for example, the required solubility).

To date, much of the research involving dendrimers as OLED components has focused on their use in the electroluminescent, emissive layer of the device. For example, branched, stilbenoid materials have been shown to display blue emission and increase device lifetime and stability, while elegant polyphenylene chemistry has been used to design red–orange OLEDs. And phosphazene-cored dendrimers with amino-pyrene moieties have shown photoluminescent quantum efficiencies in the range of 67 to 83 per cent. Hyperbranched and dendronised polymer constructs are also under investigation.

Logically, metallo-dendrimers have been examined, in particular those made with europium(II), platinum(II), and iridium(III), due to their potential to act as highly efficient phosphorescence emitters; reports of theoretical internal quantum efficiencies of 100 per cent are known. Recent integration of hole-transporting, carbazole dendrons with

iridium(III) complexes reportedly yielded soluble, easily manipulated phosphorescent materials with quantum yields of 87 and 45 per cent for solution and film measurements, respectively.

The advantages of dendritic macromolecules are straightforward when their structure is considered. The surface groups can be tuned independently of the core, allowing the processing properties, such as solubility, to be altered easily. Interfacial contact between surface groups helps avoid aggregate formation, which is often observed in non-dendritic materials. Finally, band gaps can be modulated, from the outer to the inner dendritic regions, to provide the OLED components with the best charge transport properties.

Though the field is growing rapidly and its impact is far-reaching, major challenges still remain. The lack of highly efficient, stable organic light-emitting materials, the short lifetime of OLEDs and low large-scale manufacturing yields are particular problems. These drawbacks can only be overcome by an exceptional interdisciplinary research effort bridging physics, chemistry and materials sciences.

Progress towards higher efficiencies using dendritic architectures will undoubtedly generate new OLED applications, for example in mobile phones, portable electronic games, personal digital assistants and tomorrow's yet-to-be-created gadgets and toys.

**Branched architectures shine brightly in the quest for efficient components for OLEDs**

#### Reference

S-H Hwang, C N Moorefield and G R Newkome, *Chem. Soc. Rev.*, 2008, DOI: 10.1039/b803932c

Read more in 'Dendritic macromolecules for organic light-emitting diodes' in issue 11 of Chemical Society Reviews.

# Essential elements

## Good prospects for *Lab on a Chip*

*Lab on a Chip*, the miniaturisation journal for chemistry, biology and bioengineering is now taking miniaturisation science to the next level. With journal submissions steeply rising over the past years, 2009 will see the journal increase in frequency to 24 issues per year. The new year will also herald the arrival of George Whitesides as the new editorial board chair of *Lab on a Chip*. 'There is no one in the field who is better equipped than Professor Whitesides to help *Lab on a Chip* ascend to the next level in terms of quality, visibility and impact,' comments Harp Minhas, editor of *Lab on a Chip*.

*Lab on a Chip* has established itself at the heart of the miniaturisation community through various sponsorships for prizes and awards, which recognise and highlight the contributions of young and emerging scientists in the field, to



**George Whitesides, the new editorial board chair of *Lab on a Chip***

online support via new initiatives such as 'Chips & Tips' - the quick-fix online forum providing useful advice on common practical problems for scientists in the miniaturisation world.

More issues, more leading research and a new editorial board chair - 2009 promises to be an exciting year for the *Lab on a Chip* community.

For further information visit [www.rsc.org/loc](http://www.rsc.org/loc)



## Do you know...

...which RSC journals you can access at your institution? Or whether you can use the RSC Journals Archive? If you're not sure, help is at hand.

We've introduced a special web page to help you to find out exactly what RSC content you can access. This new page is called Your RSC Subscriptions ([www.rsc.org/Publishing/your\\_access.asp](http://www.rsc.org/Publishing/your_access.asp)) and it lists all products for which your organisation has a current subscription, plus other content which may be available to you, such as the RSC Journals Archive and the RSC eBook Collection.

You can also find out about RSC content that is available free, including:

- research articles that are free for a limited time
- news articles in magazines
- free chapters from the RSC eBook Collection

Visit [www.rsc.org/Publishing/freeRSCcontent.asp](http://www.rsc.org/Publishing/freeRSCcontent.asp)

## ChemComm in Korea

The Second *ChemComm* International Symposium on Supramolecular Chemistry will take place in Korea in November 2008 with one-day meetings in Seoul, Daejeon and Pohang. This follows a successful First *ChemComm* International Symposium on Polymers and Polymer Science in China in December 2007.

*ChemComm*, with an impact factor of 5.14, publishes some of the most significant work in the chemical sciences and is

the fastest at publishing general chemistry communications. *ChemComm* Symposia aim to bring together scientists in an environment that fosters collaborations between the researchers and universities involved. All symposia are free to attend and each is devoted to a topical area of the chemical



sciences, featuring an invited programme of international and locally-based expert speakers.

In this second symposium, the programme is supplemented by a poster session, showcasing the work of local universities.

As the second symposium approaches fast and promises to be as successful as the first, plans for a third symposium

next year in China are already well underway. The Third *ChemComm* International Symposium on the topic of Organic Chemistry will be held in February 2009, with meetings in Beijing, Shanghai and Chengdu.

For more details on *ChemComm* Symposia, and full programme schedules for the Second Symposium on Supramolecular Chemistry in Korea, visit [www.rsc.org/chemcommsymposia](http://www.rsc.org/chemcommsymposia).

*Chemical Technology* (ISSN: 1744-1560) is published monthly by the Royal Society of Chemistry, Thomas Graham House, Science Park, Milton Road, Cambridge UK CB4 0WF. It is distributed free with *Chemical Communications*, *Journal of Materials Chemistry*, *The Analyst*, *Lab on a Chip*, *Journal of Atomic Absorption Spectrometry*, *Green Chemistry*, *CrystEngComm*, *Physical Chemistry Chemical Physics*, *Energy & Environmental Science* and *Analytical Abstracts*. *Chemical Technology* can also be purchased separately. 2008 annual subscription rate: £199; US \$396. All orders accompanied by payment should be sent to Sales and Customer Services, RSC (address above), Tel +44 (0) 1223 432360, Fax +44 (0) 1223 426017. Email: [sales@rsc.org](mailto:sales@rsc.org)

**Editor:** Joanne Thomson

**Deputy editor:** Michael Spencelayh

**Associate editors:** Celia Gitterman, Nina Notman

**Interviews editor:** Elinor Richards

**Web editors:** Nicola Convine, Michael Townsend, Debora Giovanelli

**Essential elements:** Kathrin Hilpert, Kathryn Lees, and Valerie Simpson

**Publishing assistant:** Jackie Cockrill

**Publisher:** Graham McCann

Apart from fair dealing for the purposes of research or private study for non-commercial purposes, or criticism or review, as permitted under the Copyright, Designs and Patents Act 1988 and the copyright and Related Rights Regulations 2003, this publication may only be reproduced, stored or transmitted, in any form or by any means, with the prior permission of the Publisher or in the case of reprographic reproduction in accordance with the terms of licences issued by the Copyright Licensing Agency in the UK. US copyright law is applicable to users in the USA.

The Royal Society of Chemistry takes reasonable care in the preparation of this publication but does not accept liability for the consequences of any errors or omissions.

Royal Society of Chemistry: Registered Charity No. 207890.

# RSC Publishing



# Chemical activation by mechanochemical mixing, microwave and ultrasonic irradiation

Rajender S. Varma\*

DOI: 10.1039/b817559b

The diverse nature of the world of chemical synthesis requires various greener pathways in our quest towards attaining sustainability. The emerging area of green chemistry envisages minimum hazard as the performance criterion when designing new chemical processes. Cleaner processes are being developed as we continue to explore alternatives to conventional chemical syntheses and transformations. One of the thrust areas for achieving this target is to explore alternative efficient reaction conditions and eco-friendly reaction media to accomplish the desired chemical transformations with minimized by-products or waste and without the use of conventional volatile organic solvents, wherever possible. Consequently, several newer strategies have appeared, such as reactions under solvent-free (dry media) conditions,<sup>1</sup> mechanochemical mixing (grinding),<sup>2,3</sup> use of solid-supported reagents and the alternate heating and activation methods that utilize microwave<sup>4</sup> (MW) and ultrasonic irradiation<sup>5</sup> for rapid syntheses. These techniques overcome some of the problems associated with excessive or wasteful heating. Ball-mill processing is a solid-state size reduction process that can be easily scaled up and has been used in the paint industry, material science, the pharmaceutical industry, and also for environmental remediation. Mechanochemical solvent-free processing of organic molecules that prevents the usage of toxic metallic species and solvents is gaining popularity.<sup>2,3</sup> While ultrasonic irradiation enhances the chemical reaction and mass transfer *via* the

process of acoustic cavitation,<sup>5</sup> MW irradiation provides the 'volumetric core' and selective heating of polar entities.<sup>6</sup> The selective absorption of microwaves by polar molecules and intermediates in a multiphase system could also substitute as a phase transfer catalyst without using any phase transfer reagent, thereby providing the observed acceleration, as has been noticed for ultrasonic irradiation.<sup>7</sup> Experimental observations in several reaction systems have been consistent with the mechanistic postulation wherein the polar transition state of the reaction is favored by MW irradiation with respect to the dielectric polarization nature of MW energy transfer.<sup>6,8</sup>

The review in this issue of *Green Chemistry* (A. Bruckmann, A. Krebs and C. Bolm, *Green Chem.*, 2008, DOI: 10.1039/b812536h) provides an overview of organocatalytic reactions using non-traditional methods. Mechanochemical organocatalytic strategy has demonstrated good stereoselectivity in asymmetric aldol reactions, Baylis–Hillman reactions, and the protection of the heterocyclic amino groups of nucleosides. On the same organocatalytic theme, MW-assisted enantioselective proline-catalyzed  $\alpha$ -aminomethylation of ketones has successfully reduced the reaction time and catalyst loading. Several reactions, the Michael addition, Baylis–Hillman and Diels–Alder, have been some of the beneficiaries of exposure to MW and ultrasonic irradiation in terms of shortening the reaction times and reducing the amount of reagents and solvents that are often used in excess.

Eco-friendly advantages of the synthetic alternatives based on unconventional activation *via* MW or ultrasound irradiation or the use of a mechanochemical approach for 'neat' reactions in the absence of any solvent are increasingly

becoming apparent and may be adopted by the pharmaceutical industry to reduce or eliminate volatile organic solvents, thus preventing pollution 'at source'. Synthetic processes using MW/ultrasonic irradiation to shorten the reaction time and eliminate or minimize side product formation are already finding acceptance in the pharmaceutical industry<sup>9</sup> (combinatorial chemistry) and polymer syntheses, and may pave the way towards a greener and more sustainable approach to chemical syntheses.<sup>10</sup> Newer developments on these themes, especially involving benign reaction media such as water<sup>11</sup> and polyethylene glycol (PEG),<sup>12</sup> in conjunction with MW and ultrasonic irradiation and/or ball-milling under solvent-free conditions, may help realize sustainable pathways for chemical synthesis and transformations, including generation of nanomaterials.<sup>13</sup>

## References

- (a) V. Polshettiwar and R. S. Varma, *Pure Appl. Chem.*, 2008, **80**, 777; (b) R. S. Varma, *Tetrahedron*, 2002, **58**, 1235; (c) R. S. Varma, *Green Chem.*, 1999, **1**, 43.
- (a) J. Mack, D. Fulmer, S. Stofel and N. Santos, *Green Chem.*, 2007, **9**, 1041; (b) V. P. Balema, J. W. Wiench, M. Pruski and V. K. Pecharsky, *J. Am. Chem. Soc.*, 2002, **124**, 6244.
- (a) D. Kumar, M. S. Sundaree, G. Patel, V. S. Rao and R. S. Varma, *Tetrahedron Lett.*, 2006, **47**, 8239; (b) D. Kumar, S. Sundaree, V. S. Rao and R. S. Varma, *Tetrahedron Lett.*, 2006, **47**, 4197; (c) D. Kumar, K. V. G. Chandra Sekhar, H. Dhillon, V. S. Rao and R. S. Varma, *Green Chem.*, 2004, **6**, 156.
- (a) V. Polshettiwar and R. S. Varma, *Acc. Chem. Res.*, 2008, **41**, 629; (b) V. Polshettiwar and R. S. Varma, *Chem. Soc. Rev.*, 2008, **37**, 1546.
- (a) V. V. Nambodiri and R. S. Varma, *Org. Letters*, 2002, **4**, 3161; (b) J. L. Luche, *Synthetic Organic Chemistry*, Plenum Press, New York, 1998.
- A. Loupy and R. S. Varma, *Chim. Oggi*, 2006, **24**, 36.
- R. S. Varma, K. P. Naicker and D. Kumar, *J. Mol. Catal. A: Chem.*, 1999, **149**, 153.

Sustainable Technology Division, National Risk Management Research Laboratory,  
U. S. Environmental Protection Agency,  
Cincinnati, Ohio, 45268, USA.  
E-mail: Varma.Rajender@epa.gov;  
Fax: +1-(513)-569-7677;  
Tel: +1-(513)-487-2701



- 8 (a) Y. Ju and R. S. Varma, *J. Org. Chem.*, 2006, **71**, 135; (b) M. Ješelnik, R. S. Varma, S. Polanc and M. Kočevár, *Green Chem.*, 2002, **4**, 35.
- 9 V. Polshettiwar and R. S. Varma, *Curr. Opin. Drug Discovery Dev.*, 2007, **10**, 723.
- 10 C. R. Strauss and R. S. Varma, *Top. Curr. Chem.*, 2006, **266**, 199.
- 11 (a) C. -J. Li and T. H. Chan, *Chem. Soc. Rev.*, 2006, **35**, 68; (b) V. Polshettiwar and R. S. Varma, *J. Org. Chem.*, 2008, **73**, 7417; (c) R. S. Varma, *Org. Chem. Highlights*, 2007, <http://www.organic-chemistry.org/Highlights/2007/01February.shtm>;
- 12 (a) J. Chen, S. K. Spear, J. G. Huddleston and R. D. Rogers, *Green. Chem.*, 2005, **7**, 64; (b) V. V. Namboodiri and R. S. Varma, *Green Chem.*, 2001, **3**, 146.
- 13 (a) B. Hu, S.-B. Wang, K. Wang, M. Zhang and S.-H. Yu, *J. Phys. Chem. C*, 2008, **112**, 11169; (b) M. N. Nadagouda and R. S. Varma, *Cryst. Growth Des.*, 2008, **8**, 291; (c) M. N. Nadagouda and R. S. Varma, *Cryst. Growth Des.*, 2007, **7**, 686; (d) M. N. Nadagouda and R. S. Varma, *Biomacromolecules*, 2007, **8**, 2762; (e) M. N. Nadagouda and R. S. Varma, *Macromol. Rapid Commun.*, 2007, **28**, 842; (f) B. Baruwati, M. N. Nadagouda, and R. S. Varma, *J. Phys. Chem. C*, 2008, 112, in press.

# Organocatalytic reactions: effects of ball milling, microwave and ultrasound irradiation

Angelika Bruckmann, Anke Krebs and Carsten Bolm\*

Received 21st July 2008, Accepted 27th August 2008

First published as an Advance Article on the web 10th October 2008

DOI: 10.1039/b812536h

Ball milling, microwave heating and ultrasound irradiation can be used to support conventional laboratory techniques. By applying them, a number of organocatalytic processes could be improved and superior results have been achieved compared to reactions performed under standard conditions. The purpose of this overview is to highlight recent advances by presenting selected examples.

## 1. Introduction

Recently, the sustainability of chemical reactions has gained relevance in scientific and political discussions.<sup>1</sup> In this context, ball milling, microwave heating and ultrasound irradiation are discussed of being complementary techniques for promoting chemical reactions. These (often called “green”) techniques can help to reduce the amount of undesired hazardous chemicals (including solvents), and increase the selectivity towards the given product/s.

The aim of this review is to show examples of advantageous applications of these techniques with a particular focus on organocatalytic reactions.

## 2. Organocatalytic reactions under ball milling conditions

Ball milling is a useful tool that allows a highly efficient mixing of reagents under solvent-free conditions.<sup>2,3</sup> In organic chemistry it found various applications including C–C bond formations,<sup>4</sup> amine condensations,<sup>5</sup> syntheses of heterocycles,<sup>5</sup> and fullerene modifications.<sup>6</sup> Furthermore, reactions with metal-organic reagents have been reported.<sup>7</sup>

Efficient mixing is particularly important in solid–solid reactions, which continuously require fresh contacts between the reacting partners.<sup>8,9</sup> Compared to grinding or sonicating, milling generates new contact sites between the solids more efficiently. This holds true for large-scale reactions as well.<sup>8</sup>

Due to the high reagent concentrations and also the efficient mixing, other solvent-free reactions, including those between solids with intermediate local melting and those with at least one liquid reagent, can benefit from the use of ball mills.

In a ball milling device the starting materials are located between surfaces and crushed due to impact and/or frictional forces that are caused by collisions. The method of how the motion leading to these collisions is affected distinguishes the various mills. In general, materials with a particle size of <100 nm can be produced.

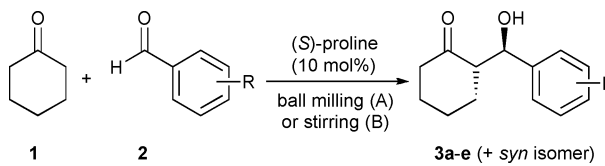
In chemical synthesis, ball milling modifies the reaction conditions and enhances the reactivity of the reagents (mechanical activation). The latter is commonly not due to an induced mechanical breaking of molecular bonds (mechanochemistry),<sup>1b,10</sup> but a result of the more efficient mixing and the enormous increase of the reagent surfaces, which both lead to a close contact between the starting materials on (an almost) molecular scale. Besides that, other factors such as an increased temperature and an enhanced pressure can be responsible for the observed reactivity changes. For example, during the milling, extreme conditions occur on the surfaces of two colliding bodies for times in the order of microseconds. According to a model developed by Urakaev and Boldyrev, local temperatures of 400–1500 K and pressures of some thousand atmospheres can be part of typical conditions in the ball mill.<sup>11</sup> As a result of these local effects, the average temperature in a ball mill typically rises by approximately 40–60 °C. A better control of these factors can be achieved by the use of temperature measurement and cooling/heating devices.

Only recently, the first examples of organocatalytic reactions performed under ball milling conditions appeared in the literature. Those will be briefly discussed, and the effect of applying a ball mill will be demonstrated by comparing the results to those of reactions carried out under conventional conditions.

### 2.1. Aldol reaction

The proline-catalysed intermolecular aldol reaction is a well-studied C–C bond-forming reaction, which proceeds *via* enamine intermediates generated *in situ*. Commonly, the products are formed with high chemo- and stereoselectivity.<sup>12</sup> With the vision that such metal-free reactions could benefit from the inherent solvent-free conditions of the ball-milling technology, Bolm and co-workers recently initiated a program that studied a combination of both approaches.<sup>13</sup> While the reaction is usually conducted in highly polar solvents, such as dimethyl sulfoxide (DMSO), only a few examples of organocatalytic aldol reactions performed in the absence of a solvent could be found in the literature.<sup>14</sup> There, high yields and acceptable stereoselectivities could only be achieved with an excess of liquid ketone ( $\geq 3$  equivalents), which in most cases appeared to act as both reactant and reaction medium. Furthermore, synthetically

Institute of Organic Chemistry, RWTH Aachen University, Landoltweg 1, D-52056, Aachen, Germany. E-mail: Carsten.Bolm@oc.rwth-aachen.de; Fax: (+49)-241-809-2391; Tel: (+49)-241-809-4675

**Table 1** The asymmetric aldol reaction under solvent-free conditions<sup>13</sup>

Entry	2/3	R =	Method	t/h	Yield (%)	anti/syn	ee (%)
1	a	4-NO <sub>2</sub>	A	5.5	99	89:11	94
2	a	4-NO <sub>2</sub>	B	24	95	89:11	94
3	b	3-NO <sub>2</sub>	A	7	94	88:12	>99
4	b	3-NO <sub>2</sub>	B	16	89	82:18	98
5	c	2-NO <sub>2</sub>	A	7	97	93:7	97
6	c	2-NO <sub>2</sub>	B	36	89	91:9	97
7	d	4-Cl	A	20	87	74:26	75
8	d	4-Cl	B	72	85	78:22	67
9	e	2-MeO	A	36	65	66:34	63
10	e	2-MeO	B	96	64	71:29	67

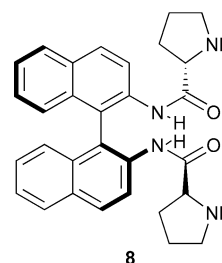
advanced variants of proline had to be used. A solvent-free approach with close to equimolar amounts of reactants and proline itself had not been reported.

In their study, Bolm and co-workers described that under solvent-free conditions an efficient mixing was vitally important to achieve high yields. In this respect, conventional magnetic stirring appeared insufficient. This limitation could be overcome by means of the ball mill, and the solvent-free ball-milling conditions allowed a highly-efficient catalysis to occur, even when solely solid reagents were employed. In all cases, the use of simple (unmodified) (*S*)-proline (10 mol%) and nearly stoichiometric amounts of ketone and aldehyde (1.1 : 1) led to the formation of *anti*-aldol products with excellent stereoselectivities (up to >99% ee, Table 1) in high yields (up to 99%). In a comparative study using conventional magnetic stirring, the aldol products were stereoselectively obtained in high yields as well, but those reactions proceeded much slower, indicating the advantage of the ball-milling technology.

The generality of the organocatalytic aldol reaction in a ball mill was examined by varying the substrate combinations. In reactions with cyclohexanone, aldehydes with electron-withdrawing substituents (**2a–c**) afforded products with high stereoselectivities in short reaction times. Those with more electron-rich groups (**2d** and **2e**) lowered both reactivity and stereoselectivity. It is noteworthy that the above-mentioned trends of the electronic effects and the dependence of the stereoselectivity on the substrate structure were analogous to those observed in aldol reactions under common reaction conditions (*e.g.* in organic or aqueous solvents and solvent-free conditions). Also, in reactions of solely solid reagents, the *anti*-aldol products **6a–d** and **7a–d** were obtained with both excellent diastereoselectivities (up to 99 : 1 *anti/syn* ratio, **7d**, Table 2) and enantioselectivities (up to 98% ee, **7c**). Presumably due to a more difficult mixing, those reactions proceeded much slower (compared to similar ones involving liquid–solid reagent combinations). Overall, the application of the ball milling technique proved particularly useful for such reactions, and compared to the use of conventional magnetic stirring (5–7 days) ball milling in reactions between solely solid

reagents led to high conversions in relatively short reaction times ( $\leq 1.6$  days).

In a similar approach, Guillena, Nájera and co-workers studied the direct aldol reaction between various ketones and aldehydes under solvent-free conditions using a combination of binam-prolinamide **8** (5–10 mol%, Fig. 1) and benzoic acid (10–20 mol%) as catalyst (Table 3).<sup>15</sup> Three different procedures were assayed: ball milling (method A), conventional magnetic stirring (method B) and conventional magnetic stirring with a pre-formed solution in THF and immediate evaporation (method C). The latter methods were intended to accelerate the reaction rate by inducing an intensive substrate-catalyst contact.

**Fig. 1** Binam-(*S*)-proline derived catalyst.<sup>15</sup>

All three methods provided the aldol product **3a** after short reaction times (1–1.5 h) with regio-, diastereo- and enantioselectivities comparable to those achieved in reactions performed in organic or aqueous solvents. No improvement was observed when the catalysis was conducted in a ball mill (Table 3, method A). Further studies revealed that when (*S*)-proline (10 mol%) was employed as catalyst under method C conditions, even after 24 h the conversion towards aldol product **3a** was only moderate (34%). Thus, the authors concluded that binam-proline **8** in combination with benzoic acid was a superior catalyst for conducting direct aldol reactions under solvent-free conditions.

**Table 2** The asymmetric aldol reaction between solely solid reactants<sup>13b</sup>

Entry	Ketone	6/7	R =	Method	t/d	Yield (%)	anti/syn	ee (%)
1	4	6a	4-NO <sub>2</sub>	A	1.4	85	91:9	91
2	4	6a	4-NO <sub>2</sub>	B	5	58	93:7	89
3	4	6b	3-NO <sub>2</sub>	A	1	80	78:22	92
4	4	6b	3-NO <sub>2</sub>	B	5	82	92:9	95
5	4	6c	2-NO <sub>2</sub>	A	1	66	81:19	88
6	4	6c	2-NO <sub>2</sub>	B	6	76	77:23	92
7	4	6d	4-Cl	A	1.6	75	92:8	93
8	4	6d	4-Cl	B	7	85	87:13	93
9	5	7a	4-NO <sub>2</sub>	A	1.4	79	96:4	90
10	5	7a	4-NO <sub>2</sub>	B	7	47	98:2	96
11	5	7b	3-NO <sub>2</sub>	A	1.5	75	88:12	89
12	5	7b	3-NO <sub>2</sub>	B	7	59	93:7	96
13	5	7c	2-NO <sub>2</sub>	A	1.5	59	82:18	96
14	5	7c	2-NO <sub>2</sub>	B	6	73	93:7	98
15	5	7d	4-Cl	A	1.4	72	95:5	85
16	5	7d	4-Cl	B	7	77	99:1	82

**Table 3** Example of an asymmetric aldol reaction catalysed by **8** under solvent-free conditions<sup>15</sup>

Entry	Method <sup>a</sup>	t/h	Conversion (%)	anti/syn	ee (%)
1	A	1.5	100	69:31	88
2	B	1.0	99	67:33	88
3	C	1.5	99	72:28	89

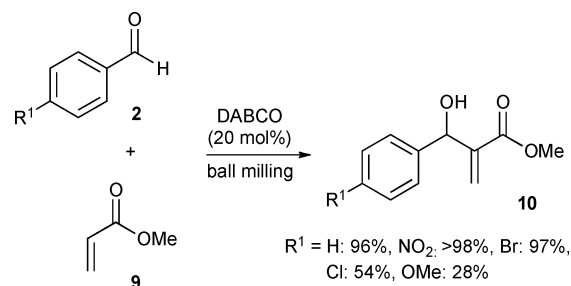
<sup>a</sup> For details see text.

## 2.2. Baylis–Hillman reaction

The Baylis–Hillman (also known as Morita–Baylis–Hillman) reaction<sup>16</sup> is an atom-economical transformation that typically involves an electron-deficient alkene, an electrophile (such as an aldehyde) and a tertiary amine as catalyst, yielding highly functionalised products. One of the main drawbacks of this powerful C–C bond-forming reaction is its low reaction rate. Thus, Baylis–Hillman reactions often require days to weeks for

completion depending on the reactivities of both the activated alkenes and the electrophiles.

With the aim of facilitating the reaction, Mack and Shumba investigated the effect of high speed milling (HSM) in Baylis–Hillman reactions.<sup>17</sup> Various *p*-substituted aromatic aldehydes **2** and methyl acrylate (**9**) served as model substrates, which were milled in the presence of 20 mol% of 1,4-diazabicyclo[2.2.2]octane (DABCO) (Scheme 1). Whereas previous studies had shown that such reactions can take 3 to 4 days at room temperature to provide the products in good yields (70–87%),<sup>18</sup> the use of HSM led to a significant rate enhancement, generating products **10** after only 0.5 hours in yields up to >98%. The temperature was neither controlled nor reduced by including breaks into the 0.5 hour milling time. It can therefore be assumed that the process was accompanied by a significant temperature increase.

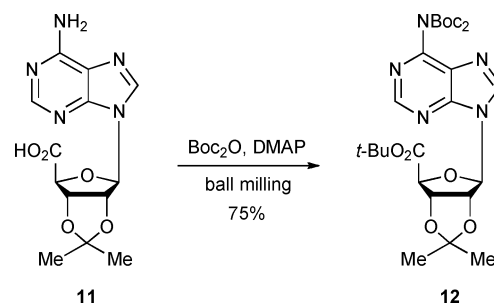
**Scheme 1** The Baylis–Hillman reaction in a high speed ball mill.<sup>17</sup>



### 2.3. Bis-*N*-Boc protections of the heterocyclic amino group of nucleosides

Protected nucleosides, such as **11**, are poorly soluble in the organic solvents that are commonly used for amide formations. Thus, when several attempts to protect the *N*-6 group of **11** with *tert*-butoxycarbamate (Boc) using standard solution protocols failed, Sikchi and Hultin considered solvent-free methods.<sup>19</sup> As a result they found that upon grinding of acid **11** with an excess of di-*tert*-butyl dicarbonate ( $\text{Boc}_2\text{O}$ ) and 4-*N,N'*-(dimethylamino)-pyridine (DMAP) in a ball mill, the corresponding bis-*N*-Boc-protected ester **12** was rapidly formed (Scheme 2). Furthermore, in contrast to many reported solution methods, the use of a strong base was not required. As  $\text{CO}_2$  (g) was liberated during the reaction, it was impossible to perform the reaction in closed glass flasks or vials. In a simple ball mill, however, the reaction proceeded well.

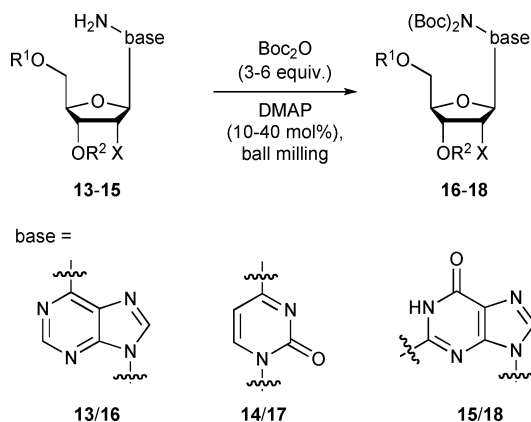
The scope of the nucleoside protection under ball milling conditions was studied by applying common *O*-protected adenosine, cytidine and guanosine derivatives **13–15**, respectively (Table 4). In almost all cases the reactions were complete within 1–7 hours, and the expected products were obtained in high yields. Only guanosine derivatives led to the formation of significant amounts of by-products. During the grinding, the formation of a liquid phase or melt was observed. Presumably, due to their lower melting points, this stage was reached earlier for the silyl-protected nucleosides than for their ester-protected counterparts. As a consequence, conversions of the former proceeded faster.



**Scheme 2** Bis-*N*-Boc protection (and ester formation) of adenosine derivative **11** under solvent-free conditions in a ball mill.<sup>19</sup>

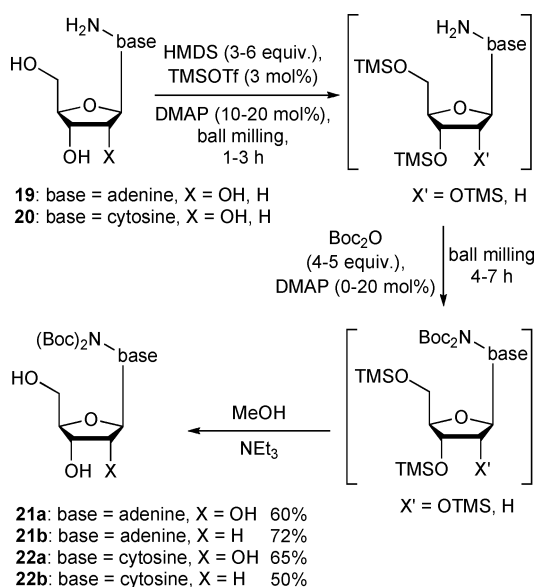
Finally, nucleosides with free OH-groups were subjected to the reaction conditions. In this case, the Boc-protection of both the amino and the sugar hydroxyl groups occurred. In order to selectively convert the former, a new procedure was developed which involved an *in situ* transient silylation of the hydroxyl groups prior to the Boc-introduction (Scheme 3). Thus, first the nucleoside was ball milled with 3–6 equiv. of HMDS and catalytic amounts of trimethylsilyl triflate and DMAP. When the silylation of the hydroxyl groups was complete,  $\text{Boc}_2\text{O}$  was added (together with additional DMAP if required) and the reaction mixture was milled a second time. Finally, the *O*-silyl groups were removed by stirring of the crude product in methanol in the presence of triethylamine over night. This sequence worked well for adenosine and cytidine derivatives, to provide the corresponding products (**21a,b** and **22a,b**) in

**Table 4** Bis-*N*-Boc protection of nucleoside derivatives **13–15** under solvent-free conditions in a ball mill<sup>19</sup>



Entry	Substrate	R <sup>1</sup>	R <sup>2</sup>	X	Method <sup>a</sup>	t/h	Yield (%)
1	<b>13a</b>	Ac	Ac	OAc	A	6	90
2	<b>13b</b>	TBDMS	TBDMS	OTBDMS	B	2	99
3	<b>13c</b>	Ac			B	4	96
4	<b>13d</b>	TBDMS			B	2	99
5	<b>13e</b>	Ac	Ac	H	B	2	99
6	<b>13f</b>	TBDMS	TBDMS	H	B	1	99
7	<b>14a</b>	TBDMS	TBDMS	OTBDMS	C	1	99
8	<b>14b</b>	TBDMS	TBDMS	H	C	1	99
9	<b>14c</b>	Ac	Ac	H	C	2	50
10	<b>15a</b>	Ac	Ac	OAc	D	7	25
11	<b>15b</b>	TBDMS	TBDMS	TBDMS	D	6	40
12	<b>15c</b>	TBDMS	TBDMS	H	E	6	70

<sup>a</sup> Method A: DMAP (30 mol%),  $\text{Boc}_2\text{O}$  (4 equiv.); Method B: DMAP (10 mol%),  $\text{Boc}_2\text{O}$  (3 equiv.); Method C: DMAP (20 mol%),  $\text{Boc}_2\text{O}$  (4 equiv.); Method D: DMAP (20 mol%),  $\text{Boc}_2\text{O}$  (5 equiv.); Method E: DMAP (40 mol%),  $\text{Boc}_2\text{O}$  (6 equiv.).



Scheme 3 One pot bis-*N*-protection using a transient silylation.<sup>19</sup>

good yields (Scheme 3). Attempts to convert guanosine-derived nucleosides led to complex product mixtures.

### 3. Organocatalytic reactions under microwave irradiation

Microwave irradiation has become a useful tool in the synthesis of organic molecules. Since the pioneering work by Gedye and co-workers in 1986 the number of publications dealing with so called microwave-assisted organic synthesis (MAOS) has rapidly increased.<sup>20</sup> The early studies were carried out using conventional microwave ovens which resulted in hardly controlled reaction conditions and poor reproducibilities. Today, specially designed microwave reactors are available allowing a careful measuring of the irradiation, the reaction temperature and the pressure inside the reaction vessel.

In many examples it has been shown that the application of microwave irradiation reduces the reaction time, increases the product yield and sometimes results in a different product distribution compared to conventional heating methods.<sup>21</sup> The observed rate acceleration upon microwave irradiation is due to material-wave interactions leading to thermal and specific effects. The thermal effects largely result from a more efficient energy transfer to the reaction mixture which is known as dielectrical heating. This phenomenon relies on the ability of a substance (solvent or reagent) to absorb microwaves and convert them into heat. The reaction mixture is heated from the inside since the microwave energy is transferred directly to the molecules (solvent, reagents, catalysts). This process is known as “volumetric core heating” and results in a temperature gradient which is reversed compared to the one resulting from conventional heating.

There is also an ongoing discussion about so called “non-thermal” microwave effects leading to differences in product distributions and yields. They could result from a decrease in activation energy due to orientation effects of polar species in the electromagnetic field. Intensive studies have been carried out

with the goal to prove their existence. However, as recently summarized by Kappe and co-workers, many of the hypothesised non-thermal effects could result from incorrect temperature measurements, since they were not observed when the reaction temperature was monitored using appropriate devices.<sup>21b</sup>

Whereas a large number of publications deals with metal catalyses under microwave irradiation, organocatalytic reactions, which are being summarised here, are still rare.

#### 3.1 Mannich reaction

The Mannich reaction offers an attractive approach towards amino-functionalised carbonyl compounds. Organocatalytic versions were independently introduced by List<sup>22</sup> and Barbas.<sup>23</sup> Although they were able to achieve impressive enantioselectivities with proline as catalyst, two major drawbacks remained: first, the catalyst loading was generally high (10 mol% and more), and second, the overall reaction rate was low resulting in long reaction times.

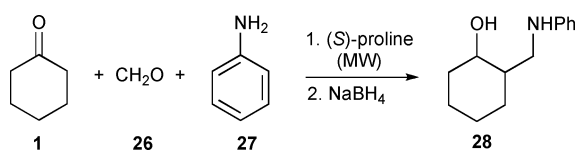
Early experiments illustrating an effect of microwave irradiation on organocatalytic Mannich reactions were included in a paper by Westermann and co-workers.<sup>24</sup> They studied the use of protected dihydroxyacetone (**23**) as three-carbon building block in proline-catalysed Mannich-type reactions with imino ester **24** (scheme in Table 5). The goal was to establish an easy access to azasugars and aminosugar derivatives, which play important roles as glycosidase inhibitors and parts of aminoglycosides. After intensive testing, 2,2,2-trifluoroethanol (TFE) was identified as the solvent of choice giving the product with excellent enantio- and diastereoselectivities in satisfactory yield (Table 5, entry 1). When the catalysis was performed under microwave irradiation the reaction rate increased considerably (entries 2 and 3). Varying the irradiation power had only a minor effect on the stereoselectivity (Table 5, entries 2 and 3).

With the aim of improving the applicability of organocatalytic Mannich reactions, Rodriguez and Bolm investigated the influence of microwave irradiation on enantioselective proline-catalysed  $\alpha$ -aminomethylations of ketones.<sup>25</sup> As a test system, the reaction between cyclohexanone (**1**), formaldehyde (**26**), and aniline (**27**) was chosen.<sup>26</sup> Under common reaction conditions both yield and enantioselectivity were high, but in order to achieve this result, 20 mol% of proline and a reaction time of 30 h were required (Table 6, entry 1). The use of microwave

Table 5 Mannich-type reaction between protected dihydroxyacetone and  $\alpha$ -imino ethyl glyoxylate<sup>24</sup>

Entry	MW/W	t/min	Yield (%)	de (%)	ee (%)
1	— <sup>a</sup>	1200	72	95	99
2	300	10	72	81	94
3	100	10	64	81	95

<sup>a</sup> Carried out at ambient temperature; no microwave irradiation.

**Table 6** Direct asymmetric Mannich reaction catalysed by (*S*)-proline<sup>25</sup>


Entry	Catalyst (mol%)	MW power/W	<i>T</i> /°C	<i>t</i> /h	Yield (%)	ee (%)
1 <sup>a</sup>	20	—	25–30	30	81	98
2 <sup>a</sup>	10	—	45–50	27	85	97
3	10	15	46	2.5	96	98
4	0.5	15	46	3	83	98

<sup>a</sup> Heating by using a conventional oil bath.

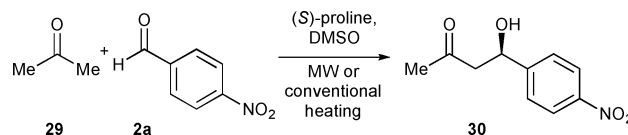
irradiation led to two improvements. First, the reaction time was shortened (to 2–3 h), and second, the catalyst loading could be significantly reduced. Under the optimized reaction conditions (involving MW irradiation with a power of 15 W under simultaneous air-cooling; followed by NaBH<sub>4</sub> reduction of the ketonic intermediate) product **28** was finally obtained with 98% ee in 83% yield after only 3 h reaction time using 0.5 mol% of (*S*)-proline (Table 6, entry 4). Studying this three-component reaction in detail revealed that thermal heating also allowed a reduction of the catalyst loading and that also under those conditions the reaction became faster retaining its high stereoselectivity.

### 3.2 Aldol reaction

List, Barbas and co-workers were the first to report organocatalytic direct aldol reactions between acetone and a variety of aldehydes.<sup>12a</sup> After testing various amino acids, they found that proline was an effective asymmetric catalyst for this synthetically highly useful C–C-bond formation. For many substrate combinations both yield and stereoselectivity reached synthetically useful levels, but the long reaction time remained the major drawback.<sup>12</sup> A solution to that problem was offered by Mossé and Alexakis, who performed organocatalytic direct aldol reactions under microwave irradiation.<sup>27</sup> They investigated the reaction between acetone (**29**) and *p*-nitrobenzaldehyde (**2a**). Product **30** was obtained with 76% ee in 68% yield by List, Barbas and co-workers using 30 mol% of (*S*)-proline in DMSO after a reaction time of 4 h (Table 7, entry 1). As discovered in the Mannich reaction by Rodriguez and Bolm,<sup>25</sup> Mossé and Alexakis found that microwave irradiation increased the reaction rate of this aldol reaction without significantly affecting the yield and the enantioselectivity (Table 7, entry 2). Furthermore, the catalyst loading could be reduced to 20 mol% (Table 7, entry 3). Also, using a pre-heated oil bath led to a shorter reaction time, but in this case both yield and ee were lower (Table 7, entry 4).

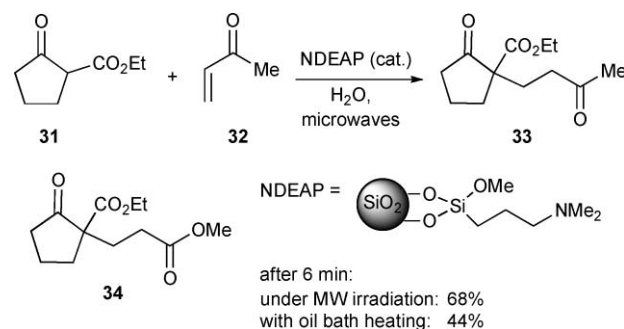
### 3.3 Michael addition

The Michael addition allows the stereocontrolled formation of new carbon–carbon and carbon–heteroatom bonds. Taking into account the observations made in organocatalytic Mannich<sup>25</sup> and aldol reactions,<sup>27</sup> it is not surprising that also Michael additions have been evaluated on their sensitivity

**Table 7** Proline-catalysed aldol reactions<sup>27</sup>


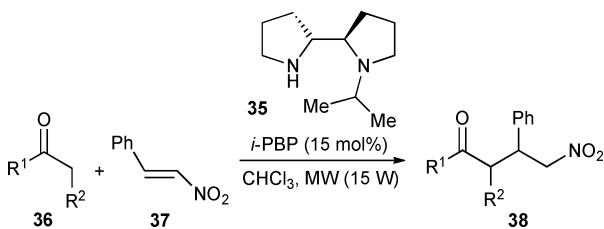
Entry	Catalyst (mol%)	<i>T</i> /°C	MW Power/W	<i>t</i> /min	Yield (%)	ee (%)
1	30	rt	—	240	68	76
2	30	35	15	15	64	72
3	20	35	15	15	69	70
4	30	35	—	15	42	62

towards microwave irradiation. In this context, Hagiwara and co-workers reported on the reactivity of 1,3-dicarbonyl compounds in water using ethyl 2-oxocyclopentanecarboxylate (**31**) and methyl vinyl ketone (**32**) as test substrates and reusable *N,N*-diethylaminopropylated silica gel (NDEAP) as catalyst (Scheme 4).<sup>28</sup> Due to the low solubility of the organic components in water, a triphasic system resulted and microwave irradiation was applied for internal heating. Under optimized conditions, addition product **33** was obtained in 92% yield after 10 min. Also, other carbonyl compounds reacted well, affording the corresponding Michael addition products with up to 94% yield. The importance of microwave irradiation was illustrated in the reaction between keto ester **31** and methyl acrylate (**9**), which afforded keto diester **34** in 68% yield after only 6 min. Performing the same reaction under analogous conditions in an oil bath (without microwave irradiation) led to **34** in only 44% yield.

**Scheme 4** Michael additions in water catalysed by NDEAP (*N,N*-diethylaminopropylated silica gel).<sup>28</sup>

The effect of microwave irradiation on an enantioselective Michael addition was investigated by Mossé and Alexakis, who studied the use of *N*-*i*-Pr-bipyrrolidine (*i*-PBP, **35**) as organocatalyst.<sup>27,29</sup> In reactions between hydroxyacetone (**36a**) and  $\beta$ -nitrostyrene (**37**) to give nitro ketone **38** they were able to shorten the required reaction time from 168 to 4 h without affecting the enantioselectivity (Table 8, entries 1 and 2). Interestingly, in the reaction with isovaleraldehyde (**36b**) even a slight ee increase was observed, when the reaction was carried out under microwave irradiation (Table 8, entries 3 and 4). Furthermore, the catalyst loading could be reduced from 15 to 5 mol% (Table 8, entry 5).

Kappe and co-workers re-evaluated the asymmetric organocatalyses described above (Mannich, aldol, and Michael

**Table 8** Asymmetric organocatalytic conjugate additions<sup>27,29</sup>


Entry	36/38	R <sup>1</sup> , R <sup>2</sup>	T/°C	t/h	Conv. (%)	Yield (%)	syn/anti	ee (%)
1 <sup>a</sup>	<b>a</b>	Me, OH	rt	168	100	79	17:83	98
2	<b>a</b>	Me, OH	28	4	100	83	11:89	98
3 <sup>a</sup>	<b>b</b>	H, <i>i</i> -Pr	rt	48	100	99	87:13	73
4	<b>b</b>	H, <i>i</i> -Pr	27	1	100	97	90:10	78
5 <sup>b</sup>	<b>b</b>	H, <i>i</i> -Pr	28	5	80	79	88:12	79

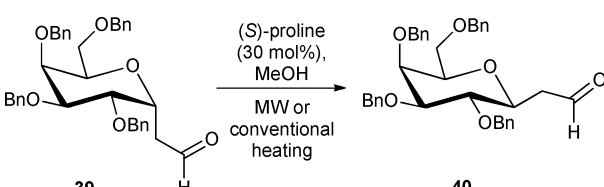
<sup>a</sup> Result obtained without microwave irradiation. <sup>b</sup> Use of 5 mol% of *i*-PBP.

reaction), and their results suggested that all differences found between reactions performed under microwave irradiation and conventional heating could be explained by the more effective energy transfer achievable by the former technique.<sup>30</sup> All proposed non-thermal effects should then be ascribed to incorrect temperature measurements during the reaction.

### 3.4 Anomerisation

Massi, Dondoni and co-workers extended the use of microwave irradiation to the anomerisation of  $\alpha$ -C-glycosylmethyl aldehydes and ketones to the corresponding  $\beta$ -isomers.<sup>31</sup> These C-glycosides are valuable precursors for other complex non-natural molecules such as C-glycopeptides. They found that the proline-catalysed anomerisation process could be significantly accelerated by microwave dielectric heating. Perbenzylated  $\alpha$ -C-galactosylmethyl aldehyde **39** was chosen as model substrate with a catalyst loading of 30 mol% and methanol as the solvent. Under conventional conditions the reaction was initiated at 0 °C and after 1 h warmed to 30 °C. Stirring at that temperature was continued for 24 h leading to C-glycoside **40** with a  $\beta$  :  $\alpha$ -ratio of 19 : 1 in 95% yield (Table 9, entry 1).

Performing the anomerisation under microwave irradiation shortened the reaction time, and complete conversion was achieved after 1 h without loss in yield and selectivity. The

**Table 9** Anomerisation of an  $\alpha$ -C-galactosylmethyl aldehyde<sup>31</sup>


Entry	MW power/W	Temp/°C	Time/h	$\beta$ : $\alpha$ ratio	Yield (%)
1	—	30	24	19:1	95
2	13	50	1	19:1	95
3	—	61	1	18:1	95

optimal reaction temperature was about 50 °C and involved external cooling (Table 9, entry 2). Being alerted by previous work,<sup>25,27,30</sup> the experiments were repeated in a conventional oil bath at elevated temperatures (Table 9, entry 3). Since almost identical results as under microwave irradiation were achieved in terms of both yield and  $\alpha$  :  $\beta$ -ratio the occurrence of non-thermal microwave effects was excluded.

### 3.5 Baylis–Hillman Reaction

The cheap and readily available starting materials, the simple reaction conditions, and the possibility to render the reaction asymmetric are just a few of the interesting features of the Baylis–Hillman reaction that have recently led to an exponential increase in synthetic studies of this reaction.<sup>16</sup> Despite all efforts, one major drawback remained: it is a rather slow C–C-bond formation, which often requires weeks to achieve complete conversion. Microwave irradiation was expected to have a positive effect on the reaction.

As early as 1994, Bhat and co-workers reported a significant rate acceleration upon microwave irradiation, shortening the reaction times in the formation of allylic alcohols **10** and **42** from days to minutes.<sup>32</sup> Selected results are summarized in Table 10.

Subsequently, Vasconcellos and co-workers studied the reaction between aromatic aldehydes such as *p*-nitrobenzaldehyde (**2a**) and methyl acrylate (**9**) using DMAP (10 mol%) as catalyst.<sup>33</sup> They found a significant rate acceleration when the reaction was carried out at elevated temperatures (Table 11, entries 1 and 2), and a further rate increase was achieved, when microwave irradiation was applied (entry 3).

### 3.6 Diels–Alder Reaction

The Diels–Alder reaction is one of the most fundamental and useful synthetic processes in organic chemistry. High regio- and stereoselectivities can be achieved. Focusing on organocatalytic versions Mossé and Alexakis investigated the microwave assisted reaction of cyclopentadiene (**44**) and cinnamaldehyde (**45**) to give products **46** and **47** catalysed by MacMillan's



**Table 10** Microwave supported Baylis–Hillman reaction<sup>32</sup>

Entry	Ar	X	Method <sup>a</sup>	t	Yield (%)
1	C <sub>6</sub> H <sub>5</sub>	COOCH <sub>3</sub> ( <b>9</b> , <b>10</b> )	A	2 d	25
2	C <sub>6</sub> H <sub>5</sub>	COOCH <sub>3</sub> ( <b>9</b> , <b>10</b> )	B	10 min	34
3	2-HOC <sub>6</sub> H <sub>4</sub>	COOCH <sub>3</sub> ( <b>9</b> , <b>10</b> )	A	3 d	10
4	2-HOC <sub>6</sub> H <sub>4</sub>	COOCH <sub>3</sub> ( <b>9</b> , <b>10</b> )	B	10 min	70
5	4-NO <sub>2</sub> C <sub>6</sub> H <sub>4</sub>	CN ( <b>41</b> , <b>42</b> )	A	3 d	45
6	4-NO <sub>2</sub> C <sub>6</sub> H <sub>4</sub>	CN ( <b>41</b> , <b>42</b> )	B	10 min	95

<sup>a</sup> Method A: Common (room temperature) reaction conditions; Method B: Performed under microwave irradiation.

**Table 11** DMAP in the Baylis–Hillman reaction<sup>33</sup>

Entry	T/°C	t	Yield (%)
1	25	4 days	72
2	76	5 h	>99
3	MW irradiation	15 min	93

**Table 12** Asymmetric Diels–Alder Reaction<sup>27</sup>

Entry	T/°C	MW Power (W)	t/h	Yield (%)	exo : endo	ee (%) exo
1 <sup>a</sup>	23	—	21	99	1.3 : 1	93
2	90	70	0.5	79	1.2 : 1	50
3	65	50	1	82	1.2 : 1	78
4 <sup>b</sup>	65	—	1	75	1.5 : 1	85

<sup>a</sup> Result obtained without microwave irradiation by MacMillan and co-workers. <sup>b</sup> Experiment was performed in a conventional preheated oil bath using a sealed tube. <sup>c</sup> In all cases the *endo* isomer had identical ees.

imidazolium salt **43**.<sup>27</sup> A microwave power of 50 W was found to be the best compromise in terms of reactivity and selectivity. Although the enantioselectivity decreased (Table 12, entries 2 and 3) compared to the room temperature reaction (entry 1),<sup>34</sup> a significant rate acceleration was observed. Performing the

cycloaddition in an oil bath at the same temperature (using a sealed tube) led to a slightly lower yield but a higher ee (entry 4). Those data were interpreted as indication for the absence of specific microwave effects.

## 4. Organocatalytic reactions under ultrasound irradiation

Besides ball milling and microwave heating ultrasound irradiation has emerged as a powerful technique for the promotion of organic reactions.<sup>35</sup> In order to affect chemical reactivity in liquids (conventional power ultrasound) its frequency range has to lie between microwaves and diagnostic ultrasound. The activation is caused by cavitation, which involves the creation, growth and collapse of micrometre-sized bubbles, that are formed when an acoustic pressure wave propagates through a liquid. According to the so-called “hot spot theory”, extreme local conditions occur inside the cavitating bubbles and their interfaces when they collapse. These have been estimated to be in the range of 4900–5200 K<sup>36</sup> and 1700 atm.<sup>35</sup> The interactions of acoustic waves with chemical systems lead to an energy transfer that can result in enhanced mechanical effects in heterogeneous processes and induced new reactivities.

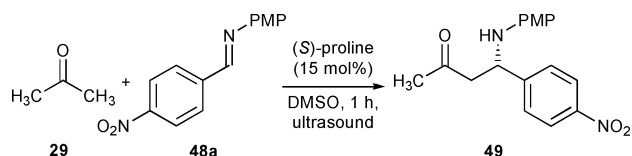
In most cases, the application of ultrasound does not affect the chemical pathways. The reaction rates are often comparable to those of non-irradiated systems and the only role of ultrasound is then to mix the phases of a heterogeneous system. Thus, the increased yields and reaction rates are due to mechanical effects associated with the sound waves. Chemical effects of ultrasound (true sonochemistry) can only be expected if high-energy species, that are released after cavitation collapse, act as reaction intermediates. In these cases, changes in product distribution, switching of reaction mechanisms or changes in regio- or diastereoselectivity may occur.<sup>37</sup>

Since the effects of ultrasound irradiation are similar to those created by ball-milling or microwave, it is not surprising that this technique has been applied to the same families of reactions. Thus, the examples for ultrasound-promoted reactions include Boc-protections of amines,<sup>38</sup> Baylis–Hillman reactions,<sup>33,39</sup> and organocatalytic Mannich reactions.<sup>40</sup> The latter shall be discussed in more detail here.

### 4.1 Mannich reaction

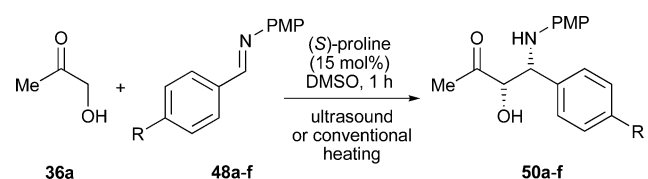
Inspired by the developments in microwave-assisted Mannich reactions, that allowed these important C–C-bond formations to be performed with good yields and selectivities in short reaction times (section 3.1), Choudary and co-workers studied the effect of ultrasound irradiation on two- and three-component Mannich reactions.<sup>40</sup> A pronounced acceleration was found in the proline-catalysed Mannich reaction between acetone (**29**) and preformed imine **48a** in a 4 : 1 mixture of DMSO–acetone affording Mannich product **49** in 50% yield after only 1 h (Scheme 5). In contrast, 24 h of reaction time were required to give the same yield of **49** when the reaction was performed under common reaction conditions without ultrasound irradiation.

When hydroxyacetone (**36a**) was employed as ketonic donor in the reaction with **48a**, Mannich product **50a** was obtained with >99% ee in remarkable 98% yield (Table 13, entry 1).



**Scheme 5** Mannich reaction performed under ultrasound irradiation.<sup>40</sup>

**Table 13** Proline-catalysed Mannich reaction under ultrasonic and conventional heating conditions<sup>40</sup>



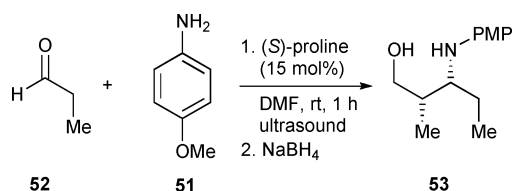
Entry	48/50	R	Method <sup>a</sup>	Yield (%)	syn/anti	ee (%)
1	<b>a</b>	NO <sub>2</sub>	A	98	94 : 6	>99
2	<b>b</b>	CN	A	98	96 : 4	99
3	<b>c</b>	Br	A	96	94 : 6	98
4	<b>d</b>	H	A	94	90 : 10	98
5	<b>d</b>	H	B	93	90 : 10	93
6	<b>e</b>	Me	A	90	85 : 15	98
7	<b>e</b>	Me	B	86	85 : 15	85
8	<b>f</b>	OMe	A	91	75 : 25	81
9	<b>f</b>	OMe	B	85	75 : 25	65

<sup>a</sup> Method A: Performed under ultrasound irradiation; Method B: Common (conventional heating) reaction conditions.

Also other electron-poor aromatic imines reacted well with **36a** leading to Mannich products **50b,c** with both high yields and excellent stereoselectivities (Table 13, entries 2 and 3). Most interestingly, in reactions of electron-rich imines **48e** and **48f** the corresponding Mannich products **50e** and **50f** were formed with significantly better selectivities and in higher yields than under conventional heating conditions (compare method A vs. B, Table 13, entries 6–9). Overall, these promoting effects by ultrasound irradiation were assumed to be due to the extreme conditions (high pressure, rapid heating and rapid cooling) that occurred during the cavitation process.

Ultrasonic conditions were also applied to three-component Mannich reactions. In most cases they delivered the corresponding Mannich products **50** with satisfying diastereo- and enantioselectivities in good yields (Table 14).

Finally, the self-Mannich reaction between propanal (**52**) and *p*-anisidine (**51**) was studied under ultrasonic conditions (Scheme 6). After only 1 h the formation of a single product was observed, and its subsequent NaBH<sub>4</sub> reduction led to amino alcohol **53** with 91% ee in 80% yield.



**Scheme 6** Self-Mannich reaction under ultrasound irradiation.<sup>40</sup>

**Table 14** Proline-catalysed three-component Mannich reactions under ultrasonic irradiation<sup>40</sup>

Entry	2/50	R	Yield (%)	syn/anti	ee (%)
1	<b>a</b>	NO <sub>2</sub>	98	94 : 6	99
2	<b>f</b>	CN	98	96 : 4	98
3	<b>g</b>	Br	94	94 : 6	96
4	<b>h</b>	H	90	90 : 10	85
5	<b>i</b>	OMe	85	75 : 25	66

## 5. Conclusions

The aforementioned examples show that ball milling, microwave heating and ultrasonic irradiation are useful tools for promoting organocatalytic reactions. In many cases their application allows reduction of the amounts of reagents (in particular solvents) and shorter reaction times, leading to a more efficient use of starting materials and energy.<sup>41,42</sup>

All three techniques have in common that they affect chemical processes requiring enhanced heat transfer and mass transport. Consequently, heterogenous reactions can particularly benefit from their application.

For several reactions discussed in this article (*e.g.* aldol, Mannich, Baylis–Hillman reaction), positive effects on the reaction outcome have been observed by applying more than one of those techniques. For example, all three of them were demonstrated to reduce the reaction time of the Baylis–Hillman reaction between methyl acrylate (**9**) and *p*-nitrobenzaldehyde (**2a**) under either DABCO or DMAP catalysis from days to a few minutes (microwave,<sup>33</sup> ball milling<sup>47</sup>) or hours (ultrasound<sup>33</sup>) affording the desired product in excellent yield. Unfortunately, a strict comparison of an asymmetric organocatalytic transformation using the same starting materials under ball milling, microwave and ultrasound conditions is still lacking.<sup>43</sup> Even more options become possible by combining the techniques as recently shown for the conjunction of ultrasound and microwave irradiation (in either simultaneous or tandem mode).<sup>35b</sup>

The modifications of the reaction conditions by the altered energy input upon applying ball milling, microwave heating and ultrasonic irradiation lead to highly complex physico-chemical phenomena, which on the molecular level are still far from being completely understood. With a deeper mechanistic knowledge, however, significant progress can be foreseen and, in particular, organocatalytic reactions will benefit from further studies rendering the entire field even more synthetically attractive.

## Acknowledgements

This work was supported by the Deutsche Forschungsgemeinschaft (DFG, SPP 1179) and the Fonds der Chemischen Industrie.

## Notes and references

- (a) For overviews on green and sustainable chemistry, see: *Green Chemistry: Theory and Practice*, ed. P. T. Anastas and J. C. Warner, Oxford University Press, Oxford, 1998; (b) *Handbook of Green Chemistry and Technology*, ed. J. Clark and D. Macquarrie, Blackwell Science, Oxford, 2002; (c) J. H. Clark, *Green Chem.*, 2006, **8**, 17–21.
- (a) Reviews: G. Kaupp, M. R. Naimi-Jamal, H. Ren and H. Zoz, in *Advanced Technologies Based on Self-Propagating and Mechanochemical Reactions for Environmental Protection*, ed. G. F. Cao, Delogu and R. Orrù, Research Signpost, Kerala, 2003, pp. 83–100; (b) E. Gaffet, F. Bernard, J.-C. Niepce, F. Charlot, C. Gras, G. Le Caër, J.-L. Guichard, P. Delcroix, A. Mocellin and O. Tillement, *J. Mater. Chem.*, 1999, **9**, 305–314; (c) S. V. Kipp, Sepelak and K. D. Becker, *Chem. Unserer Zeit*, 2005, **39**, 384–392.
- For an overview on solvent-free organic reactions, see: (a) G. W. V. Cave, C. L. Raston and J. L. Scott, *Chem. Commun.*, 2001, 2159–2169; (b) K. Tanaka, *Solvent-Free Organic Synthesis*, Wiley-VCH, Weinheim, 2003; (c) P. J. Walsh, H. Li and C. A. de Parrodi, *Chem. Rev.*, 2007, **107**, 2503–2545.
- B. Rodríguez, A. Bruckmann, T. Rantanen and C. Bolm, *Adv. Synth. Catal.*, 2007, **349**, 2213–2233.
- G. Kaupp, *CrystEngComm*, 2006, **8**, 794–804.
- K. Komatsu, *Top. Curr. Chem.*, 2005, **254**, 185–206.
- (a) A. L. Garay, A. Pichon and S. L. James, *Chem. Soc. Rev.*, 2007, **36**, 846–855; (b) J. M. Harrowfield, R. J. Hart and C. R. Whitaker, *Aust. J. Chem.*, 2001, **54**, 423–425.
- For organic solid-state synthesis, see: (a) G. Kaupp, J. Schmeyers and J. Boy, *Chemosphere*, 2001, **43**, 55–61; (b) G. Rothenberg, A. P. Downie, C. L. Raston, C. L. Raston and J. L. Scott, *J. Am. Chem. Soc.*, 2001, **123**, 8701–8708; (c) G. Kaupp, *CrystEngComm*, 2003, **5**, 117–133; (d) F. Toda, *Acc. Chem. Res.*, 1995, **28**, 480–486.
- For an overview on organic solid-state reactions mostly with application of a ball mill, see: G. Kaupp, *Top. Curr. Chem.*, 2005, **254**, 95–183.
- (a) In 1984, Heinicke defined the concept of mechanochemistry as follows: “Mechanochemistry is the branch of chemistry, which studies the solid-state physical and chemical transformations, which are induced by the application of mechanical influence”. G. Heinicke, *Tribochemistry*, Akademie Verlag, Berlin, 1984. For selected reviews on mechanochemistry, see: (b) J. F. Fernandez-Bertran, *Pure Appl. Chem.*, 1999, **71**, 581–586; (c) V. V. Boldyrev and K. Tkáčová, *J. Mater. Synth. Process.*, 2000, **8**, 121–132; (d) M. K. Beyer and H. Clausen-Schaumann, *Chem. Rev.*, 2005, **105**, 2921–2948.
- (a) F. K. Urakaev and V. V. Boldyrev, *Powder Technol.*, 2000, **107**, 93–107; (b) F. K. Urakaev and V. V. Boldyrev, *Powder Technology*, 2000, **107**, 197–206; (c) for a qualitative summary of this model, see ref. 2c.
- For some selected examples, see: (a) B. List, R. A. Lerner and C. F. Barbas III, *J. Am. Chem. Soc.*, 2000, **122**, 2395–2396; (b) P. M. Pihko, K. M. Laurikainen, A. Usano, A. I. Nyberg and J. A. Kaavi, *Tetrahedron*, 2006, **62**, 317–328; (c) Review: G. Guillena, C. Nájera and D. J. Ramón, *Tetrahedron: Asymmetry*, 2007, **18**, 2249–2293.
- (a) B. Rodríguez, T. Rantanen and C. Bolm, *Angew. Chem., Int. Ed.*, 2006, **45**, 6924–6926; B. Rodríguez, T. Rantanen and C. Bolm, *Angew. Chem.*, 2006, **118**, 7078–7080; (b) B. Rodríguez, A. Bruckmann and C. Bolm, *Chem.–Eur. J.*, 2007, **13**, 4710–4722; (c) T. Rantanen, I. Schiffrers and C. Bolm, *Org. Process Res. Dev.*, 2007, **11**, 592–597.
- (a) Y. Sekiguchi, A. Sasaoka, A. Shimomoto, S. Fujioka and H. Kotsuki, *Synlett*, 2003, 1655–1658; (b) Z. Tang, Z.-H. Yang, X.-H. Chen, L.-F. Cun, A.-Q. Mi, Y.-Z. Jiang and L.-Z. Gong, *J. Am. Chem. Soc.*, 2005, **127**, 9285–9289; (c) Y. Hayashi, T. Sumiya, J. Takahashi, H. Gotoh, T. Urushima and M. Shoji, *Angew. Chem., Int. Ed.*, 2006, **45**, 958–961; Y. Hayashi, T. Sumiya, J. Takahashi, H. Gotoh, T. Urushima and M. Shoji, *Angew. Chem.*, 2006, **118**, 972–975; (d) M. Jiang, S.-F. Zhu, Y. Yang, L.-Z. Gong, X.-G. Zhou and Q.-L. Zhou, *Tetrahedron: Asymmetry*, 2006, **17**, 384–387; (e) Y. Hayashi, S. Aratake, T. Itoh, T. Okana, T. Sumiya and M. Shoji, *Chem. Commun.*, 2007, 957–959.
- (a) G. Guillena, M. del Carmen Hita, C. Nájera and S. F. Vióquez, *Tetrahedron: Asymmetry*, 2007, **18**, 2300–2304; (b) G. Guillena, M. del Carmen Hita, C. Nájera and S. F. Vióquez, *J. Org. Chem.*, 2008, **73**, 5933–5943.
- For recent overviews on the Baylis–Hillman reaction, see: (a) D. Basavaiah, A. J. Rao and T. Satyanarayana, *Chem. Rev.*, 2003, **103**, 811–891; (b) D. Basavaiah, K. V. Rao and R. J. Reddy, *Chem. Soc. Rev.*, 2007, **36**, 1581–1588; (c) G. Masson, C. Housseman and J. Zhu, *Angew. Chem., Int. Ed.*, 2007, **46**, 4614–4628; G. Masson, C. Housseman and J. Zhu, *Angew. Chem.*, 2007, **119**, 4698–4712.
- J. Mack and M. Shumba, *Green Chem.*, 2007, **9**, 328–330.
- R. Galeazzi, G. Martelli, G. Mobbili, M. Orena and S. Rinaldi, *Org. Lett.*, 2004, **6**, 2571–2574.
- S. A. Sikchi and P. G. Hultin, *J. Org. Chem.*, 2006, **71**, 5888–5891.
- R. Gedye, F. Smith, K. Westaway, H. Ali, L. Baldisera, L. Laberge and J. R. Rousell, *Tetrahedron Lett.*, 1986, **27**, 279–282.
- For recent reviews and more detailed descriptions see: (a) C. O. Kappe, *Angew. Chem., Int. Ed.*, 2004, **43**, 6250–6284, (*Angew. Chem.*, 2004, **116**, 6408–6443); (b) M. A. Herrero, J. M. Kresmer and C. O. Kappe, *J. Org. Chem.*, 2008, **73**, 36–47; (c) M. A. Herrero, J. M. Kresmer and C. O. Kappe, *Microwaves in Organic Synthesis*, ed. A. Loupy, Wiley-VCH, Weinheim, 2nd edn, 2006; (d) L. Perreux and A. Loupy, *Tetrahedron*, 2001, **57**, 9199–9223; (e) T. Razzaq, J. M. Kresmer and C. O. Kappe, *J. Org. Chem.*, 2008, **73**, 6321–6329; (f) C. O. Kappe and A. Stadler, *Microwaves in Organic and Medicinal Chemistry*, Wiley-VCH, Weinheim, 2005; (g) P. Lidström, J. Tierny, B. Wathey and J. Westman, *Tetrahedron*, 2001, **57**, 9225–9283 and references therein.
- (a) B. List, *J. Am. Chem. Soc.*, 2000, **122**, 9336–9337; (b) B. List, P. Pojarliev, W. T. Biller and H. J. Martin, *J. Am. Chem. Soc.*, 2002, **124**, 827–833.
- (a) W. Notz, K. Sakthivel, T. Bui, G. Zhong and C. F. Barbas III, *Tetrahedron Lett.*, 2001, **42**, 199–201; (b) A. Córdova, W. Notz, G. Zhong, J. M. Betancort and C. F. Barbas III, *J. Am. Chem. Soc.*, 2002, **124**, 1842–1843; (c) W. Notz, S.-I. Watanabe, N. S. Chowdari, G. Zhong, J. M. Betancort, F. Tanaka and C. F. Barbas III, *Adv. Synth. Catal.*, 2004, **346**, 1131–1140.
- B. Westermann and C. Neuhaus, *Angew. Chem., Int. Ed.*, 2005, **44**, 4077–4079, (*Angew. Chem.*, 2005, **117**, 4145–4147).
- B. Rodríguez and C. Bolm, *J. Org. Chem.*, 2006, **71**, 2888–2891.
- For reactions of this type performed without microwave irradiation, see: (a) I. Ibrahim, J. Casas and A. Córdova, *Angew. Chem., Int. Ed.*, 2004, **43**, 6528–6531; I. Ibrahim, J. Casas and A. Córdova, *Angew. Chem.*, 2004, **116**, 6690–6693; (b) I. Ibrahim, W. Zou, J. Casas, H. Sudén and A. Córdova, *Tetrahedron*, 2006, **62**, 357–364.
- S. Mossé and A. Alexakis, *Org. Lett.*, 2006, **16**, 3577–3580.
- H. Hagiwara, S. Inotsume, M. Fukushima, T. Hoshi and T. Suzuki, *Chem. Lett.*, 2006, **35**, 926–927.
- O. Andrey, A. Alexakis, A. Tomassini and G. Bernardinelli, *Adv. Synth. Catal.*, 2004, **346**, 1147–1168.
- M. Hosseini, N. Stiasni, V. Barbieri and C. O. Kappe, *J. Org. Chem.*, 2007, **72**, 1417–1424.
- (a) A. Massi, A. Nuzzi and A. Dondoni, *J. Org. Chem.*, 2007, **72**, 10279–10282; (b) see also in: A. Massi and A. Dondoni, *Angew. Chem., Int. Ed.*, 2008, **47**, 4638–4660, (*Angew. Chem.*, 2008, **120**, 4716–4739).
- M. K. Kundu, S. B. Mukherjee, N. Balu, R. Padmakumar and S. V. Bhat, *Synlett*, 1994, 444.
- R. Octavio, M. A. de Souza and M. L. A. A. Vasconcellos, *Synth. Commun.*, 2003, **33**, 1383–1389.
- For the pioneering findings, see: (a) K. A. Ahrendt, C. J. Borths and D. W. C. MacMillan, *J. Am. Chem. Soc.*, 2000, **122**, 4243–4244; (b) W. S. Jen, J. J. M. Wiener and D. W. C. MacMillan, *J. Am. Chem. Soc.*, 2000, **122**, 9874–9875; (c) A. B. Northrup and D. W. C. MacMillan, *J. Am. Chem. Soc.*, 2002, **124**, 2458–2460.
- For reviews see: (a) G. Cravotto and P. Cintas, *Chem. Soc. Rev.*, 2006, **35**, 180–196; (b) G. Cravotto and P. Cintas, *Chem.–Eur. J.*, 2007, **13**, 1902–1909; (c) C. Einhorn, J. Einhorn and J.-L. Luche, *Synthesis*, 1989, 787–813; (d) J. L. Luche, C. Einhorn, J. Einhorn and J. V. Sinisterra-Gago, *Tetrahedron Lett.*, 1990, **31**, 4125–4128; (e) C. Einhorn, J. Einhorn, M. J. Dickens and J. L. Luche, *Tetrahedron Lett.*, 1990, **31**, 4129–4230.
- E. B. Flint and K. S. Suslick, *Science*, 1991, **253**, 1397–1399.
- For a discussion of some examples, in which “true sonochemical activation” occurs, see ref. 35a.
- J. Einhorn, C. Einhorn and J.-L. Luche, *Synlett*, 1991, 37–38.
- (a) W. P. Almeida and F. Coelho, *Tetrahedron Lett.*, 2003, **44**, 937–940; (b) F. G. Coelho, C. A. Diaz, M. Abella and W. P. Almeida, *Synlett*, 2006, 435–439.

- 
- 40 M. L. Kantam, C. V. Rajasekhar, G. Gopikrishna, K. R. Reddy and B. M. Choudary, *Tetrahedron Lett.*, 2006, **47**, 5965–5967.
- 41 Recently, a very detailed study of solvent-free Knoevenagel condensations was reported. The authors also compared the effect of ball milling and microwave irradiation. With respect to the required energy input the former technique was by far superior to the latter. For details, see: R. Trotzki, M. M. Hoffmann and B. Ondruschka, *Green Chem.*, 2008, **10**, 767–772.
- 42 A critical analysis of those issues would also have to include aspects such as solvent amount (and energy input) for product extraction, vessel cleaning, product purification by crystallization and/or chromatography *etc.* To the best of our knowledge, a comprehensive analysis of this type has yet not been reported for organocatalytic reactions.
- 43 For the application of all three techniques in Heck reactions, see: F. Alonso, I. P. Beletskaya and M. Yus, *Tetrahedron*, 2005, **61**, 11771–11835.



# Switching the basicity of ionic liquids by CO<sub>2</sub>†

Wenjing Li, Zhaofu Zhang, Buxing Han,\* Suqin Hu, Jinliang Song, Ye Xie and Xiaosi Zhou

Received 8th July 2008, Accepted 4th September 2008

First published as an Advance Article on the web 22nd September 2008

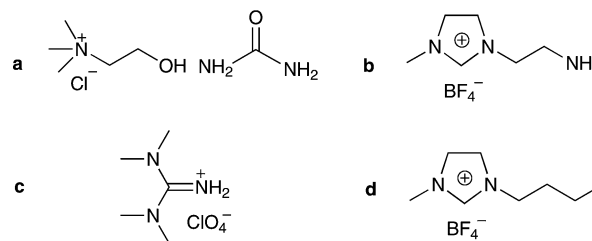
DOI: 10.1039/b811624e

The basicity of several basic ionic liquids is studied quantitatively for the first time, and the basicity of the ionic liquids can be switched repeatedly by bubbling CO<sub>2</sub> and N<sub>2</sub> through the solution alternately.

Ionic liquids (ILs) have some unusual properties, such as extremely low vapor pressure, wide liquid temperature range, high thermal and chemical stability, and ability to dissolve a wide range of organic and inorganic chemical compounds.<sup>1,2</sup> Moreover, ILs can be functionalized by designing different cations and anions. Researchers have developed large amounts of functional ILs for particular applications.<sup>3–5</sup> For example, acidic ILs have been proven to be efficient catalysts for many acid-catalysed organic reactions.<sup>6,7</sup> Basic ILs with amino groups were synthesized and used to capture CO<sub>2</sub>,<sup>8,9</sup> and H<sub>2</sub>S<sup>10</sup>, and to promote hydrogenation of CO<sub>2</sub>.<sup>11</sup> 1,1,3,3-tetramethylguanidine-based ILs have been found to be very effective to aldol reaction and absorb SO<sub>2</sub> from mixed gases.<sup>12–14</sup> Some basic ILs containing biodegradable components, including ILs derived from natural amino acids<sup>15–17</sup> and a deep eutectic mixture of choline chloride and urea,<sup>18</sup> have aroused increasing research interest and found promising application in different fields, such as separation,<sup>19</sup> catalysis<sup>20</sup> and material synthesis.<sup>21</sup>

Acidic or basic ILs represent new classes of acids or bases. The study of the properties of these ILs is of great importance from both fundamental and practical points of view. Thomazeau *et al.* characterized the Hammett acidity scale for Brønsted acid in non-chloroaluminate ILs.<sup>22</sup> Yang and Kou studied the Lewis acidity of ILs consisting of imidazolium chloride and metal chloride by monitoring the IR spectra of probes.<sup>23</sup> However, to the best of our knowledge, study of the basicity of ILs has not been reported.

Determining and tuning the basicity of ILs is a new and interesting topic because the efficiency of many processes depends on the basicity of the media or can be controlled by the basicity of the media. Moreover, considering the wide application of ILs, reversible tuning of the basicity of ILs would be more interesting and offer great advantages in applications. As an environmentally benign gas, CO<sub>2</sub> has been used to develop switchable nonpolar-to-polar solvents,<sup>24,25</sup> gelators<sup>26</sup> and surfactants.<sup>27</sup> In this work, we first studied the basicity of some amino-contained ILs (Scheme 1), choline chloride/urea (1 : 2 molar ratio, CH/urea), 1-aminoethyl-3-methyl imidazolium tetrafluoroborate-



**Scheme 1** Structure of the ILs investigated in this work. (a) CH/urea, (b) [AEMIM][BF<sub>4</sub>], (c) [TMG][ClO<sub>4</sub>], (d) [BMIM][BF<sub>4</sub>].

rate ([AEMIM][BF<sub>4</sub>]), and 1,1,3,3-tetramethylguanidinium perchlorate ([TMG][ClO<sub>4</sub>]). The basicity is evaluated by the Hammett function. The Hammett function of the commonly used IL, 1-butyl-3-methylimidazolium tetrafluoroborate ([BMIM][BF<sub>4</sub>]) was also determined for comparison. Then, we proposed a method to tune the basicity of the ILs using CO<sub>2</sub>. It was found that adding CO<sub>2</sub> of ambient pressure to the ILs could reduce the basicity of the ILs significantly, and the basicity of the ILs was readily recovered after removing CO<sub>2</sub> by bubbling N<sub>2</sub> through the solutions. This novel, simple, green and reversible method to tune the basicity of ILs has potential application in different fields.

The Hammett function was proposed by Hammett and Deyrup in the early 1930s to evaluate the acidity and basicity outside the pH range in water and the acidity in nonaqueous solvents by determining the ionization ratio of indicators in a solution.<sup>28,29</sup> For a basic solution, the Hammett function measures the tendency of the solution to capture protons. When weak acids were chosen as indicators, the Hammett function  $H_-$  is defined by the following equation.

$$H_- = \text{p}K(\text{HI}) + \log\left(\frac{[\text{I}^-]}{[\text{HI}]}\right) \quad (1)$$

where  $\text{p}K(\text{HI})$  is the thermodynamic ionization constant of the indicator in water, [I<sup>-</sup>] and [HI] stand for the molar concentrations of anionic and neutral forms of the indicator, respectively. Clearly, a medium with larger  $H_-$  value has stronger basicity. Usually, an indicator is only applicable to a narrow  $H_-$  range. The commonly used method to study the Hammett function in wide range is to use different indicators because different indicators give approximately the same Hammett value for a solution, especially when using indicators of the same charge type and similar structure.<sup>28–31</sup> In this work we used three indicators, 4-nitrobenzylcyanide, 4-nitrophenol and 2,5-dinitrophenol to determine the basicity of the ILs with and without CO<sub>2</sub> at 25 °C. Their  $\text{p}K(\text{HI})$  values are 13.43,<sup>30</sup> 7.15<sup>32</sup> and 5.15,<sup>33</sup> respectively.

The absorption of the neutral form of the indicators is negligible at the wavelength monitored in this work. Therefore,

Beijing National Laboratory for Molecular Sciences, Institute of Chemistry, Chinese Academy of Sciences, Beijing, 100080, PR China. E-mail: hanbx@iccas.ac.cn; Fax: 86-10-62559373; Tel: 86-10-62562821

† Electronic supplementary information (ESI) available: Preparation of ILs and experimental details. See DOI: 10.1039/b811624e

**Table 1**  $H_-$  values for hydrazine aqueous solution measured in this work and reported in the literature

Hydrazine (wt%)	$H_-$ (measured, $\pm 0.01$ )	$H_-$ (literature)
10	11.55	11.55
15	11.86	11.93
20	12.18	12.29
25	12.62	12.72
30	12.97	13.15

the ratio  $[I^-]/[HI]$  can be known from UV-Vis spectra by applying Beer's law.<sup>22,28–31</sup>

$$[I^-]/[HI] = \varepsilon/(\varepsilon_1^- - \varepsilon) \quad (2)$$

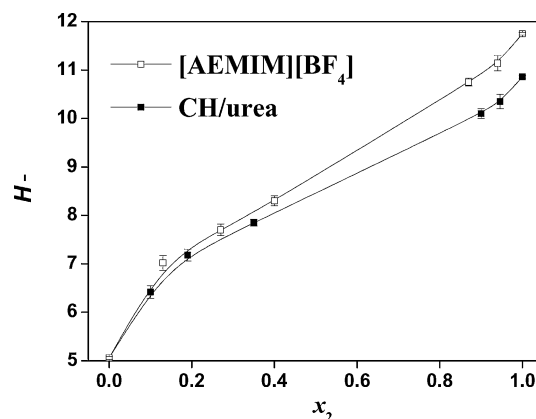
where  $\varepsilon$  is the measured extinction coefficient of the indicator at a given wavelength, and  $\varepsilon_1^-$  represents the extinction coefficient at the same wavelength of the indicator completely in the anionic form. We first determined the  $H_-$  values of hydrazine aqueous solutions of different concentrations to verify the reliability of our experimental method, and the results are presented in Table 1 together with those reported by other authors. It can be observed that the results determined in this work agree well with the literature values.<sup>30</sup>

The basicity of the ILs was determined with 4-nitrobenzylcyanide and 2,5-dinitrophenol. The absorption maximum of the anionic form of was 4-nitrobenzylcyanide at about 540 nm in CH/urea and [AEMIM][BF<sub>4</sub>]. For [TMG][ClO<sub>4</sub>] and [BMIM][BF<sub>4</sub>], 2,5-dinitrophenol was used. Value of  $\varepsilon_1^-$  is necessarily measured in solutions with sufficient high basicities.<sup>28,31</sup> In this work,  $\varepsilon_1^-$  was determined in the mixed solution of the ILs and ethylenediamine (30 wt%) in which the absorption band of the neutral form of the indicator disappeared completely, indicating that the indicator existed entirely in the anionic form in the solution. The  $H_-$  values of the ILs determined are presented in Table 2. CH/urea and [AEMIM][BF<sub>4</sub>] behave as bases and exhibit high  $H_-$  values, while [TMG][ClO<sub>4</sub>] have much lower value similar to that of the neutral IL [BMIM][BF<sub>4</sub>]. It should be noted that the [BF<sub>4</sub>] anion might be hydrolysed in the presence of water, which may have some effect on the  $H_-$  measurements. However, we have found that the  $H_-$  values of ILs remained constant after the dried ILs were preserved for several days. Guanidine and its derivatives are known to be very strong organic bases of the order of strength of potassium hydroxide.<sup>34</sup> Therefore, the neutralization of 1,1,3,3-tetramethylguanidine by the strong perchloric acid leads to a neutral product.

It is known that most ILs are hygroscopic and water could affect the properties of ILs, such as density, viscosity and polarity.<sup>35,36</sup> The ILs used here were dried under vacuum for at

least 24 h at 70 °C prior to use and the water content determined by Karl Fischer titration was less than 100 ppm. To study the effect of the remaining water on the  $H_-$  values of the dried ILs, we measured the  $H_-$  values of ILs with 1 wt% and 3 wt% added water, and the results are also presented in Table 2. It can be seen that water slightly reduces the basicity of CH/urea and [AEMIM][BF<sub>4</sub>], due to the hydrogen bonding between water and amino group. On the other hand, the addition of water results in slight increase of  $H_-$  values in the case of [TMG][ClO<sub>4</sub>] and [BMIM][BF<sub>4</sub>]. The values of  $H_-$  for the IL/water mixtures did not change over three days, indicating that the hydrolysis was negligible under the conditions.

The basicity of mixed ILs was also determined. Fig. 1 shows the  $H_-$  values of binary mixtures of basic ILs and neutral [BMIM][BF<sub>4</sub>] with different concentrations. The three indicators described before were used in a different  $H_-$  range.  $x_2$  represents the mole fraction of the basic ILs, CH/urea and [AEMIM][BF<sub>4</sub>]. As illustrated in Fig. 1, the basicity of the mixtures increases significantly with the increase of  $x_2$ . The change in the basicity is more rapid in the neutral IL-rich region and basic IL-rich region, which is similar to the basic aqueous system.<sup>30</sup>



**Fig. 1** The  $H_-$  values of CH/urea + [BMIM][BF<sub>4</sub>] and [AEMIM][BF<sub>4</sub>] + [BMIM][BF<sub>4</sub>] mixed ILs as a function of the mole fraction of basic ILs  $x_2$ .

It is very interesting to switch the basicity of ILs repeatedly using simple and green method. In this work, we studied the effect of CO<sub>2</sub> on the  $H_-$  values of the ILs. The above data were obtained using 4-nitrobenzylcyanide as the indicator. Our experiments showed that the addition of CO<sub>2</sub> of ambient pressure to [AEMIM][BF<sub>4</sub>] and CH/urea made the bands of the indicator at 540 nm disappear completely. This means that the basicity of the two ILs is reduced significantly after adding CO<sub>2</sub>

**Table 2**  $H_-$  values of the ILs with and without additives at 25 °C

Additives	$H_-$ ( $\pm 0.02$ )			
	CH/urea	[AEMIM][BF <sub>4</sub> ]	[TMG][ClO <sub>4</sub> ]	[BMIM][BF <sub>4</sub> ]
Without additive	10.86 <sup>a</sup>	11.75 <sup>a</sup>	4.35	5.06
1 wt% water	10.77 <sup>a</sup>	11.65 <sup>a</sup>	4.40	5.12
3 wt% water	10.65 <sup>a</sup>	11.49 <sup>a</sup>	4.47	5.20
CO <sub>2</sub> of 1 atm	6.25	4.96	4.35	5.06

<sup>a</sup> The values were determined by 4-nitrobenzylcyanide, the other values were determined by 2,5-dinitrophenol.

and the indicator is not applicable to determine the  $H_-$  values of the ILs in the presence of  $\text{CO}_2$ . Therefore, we use another indicator, 2,5-nitrophenol, which is suitable for lowering  $H_-$  values. The absorbance of the indicator in the corresponding neat ILs was used as the reference absorbance of the total anionic form because only the absorbance of the anionic form can be observed in the neat ILs for the indicator. The  $H_-$  values of the ILs after equilibration under ambient  $\text{CO}_2$  pressure are presented in Table 2. It can be observed that the basicity of [AEMIM][ $\text{BF}_4$ ] and CH/urea decreased significantly after adding  $\text{CO}_2$ . Especially, the  $H_-$  value of [AEMIM][ $\text{BF}_4$ ] after  $\text{CO}_2$  treatment is nearly the same as the neutral [BMIM][ $\text{BF}_4$ ]. This is because that  $\text{CO}_2$  reacts with primary and secondary amines to form ammonium carbamates,<sup>8,25,26</sup> which reduces the basicity. As expected, the effect of  $\text{CO}_2$  on the basicity of [TMG][ $\text{ClO}_4$ ] and [BMIM][ $\text{BF}_4$ ] is negligible, because there is no chemical reaction between the ILs and  $\text{CO}_2$ .

Our experiments showed that the  $H_-$  value of IL samples with absorbed  $\text{CO}_2$  returned to that of the neat ILs after bubbling  $\text{N}_2$  through the solutions. As example, Fig. 2 demonstrates the change of  $H_-$  values of CH/urea by bubbling  $\text{CO}_2$  and  $\text{N}_2$  through the solution over three cycles. Clearly, the basicity of the ILs can be switched repeatedly and reversibly by bubbling  $\text{CO}_2$  and  $\text{N}_2$  alternatively. This is understandable because the  $\text{CO}_2$  absorbed by amino group can be released.<sup>8,26</sup> This novel method to tune the basicity of ILs may find wide application in different fields, such as separation, chemical reactions and smart materials. As an example, we studied the switching of absorbance of 4-nitrophenol in CH/urea. 4-Nitrophenol in CH/urea is bright yellow. It quickly became colourless after was exposed to  $\text{CO}_2$  of ambient pressure for five minutes under stirring. After bubbling  $\text{N}_2$  at  $60^\circ\text{C}$  for thirty minutes, the solution reverted back to its original colour. The photographs of this process are shown in Fig. 3.

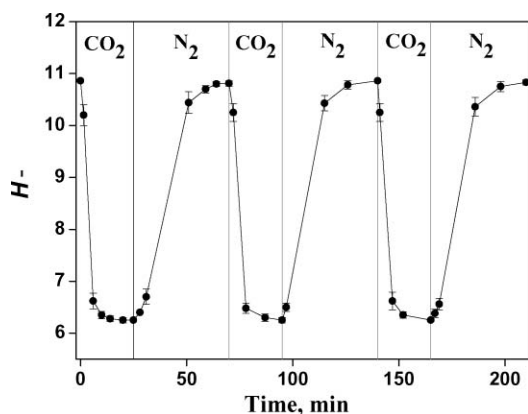


Fig. 2 The  $H_-$  value of CH/urea as a function of time during three cycles of treatment with  $\text{CO}_2$  at  $25^\circ\text{C}$  followed by  $\text{N}_2$  at  $60^\circ\text{C}$ .

In summary, the basicity of several ILs were determined. Most importantly, the basicity of the amino-group containing ILs can be tuned repeatedly and reversibly by bubbling  $\text{CO}_2$  and  $\text{N}_2$  through the solutions alternately. We believe that this novel, simple, green and reversible method to tune the basicity of ILs has potential applications in different fields.

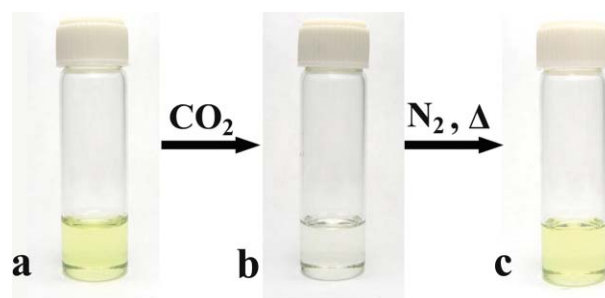


Fig. 3 The color change of 4-nitrophenol in CH/urea. (a) in neat CH/urea, (b) after bubbling  $\text{CO}_2$  for five minutes at  $25^\circ\text{C}$ , (c) after bubbling  $\text{N}_2$  for half an hour at  $60^\circ\text{C}$ . The concentration of the dye is  $5 \times 10^{-5} \text{ mol L}^{-1}$ .

## Acknowledgements

The authors are grateful to the National Natural Science Foundation of China (20533010) and Chinese Academy of Sciences (KJCX2.YW.H16).

## Notes and references

- P. Wasserscheid and T. Welton, *Ionic Liquids in Synthesis*, Wiley-VCH, Weinheim, Germany, 2003.
- R. D. Rogers and K. R. Seddon, *Ionic Liquids: Industrial Applications to Green Chemistry*, ACS, Washington, DC, USA, 2002.
- V. I. Parvulescu and C. Hardacre, *Chem. Rev.*, 2007, **107**, 2615.
- T. L. Greaves and C. J. Drummond, *Chem. Rev.*, 2008, **108**, 206.
- S. G. Lee, *Chem. Commun.*, 2006, 1049.
- Y. L. Gu, J. Zhang, Z. Y. Duan and Y. Q. Deng, *Adv. Synth. Catal.*, 2005, **347**, 512.
- A. C. Cole, J. L. Jensen, I. Ntai, K. L. T. Tran, K. J. Weaver, D. C. Forbes and J. H. Davis, Jr., *J. Am. Chem. Soc.*, 2002, **124**, 5962.
- E. D. Bates, R. D. Mayton, I. Ntai and J. H. Davis, Jr., *J. Am. Chem. Soc.*, 2002, **124**, 926.
- J. M. Zhang, S. J. Zhang, K. Dong, Y. Q. Zhang, Y. Q. Shen and X. M. Lv, *Chem.–Eur. J.*, 2006, **12**, 4021.
- J. H. Davis, Jr., *Green Industrial Applications of Ionic Liquids*, NATO Science Series, vol. 92, ed. R. D. Rogers, K. R. Seddon and S. Volkov, Kluwer Academic Publishers, Dordrecht, 2000.
- Z. F. Zhang, Y. Xie, W. J. Li, S. Q. Hu, J. L. Song, T. Jiang and B. X. Han, *Angew. Chem., Int. Ed.*, 2008, **47**, 1127.
- H. X. Gao, B. X. Han, J. C. Li, T. Jiang, Z. M. Liu, W. Z. Wu, Y. H. Chang and J. C. Zhang, *Synth. Commun.*, 2004, **34**, 3083.
- A. L. Zhu, T. Jiang, B. X. Han, J. C. Zhang, Y. Xie and X. M. Ma, *Green Chem.*, 2007, **9**, 169.
- W. Z. Wu, B. X. Han, H. X. Gao, Z. M. Liu, T. Jiang and J. Huang, *Angew. Chem., Int. Ed.*, 2004, **43**, 2415.
- K. Fukumoto, M. Yoshizawa and H. Ohno, *J. Am. Chem. Soc.*, 2005, **127**, 2398.
- G. H. Tao, L. He, N. Sun and Y. Kou, *Chem. Commun.*, 2005, 3562.
- S. Q. Hu, T. Jiang, Z. F. Zhang, A. L. Zhu, B. X. Han, J. L. Song, Y. Xie and W. J. Li, *Tetrahedron Lett.*, 2007, **48**, 5613.
- A. P. Abbott, G. Capper, D. L. Davies, R. K. Rasheed and V. Tambyrajah, *Chem. Commun.*, 2003, 70.
- A. P. Abbott, G. Capper, D. L. Davies, R. K. Rasheed and P. Shikotra, *Inorg. Chem.*, 2005, **44**, 6497.
- A. L. Zhu, T. Jiang, D. Wang, B. X. Han, L. Liu, J. Huang, J. C. Zhang and D. H. Sun, *Green Chem.*, 2005, **7**, 514.
- E. R. Cooper, C. D. Andrews, P. S. Wheatley, P. B. Wedd, P. Wormald and R. E. Morris, *Nature*, 2004, **430**, 1012.
- A. Thomazeau, H. Olivier-Bourbigou, L. Magna, S. Luts and B. Gilbert, *J. Am. Chem. Soc.*, 2003, **125**, 5264.
- Y. L. Yang and Y. Kou, *Chem. Commun.*, 2004, 226.
- P. G. Jessop, D. J. Heldebrant, X. W. Li, C. A. Eckert and C. L. Liotta, *Nature*, 2005, **436**, 1102.
- T. Yamada, P. J. Lukac, M. George and R. G. Weiss, *Chem. Mater.*, 2007, **19**, 967.
- M. George and R. G. Weiss, *J. Am. Chem. Soc.*, 2001, **123**, 10393.

- 27 Y. X. Liu, P. G. Jessop, M. Cunningham, C. A. Eckert and C. L. Liotta, *Science*, 2006, **313**, 958.
- 28 M. A. Paul and F. A. Long, *Chem. Rev.*, 1957, **57**, 1.
- 29 L. P. Hammett, *Chem. Rev.*, 1935, **16**, 67.
- 30 N. C. Deno, *J. Am. Chem. Soc.*, 1952, **74**, 2039.
- 31 R. J. Gillespie and T. E. Peel, *J. Am. Chem. Soc.*, 1973, **95**, 5173.
- 32 R. G. Bates and G. Schwarzenbach, *Helv. Chim. Acta*, 1955, **38**, 699.
- 33 S. J. Broderius, M. D. Kahl and M. D. Hoglund, *Environ. Toxicol. Chem.*, 1995, **14**, 1591.
- 34 T. C. Davis and R. C. Elderfield, *J. Am. Chem. Soc.*, 1932, **54**, 1499.
- 35 K. R. Seddon, A. Stark and M. J. Torres, *Pure Appl. Chem.*, 2000, **72**, 2275.
- 36 S. N. V. K. Aki, J. F. Brennecke and A. Samanta, *Chem. Commun.*, 2001, 413.



# Comparative assessment of an alternative route to (5-benzylfuran-3-yl)methanol (Elliott's alcohol), a key intermediate for the industrial production of resmethrins†

Goffredo Rosini,<sup>a</sup> Valerio Borzatta,<sup>b</sup> Claudio Paolucci<sup>a</sup> and Paolo Righi<sup>\*a</sup>

Received 29th May 2008, Accepted 28th July 2008

First published as an Advance Article on the web 19th September 2008

DOI: 10.1039/b809088b

Industrial preparation of resmethrin, one of the first members of the pyrethroid family to be introduced, is achieved *via* Elliott's alcohol. Available procedures make use of stoichiometric amounts of pyridine, thionyl chloride, fuming nitric acid and a lot of chlorinated by-products are generated. We present here an alternative route to Elliott's alcohol, based on Baylis–Hillman reaction in aqueous media. A comparative quantitative assessment of the “greenness” was performed, using the freeware package EATOS which takes into account both the mass economy and the environmental impact of the materials involved.

## Introduction

Pyrethroids are synthetic insecticides possessing greater insecticidal potency and enhanced photostability than plant-derived pyrethrins. Thanks to their low mammalian toxicity and biodegradability, they have emerged as a replacement for DDT since the late 1960s. The demand for pyrethroids is increasing, also due to the upgraded agriculture technologies of “emerging countries” such as China.<sup>1</sup> Resmethrin (Fig. 1) was one of the first members of the pyrethroid family to be used. It is commercialized as the mixture of the four stereoisomers, while the most active (1*R*,3*R*)-*trans* stereoisomer is sold under the name bioresmethrin. Bioresmethrin is one of the most effective broad spectrum insecticides currently available. It exhibits a high order of insecticidal activity, which is coupled with its excellent toxicological properties.<sup>2</sup>

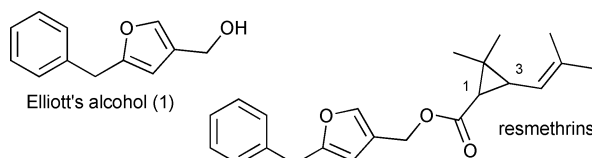
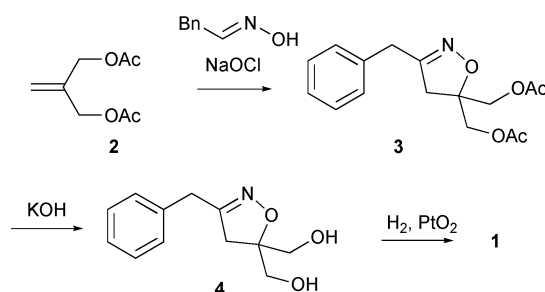


Fig. 1 Elliott's alcohol and resmethrins.

They are both chrysanthemic acid esters of (5-benzylfuran-3-yl)methanol (Elliott alcohol, **1**).<sup>3</sup> Patented methods<sup>4</sup> for the industrial preparation of Elliott's alcohol are demanding and as such hardly exploited in industrial-scale plants. For instance, in one of these methods<sup>5</sup> (5-benzyl-3-furyl)methanol is obtained

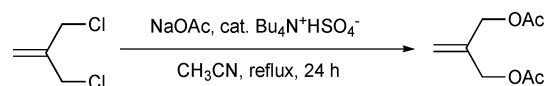
by a sequence of Claisen condensation of benzylcyanide and a dialkylsuccinate, hydrolysis, esterification, protection of the ketone group, formylation, cyclization to 5-benzyl-3-furfuryl ester, and reduction to alcohol with lithium aluminium hydride. The process is particularly laborious, it requires anhydrous solvents and uses lithium aluminium hydride the handling of which requires numerous precautions.

More promising, in terms of “green” efficiency, was the procedure<sup>6</sup> for obtaining **1** (Scheme 1). The key step of this procedure is an extremely atom efficient and regioselective dipolar cycloaddition between an *in situ* generated nitrile oxide and isobutene diacetate (**2**). The cycloadduct is then converted into **1** by a simple saponification/hydrogenolysis/furane ring formation three-step sequence.



Scheme 1 BASF procedure for Elliott's alcohol.

The weak point of this method is the supply of isobutene diacetate (**2**) which is expensive and difficult to find in bulk quantities, or can be prepared by a double nucleophilic displacement from the corresponding dichloride **5** (Scheme 2).



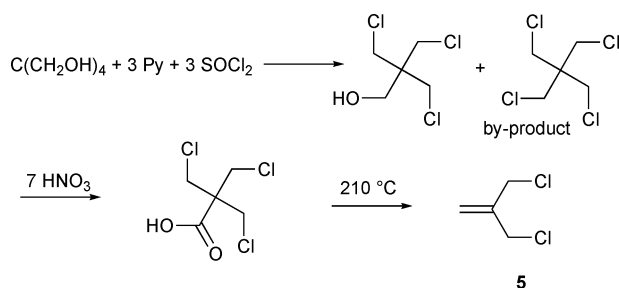
Scheme 2 Preparation of diacetate **2**.

<sup>a</sup>Dipartimento di Chimica Organica “A. Mangini”, Alma Mater Studiorum–Università di Bologna, Viale del Risorgimento, 4, I-40136, Bologna, Italy. E-mail: paolo.righi@unibo.it; Fax: +39 051 20 93630; Tel: +39 051 20 93625

<sup>b</sup>ENDURA SpA, Viale Pietramellara, 5, 40131, Bologna, Italy

† Electronic supplementary information (ESI) available: Details of the comparative quantitative greenness assessment calculations performed with the EATOS tool. See DOI: 10.1039/b809088b

A recent preparation of dichloride **5**,<sup>7</sup> claimed as safer and more convenient, is depicted in Scheme 3.



Scheme 3 Preparation of isobutene dichloride.

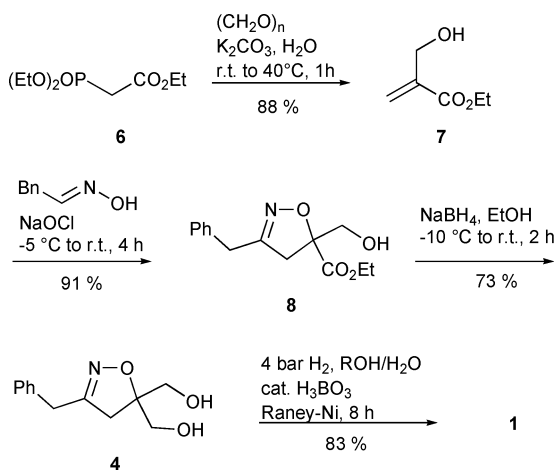
Of course, this preparation poses a heavy burden on the environment. In the first step huge amounts of pyridinium salts and SO<sub>2</sub> are generated along with 20% of an useless tetrachlorinated by-product, which has to be discarded in the following step. The second step is accompanied by a large NO<sub>x</sub> evolution, while the final step releases carbon dioxide and HCl.

## Results and discussion

### An alternative synthesis of Elliott's alcohol

On the outset of this project,<sup>8</sup> we were interested in finding an alternative procedure for obtaining Elliott's alcohol, based on the efficient cycloaddition reaction, but avoiding the use of the isobutene diacetate and all the wastes associated with its preparation (Schemes 3 and 2).

As an alternative building block for the cycloaddition step, we thought of ethyl 2-(hydroxymethyl)acrylate (**7**), which can be easily prepared *via* a known<sup>9</sup> tandem olefination/Baylis–Hillmann sequence (Scheme 4) from commercially available and inexpensive triethyl phosphonoacetate (**6**), paraformaldehyde, potassium carbonate as the base, in water at 40 °C for 1 h.<sup>10</sup>



Scheme 4 Alternative route to Elliott's alcohol.

Though structurally similar to diester **2**, dienophile **7** is electron-poor while **2** is electron-rich. So, choosing **7** as the new starting material posed at least three questions: (i) would **7** react at all, in the cycloaddition step? (ii) would this reaction

regiospecifically afford the desired isomer? and (iii) can the new cycloadduct be converted into Elliott's alcohol?

We were glad to find that by treating **7** with phenylacetaldehyde aldoxime and 10% NaOCl the desired cycloadduct **8** is regiospecifically obtained in high yield (Scheme 4). After the extractive work-up the product is obtained pure enough to be used in the next step without any further purification.

With this result in hand, the attention was shifted to find an effective reduction of the carboxylate moiety to obtain the bishydroxyl derivative **4**, the intermediate that is in common with the procedure depicted in Scheme 1. The reduction does not need problematic aluminium hydride reagents, and can be performed, in good yields, with easier-to-handle granular sodium borohydride in lower alcohols. Finally, the conversion of **8** into Elliott's alcohol can be carried out according to the original procedure<sup>6</sup> or by hydrogenation in lower alcohols/water solution in the presence of Raney nickel and orthoboric acid.<sup>11</sup>

Summarizing, an alternative route to Elliott's alcohol (**1**) was found. The new procedure makes use of 2-(hydroxymethyl)acrylic acid esters, such as **7**, as the new starting materials. On the “green” side, the choice of this alternative starting material, allows us to keep the atom economic efficient cycloaddition step of the existing procedure, while producing a great reduction of steps, waste amount, and waste toxicity and hazards. In fact, the existing synthetic sequence (Schemes 3 and 2) is now replaced by one step only: the first step depicted in Scheme 4. Thus, the wastes associated with the existing methodology (3 SO<sub>2</sub>, 3 pyridium salts, the tetrachlorinated by-product, 7 NO<sub>x</sub>, CO<sub>2</sub>, HCl) are now replaced by the wastes associated with the first step of Scheme 4 (excess CH<sub>2</sub>O and phosphate salts).

However we felt that this kind of “qualitative” greenness assessment, based only the visual inspection of reaction schemes may be too limited and may lead to erroneous conclusions. So we decided to perform a rapid “quantitative” greenness assessment of the two routes: the best existing one,<sup>6</sup> and our new route (Scheme 4).

### Comparative assessment of alternative routes to Elliott's alcohol

The quantitative evaluation of chemical processes in terms of environmental impact and eco-friendliness has gradually become a topic of great interest since the original introduction of the Atom Economy (AE) by Trost,<sup>12</sup> and the E-factor by Sheldon.<sup>13</sup> Since then, other indexes have been proposed for the green metrics of chemical processes, such as Effective Mass Yield (EMY),<sup>14</sup> Reaction Mass Efficiency (RME),<sup>15</sup> Mass Intensity (MI),<sup>16</sup> along with unification efforts,<sup>17,18</sup> and comparisons among these indexes.<sup>19</sup>

All the above metrics are only based on masses of waste: they do not take into account the nature of the waste. The necessity of metrics that consider not just the amount of the waste, but also its environmental impact was first recognized by Sheldon.<sup>20</sup> To put it in his words: “Comparing alternative routes solely on the basis of the amount of waste is to grossly oversimplify”. So, he defined the *environmental quotient* (EQ) as the product between the *E-factor* (*E*) and an unfriendliness quotient, *Q*.

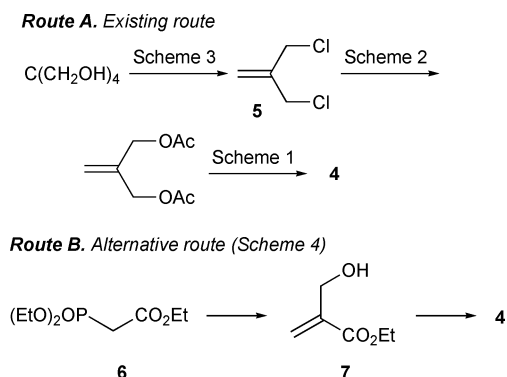
However, despite the simplicity of this definition, the quantitative assessment of *Q* is not so obvious. Sheldon's original

proposal to arbitrarily assign to any substance a  $Q$  value relative to that of NaCl, which is set to 1, does not fully solve the problem. This has been followed by a few papers dealing with this problem.<sup>21</sup> However, the methods proposed suffer from a difficult calculation basis and therefore are not amenable for a rapid evaluation and/or screening of the environmental impact of alternative synthetic pathways.

In 2002, Eissen and Metzger proposed EATOS—an environmental assessment tool for organic syntheses—an environmental performance metrics for daily use in synthetic chemistry.<sup>22</sup> This tool allows rapid quantitative assessment of both the  $E$ -factor and the potential environmental impact (PEI, Sheldon's  $Q$ ) of a process. They also provided a software application to perform this calculation, which is available from them.<sup>23</sup> With this tool, Sheldon's  $Q$  can be quantitatively assessed for both the feedstock and the output (product and wastes) of a multi-step synthesis. The assessment is made on the basis of the available substance's ecotoxicological and human toxicological data.

Here we present a comparative assessment of our new route to Elliott's alcohol and the existing route.<sup>6</sup> The assessment was made with the aid of the EATOS tool and takes into consideration both the masses ( $E$ -factor) as well as environmental impact of the substances employed and released by the processes (Sheldon's  $Q$ ).

This assessment compares the two routes to the common Elliott's alcohol intermediate **4**, depicted in Scheme 5.



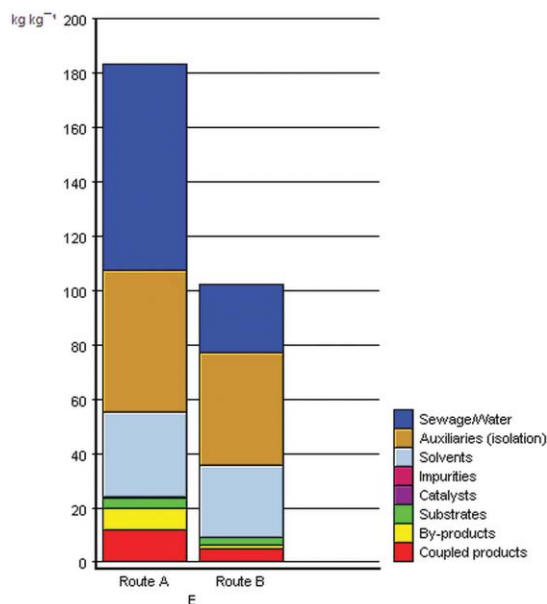
**Scheme 5** Alternative routes to Elliott's alcohol common intermediate **4**.

So, which is the greener route? This evaluation is usually done qualitatively by visual inspection of the reaction scheme. At a first glance, the shorter route B probably has the lower  $E$ -factor. But how much lower? And what about the environmental impact? Will the use of problematic formaldehyde in route B counterbalance the use of problematic pyridine and  $SOCl_2$  in route A? Obviously to answer these and other questions a *quantitative* assessment is needed.

### Comparison of $E$ -factor

The  $E$ -factor was calculated for both routes considering the amounts and yields reported in refs. 6 and 7 for route A and in the Experimental section of this paper for route B.

Comparison of  $E$ -factors (Fig. 2) clearly shows how route B is much less mass intensive than route A. In fact, for each kilogram



**Fig. 2** Comparison of  $E$ -factors (kg waste/kg product).

of compound **4**, route A produces 183 kg of wastes while route B produces only 102 kg, that is a net 44% reduction.

Inspection of EATOS graphical output (Fig. 2) allows us also to see where these wastes come from. Much of the wastes produced in route A (76 kg out of 183 kg; blue block) are aqueous and come from aqueous reagents and aqueous work-up. Further inspection of this segment† with EATOS tool shows that the majority of this aqueous waste is produced in the early steps of route A (Scheme 3), especially from the use and subsequent removal of mineral acids and their salts. Inspection of the wastes produced in Route B shows that most of them come from the auxiliaries materials used during isolation steps (41 kg out of 102 kg; brown block) of the process (Scheme 4). Overall isolation steps produce most of the wastes in both routes: the figures are 105 kg waste/kg product (57% of the total waste produced) for Route A and 51 kg waste/kg product (50% of the total waste produced) for Route B.

These figures speak very well on how misleading could be the “greenness” evaluation of a process based only on the “visual inspection” of synthetic schemes: a very large part of the waste comes from isolation steps, which do not even appear in synthetic schemes. Moreover, some green metrics, such as atom economy do not consider at all this portion of waste.

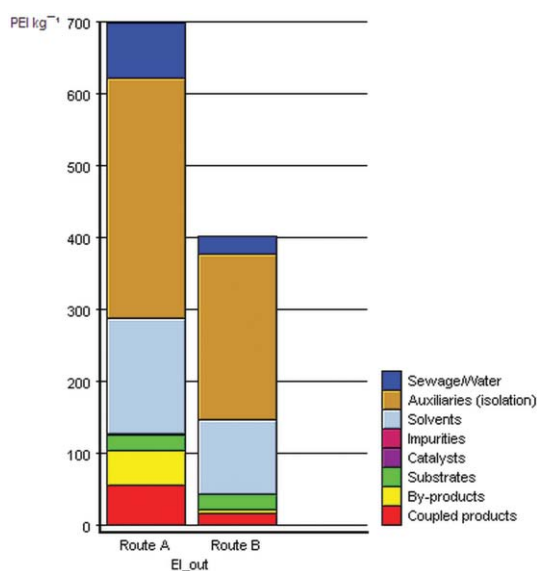
### Comparison of waste environmental impact

For the assessment of the environmental impact of chemical processes, EATOS can take into consideration up to ten different substances' ecotoxicological and human toxicological parameters, and each parameter can be given a different weight. Such substances' parameters are then normalized (each parameter is made to vary from 1 to 10) and then combined to afford an environmental quotient  $EI$  (much the same of Sheldon's  $Q$ ). So each different component of the waste can be assigned a quantitative potential environmental impact  $PEI_{out}$  (much the same of Sheldon's environmental quotient  $EQ$ ), defined as the

product of its mass (relative to the product unit mass) with its  $EI$ .

In this work the parameters taken into account for the assessment of  $EI_{out}$  of the waste are: MAK,<sup>24</sup> TLV, Hazard Symbol, or  $LX_{50}$  for human acute toxicity; any suspect carcinogen, mutagen or teratogen for chronic human toxicity; and WGK<sup>25</sup> or  $LC_{50}$  to fish for ecotoxicology. These data were obtained from substances Material Safety Data Sheets, the European Chemicals Bureau,<sup>26</sup> the Hazardous Substance DataBank.<sup>27</sup> When insufficient data were available for human chronic toxicity, a prediction of the carcinogenic and mutagenic effects was performed with the OSIRIS tool, available at the Organic Chemistry Portal.<sup>28</sup>

The quantitative comparison of potential environmental impact of waste ( $PEI_{out}$ ) is reported in Fig. 3.



**Fig. 3** Graphical comparison of potential environmental impact of waste.

Fig. 3 allows us to see immediately that Route B also allows a large decrease in waste environmental impact: the figures are 697 PEI unit/kg product while Route B is at 402 PEI unit/kg product, that is Route B achieves a net 40% reduction in waste potential environmental impact.

In both routes most of the environmental impact is generated by auxiliaries materials (those needed only for product isolation, brown blocks in Fig. 3). In particular,† in Route A nearly all (96%) of auxiliaries waste is due to the dichloromethane used for product extraction in three different steps of the process. In route B, again most of the auxiliaries waste comes from solvents needed for product isolation.

Further inspection Fig. 3 and its comparison with Fig. 2 affords some other useful insights. The aqueous waste (blue block) although relevant in mass terms (Fig. 2), is much less relevant in environmental impact terms: in Route A the aqueous waste is more than 40% of the waste total mass (Fig. 2) while it contributes to only less than 11% of the waste total potential environmental impact (Fig. 3). On the contrary auxiliary materials of Route A accounts for 25% of the waste

mass (Fig. 2) and for nearly 50% of waste environmental impact. Similar value are found for reaction solvents.

Again, it is important to stress how misleading could be an environmental assessment based only on waste masses: relatively small portions of the waste mass can account for relatively large environmental impacts.

Comparison of the waste produced by the two routes, shows that Route A suffers from poor reaction conditions more than Route B. In fact, in Route A the environmental impact of the waste related to reaction—*i.e.* coupled products, by-products, and excess substrates—accounts for 124 PEI  $kg^{-1}$  (nearly 20% of the total waste). Nearly all of this waste is produced in the early steps of route A (Scheme 3). In route B the same figure is 41 PEI  $kg^{-1}$  (10% of the total waste of route B). Fig. 3 shows how Route B, compared to Route A, produces very little by-products (yellow block) and less coupled products (red block), while has a similar impact due to excess substrate waste (green block), which for Route B is essentially due to excess paraformaldehyde and NaOCl, respectively, used in the first and second steps of Scheme 4.

So the environmental analysis performed with the aid of EATOS makes clear (in quantitative terms) that any effort for the reduction of the environmental impact of both processes should take into consideration, in the first place, the improvement of isolation procedures, that is using less and/or *less toxic* auxiliaries; a result that would not have been possible at all considering other metrics such as atom economy, or would have been greatly underestimated using metrics based only on masses.

### Comparison of feedstock environmental impact

The environmental impact can also be calculated for the feedstock of the process ( $PEI_{in}$ ), allowing us to assess the hazards and the costs associated with the use of the starting materials of a particular process. This should always be done to make sure that a decrease of the environmental impact of waste is not made at the expense of using more hazardous or (environmentally) expensive starting materials.

For the feedstock environmental impact evaluation, EATOS considers risk-phrases and the cost<sup>29</sup> associated with each substance. These data were obtained for all substances of both routes, from the 2007 Sigma-Aldrich catalogue.

Fig. 4 reveals that Route B allows also a decrease (33%) in the potential environmental impact of materials used for the preparation of Elliott's alcohol intermediate **4**. Again, most the hazards and costs come from the use of auxiliaries. For Route A a significantly higher proportion of the potential environmental impact of the materials used is due to reaction substrates (green block) and especially to thionyl chloride.†

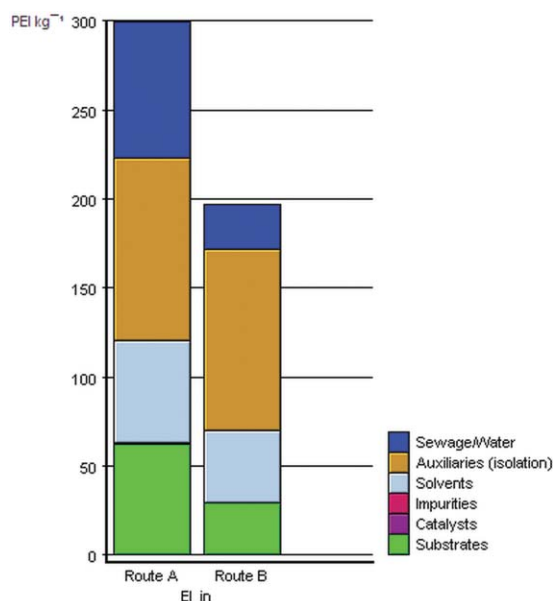
The results obtained are summarized in Table 1. Route B achieves a decrease over Route A, in the environmental impact of the waste produced ( $EI_{out}$ : -42%), and this is not done at the expense of more hazardous starting materials. In fact, the environmental impact of starting material is also decreased in Route B ( $EI_{in}$ : -34%). From Table 1, it is also possible to see the largest relative reduction that Route B brought about were in the environmental impact of the aqueous waste (-66%), in the solvents (-58%), and in the by-product (-89%).



**Table 1** Comparison of EATOS environmental indexes of waste ( $EI_{out}$ ) and of feedstock ( $EI_{in}$ ) for both synthetic routes

Category	$EI_{out}^a$			$EI_{in}^a$		
	Route A	Route B	Diff. <sup>b</sup>	Route A	Route B	Diff. <sup>b</sup>
Aqueous	76.07	25.48	-66%	76.07	25.48	-66%
Auxiliaries	333.38	230.79	-31%	102.31	101.61	-1%
Solvents	161.54	103.56	-58%	57.39	40.59	-29%
Substrates	21.64	21.07	-3%	61.83	28.65	-54%
By-products	47.90	5.35	-89%			
Co-products	54.70	15.23	-72%			
Total	696.65	401.63	-42%	298.49	196.38	-34%

<sup>a</sup> EATOS units.<sup>24</sup> <sup>b</sup> % Difference between Route B and Route A.

**Fig. 4** Graphical comparison of potential environmental impact of feedstock of synthetic routes depicted in Scheme 5.

### Driving the “green” improvement

EATOS can also be used as powerful tool to drive the “green” improvement of a chemical synthetic sequence. For example, analysing Table 1 it is clear that, in absolute terms, the greatest contribution to environmental impact of both routes comes from the auxiliaries materials, that is materials used for isolation and/or purification of the product. Then, efforts to further decrease waste environmental impact should be directed, in the first place, in finding alternative and greener isolation procedures.

In this sense, EATOS can again be very useful since it can be used to rapidly answer a manifold of “what if” questions.

Further insight into waste environmental impact generated by the auxiliary materials used in Route B,<sup>†</sup> shows that 225 out of 230 of this impact is due to the solvents (diethyl ether and dichloromethane) used for extractions in the synthesis. For example, what if we could manage to replace those solvents with the *same amounts* of ethyl acetate? Using EATOS this question is rapidly answered and the answer is that the environmental impact of the waste generated by the auxiliary materials would be dramatically reduced from 230 to only 40 EATOS units. At this point, it is important to stress that the use of any other

green metrics based on masses only (Atom Economy, RME, MI, *etc.*) leads to the wrong conclusions. In fact, these metrics would record no change in the “greenness” of the process, since toxic solvents are replaced by the *same amounts* of the less toxic ethyl acetate.

## Experimental section

### General

<sup>1</sup>H NMR spectra were recorded at 300.00 MHz at 20 °C with either tetramethylsilane ( $\delta$  0.00) or chloroform ( $\delta$  7.26) as the internal standard. <sup>13</sup>C NMR spectra were recorded at 75.46 MHz at 20 °C with chloroform ( $\delta$  77.7) as the internal standard. <sup>13</sup>C NMR signal multiplicities were established by DEPT experiments. Melting points were determined through a Büchi instrument and are uncorrected. Flash chromatographic separations were performed over Merck Silica gel 60 (230–400 mesh), tlc analyses were performed over Merck precoated tlc plates (Silica gel 60 GF<sub>254</sub> 0.25 mm). Tetrahydrofuran was obtained anhydrous over sodium and benzophenone. Unless otherwise stated, other solvents and reagents were used as commercially available. For EATOS calculations, when insufficient experimental details on work-up procedures were encountered, the following assumptions were made:<sup>30</sup> (a) extraction from aqueous media: 300 mL of organic solvent per litre of aqueous solution; (b) washing water: 300 mL per litre of organic solvent; (c) brine: 100 mL per litre of organic solvent; (d) solid inorganic drying agent: 20 g per litre of organic solvent.

### Ethyl 2-(hydroxymethyl)acrylate (7)

A 1 L reactor is charged with paraformaldehyde (96 g; 3.2 mol), 1 N orthophosphoric acid (H<sub>3</sub>PO<sub>4</sub>; 8 mL) and water (220 mL). The stirred mixture is heated to 90 °C for 1.5 h. The clear solution is then cooled to room temperature. Triethylphosphonoacetate (60.86 g; 0.27 mol), and a solution of potassium carbonate (41.04 g; 0.44 mol) in water (41 mL) under vigorous stirring at a rate so as to maintain internal temperature below 40 °C. Once the addition is complete, the solution is allowed to stir at 40 °C for 5 min, then it is quickly cooled to room temperature. Diethyl ether (200 mL) and brine (150 mL) are added in sequence. The two phases are separated and the aqueous phase is retroextracted with diethyl ether. The organic phases are reunited, washed with brine, and then dried over sodium sulfate. Evaporation of the solvent afforded 41.55 g of crude product as an orange oil, which was purified by distillation (70–72 °C/1 mmHg) to obtain a clear oil (30.89 g; 88%). <sup>1</sup>H NMR (CDCl<sub>3</sub>)  $\delta$  1.32 (t, 3H), 3.35 (bs, 1H), 4.25 (q, 2H), 4.35 (s, 2H), 5.86 (m, 1H), 6.26 (m, 1H) ppm. <sup>13</sup>C NMR (CDCl<sub>3</sub>)  $\delta$  14.60 (q), 61.33 (t), 62.31 (t), 125.66 (t), 140.21 (s), 166.85 (s) ppm.

### 3-Benzyl-5-hydroxymethyl-5-carboxyethyl isoxazoline (8)

A 1 L flask, equipped with a mechanical stirrer, thermometer and two dropping funnels, is charged with ethyl 2-(hydroxymethyl)acrylate (7) (39.0 g, 0.3 mol) and methylene chloride (115 mL). The mixture is cooled to -5 °C, then a solution of phenylacetaldehyde oxime (42.0 g, 0.3 mol) in methylene chloride (350 mL) and sodium hypochlorite solution

(active chlorine 10%, titrated before use, 343 mL equivalent to 0.48 mol of NaOCl) are simultaneously added dropwise in 2 h. Once the addition is complete, the mixture is allowed to stir at room temperature for 2 h. Conventional work-up afforded the product (71.55 g, 91%, >95% pure, by uncalibrated GC analysis), used as such in the subsequent step.

### 3-Benzyl-5,5-bis(hydroxymethyl)isoxazoline (4)

A 1 L flask, equipped with thermometer and mechanical stirrer, is charged with isoxazoline **8** (71.55 g, 0.272 mol), and ethanol (500 mL). The solution is cooled to  $-10^{\circ}\text{C}$  and  $\text{NaBH}_4$  (granules 10–40 mesh, 10.29 g, 0.272 mol) is added in 1 h. Once the addition is completed the temperature is increased to room temperature and the solution is allowed to stir for an additional 1.5 h. Conventional work-up afforded a raw orange oil (59.85 g). Crystallization from ethyl acetate and hexanes afforded the title compound (39.91 g) as a pale yellow solid. A second crop of product (4.16 g, 73% overall) is recovered from the mother liquors.

### Conclusions

In this paper, we have presented a quantitative assessment of the environmental impact of an alternative procedure for the preparation of Elliott's alcohol, an important industrial intermediate of the pyrethroid resmethrin. The assessment was made with the aid of the EATOS tool. The results show that the alternative process we propose, allows a significant reduction of the mass of waste, the environmental impact of waste and of the hazards and costs associated with the materials used for the process. With the aid of EATOS tools we were also able to establish the process zones where most of the environmental impact is produced. We have also shown how the use of other green metrics based only on waste mass would have led to different or underestimated results.

### Acknowledgements

This research was supported in part by Alma Mater Studiorum–Università di Bologna, and MiUR, Italy (PRIN 2005: “Stereo-selezione in Sintesi Organica. Metodologie ed Applicazioni”).

### Notes and references

- 1 United Nations FADINAP (2002) Agro-chemical Reports 2: 29–35.
- 2 M. G. Ford and D. R. Pert, *Pestic. Sci.*, 1974, **5**, 635–641; T. B. Gaines and R. E. Linder, *Fundam. Appl. Toxicol.*, 1986, **7**, 299–308.

- 3 (a) M. Elliott, A. W. Farnham, N. F. Janes, P. H. Needham and B. C. Pearson, *Nature*, 1967, **213**, 493–494; (b) M. Elliott, *Chem. Ind.*, 1969, 776–781; (c) M. Elliott, N. F. Janes and B. C. Pearson, *J. Chem. Soc. C*, 1971, 2551–2554.
- 4 For alternative procedures for the preparation of **1** see: K. Naumann, Synthetic Pyrethroid Insecticides: Chemistry and Patents, in *Chemistry of Plant Protection*, ed. W. S. Bowers, W. Ebing, D. Martin and R. Wegler, Springer-Verlag, Berlin, 1990, vol. 5, ch. 2, pp. 112–115.
- 5 *US Pat.*, 3 466 304, 1969.
- 6 *EP Pat.*, 0 187 345, 1986; *US Pat.*, 4 954 633, 1990.
- 7 K. Mondanaro Lynch and W. P. Dailey, *Org. Synth.*, 1998, **75**, 89.
- 8 ENDURA, PTC WO 02/090341.
- 9 J. Villieras and M. Rambaud, *Org. Synth.*, 1988, **66**, 220.
- 10 (a) For alternative and efficient preparations of hydroxymethacrylate esters via Baylis–Hilman reactions in aqueous media, see: P. J. Dunn, M. L. Hughes, P. M. Searle and A. S. Wood, *Org. Process Res. Dev.*, 2003, **7**, 244–253; (b) L. J. Mathias, S. H. Kusefoglu and A. O. Kress, *Macromolecules*, 1987, **20**, 2326–2328.
- 11 D. P. Curran, *J. Am. Chem. Soc.*, 1982, **104**, 4024.
- 12 B. M. Trost, *Science*, 1991, **254**, 1471; B. M. Trost, *Acc. Chem. Res.*, 2002, **35**, 695; B. M. Trost, *Angew. Chem., Int. Ed. Engl.*, 1995, **34**, 259.
- 13 R. A. Sheldon, *Chem. Ind. (London)*, 1992, 903–906; R. A. Sheldon, *Green Chem.*, 2007, **9**, 1273–1283.
- 14 T. Hudlicky, D. A. Frey, L. Koroniak, C. D. Claeboe and L. E. Brammer, *Green Chem.*, 1999, **1**, 57–59.
- 15 A. D. Curzons, D. J. C. Constable, D. N. Mortimer and V. L. Cunningham, *Green Chem.*, 2001, **3**, 1–6.
- 16 D. J. C. Constable, A. D. Curzons, L. M. Freitas dos Santos, G. R. Green, R. E. Hannah, J. D. Hayler, J. Kitteringham, M. A. McGuire, J. E. Richardson, P. Smith, R. L. Webb and M. Yu, *Green Chem.*, 2001, **3**, 7–9.
- 17 J. Augé, *Green Chem.*, 2008, **10**, 225–231.
- 18 J. Andraos, *Org. Process Res. Dev.*, 2005, **9**, 149–163; J. Andraos, *Org. Process Res. Dev.*, 2005, **9**, 404–431; J. Andraos, *Org. Process Res. Dev.*, 2006, **10**, 212–240.
- 19 D. J. C. Constable, A. D. Curzons and V. L. Cunningham, *Green Chem.*, 2002, **4**, 521–527.
- 20 R. A. Sheldon, *Chemtech*, 1994, 38–47.
- 21 E. Heinzle, D. Weirich, F. Brogli, V. H. Hoffmann, G. Koller, M. A. Verduyn and K. Hungerbühler, *Ind. Eng. Chem. Res.*, 1998, **37**, 3395–3407; G. Koller, D. Weirich, F. Brogli, E. Heinzle, V. H. Hoffmann, M. A. Verduyn and K. Hungerbühler, *Ind. Eng. Chem. Res.*, 1998, **37**, 3408–3413; P. Lepper, D. Keller, M. Herrchen, U. Wahnschaffe and I. Mangelsdorf, *Chemosphere*, 1997, **35**, 2603–2618; A. Steinbach and R. Winkenbach, *Chem. Eng.*, 2000, **4**, 94–100; G. Koller, U. Fischer and K. Hungerbühler, *Ind. Eng. Chem. Res.*, 2000, **37**, 960–972.
- 22 M. Eissen and J. O. Metzger, *Chem.–Eur. J.*, 2002, **8**, 3580–3585.
- 23 <http://www.chemie.uni-oldenburg.de/oc/metzger/eatos/>.
- 24 Maximale Arbeitsplatz-Konzentration (MAK).
- 25 Wassergefährdungsklassen: “Water Hazard Class”. <http://www.umweltbundesamt.de/wgs-e/index.htm>.
- 26 <http://ecb.jrc.it/>.
- 27 <http://toxnet.nlm.nih.gov/>.
- 28 <http://www.organic-chemistry.org/prog/peo/>.
- 29 For a discussion on the cost as a metric for starting material environmental impact, see ref. 22.
- 30 These assumptions are recommended by EATOS' authors.

# Purity specification methods for ionic liquids

Annegret Stark,<sup>\*a</sup> Peter Behrend,<sup>b</sup> Oliver Braun,<sup>a</sup> Anja Müller,<sup>b</sup> Johannes Ranke,<sup>\*b</sup> Bernd Ondruschka<sup>a</sup> and Bernd Jastorff<sup>†b</sup>

Received 20th May 2008, Accepted 21st July 2008

First published as an Advance Article on the web 18th September 2008

DOI: 10.1039/b808532c

In the last decade, ionic liquids have shown great promise in a plethora of applications. However, little attention has been paid to the characterisation of the purity of these fluids, which has ultimately led to non-reproducible data in the literature. In order to facilitate specification of ionic liquids, a number of analytical protocols with their limits of detection (where available) have been compiled, including methods of other authors. In particular, quantitative methods have been developed and summarised for the determination of the total ionic liquid content, residual unreacted ionic liquid starting material and by-products (amines, alkylating agents, inorganic halides), solvents from extraction procedures and water, in addition to decomposition products and total volatiles.

## Introduction

Since 1992,<sup>1</sup> ionic liquids have increasingly been investigated in particular as solvents for various reactions,<sup>2</sup> and have been applied to other fields, for example as electrolytes, as entrainers in extractive distillations,<sup>3</sup> in metal deposition<sup>4</sup> and fuel cells.<sup>5</sup> In parallel to technical developments, there is plenty of ongoing research in the field of sustainable product design of ionic liquids.<sup>6</sup>

It has been pointed out<sup>7</sup> that, considering the exponential increase in publications in this field in the last 15 years, very little information on routine analytical methods for the determination of impurities in ionic liquids has been published. Such methods are especially important, as many conventionally used operations for the purification of organic compounds, such as distillation or extraction, are aggravated by the unique properties of ionic liquids, such as negligibly low vapour pressure and high solvating power.

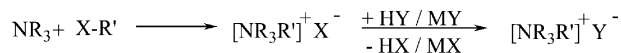
In this article, we summarise the established and published methods and present our own efforts in providing reliable and practicable analytical techniques.

## Origin of potential impurities

The most important source of impurities in ionic liquids originates from ionic liquid preparation. Their analysis is the topic of this contribution, with special emphasis on the quantitative determination of the total ionic liquid content and the different types of impurities occurring.

Although many thousands of ionic liquids are conceivable,<sup>8</sup> their preparation follows, in the majority of cases, the same procedure: alkylation, first work-up (organic solvent extraction), ion exchange, second work-up (aqueous extraction/steam distillation/precipitation), diligent drying, and, where required, removal of discolorations.

Thus, a Lewis base (an amine, phosphine or sulfide) is alkylated by nucleophilic substitution of an alkyl halide. After extraction of the intermediate halide salt with an organic solvent to remove unreacted starting material, the halide is exchanged with the required anion. There are, in principle, two methods to achieve this, *i.e.* exchange with the corresponding acid HY, or the Group 1 metal salt MY. In this latter instance, sodium, potassium and lithium are most frequently employed. The anion exchange is carried out in a solvent and at room-temperature, and the respective halide-containing acids HX or salts MX are formed as side-product. Scheme 1 illustrates the general synthetic steps for the preparation of amine-based ionic liquids.



Scheme 1 Typical preparation of ionic liquids.

In order to be able to quantitatively remove these side-products with a reasonable extractive effort, the anion Y<sup>-</sup> must render the ionic liquid hydrophobic enough to allow for aqueous extraction of HX or MX. Examples of such anions are tetrafluoroborate, hexafluorophosphate, bis(trifluoromethanesulfonyl)amide and trifluoromethylsulfonate. It should be noted here that 'hydrophobic' is not meant to imply 'water-immiscible', but rather that a biphasic ionic liquid–water system is attained at certain mole fractions and temperatures, depending also on the cation substitution.

In those cases, however, where the required anion gives a water-soluble ionic liquid, the extraction with water described above is not easily feasible, and cumbersome work-ups result: HX is driven out by frequent addition of water and successive

<sup>a</sup>Institute for Technical Chemistry and Environmental Chemistry, Friedrich-Schiller University Jena, Lessingstr. 12, 07743, Jena, Germany. E-mail: annegret.stark@uni-jena.de; Fax: ++49 3641 948402; Tel: ++49 3641 948413

<sup>b</sup>UFT Centre of Environmental Research and Environmental Technology, University of Bremen, Leobener Strasse 1, 28359, Bremen, Germany. E-mail: jranke@uni-bremen.de; Fax: ++49 4212 1863375; Tel: ++49 4212 1863373

drying *in vacuo* ('steam distillation').<sup>9,10</sup> MX, on the other hand, can be precipitated from the dry ionic liquid or its solution in chloroform at low temperatures,<sup>11</sup> followed by several filtration steps. However, both alternatives result in products containing >5% residual halide.<sup>12</sup>

A viable, albeit very cost-intensive method has been proposed<sup>13</sup> in which the halide is precipitated as AgX by addition of *e.g.* Ag[NO<sub>3</sub>]. Residual silver ions can be removed electrochemically.<sup>13</sup> However, this involves yet another clean-up stage, and silver salts are produced as by-products.

In the few cases where alkylating agents such as dialkyl sulfate, alkyl trifluoromethanesulfonate, alkyl trifluoroacetate or alkyl bis(trifluoromethanesulfonyl)amide<sup>14</sup> are available, the general two-step synthesis is circumvented and the direct preparation of ionic liquids is feasible.

After work-up, the product is dried (80 °C, 12 h, high vacuum) in order to remove any volatiles remaining from the preparation. Under these conditions, we found that the alkylating agents and organic solvents are quantitatively removed. In the case of water-soluble ionic liquids, water (stemming either from the preparation or from absorption from air)<sup>9</sup> may still be present in trace amounts.

Due to the high boiling points and affinities of polar compounds, in particular imidazoles and pyridine, to ionic liquids, their quantitative removal is not achieved. Higher temperatures (during drying or also during synthesis) often result in thermal degradation of the ionic liquid,<sup>15–18</sup> as observed by a honey-yellow to brown tint, the origin of which still remains unknown. In our experience, however, the colour of an ionic liquid is neither correlated to its physical properties nor to its performance as solvent, and coloured impurities have not been observed in any of our IR, HPLC or NMR measurements. However, for more sensitive spectroscopic applications or from the point of view of commercial ionic liquid suppliers, colourless ionic liquids may be desirable.

The removal of any discoloration has been reported using activated charcoal, acidic or neutral alumina followed by filtration through kieselguhr.<sup>19–23</sup> In our laboratories, decolourisation (Fig. 1) is carried out by stirring the ionic liquid with activated charcoal (charcoal : ionic liquid 1 : 4) in acetone at room-temperature for 20 min. A rather large physical loss of about 20% results, and the method was found not to be applicable for chloride- or bromide-based ionic liquids.

### Relevance of the purity of ionic liquids

Although the use of high-purity ionic liquids may not be necessary for every purpose, several authors have highlighted that residual water, halide or 1-methylimidazole exhibit (often severe) effects on the rate and/or selectivity of reactions carried out in ionic liquids and their physical properties.<sup>24–37</sup> Electrochemical studies have recently shown that impurities in ionic liquids *inter alia* narrow the apparent electrochemical window and decomposition products may alter the electrode surface. Hence, the use of ultra high purity ionic liquids is necessary to achieve reproducible results.<sup>38</sup>

It has been pointed out that the apparent lack of physical data impedes the industrial application of ionic liquids in industry.<sup>39</sup> The situation is made worse by the fact that most available data



**Fig. 1** [C<sub>6</sub>dmim][BF<sub>4</sub>], before (left) and after (right) treatment with activated charcoal in acetone at room-temperature.

was obtained with ionic liquids of an unknown purity level. For example, melting points published for the same ionic liquid, *e.g.* [C<sub>2</sub>mim][BF<sub>4</sub>], deviate by almost 10 °C,<sup>1,40</sup> and the viscosity varies by 140 cP for [C<sub>4</sub>mim][PF<sub>6</sub>].<sup>11,41</sup>

Likewise, reaction kinetics are not comparable unless the purity of the medium is reported. From an engineering point of view, the presence of halides will affect the choice of constructional material, as these anions are known for their corrosiveness.

Another important factor to be considered is the dependence of water content on ionic liquid stability. For example, water leads to a significant loss in stability of ionic liquids based on the tetrafluoroborate<sup>42</sup> or hexafluorophosphate<sup>43</sup> anion, which decompose to yield HF<sup>44</sup> and other by-products.

Finally, purity has an influence on the safety of ionic liquids for man and the environment. The formation of HF, for example, can lead to corrosion and successive leaking of glassware which significantly increases the risk of a direct exposure of the skin and respiratory tract. In theory, there is also the possibility that impurities lead to more toxic mixtures than the pure ionic liquid itself. It is known that the toxicity of ionic liquids increases with alkyl chain length,<sup>45,46</sup> or more generally with cation hydrophobicity.<sup>47</sup> Therefore, the by-product *N,N*-dihexylpyrrolidinium in *N*-hexyl-*N*-methylpyrrolidinium ionic liquids can be expected to substantially increase the mixture's toxicity.

It is clear that highly pure ionic liquids are not necessary for every application. However, at this present stage of ionic liquid development, we believe that any literature data should be accompanied with an analytical specification of impurities that are potentially relevant for the data in order to allow for the comparison of results between different research groups.

The quantification of the total ionic liquid content and the determination of the amounts of impurities are thus considered as follows:

- Total ionic liquid content
- Unreacted organic starting material (amine, alkylating agent)



- Unreacted inorganic starting material (HY, MY) and by-products (MX, HX)
- Solvents from extraction procedures and water absorbed from the atmosphere
- Decomposition products and other volatiles.

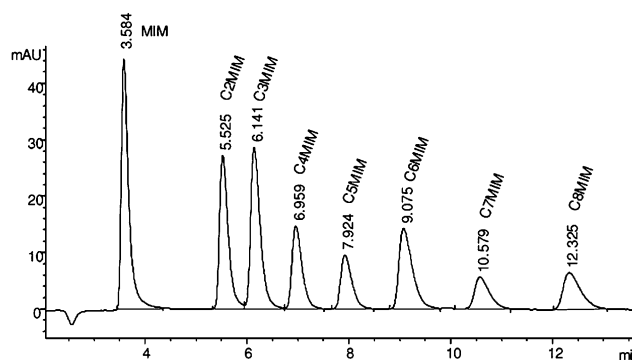
The focus of this article is on providing a set of practicable methods from which interested readers can choose the ones that are relevant to their work. For the groups of impurities listed above, some of the established quantitative methods from literature are summarised, and our own analytical methods for the specification of ionic liquids are introduced. In many cases, the calibration and validation of analytical techniques is hampered by the fact that ionic liquids in analytical standard quality are not yet commercially available. Nevertheless, interest in the development of analytical techniques for ionic liquids has risen in recent years, albeit much slower than investigations on ionic liquids in catalysis or organic synthesis, and includes sometimes rather sophisticated apparatus.

## Results and discussion

### Total ionic liquid content

Traditionally, the purity of ionic liquids has been qualitatively determined using  $^1\text{H}$  NMR spectroscopy. However, at impurity levels  $<3$  mol% the limit of detection is reached, and organic compounds such as 1-methylimidazole, which exhibit a strong effect on the reaction outcome remain undetected.<sup>37</sup> The quantitative analysis of the total ionic liquid content has been reported by UV-Vis,<sup>29,48</sup> electrospray ionisation mass spectrometry,<sup>49</sup> capillary electrophoresis (limit of detection  $<2$  ppm<sup>50</sup> and 10 ppb for  $[\text{C}_2\text{mim}]^+$ -based ionic liquids)<sup>51</sup> and hydrophilic interaction liquid chromatography (HILIC).<sup>52</sup>

Building on an HPLC-UV-method developed for the separation of ionic liquids with longer alkyl chain substitution on an RP-8 column using a phosphate buffer–acetonitrile eluent,<sup>53,54</sup> we found a phosphoric acid–dihydrogenphosphate buffer with a pH of 2.8 or 3 to be necessary to prevent excessive tailing of the quaternary ammonium cations, which is probably due to interactions with dissociated, negatively charged silanol groups even on end-capped RP columns. Using phosphate buffer, UV detection is best at 208 nm for imidazole-derivatives. Isocratic methods can be applied for the quantification of several ionic liquid cations. For example, we calibrated with  $[\text{C}_4\text{MIM}]$  and  $[\text{C}_8\text{MIM}]$  tetrafluoroborate solutions, reaching detection limits of about  $2.5$  mg  $\text{L}^{-1}$  and a linear response up to at least  $250$  mg  $\text{L}^{-1}$ . It should be noted that this method does not allow for the separation of 1-methylimidazole or 1,2-dimethylimidazole from imidazolium-derivatives with short alkyl chain substitution (*vide infra*). Satisfactory retention of ionic liquid cations with short chains such as 1-ethyl-3-methylimidazolium ( $[\text{C}_2\text{MIM}]$ ) in reversed phase HPLC is only possible with special RP phases, *e.g.* with pentafluorophenylpropyl groups (Fig. 2), or by switching to HILIC or cation exchange chromatography columns. For non-aromatic cations, such as pyrrolidinium, morpholinium or phosphonium derivatives, an alternative acetic acid/acetate buffer can be used, which has better compatibility with MS-coupled electrospray ionisation (ESI-MS) (see Experimental). The resulting method for cation analysis has been shown to



**Fig. 2** Chromatogram of 1-methylimidazole and the homologous series of 1-alkyl-3-methylimidazolium cations on a pentafluorophenylpropyl HPLC column. Alkyl chains are from ethyl ( $[\text{C}_2\text{MIM}]$ ) to octyl ( $[\text{C}_8\text{MIM}]$ ). Note the strong separation of 1-methylimidazole from the short chain  $[\text{C}_2\text{MIM}]$  cation.

be applicable to almost the entire range of cations found in ionic liquids.<sup>47</sup> However, precautions for quantification with the non-linear and matrix-dependent ESI have to be taken, *i.e.* a non-linear calibration might have to be used in order to obtain a viable working range of the method, and the purity of the cation peak has to be tested either by MS<sup>2</sup> or by cross-checking under different chromatographic conditions.

All of these relative methods rely on the availability of a standard ionic liquid with maximum purity, and can only be as good as this standard. This means that their application is confined to the comparison of different batches of ionic liquids, and the monitoring of cation content of ionic liquids.

### Unreacted organic starting material

Of the organic impurities (amines, *e.g.* pyridine/imidazole, alkylating agent, water and organic solvents), only the amine and water have been recognised as synthesis-inherent (and difficult to remove) impurities to influence ionic liquid performance (*vide supra*). In our experience, the alkylating agents are quantitatively extracted with ether or other nonpolar extracting agents,<sup>55</sup> and the organic solvents are removed during the extensive drying process following the preparation. However, the Lewis bases, in particular 1-methylimidazole and pyridine, possess both high boiling points and affinities towards the ionic liquid, and are therefore in most cases not quantitatively removed.

Holbrey *et al.*<sup>56</sup> devised a protocol for the quantification of 1-methylimidazole during the synthesis of 1-ethyl-3-methylimidazolium chloride. The procedure is based on the formation of the  $[\text{Cu}(\text{MIM})_4]^{2+}$  ion (where MIM = 1-methylimidazole) from copper(II)chloride and 1-methylimidazole, which is blue. The shift of the maxima in the electronic absorbance spectra is exponentially related to the 1-methylimidazole concentration. The method can be used for the quantification of 1-methylimidazole between 0.2 and 8 mol% in ionic liquids.<sup>55</sup> The separation, detection and quantification of imidazoles has also been achieved by zone electrophoresis,<sup>50,57</sup> with a low limit of detection ( $<1$  ppm) for 1-methylimidazole and 1,2-dimethylimidazole on a  $\alpha$ -cyclodextrin-modified capillary.<sup>50</sup>

We have developed both GC- and HPLC-based methods for the quantification of residual imidazoles and pyridine, and a UV-based method for primary and secondary aliphatic amines.

**Determination of 1-methylimidazole impurity in ionic liquids by GC using the standard addition method.** A viable method to establish the amount of 1-methylimidazole in a sample of an ionic liquid is the standard addition method combined with GC-FID analysis: the sample is dissolved in acetonitrile, and spiked with known amounts of 1-methylimidazole before analysis (see Experimental). The GC injector should be equipped with a glass insert or a tuft of glass wool preventing the non-volatile ionic liquid from accumulating on the column. By extrapolation, the concentration of the original solution is derived (Fig. 3, 2.5 wt%, or 5.2 mol% MIM).

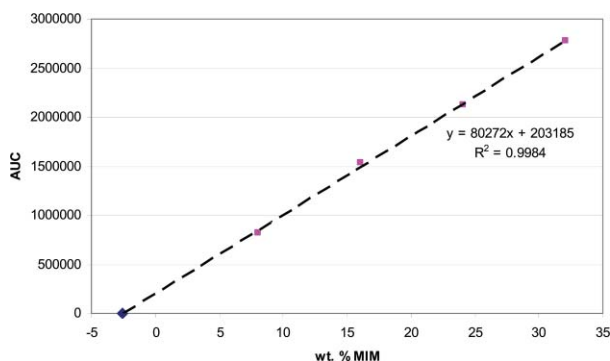


Fig. 3 GC determination of 1-methylimidazole (MIM) using the standard addition method.

**Determination of imidazole and pyridine impurities in ionic liquids by HPLC.** Reversed-phase HPLC with UV detection was evaluated for the quantification of UV active substrates, such as residual imidazole in ionic liquids. 1,2-Dimethylimidazole (DMIM) or 1-methylimidazole (MIM) was analysed as both the respective halide precursor, and the tetrafluoroborate ionic liquid. Preliminary results show that the same methodology is applicable to pyridinium-based ionic liquids.

During the development of the optimal eluent system, we discovered that the use of an acetate buffer–acetonitrile eluent<sup>58</sup> only allowed for detection at 220 nm, and thus gave a low response.<sup>59</sup> When a phosphate buffer (see Experimental) is used, on the other hand, measurement was possible around the absorption maxima of the imidazoles, e.g. at 208 nm.

It was found that the retention times (for exact values, see Experimental) on a standard C-8 HPLC column are solely dependent on the nature of the cation, and increase with increasing alkyl chain. Also, ionic liquids which are methylated in the C-2 position elute somewhat later than their non-methylated homologues. Unfortunately, the quantification of 1-methylimidazole in [C<sub>2</sub>mim]<sup>+</sup> or [C<sub>4</sub>mim]<sup>+</sup>-based ionic liquids is not feasible, due to poor separation, verifying results obtained by Stepnowski *et al.*<sup>55</sup> In these cases, a less polar column has to be used to achieve separation (*vide supra*).

However, lengthening of the alkyl chain increases the retention time, and 1,2-dimethylimidazole is fully separated from [C<sub>4</sub>dmim]<sup>+</sup> or longer alkyl chain substituted ionic liquids. Furthermore, the method is characterised by a short analysis

**Table 1** Parameters and performance characteristics for the determination of 1-methylimidazole (MIM) and 1,2-dimethylimidazole (DMIM) by HPLC

Parameter	MIM	DMIM	MIM <sup>a</sup>
Sensitivity/L mg <sup>-1</sup>	9.655	10.594	28.270
Residual SD <sup>b</sup>	26.646	54.161	13.612
SD <sup>b</sup> of method/mg L <sup>-1</sup>	2.6	5.1	0.5
LOD <sup>c</sup> /mg L <sup>-1</sup>	10	20	1.5
Linear range <sup>d</sup> /mg L <sup>-1</sup>	10–468	10–446	5–65
Correlation coefficient	0.9999	0.9995	0.9998

<sup>a</sup> Low content calibration. <sup>b</sup> SD = standard deviation. <sup>c</sup> LOD = limit of detection, determined according to DIN 32645. <sup>d</sup> Linear range was ascertained using the MANDEL test of goodness of fit.

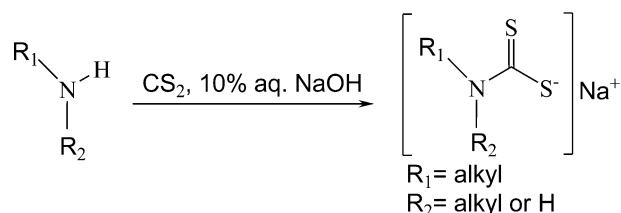
time (<7.05 min in the case of [C<sub>8</sub>dmim]<sup>+</sup>), and can therefore be used for in-process control.

The content of the imidazole impurity is determined from a linear calibration curve obtained for both, the MIM and DMIM impurity by measuring the responses for equidistant standard concentrations between 0 and 500 mg L<sup>-1</sup>.

As shown in Table 1, the detection limit of the method for MIM and DMIM is 10 and 20 mg L<sup>-1</sup>, respectively. In the case of MIM, the given limit of detection translates into 0.17% w/w for any 1-methylimidazole-based ionic liquid, or between 0.35 mol% (for the ionic liquid with the lowest molecular weight analysable by this method: [C<sub>4</sub>mim]Cl) and 0.57 mol% (for an ionic liquid with relatively high molecular weight: [C<sub>8</sub>mim][BF<sub>4</sub>]). For DMIM, the corresponding percentages are 0.33% w/w, and 0.66 mol% (for [C<sub>4</sub>dmim]Cl) to 1.01 mol% (for [C<sub>8</sub>dmim][BF<sub>4</sub>]), respectively.

In order to further lower the detection limit, the total concentration of the sample can be increased; however, with the risk of overloading the column and reducing column lifetime. Alternatively, a calibration at lower concentration can be carried out, resulting in a detection limit of 0.025 wt% if a sample concentration of 6 g L<sup>-1</sup> is used. The analytical parameters and performance characteristics are summarised in Table 1.

**Determination of primary and secondary amine impurities in ionic liquids by UV-spectroscopy.** There is a lack of analytical procedures for the determination of non-aromatic amines in ionic liquids, although these are important starting materials for alternative systems, such as tetraalkylammonium,<sup>60</sup> pyrrolidinium<sup>61</sup> or morpholinium<sup>62</sup> ionic liquids. During our studies of these materials, we adapted a facile method<sup>63</sup> to assess the content of non-aromatic primary and secondary amines based on the quantitative formation of UV-active dithiocarbamates in an aqueous sodium hydroxide/carbon disulfide biphasic reaction mixture (see Scheme 2).<sup>64</sup>



**Scheme 2** Reaction scheme of primary and secondary amines with carbon disulfide to yield UV-active dithiocarbamates.

**Table 2** HPLC conditions for the determination of imidazole and pyridine impurities

Column	Hyperchrome 125-4 Prontosil 120-5-C8-SH 5.0 $\mu\text{m}$ Bischoff
Eluent	A = acetonitrile B = 0.02 M sodium dihydrogenphosphate
Programme	30% v/v A, isocratic, 8 min
Column temperature	30 $^{\circ}\text{C}$
Flow rate	1.2 mL min $^{-1}$
Injected volume	5 $\mu\text{L}$
Detection	UV-DAD, $\lambda_{\text{Absorption}} = 208 \text{ nm}$
Retention times/min	MIM 1.00 DMIM 1.00 [C <sub>2</sub> mim] <sup>+</sup> 0.98 [C <sub>4</sub> mim] <sup>+</sup> 1.21 [C <sub>6</sub> mim] <sup>+</sup> 2.24 [C <sub>8</sub> mim] <sup>+</sup> 5.56 [C <sub>4</sub> dmim] <sup>+</sup> 1.33 [C <sub>6</sub> dmim] <sup>+</sup> 2.55 [C <sub>8</sub> dmim] <sup>+</sup> 7.05

Besides the specification of the ionic liquids themselves, this procedure may also be employed to follow reactions in ionic liquids which use primary or secondary amines as reactants.

Statistical comparison of the calibration of the amines (pyrrolidine, morpholine, *n*-butylamine, *n*-propylamine) in the absence of ionic liquid with the standard addition calibration performed in the presence of ionic liquid confirmed that no proportional or constant systematic error occurred in the concentration ranges indicated in Table 3. The recovery was  $96.0 \pm 2.8\%$  for pyrrolidine,  $98.7\% \pm 9.8\%$  for morpholine,  $101.5 \pm 3.5\%$  for *n*-butylamine and  $82.8 \pm 5.2\%$  for *n*-propylamine in 1-butyl-3-methylimidazolium chloride. For the method described (see Experimental), the detection limit of amines in ionic liquids is 0.2 wt%. For water soluble ionic liquids, the detection limit may be further decreased by increasing the amount of sample used for analysis.

To test the applicability of the protocol, the recovery of 1% of pyrrolidine in 1-butyl-3-methylimidazolium chloride (Fig. 4), to which standards of various pyrrolidine concentrations were added, was carried out. Although 1,3-dialkylimidazolium-based ionic liquids are able to form carbenes in the presence of a base such as NaOH,<sup>65</sup> this did not interfere with the analysis. All other amines investigated gave spectra of similar appearance.

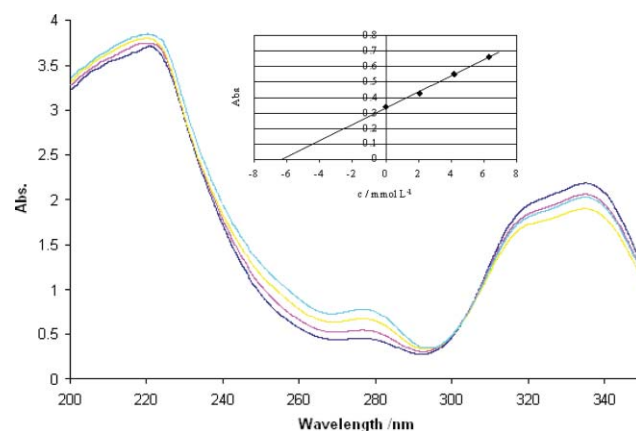
### Unreacted inorganic starting material (HY, MY) and by-products (MX, HX)

The complete removal of the acidic by-product HX and excess reactant HY, which is used for the anion exchange, is

**Table 3** Method characteristics for the amines investigated

Amine	$\lambda/\text{nm}$	Linear range <sup>a</sup> /mmol L $^{-1}$	Linear range/ $\mu\text{g L}^{-1}$	SD <sup>b</sup> /[%]	Slope	Intercept (abs.)	LOD <sup>c</sup> /mmol L $^{-1}$	LOQ <sup>d</sup> /mmol L $^{-1}$
Pyrrolidine	277	1.4–12.0	0.31–2.78	5.42	0.792	−0.034	1.0	2.7
Morpholine	285	1.1–9.8	0.49–4.18	3.04	0.596	−0.011	0.5	1.3
Butylamine	283	1.3–13.7	0.38–4.00	4.76	0.601	−0.033	0.9	2.5
Propylamine	283	1.7–17.0	0.40–4.01	2.54	0.965	−0.025	0.6	1.7

<sup>a</sup> Verified by the MANDEL test of goodness of fit. <sup>b</sup> SD = standard deviation. <sup>c</sup> LOD = limit of detection, determined according to DIN 32645. <sup>d</sup> LOQ = limit of quantification ( $k = 3$ ).



**Fig. 4** UV-spectra of 1-butyl-3-methylimidazolium chloride spiked with 1% pyrrolidine (blue) as impurity model, and three standard additions of pyrrolidine (2.1, 4.2, 6.3 mmol L $^{-1}$ , red, yellow and turquoise, respectively), and standard addition plot (insert) corrected by ionic liquid-caused offset ( $\lambda = 277 \text{ nm}$ ;  $y = 0.331 + 0.052x$ ;  $R^2 = 0.9978$ ).

conveniently assured by following each step of the aqueous extraction or steam distillation using indicator paper, colorimetric methods<sup>44</sup> or a pH-meter. The salts MX and MY possess a very limited solubility in most dry ionic liquids, which has been previously shown by sodium-selective electrode measurements on the example of Na[NO<sub>3</sub>], NaCl and Na[BF<sub>4</sub>]. Therefore, residual halide impurity originates rather from unreacted [C<sub>*n*</sub>mim]X/[C<sub>*n*</sub>py]X than from MX.<sup>9,41</sup> However, lithium salts possess higher solubilities than analogous sodium salts. The lithium content can be determined by counterflow electrophoresis<sup>54</sup> at ppb level.

By now, a plethora of analytical techniques have been developed to determine the halide content in ionic liquids: the use of a chloride-selective electrode has been described,<sup>9</sup> requiring the preparation of standard chloride solutions containing the same cation as the sample ionic liquid, since both the slope and intercept vary from that obtained from standard NaCl. The reproducibility of the electrode is  $\pm 2\%$ , and a detection limit of 2 ppm is obtained using a four-point calibration. The error of measurement was determined to be 3%. In addition to the laborious calibration and sample preparation, the possible interference of other ions is a disadvantage, and for ionic liquids containing alkyl chains longer than octyl, only unstable meter readings are obtained. However, compared to the Volhard titration (*vide infra*), only a small sample size of 0.15–0.3 g is necessary.<sup>9</sup>

Ion chromatography has been described for the determination of chloride,<sup>66,67</sup> featuring a detection limit well below 1 ppm for IL–water or acetonitrile–water solutions, corresponding to below 10 ppm chloride in the pure ionic liquid (water miscible and immiscible ones), but due to the strong retention of some anions, analysis time may be prohibitive.<sup>42,68</sup> Capillary electrophoresis<sup>69</sup> was established for  $[\text{C}_4\text{mim}][(\text{CF}_3\text{SO}_2)_2\text{N}]$  and  $[\text{C}_4\text{mim}][\text{PF}_6]$  with detection limits  $< 10$  ppm. Problems were encountered due to limited homogenisation of viscous samples. Alternatively, linear-sweep and square-wave voltammetry<sup>42,70,71</sup> feature a detection limit at ppb level, but are applicable only to a narrow range of chloride concentrations. For water-soluble ionic liquids, low detection limits (10 ppb) of total chlorine content are achieved by using inductively coupled plasma-mass spectrometry.<sup>12</sup> An ion exchange chromatographic column has been used for the analysis of 1-butyl-3-methylimidazolium chloride in the concentration range of 1–100  $\mu\text{M}$ , yielding a detection limit of 20  $\mu\text{g}$ .<sup>53</sup>

**Determination of the halide content by Volhard titration ( $[\text{X}^-] > 1 \text{ wt}\%$ ).** As pointed out above, methods for the determination of halides at extremely low concentrations have been developed. However, since most of them require rather sophisticated apparatus, we have looked further into the potentials of the Volhard titration, since it requires only standard glassware and can thus be carried out in any laboratory. The principle of this method is to precipitate all halide ions present in an aqueous sample solution by addition of an excess of silver nitrate. The precipitate is filtered off, and excess silver is back-titrated with a solution of thiocyanate. Excess thiocyanate, in turn, forms the reddish-brown thiocyanatoiron(III) complex with the indicator, and the endpoint of the titration is determined visually by the first permanent appearance of red.<sup>72</sup> The standard Volhard method has previously been validated using a chloride-selective electrode.<sup>9</sup> For samples containing either chloride or bromide impurities, the detection limit is 0.4 wt% and 0.9 wt%, respectively. Lower limits of detection are achieved by further increasing the weighted sample, or with an alternative, semi-quantitative method using Nessler cylinders (*vide infra*).

Because the original Volhard protocol is only applicable to water-soluble ionic liquids, it was extended to water-insoluble ionic liquids. Various organic solvents were elucidated using the principally water-soluble  $[\text{C}_4\text{mim}][\text{BF}_4]$  as a standard both in deionised water and the respective solvent. Acetone was found to give reproducible results which agreed within 2% with the values obtained with water.

Although the Volhard method is very reliable, some disadvantages are intrinsic: a large amount of sample (0.5 g) is used and can not be regenerated, thus, the halide content of small samples can not be determined. Due to the necessary filtration step, the method is relatively time-consuming, and thiocyanate waste is generated. Also, ionic liquids containing pseudo-halide anions, such as  $[\text{SCN}]^-$  and  $[(\text{CN})_2\text{N}]^-$ , can not be analysed.

**Semi-quantitative determination of trace amounts of halide ( $[\text{X}^-] > 10 \text{ ppm}$ ).** The principle of the Nessler cylinder method is based on the fixation of any halide anion as  $\text{AgX}$  in acidic aqueous solution in the presence of silver nitrate. The opacity of the samples is visually compared to standard solutions (0, 10, 20, 40, 60 ppm) contained in colorimetric Nessler cylinders

(Fig. 5). These cylinders feature a precise volume of 50 mL with a constant height, and their bases are manufactured to be plane to prevent the diffraction of light when placed on a dark background and examined from above. The standard solution which is slightly more turbid than the sample is visually selected, and the halide content of the sample is thus lower than the respective standard ppm value. For water-insoluble ionic liquids, ethanol was found to reliably substitute for distilled water.



**Fig. 5** Colorimetric Nessler cylinders containing standard solutions of NaCl (0, 10, 20, 40 and 60 ppm) for semi-quantitative determination of halides.

#### Solvents from extraction procedures and water absorbed from the atmosphere

In our experience, the only commonly used solvent in ionic liquid synthesis that may not be quantitatively removed from ionic liquids after the preparation is water, especially if the stringent drying procedure is not followed. All other solvents (diethylether, chloroform, dichloromethane, ethyl acetate *etc.*) are sufficiently volatile to be quantitatively removed and do not pose a problem. However, as pointed out above, water is accumulated if exposed to the atmosphere due to the hygroscopic nature of ionic liquids. If ionic liquids are exposed to air frequently and over a prolonged period of time, their water content should be determined regularly.

**Water by Karl–Fischer titration.** Automated Karl–Fischer titration ideally lends itself to this purpose, since the determination can be carried out within a few minutes without sample preparation, and only small amounts of ionic liquid are required.<sup>14,73</sup> This quick method requires only a small sample size (approx. 0.05–0.1 g), and 0.01 to 0.1 mg water content per sample, with a detection limit of 0.01 mg water, can be determined.

Although the water content of any conventional ionic liquid can be measured, it should be noted that samples containing strong acids or bases as functional groups will result in a



destabilisation of the buffered Karl–Fischer analyte mixture. Also, oxidising and reducing agents, such as chromates, oxides, copper(II) or Fe(III) salts, thiosulfates and sulfides, basic oxides or salts of weak oxy-acids, such as hydrogen carbonate, interfere with the Karl–Fischer titration. It was found that ionic liquids containing nitrite or alkylsulfite could not reproducibly be measured using this method, whereas no problems were encountered with ionic liquids based on chloride, bromide, tetrafluoroborate, trifluoromethane-sulfonate *etc.*

Since Karl–Fischer titration is not applicable to ionic liquids containing oxidising or reducing anions, it is favourable to compare/calibrate this method with the direct determination of water using gas chromatography.

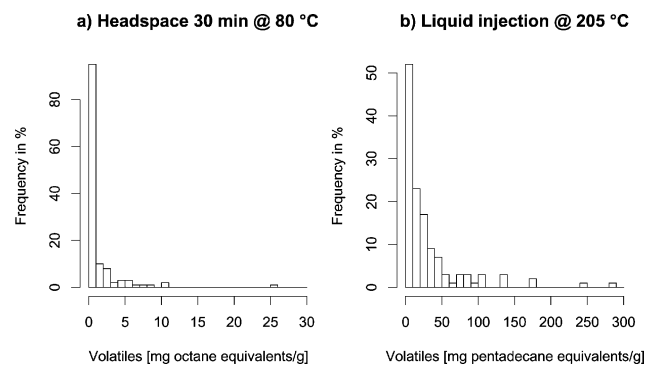
**Water by GC.** The determination of water by gas chromatography has been used as a reference method in the field of food analysis for about two decades and has recently been adapted to the moisture analysis of various ionic liquids. Instead of calculating the sample's water content by the consumption of the Karl–Fischer reagent from the sample, a well defined single peak of H<sub>2</sub>O is used which is independent of the presence of further components in any individual sample-provided the H<sub>2</sub>O peak is properly separated from other interfering peaks. Using a special GC column, no interferences were found by GC with thermal conductivity detection (TCD), which was verified by GC-MS.

During our investigations, we found that the moisture content in air is the main factor disturbing analytical results below the 0.01% range. The equipment used has to be dried carefully and the condensation of moisture from environmental air has to be carefully prevented.

### Decomposition products and other volatiles

Ionic liquids are relatively thermally stable, but decompose under certain circumstances, as observed by thermogravimetric analysis.<sup>15–18</sup> Chemical decomposition may also occur, dependent on the reaction conditions. Since little attention has been paid to this aspect, we have developed methods to quantify the amount of total volatiles as a sum parameter. Thus, impurities that are volatile at temperatures up to the decomposition of the ionic liquids can be monitored by gas chromatography. In general, these are non-ionic substances such as the alkyl halides that are frequently used for the alkylation reaction, the Lewis base starting material, or the decomposition products of the cations, such as alkenes and alkyl halides from the Hofmann elimination and the reversed Menshutkin reaction, respectively. For the quantification of volatile impurities, a combination of headspace sampling and liquid injection has been chosen in order to cover an optimum range of possible impurities.

**Headspace GC.** Purity screening of a large, random part of our compound library (133 out of about 300 ionic liquids) with this method (30 min equilibration time at 80 °C) yielded results ranging from no detectable impurities to frequent occurrence of impurities in concentrations smaller than 1 mg g<sup>-1</sup> up to several mg g<sup>-1</sup> volatile and semi-volatile impurities, expressed as octane equivalents (Fig. 6a). It has to be noted, however, that these values can only be taken as approximations since the real response of the impurities will be different from octane and the



**Fig. 6** Histograms of volatile compounds detected by GC-FID after (a) 30 min equilibration at 80 °C and (b) liquid injection at 205 °C for a set of 133 ionic liquid samples.

equilibrium concentration of the impurities within the gas phase are dependent on the matrix as well as on the kinetics of reaching this equilibrium.

**Liquid injection.** By this method, semi-volatile substances up to the boiling point range of C<sub>24</sub> alkanes can be detected. Impurities are again assessed in a semi-quantitative way with FID detection, and expressed as pentadecane equivalents.

In particular, the presence of higher alkyl chlorides and nucleophiles (1-methylimidazole, methylpyridine *etc.*) can be determined by this method.

Samples screened with this method generally indicated higher levels of contamination than found with the headspace method, although some substances did not show any measurable impurities. Semi-quantitative assessment leads to sum values of up to 100 mg g<sup>-1</sup> and greater (Fig. 6b), pointing to thermal instability of the compounds at the chosen conditions. Results have to be carefully compared to thermogravimetric observations, in order to draw correct conclusions. Strictly speaking, the thermogravimetry of the pure compound has to be known in order to interpret the results from this method.

## Experimental

### Total ionic liquid content

For UV-absorbing ionic liquid cations such as imidazolium, pyridinium or quinolinium derivatives, standard reversed phase chromatography with UV detection can be applied with mixtures of acetonitrile and a sufficiently acidic buffer, preferably phosphoric acid/dihydrogen phosphate. The separation of complex ionic liquid mixtures in Fig. 2 was achieved using 70% acetonitrile (gradient grade, Fluka, Buchs, Switzerland), and 30% of a 5 mM solution of ammonium acetate in 0.1% acetic acid (p.a., Fluka). The column was a 150 mm Monochrom<sup>®</sup> MS column (Varian), with 3 mm i.d. and 5 μm particle size, operated at a flow rate of 0.5 mL min<sup>-1</sup> with an injection volume of 2 μL on a Hewlett Packard system Series 1100, with online degasser, autosampler and gradient pump and both a variable wavelength UV/VIS detector and a Bruker Esquire ESI-MS ion trap detector. Using the acetate buffer made it possible to identify non-UV-absorbing cations with the mass selective detector.

## Unreacted organic starting material

**Determination of 1-methylimidazole impurity in ionic liquids by GC using the standard addition method.** To 1 mL of a solution of  $[C_4mim]Cl$  ( $492 \text{ g L}^{-1}$ , *i.e.* approx.  $2.82 \text{ mol L}^{-1}$ ) in acetonitrile, a solution of 1-methylimidazole in acetonitrile ( $394.9 \text{ g L}^{-1}$ , *i.e.* approx.  $4.8 \text{ mol L}^{-1}$ ) was added in increments of 0.1, 0.2, 0.3 and 0.4 mL. All samples were diluted with acetonitrile to the 5 mL mark volumetric flasks, thus keeping the relative concentration of the ionic liquid constant. A  $3 \mu\text{L}$  sample was inserted into the GC-injector, which was equipped with a glass insert to prevent the accumulation of non-volatile ionic liquid on the column. Analysis was performed using on a gas chromatograph equipped with a PONA column, and FID detector operated at  $300 \text{ }^\circ\text{C}$ . The retention time of 1-methylimidazole was 12.5 min using this method (injector temperature  $250 \text{ }^\circ\text{C}$ , initial column temperature  $120 \text{ }^\circ\text{C}$ , rate  $4 \text{ }^\circ\text{C min}^{-1}$ , final temperature  $300 \text{ }^\circ\text{C}$ ), and resulted in a good  $R^2$  of 0.9984. The limit of detection of this method is  $2 \text{ g L}^{-1}$ .

**Determination of imidazole and pyridine impurities in ionic liquids by HPLC.** HPLC set-up: degasser: Degasys DG-1310, Uniflows (Japan); pumps: Model 2250, Bischoff (Germany); autosampler: "Triathlon" Type 900, Spark Holland BV; column thermostat: "Mistral" Type 880, Spark Holland BV; 20/20 diode array detector (UV-DAD): Groton (USA); instrument interface and data acquisition unit: McDAcq32 Chromatography Control System, Bischoff (Germany); software: Bischoff Chromatography Data Acquisition (Version: 2.1).

Sample preparation: approx. 150 mg of ionic liquid is weighed into a 25 mL volumetric flask and dissolved in the eluent mixture (30% v/v A, 70% v/v B, Table 2). The solution is transferred to a sample vial and analysed.

**Determination of primary and secondary amine impurities in ionic liquids by UV-spectroscopy.** Due the high toxicity (toxic to reproduction, cat. 3) of carbon disulfide, exposure must be avoided and all experiments carried out under the recommended safety precautions. It should be noted that due to the biphasic system and a consecutive dilution step, all concentrations given in the following ( $\text{mmol L}^{-1}$ ) refer to the amount of amine in the 2 mL aqueous phase prior to the addition of  $\text{CS}_2$ . The reliability of the method is critically dependent on two factors: firstly, best results were obtained with a 10% aqueous sodium hydroxide solution. Secondly, a constant reaction time (30 min) and reproducible intervals between derivatisation and UV-measurements have to be adhered to, due to the limited stability of the dithiocarbamates formed.

A seven point calibration with solutions of the pure amines was performed in the concentration ranges indicated in Table 3, *i.e.* in the absence of ionic liquid. A blank value was obtained by adding 0.100 mL of distilled water to 1.900 mL sodium hydroxide solution.

From a solution prepared from 0.5 g of the ionic liquid in 10 mL of an aqueous 10% sodium hydroxide solution, 1.900 mL are transferred to each of four test tubes. 0.100 mL of aqueous amine solutions with four equidistant concentrations (*e.g.* 0, 0.041, 0.082 and  $0.123 \text{ mol L}^{-1}$  for *n*-butylamine) are added to give 2.000 mL. 1.000 mL carbon disulfide is added

under cooling. The biphasic reaction mixtures are vigorously shaken for exactly 30 min at room temperature. 0.100 mL of the upper yellowish aqueous phases containing the hydrophilic dithiocarbamate are diluted to 25 mL in volumetric flasks and analysed immediately by UV-spectroscopy (SHIMADZU UV-2102 PC, 1 cm quartz cell, against sodium hydroxide solution). The spectra are recorded from 200 to 350 nm. The detection wavelength used depends on the amine analysed (Table 3) and ranges between 277 and 285 nm.

## Unreacted inorganic starting material (HY, MY) and by-products (MX, HX)

**Determination of halide content by Volhard titration ( $[X]^- > 1 \text{ wt.}\%$ ).** Approximately 0.5 g of ionic liquid is weighed into a volumetric flask (250 mL) and dissolved in either deionised water or acetone to give the sample solution. In an Erlenmeyer flask (250 mL), the sample solution (25 mL) is acidified with nitric acid (6 M, 5 mL). Silver(I) nitrate (Aldrich, volumetric standard, 0.100 M, 5 mL) is added to precipitate the halide. After swirling the mixture, the white precipitate is removed by gravity filtration, and the filtrate washed with three portions of dilute nitric acid. To the combined washings, 1 mL of the indicator (saturated, aqueous ammonium iron(III)sulfate) is added, and the solution titrated with potassium thiocyanate solution (Aldrich, volumetric standard, 0.100 M) until the first permanent reddish colour occurs. The endpoint is read from the burette (10 mL, class A). For each sample, this procedure is repeated three times, and the average of these titrations forms the final result.

**Semi-quantitative determination of trace amounts of halide ( $[X]^- > 10 \text{ ppm}$ ).** Chemicals: nitric acid 65% (Fluka, puriss. p.a. grade), chloride standard  $1 \text{ g L}^{-1}$  (Fluka, chloride ion chromatography standard solution), silver nitrate (Fluka, puriss. p.a. ACS reagent), ethanol (Fluka, absolute, denaturised with 1% toluene), acetone (Aldrich, HPLC grade). Silver nitrate solution (0.1 N) was obtained by dissolution of 17 g of silver(I)nitrate in 1000 mL deionised water.

In a Nessler cylinder, 2.5 g of the sample is dissolved in 30 mL deionised water and 1 mL nitric acid (65%) added. 1 mL silver nitrate (0.1 N) is added, and the mixture diluted to 50 mL with deionised water. Samples which are not soluble in water can be dissolved in up to 20 mL of ethanol.

For the 10 ppm standard, 25  $\mu\text{L}$  of the standard chloride solution ( $1 \text{ g L}^{-1}$ ), 30 mL deionised water and 0.5 mL of nitric acid (65%) are combined in a Nessler cylinder. 1 mL silver nitrate solution (0.1 N) is added and the mixture diluted to 50 mL.

Similarly, 0, 20, 40, 60 ppm standard solutions are prepared by using 0, 50, 100 and 150  $\mu\text{L}$  of the standard chloride solution ( $1 \text{ g L}^{-1}$ ), respectively. All solutions are allowed to stand in the dark for 30 min, before comparison to the standard solutions is made.

It should be noted that all glassware must be absolutely free of halide ions. This is achieved by maintaining a cleansing procedure, starting with soaking all glassware in concentrated nitric acid, rinsing with deionised water, followed by rinsing with high-purity acetone, and subsequent drying in an oven.

## Solvents from extraction procedures and water absorbed from the atmosphere

**Water by Karl–Fischer titration.** A Karl–Fischer Mettler DL37 Coulometer was used for the determination of water, using Hydranal®-Coulomat A and C (both from Riedel-deHaën). Samples are inserted into the titrator using a disposable 1 mL syringe, and approx. 0.05–0.10 mL injected. Solid samples are dissolved in chloroform with known water content, and analysed. The measurements are performed in duplicate, and agree within 5%.

**Water by GC.** We used extra dry pyridine (molecular sieve) from Acros Organics and 10 mL headspace vials with Teflon® layered silicone crimp caps for extraction. Depending on the expected moisture content of the sample, 5.0 mL of pyridine are mixed with *e.g.* 10 to 100 mg of sample and shaken extensively by using a shaker assembly, by ultrasonic or a rotor stator blender. For GC analysis, a 10 m × 0.32 mm (0.25 mm for GC-MS) Chrompack CP Porabond-Q column with 5 µm coating from Varian was used. Water analysis was carried out isothermally at 50 °C with a subsequent temperature ramp up to 240 °C in order to remove higher boiling compounds from the column. We found a non-linear relationship between peak area and concentration. Therefore, the standard addition method was not feasible and a polynomial was used for calibration.

## Decomposition products and other volatiles

**Headspace GC.** For headspace-GC, 100 mg ionic liquid sample are introduced in 20 mL vials, which are in turn placed into a headspace auto-sampler. Samples are equilibrated for 30 min at 80 °C, and chromatographed on a 50 m × 3 µm SE-54 column at a flow rate of about 3 mL min<sup>-1</sup>. With this method, a linear response can be expected for compounds up to the boiling point range of C<sub>10</sub>–C<sub>12</sub> alkanes. Detection by a flame ionisation detector (FID) allows for a semi-quantitative assessment of volatile to semi-volatile compounds, expressed as octane equivalents (response factor of octane = 1).

**Liquid injection.** In order to capture less volatile impurities, liquid injection on a standard injector (liner filled with quartz wool) is used. 100 mg of sample are dissolved in 10 mL of a solvent suitable for controlled evaporation (*e.g.* MeOH/EtOH). Care has to be taken that the sample is completely dissolved. The injector temperature is 200 °C. After dosage of 1 µL of the sample solution, the split of the injector is opened in order to get rid of any decomposition products that may form after volatiles have evaporated. The glass wool in the liner has to be replaced and the liner has to be thoroughly cleaned on a regular basis. The choice of the column is less critical than in the above method, a DB-5 column with 0.25 µm film has proven adequate. By this method, semi-volatile substances up to the boiling point range of C<sub>24</sub> alkanes can be detected. Impurities are again assessed in a semi-quantitative way with FID detection, and expressed as pentadecane equivalents.

## Conclusions

In summary, the precise determination of impurities in ionic liquids is of utmost importance. We have shown that widely-

available, reliable methods exist, so that any laboratory should be able to specify the materials their data is derived from. At present, a detailed specification of the quality of ionic liquids (irrespective of them being self-made or from a commercial source) used for each experiment is most likely more essential than working with ultra-pure, expensive material.

A thorough drying step (*in vacuo* at 80 °C for 12 h) must follow the preparation of each batch, and subsequent sample preparation should optimally be carried out in a dry-box. Alternatively, the water content must be determined at the time of the experiment.

Very little attention has been paid to impurities already present in the starting materials of ionic liquids. These may be negligible in R&D, since usually reactants of high purity are being used. However, due to the unique nature of ionic liquids, analytical problems may arise during the transfer of a process to industrial scale, especially if the impurities are high-boiling compounds or salts with a high affinity to the ionic liquid phase.

Hence, in order to provide reliable data on ionic liquids, future work should include a minimum of relevant analytical specifications, *i.e.* water, amine and halide contents.

## Acknowledgements

The donation of ionic liquid samples (BASF SE, Merck KGaA, Sigma–Aldrich Chemie GmbH (Dr G. Müller)), is greatly appreciated. The authors thank C. Palik and A. Wermann for their valuable contributions in the laboratory. A.S. is indebted to the Friedrich-Schiller University (HWP) and the DFG for funding within the Priority programme SPP 1191 Ionic Liquids. The UFT ionic liquid team (here P. B., A. M., J. R. and B. J.) is thankful for support by Merck KGaA in the context of a strategic partnership.

## Notes and references

- 1 J. S. Wilkes and M. J. Zaworotko, *J. Chem. Soc., Chem. Commun.*, 1992, 965.
- 2 P. Wasserscheid, and T. Welton, *Ionic Liquids in Synthesis*, 2nd edn, Wiley-VCH, 2008.
- 3 M. Seiler, C. Jork and W. Arlt, *Chem.-Ing.-Tech.*, 2004, **76**, 735.
- 4 A. P. Abbott and K. J. McKenzie, *Phys. Chem. Chem. Phys.*, 2006, **8**, 4265.
- 5 R. F. de Souza, J. C. Padilha, R. S. Goncales and J. Dupont, *Electrochem. Commun.*, 2003, **5**, 728.
- 6 J. Ranke, S. Stolte, R. Störmann, J. Arning and B. Jastorff, *Chem. Rev.*, 2007, **107**, 2183.
- 7 P. J. Scammells, J. L. Scott and R. D. Singer, *Aust. J. Chem.*, 2005, **58**, 155.
- 8 K. R. Seddon, in *The International George Papatheodorou Symposium*, ed. S. Boghosian, V. Dracopoulos, C. G. Kontoyannis and G. A. Voyiatzis, Patras, 1999, 131.
- 9 K. R. Seddon, A. Stark and M. J. Torres, *Pure Appl. Chem.*, 2000, **72**, 2275.
- 10 A. Stark and K. R. Seddon, *Ionic Liquids*, ed. A. Seidel, John Wiley & Sons, Inc., Hoboken NJ, vol. 26, 2007, 836.
- 11 P. A. Z. Suarez, S. Einloft, J. E. L. Dullius, R. F. de Souza and J. Dupont, *J. Chim. Phys. Phys.-Chim. Biol.*, 1998, **95**, 1626.
- 12 K. McCamley, N. A. Warner, M. M. Lamoureux, P. J. Scammells and R. D. Singer, *Green Chem.*, 2004, **6**, 341.
- 13 R. C. Thied, K. R. Seddon, W. R. Pitner, and D. W. Rooney, Treatment of molten salts reprocessing wastes, *World Pat.* WO9941752, 1999.
- 14 P. Bonhôte, A. P. Dias, N. Papageorgiou, K. Kalyanasundaram and M. Grätzel, *Inorg. Chem.*, 1996, **35**, 1168.



- 15 H. L. Ngo, K. LeCompte, L. Hargens and A. B. McEwen, *Thermochim. Acta*, 2000, **357**, 97.
- 16 J. G. Huddleston, A. E. Visser, W. M. Reichert, H. D. Willauer, G. A. Broker and R. D. Rogers, *Green Chem.*, 2001, **3**, 156.
- 17 J. D. Oxley, T. Prozorov and K. S. Suslick, *J. Am. Chem. Soc.*, 2003, **125**, 11138.
- 18 K. J. Baranyai, G. B. Deacon, D. R. MacFarlane, J. M. Pringle and J. L. Scott, *Aust. J. Chem.*, 2004, **57**, 145.
- 19 C. M. Gordon, A. J. McLean, M. J. Muldoon and I. R. Dunkin, Ionic Liquids As Green Solvents: Progress and Prospects, *ACS Symp. Ser.*, 2003, **856**, 357.
- 20 I. Billard, G. Moutiers, A. Labet, A. El Azzi, C. Gaillard, C. Mariet and K. Lutzenkirchen, *Inorg. Chem.*, 2003, **42**, 1726.
- 21 D. L. Boxall and R. A. Osteryoung, *J. Electrochem. Soc.*, 2004, **151**, E41.
- 22 P. Nockemann, K. Binnemans and K. Driesen, *Chem. Phys. Lett.*, 2005, **415**, 131.
- 23 M. J. Earle, C. M. Gordon, N. V. Plechkova, K. R. Seddon and T. Welton, *Anal. Chem.*, 2007, **79**, 758.
- 24 Y. Chauvin, L. Mussmann and H. Olivier, *Angew. Chem., Int. Ed. Engl.*, 1996, **34**, 2698.
- 25 P. A. Z. Suarez, J. E. L. Dullius, S. Einloft, R. F. deSouza and J. Dupont, *Inorg. Chim. Acta*, 1997, **255**, 207.
- 26 B. Ellis, W. Keim and P. Wasserscheid, *Chem. Commun.*, 1999, 337.
- 27 A. J. Carmichael, M. J. Earle, J. D. Holbrey, P. B. McCormac and K. R. Seddon, *Org. Lett.*, 1999, **1**, 997.
- 28 C. E. Song and E. J. Roh, *Chem. Commun.*, 2000, 837.
- 29 J. L. Anthony, E. J. Maginn and J. F. Brennecke, *J. Phys. Chem. B*, 2001, **105**, 10942.
- 30 K. R. Seddon and A. Stark, *Green Chem.*, 2002, **4**, 119.
- 31 G. S. Owens and M. M. Abu-Omar, Ionic Liquids- Industrial Applications for Green Chemistry, *ACS Symp. Ser.*, 2002, **818**, 321.
- 32 R. F. de Souza, V. Rech and J. Dupont, *Adv. Synth. Catal.*, 2002, **344**, 153.
- 33 M. A. Klingshirn, G. A. Broker, J. D. Holbrey, K. H. Shaughnessy and R. D. Rogers, *Chem. Commun.*, 2002, 1394.
- 34 R. A. Sheldon, R. Madeira Lau, M. J. Sogredrager, F. van Rantwijk and K. R. Seddon, *Green Chem.*, 2002, **4**, 147.
- 35 V. Gallo, P. Mastrolilli, C. F. Nobile, G. Romanazzi and G. P. Suranna, *J. Chem. Soc., Dalton Trans.*, 2002, 4339.
- 36 D. L. Davies, S. K. Kandola and R. K. Patel, *Tetrahedron: Asymmetry*, 2004, **15**, 77.
- 37 A. Stark, M. Ajam, M. Green, H. G. Raubenheimer, A. Ranwell and B. Ondruschka, *Adv. Synth. Catal.*, 2006, **348**, 1934.
- 38 M. C. Buzzeo, R. G. Evans and R. G. Compton, *ChemPhysChem*, 2004, **5**, 1106.
- 39 M. P. Atkins, P. Davey, G. Fitzwater, O. Rouher, K. R. Seddon, and J. Swindall, *Ionic Liquids: A Map for Industrial Innovation*, Q001, London, 2004; BCS Incorporated, Accelerating ionic liquids commercialisation, *Chemical Vision 2020 Technology Partnership*, Department of Energy Industrial Technologies Programme, American Chemical Society, 2004.
- 40 J. D. Holbrey and K. R. Seddon, *Clean Prod. Process.*, 1999, **1**, 223.
- 41 L. C. Branco, J. N. Rosa, J. J. M. Ramos and C. A. M. Afonso, *Chem.-Eur. J.*, 2002, **8**, 3671.
- 42 C. Villagran, C. E. Banks, M. Deetlefs, G. Driver, W. R. Pitner, R. G. Compton and C. Hardacre, Ionic Liquids IIIb: Fundamentals, Progress, Challenges and Opportunities: Transformations and Processes, *ACS Symp. Ser.*, 2005, **902**, 244.
- 43 A. E. Visser, R. P. Swatloski, W. M. Reichert, S. T. Griffin and R. D. Rogers, *Ind. Eng. Chem. Res.*, 2000, **39**, 3596.
- 44 G. A. Baker and S. N. Baker, *Aust. J. Chem.*, 2005, **58**, 174.
- 45 J. Pernak, K. Sobaszekiewicz and I. Mirska, *Green Chem.*, 2003, **5**, 52.
- 46 J. Ranke, K. Molter, F. Stock, U. Bottin-Weber, J. Poczubutt, J. Hoffmann, B. Ondruschka, J. Filser and B. Jastorff, *Ecotoxicol. Environ. Saf.*, 2004, **58**, 396.
- 47 J. Ranke, F. Stock, A. Müller, S. Stolte, R. Störmann, U. Bottin-Weber and B. Jastorff, *Ecotoxicol. Environ. Saf.*, 2007, **67**, 430.
- 48 A. M. Scurto, S. Aki and J. F. Brennecke, *J. Am. Chem. Soc.*, 2002, **124**, 10276.
- 49 Z. B. Alfassi, R. E. Huie, B. L. Milman and P. Neta, *Anal. Bioanal. Chem.*, 2003, **377**, 159.
- 50 W. D. Qin, H. P. Wei and S. F. Y. Li, *Analyst*, 2002, **127**, 490.
- 51 M. J. Markuszewski, P. Stepnowski and M. P. Marszall, *Electrophoresis*, 2004, **25**, 3450.
- 52 G. Le Rouzo, C. Lamouroux, C. Bresson, A. Guichard, P. Moisy and G. Moutiers, *J. Chromatogr., A*, 2007, **1164**, 139.
- 53 P. Stepnowski and W. Mroziak, *J. Sep. Sci.*, 2005, **28**, 149.
- 54 M. Urbánek, A. Varenne, P. Gebauer, L. Křivánková and P. Gareil, *Electrophoresis*, 2006, **27**, 4859.
- 55 J. F. Brennecke, L. A. Blanchard, J. L. Anthony, Z. Gu, I. Zarraga and D. T. Leighton, Clean Solvents—Alternative Media for Chemical Reactions and Processing, *ACS Symp. Ser.*, 2002, **819**, 82.
- 56 J. D. Holbrey, K. R. Seddon and R. Wareing, *Green Chem.*, 2001, **3**, 33.
- 57 P. Stepnowski, J. Nichthäuser, W. Mroziak and B. Buszewski, *Anal. Bioanal. Chem.*, 2006, **385**, 1483.
- 58 P. Stepnowski, A. Miller, P. Behrend, J. Ranke, J. Hoffmann and B. Jastorff, *J. Chromatogr., A*, 2003, **993**, 173.
- 59 S. Kromidas, *HPLC Tips für Anwender*, Hoppenstedt Bonnier Zeitschriften, 2003.
- 60 H. Matsumoto, H. Kageyama and Y. Miyazaki, *Chem. Lett.*, 2001, 182.
- 61 S. Forsyth, J. Golding, D. R. MacFarlane and M. Forsyth, *Electrochim. Acta*, 2001, **46**, 1753.
- 62 K. S. Kim, S. Choi, D. Dembereinyamba, H. Lee, J. Oh, B. B. Lee and S. J. Mun, *Chem. Commun.*, 2004, 828.
- 63 A. W. M. Lee, W. H. Chan, C. M. L. Chiu and K. T. Tang, *Anal. Chim. Acta*, 1989, **218**, 157.
- 64 A. Stark, O. Braun and B. Ondruschka, *Anal. Sci.*, 2008, **24**, 681.
- 65 W. A. Herrmann and C. Koecher, *Angew. Chem., Int. Ed. Engl.*, 1997, **36**, 2162.
- 66 J. L. Anderson, J. Ding, T. Welton and D. W. Armstrong, *J. Am. Chem. Soc.*, 2002, **124**, 14247.
- 67 J. L. Anderson and D. W. Armstrong, *Anal. Chem.*, 2003, **75**, 4851.
- 68 C. Villagran, M. Deetlefs, W. R. Pitner and C. Hardacre, *Anal. Chem.*, 2004, **76**, 2118.
- 69 D. Berthier, A. Varenne, P. Gareil, M. Digne, C. P. Lienemann, L. Magna and H. Olivier-Bourbigou, *Analyst*, 2004, **129**, 1257.
- 70 L. Xiao and K. E. Johnson, *J. Electrochem. Soc.*, 2003, **150**, E307.
- 71 C. Villagran, C. E. Banks, C. Hardacre and R. G. Compton, *Anal. Chem.*, 2004, **76**, 1998.
- 72 A. I. Vogel, in *Textbook of quantitative inorganic analysis*, eds. J. Mendham, R. C. Denney, J. D. Barnes, and M. J. K. Thomas, Longmans, Green and Co., London, 2000.
- 73 K. R. Seddon, A. Stark and M. J. Torres, Clean Solvents- Alternative Media for Chemical Reactions and Processing, *ACS Symp. Ser.*, 2002, **819**, 34.



# The role of the support in achieving high selectivity in the direct formation of hydrogen peroxide

Edwin Ntainjua N.,<sup>a</sup> Jennifer K. Edwards,<sup>a</sup> Albert F. Carley,<sup>a</sup> Jose Antonio Lopez-Sanchez,<sup>a</sup> Jacob A. Moulijn,<sup>a</sup> Andrew A. Herzing,<sup>b,c</sup> Christopher J. Kiely<sup>b</sup> and Graham J. Hutchings<sup>\*a</sup>

Received 11th June 2008, Accepted 31st July 2008

First published as an Advance Article on the web 26th September 2008

DOI: 10.1039/b809881f

Pd-only, Au-only and bimetallic AuPd catalysts supported on a range of supports ( $\text{Al}_2\text{O}_3$ ,  $\text{TiO}_2$ ,  $\text{MgO}$ , and C) have been prepared by impregnation and tested for the hydrogenation and decomposition of hydrogen peroxide under conditions similar to those used in direct synthesis of hydrogen peroxide. Hydrogenation and decomposition are the main pathways for loss of selectivity and yield in the direct synthesis reaction, and the support is found to be a crucial parameter with respect to hydrogenation and decomposition activity. We show that by making the right choice of support for both the monometallic and bimetallic Au and Pd catalysts, it is possible to achieve very low hydrogen peroxide hydrogenation and decomposition activity, thus enhancing hydrogen peroxide productivity during synthesis. Carbon is found to be the optimal support for both monometallic Au and Pd catalysts as well as Au–Pd alloys, since carbon-supported catalysts gave the lowest hydrogenation and decomposition activities. Au-only catalysts were generally less active than Pd-only catalysts when utilizing the same support and metal loading. The addition of Au to Pd catalysts supported on  $\text{TiO}_2$  and carbon resulted in a decrease in both  $\text{H}_2\text{O}_2$  hydrogenation and decomposition while the reverse effect was observed for the  $\text{Al}_2\text{O}_3$  and  $\text{MgO}$ -supported catalysts. These effects are discussed in terms of the basicity of the support, and in particular the isoelectronic point of the support, which is a major factor in controlling the stability of hydrogen peroxide under reaction conditions.

## Introduction

Hydrogen peroxide ( $\text{H}_2\text{O}_2$ ) is an important chemical with many industrial applications, being mainly used as a bleach and disinfectant.<sup>1</sup> It also has a great potential for use as an oxidant for the production of numerous valuable organic compounds such as epoxides. The current commercial process for the production of  $\text{H}_2\text{O}_2$  involves the sequential hydrogenation and oxidation of an alkyl anthraquinone, thereby avoiding the potential for explosive contact between hydrogen and oxygen to occur.<sup>1</sup> This indirect process is both well established and operated around the world, and the annual production of  $\text{H}_2\text{O}_2$  is about 2 M tonnes using this route. The process has many non-green features, the most important being that the process is only economic on a large scale, and this necessitates the production of very concentrated solutions of aqueous  $\text{H}_2\text{O}_2$  which incurs very high energy utilisation. These concentrated solutions are then shipped to the point of use, which incurs further energy costs due to transportation. In contrast, most uses of  $\text{H}_2\text{O}_2$  require

relatively dilute solutions of  $\text{H}_2\text{O}_2$  and so there is a marked mismatch between production and utilisation. The introduction of a direct process would overcome the requirement to produce concentrated solutions of  $\text{H}_2\text{O}_2$  since it could be used at the point of production as a dilute solution. Also, the alkyl anthraquinone used in the indirect process degrades over time and this produces additional waste.

The direct synthesis of  $\text{H}_2\text{O}_2$  from molecular hydrogen and oxygen using metal-supported catalysts is considered to be an environmentally benign and economically attractive to the indirect process.<sup>2–16</sup> It could soon compete with the indirect process if selectivities based on  $\text{H}_2$  utilisation can be improved. Indeed, a pilot plant for the direct process is currently being constructed.<sup>17</sup> Pd-based catalysts are by far the most extensively investigated catalysts for the direct process.<sup>2–15,18–21</sup> However, in recent studies,<sup>22–29</sup> it has been shown that a combination of Pd with Au promotes both the activity and selectivity for the direct synthesis reaction. Despite the high selectivity achieved by the use of these bimetallic Au/Pd catalysts, there remains the challenge to deal with the non-selective hydrogenation and decomposition of  $\text{H}_2\text{O}_2$  for which these catalysts can still be active.<sup>27–29</sup> Both of these reactions limit the selectivity that can be achieved with the direct synthesis process. This has previously been the subject of many studies for supported Pd catalysts,<sup>18–21</sup> and dilute acids or halides have to be added to the reaction mixture to suppress the hydrogenation and decomposition of  $\text{H}_2\text{O}_2$ . However, the addition of these materials is both non-green

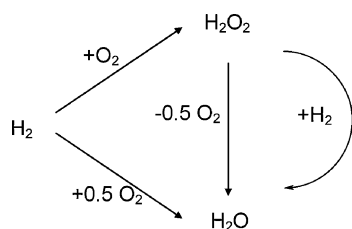
<sup>a</sup>Cardiff University, School of Chemistry, Main Building, Park Place, Cardiff, UK CF10 3AT. E-mail: hutch@cardiff.ac.uk; Fax: +44 29 2087 4059; Tel: +44 29 2087 4059

<sup>b</sup>Center for Advanced Materials and Nanotechnology, Lehigh University, 5 East Packer Avenue, Bethlehem, PA, 18015-3195, USA

<sup>c</sup>National Institute of Standards and Technology, Surface and Microanalysis Science Division, 100 Bureau Drive, Mailstop 8371, Gaithersburg, MD, 20899-8371, USA

and is likely to increase significantly the cost of production as further treatment is required to separate the acid or halide from the final product. In addition there are major corrosion problems associated with the use of these chemicals. Interestingly, the Au–Pd alloy catalysts do not require the use of these additives to achieve high selectivity and this represents a major potential advantage for utilizing these bimetallic catalysts.

We have previously shown that the nature of support is crucial for the direct synthesis of  $\text{H}_2\text{O}_2$  over Au/Pd-supported catalysts.<sup>28,29</sup> To identify if the major reason for these differences in activity are mainly associated with sequential  $\text{H}_2\text{O}_2$  hydrogenation and/or decomposition (Scheme 1) we have now investigated the role of the support in controlling these reactions. In this paper we investigate the effect of different supports ( $\text{Al}_2\text{O}_3$ ,  $\text{TiO}_2$ ,  $\text{MgO}$ , and carbon) on both hydrogenation and decomposition of  $\text{H}_2\text{O}_2$  over monometallic Au- and Pd-supported catalysts as well as the more active bimetallic Au/Pd-supported catalysts. The study therefore provides valuable insights into the design of suitable catalyst formulations for the direct synthesis of  $\text{H}_2\text{O}_2$ .



Scheme 1

## Experimental

### Catalyst preparation

Catalysts comprising 2.5 wt% Au/2.5 wt% Pd/support were prepared using the following standard method (all quantities stated are per g of finished catalyst)  $\text{PdCl}_2$  (0.042 g, Johnson Matthey) was added to an  $\text{HAuCl}_4 \cdot 3\text{H}_2\text{O}$  solution (2.5 ml, 5 g in 250 ml) and stirred at 80 °C until the Pd dissolved completely. The appropriate support (0.95 g;  $\text{TiO}_2$  (P25, Degussa),  $\text{Al}_2\text{O}_3$  (CA-150 mesh, Aldrich),  $\text{MgO}$  (BDH Chemicals Ltd, > 90%), or C (G60, Aldrich)) was then added to the solution and stirred to form a paste. The paste was dried (110 °C, 16 h) before calcination (400 °C, 3 h). Monometallic 5 wt% Au and 5 wt% Pd-supported catalysts were prepared in a similar way using appropriate amounts of  $\text{PdCl}_2$  or  $\text{HAuCl}_4 \cdot 3\text{H}_2\text{O}$  solution and support. Deionised water (2–3 ml) was used to dissolve the  $\text{PdCl}_2$  for preparation of Pd-only supported catalysts.

### Catalyst characterisation and testing

XPS measurements were made on a Kratos Axis Ultra DLD spectrometer. Samples were mounted using double-sided adhesive tape, and binding energies referenced to the C(1 s) binding energy of adventitious carbon contamination taken to be 284.7 eV. Monochromatic Al  $K\alpha$  radiation was used for all analyses except for Au–Pd/MgO where we employed a non-monochromatised Mg  $K\alpha$  source to avoid overlap of the Au(4d)–Pd(3d) region with intense features arising from KLL

Auger transitions. For the Au–Pd/MgO sample there was also significant overlap between the Mg(2 s) signal and the much weaker Au(4f) peaks. It was possible to extract the intensity of the Au(4f<sub>7/2</sub>) component by means of curve-fitting and this intensity was scaled appropriately to obtain the intensity of the Au(4f) doublet. The intensities of the Au(4f) and Pd(3d) features were used to derive Pd : Au surface molar ratios.

Samples were prepared for electron microscopy analysis by dispersing the powders in high-purity ethanol and allowing a drop of the solution to dry on a 300-mesh, Cu-supported lacey carbon film (SPI). Scanning transmission electron microscopy (STEM) annular dark-field (ADF) imaging and X-ray energy dispersive spectroscopy (XEDS) was carried out using a VG HB603 dedicated STEM operating at 300 kV comprising a Nion Co. spherical aberration corrector. The instrument was also equipped with an Oxford Inca 300 system for the acquisition of XEDS spectra images. An entire X-ray spectrum from 0–20 keV at 20 eV channel<sup>-1</sup> was acquired for 250 ms at each pixel position.

Hydrogen peroxide hydrogenation and decomposition was evaluated using a Parr Instruments stainless steel autoclave with a nominal volume of 50 ml and a maximum working pressure of 14 MPa. To test each catalyst for  $\text{H}_2\text{O}_2$  hydrogenation, the autoclave was charged with catalyst (0.01 g) and a solution containing 4 wt%  $\text{H}_2\text{O}_2$  (5.6 g MeOH, 2.22 g  $\text{H}_2\text{O}$  and 0.68 g  $\text{H}_2\text{O}_2$  (50%)). The charged autoclave was then purged three times with 5%  $\text{H}_2/\text{CO}_2$  (0.7 MPa) before filling with 5%  $\text{H}_2/\text{CO}_2$  to a pressure of 2.9 MPa at 20 °C. The temperature was allowed to decrease to 2 °C followed by stirring (at 1200 rpm) of the reaction mixture for 30 min. The above reaction parameters represent the optimum conditions we have established for the synthesis of  $\text{H}_2\text{O}_2$ .<sup>23</sup> The only difference is the absence of  $\text{O}_2$  and the addition of  $\text{H}_2\text{O}_2$  in the reaction mixture. Catalysts were tested for decomposition of  $\text{H}_2\text{O}_2$  using a similar procedure to that described above but without adding  $\text{H}_2/\text{CO}_2$  to the reaction mixture. All decomposition experiments were also performed at 2 °C for 30 min duration. The wt% of  $\text{H}_2\text{O}_2$  hydrogenated or decomposed was determined by titrating aliquots of the fresh solution and the solution after reaction with acidified  $\text{Ce}(\text{SO}_4)_2$  (0.0288 M) in the presence of two drops of ferroin indicator.

Synthesis of  $\text{H}_2\text{O}_2$  from  $\text{H}_2$  and  $\text{O}_2$  was performed using similar conditions in the presence of  $\text{O}_2$  and with no added  $\text{H}_2\text{O}_2$  (5%  $\text{H}_2/\text{CO}_2$  and 25%  $\text{O}_2/\text{CO}_2$ , 1:2  $\text{H}_2/\text{O}_2$  at 3.7 MPa, 5.6 g MeOH, 2.9 g  $\text{H}_2\text{O}$ , 0.01 g catalyst and 1200 rpm).  $\text{H}_2\text{O}_2$  productivity was determined by titration of the final filtered solution as described previously.  $\text{H}_2$  conversion was calculated by gas analysis before and after reaction using a GC with TCD and CP, CarboPlot P7 column (25 m, 0.53 mm id).

## Results and discussion

### Hydrogen peroxide hydrogenation and decomposition

We initially investigated the hydrogenation, decomposition and synthesis of hydrogen peroxide over the individual supports using our standard reaction conditions. Experiments in the absence of catalyst under these conditions did not hydrogenate, decompose or produce hydrogen peroxide, indicating the absence of any background homogeneous reactions. As

expected the supports (Table 1) were not active as catalysts for the synthesis of hydrogen peroxide in the absence of gold and palladium. Carbon and MgO did show activity for both hydrogen peroxide hydrogenation and decomposition. On the basis of these initial results one would be tempted to postulate that the use of Al<sub>2</sub>O<sub>3</sub> or TiO<sub>2</sub> as supports would be beneficial in the design of active catalysts for the synthesis of hydrogen peroxide. Although we have previously shown that TiO<sub>2</sub> is a very effective support for Au–Pd bimetallic catalysts,<sup>26</sup> we have also demonstrated that carbon supported catalysts are far more effective.<sup>27</sup>

The hydrogenation and decomposition of hydrogen peroxide were investigated using the mono-metallic catalysts and the results are shown in Tables 2 and 3. The Pd catalysts (Table 2) all show increased rates of hydrogenation and decomposition when compared with the bare support (Table 1). This result is to be expected since both of these reactions are known to be very problematic with supported Pd catalysts for the direct synthesis reaction, and acid and halide additives have to be used to control these sequential reactions.<sup>18–21</sup> Specifically, the carbon-supported Pd catalyst displays the lowest rate of hydrogenation of hydrogen peroxide, and consequently gives the highest rate of synthesis of hydrogen peroxide in the direct reaction. However, there is no obvious trend relating hydrogen peroxide synthesis and hydrogenation activity for these supported Pd catalysts. This

is more apparent for the supported Au mono-metallic catalysts (Table 3), all of which showed very little activity in the synthesis of hydrogen peroxide under standard conditions. However, apart from the carbon-supported catalysts all gave higher rates of hydrogen peroxide hydrogenation compared with synthesis. This suggests that there is no direct link between the activity for the initial hydrogenation of oxygen to form hydrogen peroxide, and its subsequent hydrogenation. Hence it is possible that distinctly different sites may be responsible for these two reactions and this feature may be of considerable value in designing more selective catalysts. Interestingly, the Au/carbon catalyst showed no activity for hydrogen peroxide decomposition and hydrogenation, whereas the carbon support was active for both these reactions. The Au/MgO catalyst also showed a lower rate of hydrogenation of hydrogen peroxide than the bare MgO support. This may indicate that the gold nanoparticles are in fact decorating and blocking the sites responsible for these sequential reactions of hydrogen peroxide, which again suggests that the sites for synthesis and hydrogenation may be different.

The catalytic data for the bimetallic Au–Pd catalysts is shown in Table 4. We have previously reported that Au-rich core/Pd-rich shell structures form on Al<sub>2</sub>O<sub>3</sub>,<sup>23</sup> TiO<sub>2</sub>,<sup>26</sup> and Fe<sub>2</sub>O<sub>3</sub>,<sup>25</sup> supports, based on detailed XPS and STEM-XEDS measurements. In the case of Au–Pd/MgO we find the Pd : Au molar ratio derived from the XPS intensities is *ca* 16 : 1, which contrasts

**Table 1** Hydrogen peroxide hydrogenation, decomposition and synthesis over bare supports

Support	H <sub>2</sub> O <sub>2</sub> hydrog. <sup>a</sup> (wt%)	H <sub>2</sub> O <sub>2</sub> hydrog. rate <sup>a</sup> / mol kg <sub>cat</sub> <sup>-1</sup> h <sup>-1</sup>	H <sub>2</sub> O <sub>2</sub> decomp. <sup>b</sup> (wt%)	H <sub>2</sub> O <sub>2</sub> decomp. rate <sup>b</sup> / mol kg <sub>cat</sub> <sup>-1</sup> h <sup>-1</sup>	H <sub>2</sub> O <sub>2</sub> productivity <sup>c</sup> / mol kg <sub>cat</sub> <sup>-1</sup> h <sup>-1</sup>
Al <sub>2</sub> O <sub>3</sub>	0	0	0	0	0
TiO <sub>2</sub>	0	0	0	0	0
MgO	10	206	10	217	0
Carbon	4	94	1	24	0

<sup>a</sup> hydrog. = wt% H<sub>2</sub>O<sub>2</sub> hydrogenated, hydrog. rate = rate of hydrogenation of H<sub>2</sub>O<sub>2</sub> calculated from H<sub>2</sub>O<sub>2</sub> hydrogenated using standard reaction conditions: 4 wt% H<sub>2</sub>O<sub>2</sub> in solvent (5.6 g MeOH, 2.22 g H<sub>2</sub>O and 0.68 g 50% H<sub>2</sub>O<sub>2</sub>), 0.01 g catalyst, 2.9 MPa 5% H<sub>2</sub>/CO<sub>2</sub>, 2 °C, 1200 rpm. <sup>b</sup> decomp. = wt% H<sub>2</sub>O<sub>2</sub> decomposed to water and O<sub>2</sub>, decomp. rate = rate of decomposition of H<sub>2</sub>O<sub>2</sub> calculated from H<sub>2</sub>O<sub>2</sub> decomposed using standard reaction conditions: 4 wt% H<sub>2</sub>O<sub>2</sub> in solvent (5.6 g MeOH and 2.9 g H<sub>2</sub>O), 0.01 g catalyst, 2 °C, 1200 rpm. <sup>c</sup> Rate of hydrogen peroxide production determined after reaction: 5% H<sub>2</sub>/CO<sub>2</sub> and 25% O<sub>2</sub>/CO<sub>2</sub>, 1 : 2 H<sub>2</sub>/O<sub>2</sub> at 3.7 MPa, 5.6 g MeOH, 2.9 g H<sub>2</sub>O, 0.01 g catalyst and 1200 rpm).

**Table 2** Effect of support on hydrogen peroxide hydrogenation, decomposition and synthesis over monometallic Pd-supported catalysts

Catalyst	H <sub>2</sub> O <sub>2</sub> hydrog. <sup>a</sup> (wt%)	H <sub>2</sub> O <sub>2</sub> hydrog. rate <sup>a</sup> / mol kg <sub>cat</sub> <sup>-1</sup> h <sup>-1</sup>	H <sub>2</sub> O <sub>2</sub> decomp. <sup>a</sup> (wt%)	H <sub>2</sub> O <sub>2</sub> decomp. rate <sup>a</sup> / mol kg <sub>cat</sub> <sup>-1</sup> h <sup>-1</sup>	H <sub>2</sub> O <sub>2</sub> productivity <sup>a</sup> / mol kg <sub>cat</sub> <sup>-1</sup> h <sup>-1</sup>
5%Pd/Al <sub>2</sub> O <sub>3</sub>	11	200	1	24	9
5%Pd/TiO <sub>2</sub>	16	288	12	247	30
5%Pd/MgO	29	582	18	405	29
5%Pd/carbon	6	135	5	118	55

<sup>a</sup> Defined in Table 1.

**Table 3** Effect of support on hydrogen peroxide hydrogenation, decomposition and synthesis over monometallic Au-supported catalysts

Catalyst	H <sub>2</sub> O <sub>2</sub> hydrog. <sup>a</sup> (wt%)	H <sub>2</sub> O <sub>2</sub> hydrog. rate <sup>a</sup> / mol kg <sub>cat</sub> <sup>-1</sup> h <sup>-1</sup>	H <sub>2</sub> O <sub>2</sub> decomp. <sup>a</sup> (wt%)	H <sub>2</sub> O <sub>2</sub> decomp. rate <sup>a</sup> / mol kg <sub>cat</sub> <sup>-1</sup> h <sup>-1</sup>	H <sub>2</sub> O <sub>2</sub> Productivity <sup>a</sup> / mol kg <sub>cat</sub> <sup>-1</sup> h <sup>-1</sup>
5%Au/Al <sub>2</sub> O <sub>3</sub>	10	229	1	18	2.6
5%Au/TiO <sub>2</sub>	4	71	1	24	7
5%Au/MgO	5	100	1	12	0
5%Au/carbon	0	0	0	0	1

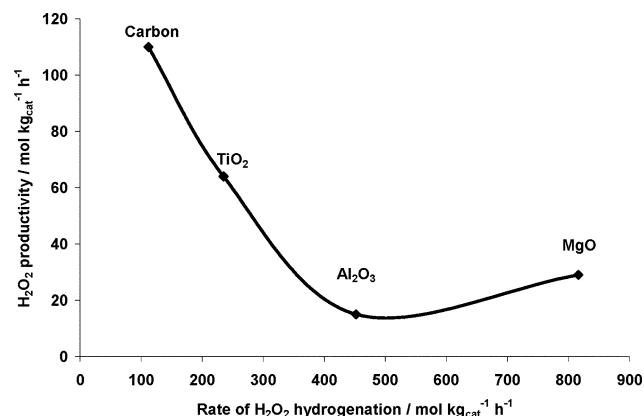
<sup>a</sup> Defined in Table 1.

**Table 4** Effect of support on hydrogen peroxide hydrogenation, decomposition, and synthesis over bimetallic Au/Pd-supported catalysts

Catalyst	H <sub>2</sub> O <sub>2</sub> hydrog. <sup>a</sup> (wt%)	H <sub>2</sub> O <sub>2</sub> hydrog. rate <sup>a</sup> / mol kg <sub>cat</sub> <sup>-1</sup> h <sup>-1</sup>	H <sub>2</sub> O <sub>2</sub> decomp. <sup>a</sup> (wt%)	H <sub>2</sub> O <sub>2</sub> decomp.rate <sup>a</sup> / mol kg <sub>cat</sub> <sup>-1</sup> h <sup>-1</sup>	H <sub>2</sub> O <sub>2</sub> Productivity <sup>a</sup> / mol kg <sub>cat</sub> <sup>-1</sup> h <sup>-1</sup>	H <sub>2</sub> sel. <sup>b</sup> (%)
Au–Pd/Al <sub>2</sub> O <sub>3</sub>	24	452	3	59	15	14
Au–Pd/TiO <sub>2</sub>	12	235	6	129	64	70
Au–Pd/MgO	39	817	25	535	29	38
Au–Pd/C	5	117	2	41	110	80

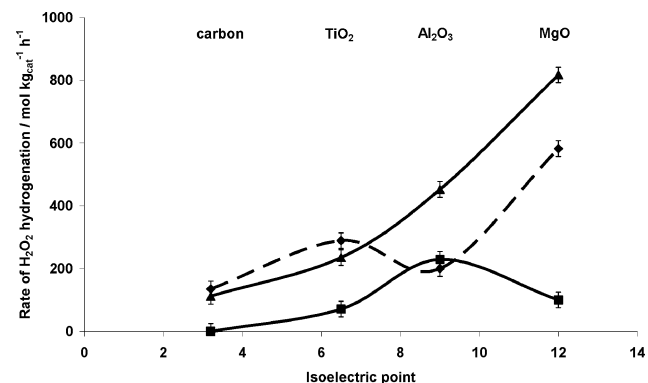
<sup>a</sup> Defined in Table 1. <sup>b</sup> Hydrogen selectivity calculated by analysis of the reaction gases before and after reaction using the standard condition.

markedly with the expected value of 1.9 : 1 for a homogeneous alloy (Pd : Au = 1 : 1 by weight), and is also therefore consistent with a core–shell structure for the bimetallic particles: in addition the Pd is noted to be in the +2 oxidation state, indicating the surface layer has been oxidised. Except for the MgO supported catalysts, the bimetallic catalysts are all more active for the synthesis of hydrogen peroxide. The addition of Au to Pd catalysts supported on TiO<sub>2</sub> and carbon resulted in a decrease in both H<sub>2</sub>O<sub>2</sub> hydrogenation and decomposition while the reverse effect was observed for the Al<sub>2</sub>O<sub>3</sub> and MgO-supported catalysts (Tables 2 and 4). The MgO-supported catalyst gave the highest rates of hydrogenation and decomposition, and the H<sub>2</sub> selectivity observed in the direct synthesis reaction is broadly in line with the levels of hydrogen peroxide hydrogenation and decomposition. There is an inverse correlation between the rate of H<sub>2</sub>O<sub>2</sub> formation and hydrogenation (Fig. 1) and Au–Pd catalysts with high rates of H<sub>2</sub>O<sub>2</sub> hydrogenation give very low rates of H<sub>2</sub>O<sub>2</sub> synthesis. Hence, it is the loss of the selective product *via* sequential hydrogenation that causes the poorer performance observed with Al<sub>2</sub>O<sub>3</sub>- and MgO-supported Au–Pd catalysts. Hence hydrogenation plays a key role in lowering H<sub>2</sub>O<sub>2</sub> production suggesting that the concentration of hydrogen relative to oxygen should be low under synthesis conditions. The importance of sequential hydrogenation has been recognized in the previous studies concerning supported Pd catalysts.<sup>18–21</sup> For Pd monometallic catalysts phosphoric acid and halide are added to stabilize the hydrogen peroxide.<sup>18–21</sup> However, we have previously demonstrated that with our most active and selective supported Au–Pd catalysts the addition of these compounds is deleterious.<sup>29</sup>



**Fig. 1** Relationship between H<sub>2</sub>O<sub>2</sub> production and H<sub>2</sub>O<sub>2</sub> hydrogenation rate over Au/Pd-supported catalysts.

Previous studies have also shown that in the direct synthesis reaction with Pd only catalysts phosphoric acid has to be added to arrest the sequential hydrogenation of the product.<sup>18–21</sup> We have demonstrated that the addition of acid is not required when employing Au–Pd bimetallic catalysts using our reaction conditions as the CO<sub>2</sub> diluent acts as an *in-situ* acid promoter.<sup>29</sup> However, it is apparent that the support has a major effect on both the synthesis of hydrogen peroxide as well as its hydrogenation, as shown in Fig. 1, and its decomposition. In these experiments we have in fact examined a range of supports that display different surface charges under reaction conditions. The degree of surface charging is controlled by the isoelectronic point of the support. To determine if this is a major parameter influencing the reactivity of the supported catalysts we have plotted the reactivity for hydrogenation, decomposition and synthesis against the isoelectronic point of the supports,<sup>30–33</sup> and the data are shown in Fig. 2–4. From these data it is clear that for the Au–Pd catalysts, in general, supports with a high isoelectronic point tend to hydrogenate hydrogen peroxide with high rates (Fig. 2). Interestingly, the Au mono metallic catalysts all show relatively low rates of hydrogenation. The trend is not so clear for decomposition (Fig. 3) as the Al<sub>2</sub>O<sub>3</sub>-supported catalysts all show very low rates of decomposition. However, the Al<sub>2</sub>O<sub>3</sub>-supported catalysts are not particularly active for the synthesis of H<sub>2</sub>O<sub>2</sub>; whereas, the observation of decreased H<sub>2</sub>O<sub>2</sub> decomposition with Al<sub>2</sub>O<sub>3</sub> as a support may be a useful feature when designing catalysts that use H<sub>2</sub>O<sub>2</sub> as an oxidant. The correlation between the rates of hydrogenation and H<sub>2</sub>O<sub>2</sub> synthesis indicates that the surface basicity is a major factor for these reactions. This effect cannot be totally ascribed to the addition of acid in the reaction mixture (*e.g.* the *in-situ* introduction of an acid by using CO<sub>2</sub> as diluent) since



**Fig. 2** H<sub>2</sub>O<sub>2</sub> hydrogenation as a function of the isoelectronic point of support. Key: ◆ Pd-only, ■ Au-only, ▲ Au–Pd.



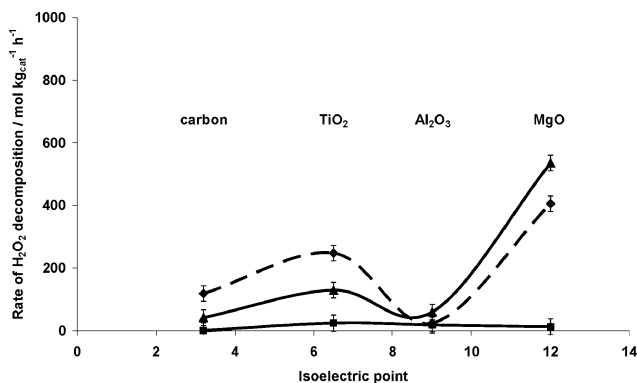


Fig. 3  $\text{H}_2\text{O}_2$  decomposition as a function of the isoelectronic point of support. Key:  $\blacklozenge$  Pd-only,  $\blacksquare$  Au-only,  $\blacktriangle$  Au-Pd.

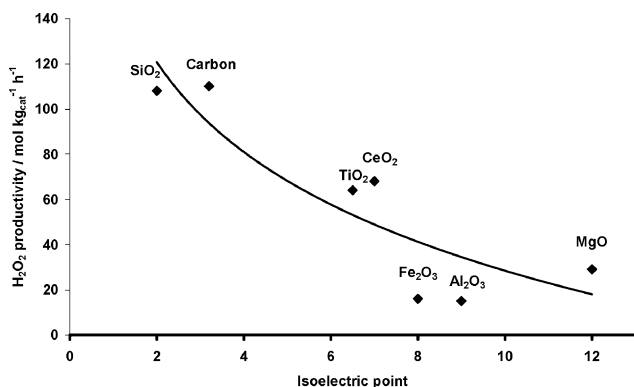


Fig. 4  $\text{H}_2\text{O}_2$  productivity over Au-Pd catalysts as a function of the isoelectronic point of support.

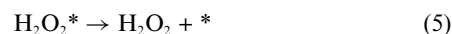
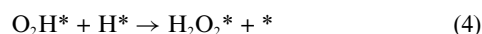
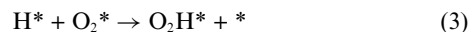
all our data are obtained under identical reaction conditions. Most importantly there is a definite correlation between the rate of hydrogen peroxide synthesis and the surface charge on the support (Fig. 4), since supports with low isoelectronic points (*i.e.* carbon and silica) give the highest rates of synthesis. In this correlation we have also included synthesis data obtained under the same reaction conditions using  $\text{CeO}_2$ , silica- and iron oxide-supported catalysts.<sup>24,29</sup> This correlation implies that the isoelectronic point of the support is an important design parameter for Au-Pd catalysts. In general the high rates of  $\text{H}_2\text{O}_2$  synthesis we observe are, in part, a consequence of the decreased rates of sequential hydrogenation (Fig. 1). Other design parameters will also be important, (*e.g.* dispersion of the metals and the degree of alloying of the Au-Pd bimetallic nanoparticles), however, we have now identified the isoelectronic point of the support as a major catalyst design parameter, and future studies will need to focus on exploiting this observation.

It is important to consider the factors that influence the selective formation of  $\text{H}_2\text{O}_2$ , since in the direct synthesis reaction several reactions take place simultaneously. Indeed, the mechanism and kinetics of  $\text{H}_2\text{O}_2$  synthesis and decomposition have been studied in detail previously.<sup>33-37</sup> The key reactions can be divided into four classes (see Scheme 1), namely:

1. Production of hydrogen peroxide from syngas
2. Production of water from syngas
3. Decomposition of hydrogen peroxide
4. Reduction of hydrogen peroxide by hydrogen

*A priori*, in our opinion, it is to be expected that these reactions are not independent reactions, but it is probable that they occur, at least partially, *via* common surface species. Based on our observations, and consideration of the previous studies, we suggest the following kinetic scheme.

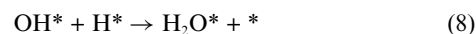
(i) Production of hydrogen peroxide (reaction (1)) takes place *via* the elementary steps:



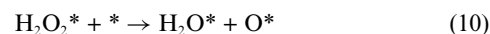
where  $^*$  denotes a vacant surface site.

So, in this proposal the formation of hydrogen peroxide occurs *via* a two step hydrogenation of adsorbed  $\text{O}_2$ . Conceptually, it is feasible that hydrogen peroxide could be generated by the combination of two surface hydroxyl radicals formed by initial oxygen bond scission and hydrogenation; but, this pathway will kinetically favour water synthesis by sequential hydrogenation, as discussed below.

(ii) Undesired side reactions leading to water (reactions (2), (3) and (4)) involve the dissociative adsorption of  $\text{O}_2$ :

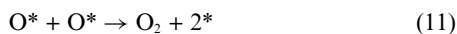


(iii) Direct dissociation of adsorbed  $\text{H}_2\text{O}_2$ , which is analogous to the dissociation of  $\text{N}_2\text{O}$ ,<sup>38</sup> might take place *via*:



This kinetic scheme describes the observed reactions, *viz.*, production of hydrogen peroxide and water from the  $\text{H}_2$  and  $\text{O}_2$  syngas, decomposition of hydrogen peroxide and the hydrogenation of hydrogen peroxide in terms of a relatively small number of elementary steps. It was decided to limit them to the smallest number of steps necessary for explaining the data while being in agreement with our observations. Although the data suggests that synthesis and hydrogenation might occur on different sites, at this stage it was decided not to include this in the kinetic scheme. We have not included the interaction with methanol, which we feel is justified because we observe no perceptible oxidation of methanol under our reaction conditions and the role of methanol is to increase the solubility of hydrogen under reaction conditions. Due to the low reaction temperature it is to be expected that strong adsorption takes place and the desorption step might be dominating the observed kinetics. According to the scheme decomposition of hydrogen peroxide takes place by reaction with a neighbouring empty site (eqn (10)). Under the conditions of hydrogenation the hydrogen will act as a scavenger (eqn (3) and (8)) and the concentration of empty

sites will increase as will the decomposition rate of hydrogen peroxide. A related alternative mechanism is the following. In the decomposition reaction the reverse step of eqn (2) has to take place:



When this reaction is slow the action of  $\text{H}_2$  would be to create a second channel for the removal of  $\text{O}^*$ . In  $\text{N}_2\text{O}$  decomposition this kinetic scheme was observed for ZSM-5 catalysts.<sup>38</sup> Hence, the above kinetic scheme can explain the fact that the rate of decomposition is increased when hydrogen is present and this effect will get stronger as the rate of dissociation of hydrogen increases.

The data show that monometallic Au based catalysts are not very effective in the production of hydrogen peroxide. They show relatively high hydrogenation rates (Table 3) and this suggests that under hydrogen peroxide production conditions the  $\text{O}^*$  concentration is high, efficiently reducing the rate of decomposition but also the rate of formation of hydrogen peroxide. When alloyed with Pd the addition of Au increases both the rate of hydrogen peroxide synthesis and the hydrogen selectivity and this effect may be related to the optimising the  $\text{O}^*$  concentration. Overall, MgO is a poor support, since it is very active in decomposing hydrogen peroxide. The reason for this is not related to its hydrogenation activity, but rather its basicity leads to high rates of decomposition of the desired product, and this suggests that other basic supports will be equally poor.

As the isoelectronic point of the support is a major factor in controlling the activity of the catalyst, it is interesting to consider whether there are additional factors that play a role during catalyst synthesis. The Au–Pd catalysts are prepared by wet impregnation from aqueous solutions of  $\text{HAuCl}_4$  and  $\text{PdCl}_2$ . Hence, there is the possibility that  $\text{Cl}^-$  could be retained on the surface of the catalysts using this preparation method. While the addition of halide during hydrogen peroxide synthesis is deleterious with Au–Pd catalysts,<sup>29</sup> it is possible, as discussed previously,<sup>27,39</sup> that the residual halide could be acting as an *in-situ* promoter. In addition, it is plausible that the surface charge of the support could affect the amount of  $\text{Cl}^-$  that is retained. As an initial investigation of this factor we have qualitatively monitored the amount of residual Cl in fresh catalysts using STEM-XEDS mapping of Cl on the surface of the carbon-,  $\text{TiO}_2$ - and  $\text{Al}_2\text{O}_3$ -supported unused Au–Pd catalysts following calcination at 400 °C. Fig. 5 shows a typical STEM-ADF image and the corresponding Pd  $L\alpha$  and Cl  $K\alpha$  elemental maps acquired from the Au–Pd/C catalyst. One of the major advantages

of the STEM-XEDS spectrum image technique is the ability to produce such maps with a very high spatial-resolution as demonstrated by the coincidence of the Pd  $L\alpha$  map (Fig. 5b) with the bright particles detected *via* ADF imaging (Fig. 5a). However, the map produced using the Cl  $K\alpha$  peak (Fig. 5c) is rather noisy since the amount of Cl present in the sample is very small and the resulting signal is barely resolved above the background. In this case, a more advantageous method of analyzing the STEM-XEDS spectrum images is to mine specific pixel areas of the data cubes which correspond to particular sample features (*i.e.* particles, and support only areas) and to examine the spectra they contain. This was carried out for the spectrum image data sets collected from the 2.5wt.%Au–2.5wt.%Pd catalysts supported on carbon (Fig. 6(a,b)),  $\text{Al}_2\text{O}_3$  (Fig 6(c,d)), and  $\text{TiO}_2$  (Fig. 6(e,f)). The X-ray spectra were extracted from pixels associated with either the metal particles (Fig. 6a–c) or the underlying support (Fig. 6d–f) and these spectra were then summed to produce a statistically more meaningful sum spectrum. The data clearly show that residual Cl is a significant component of the metal particles *and* the support areas in the carbon and  $\text{Al}_2\text{O}_3$  supported catalysts. In the case of the  $\text{TiO}_2$  supported catalyst, compared to the Pd  $L\alpha$  peak intensity the observed Cl  $K\alpha$  signal is significantly weaker in both the particle and support spectra than that in the spectra extracted from the C and  $\text{Al}_2\text{O}_3$  supported catalysts. In fact, in the  $\text{TiO}_2$  support spectra, the Cl  $K\alpha$  peak is just barely resolved above the background, suggesting that the residual Cl present in this sample is less than that detected in the carbon-supported catalyst and considerably less than that in the  $\text{Al}_2\text{O}_3$ -supported catalyst. These measurements suggest the amount of residual Cl does not simply correlate with the surface charge of the support, and, furthermore, does not appear to correlate with catalyst performance. However, it is also possible that only a trace amount of residual Cl is all that may be required to act as an *in-situ* promoter and this factor will be considered in a future detailed study.

## Conclusions

The role of support in the hydrogenation and decomposition of  $\text{H}_2\text{O}_2$  over Au-only, Pd-only, and Au–Pd-supported catalysts has been evaluated. Carbon-based catalysts showed the lowest  $\text{H}_2\text{O}_2$  hydrogenation and decomposition activity, making carbon the ideal support for Pd-only and Au–Pd-supported catalysts for  $\text{H}_2\text{O}_2$  synthesis. Indeed, carbon-supported catalysts gave the highest  $\text{H}_2\text{O}_2$  productivity. While many factors may

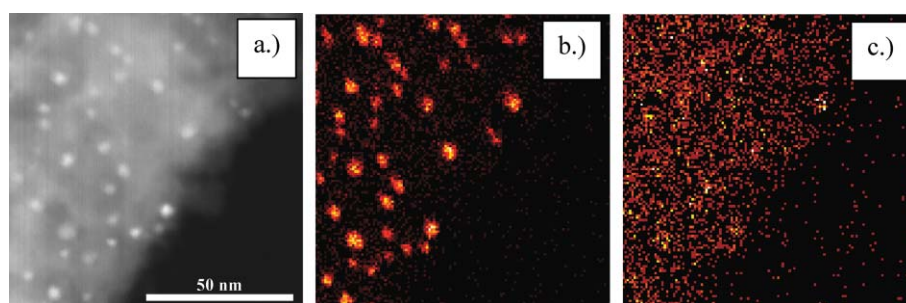
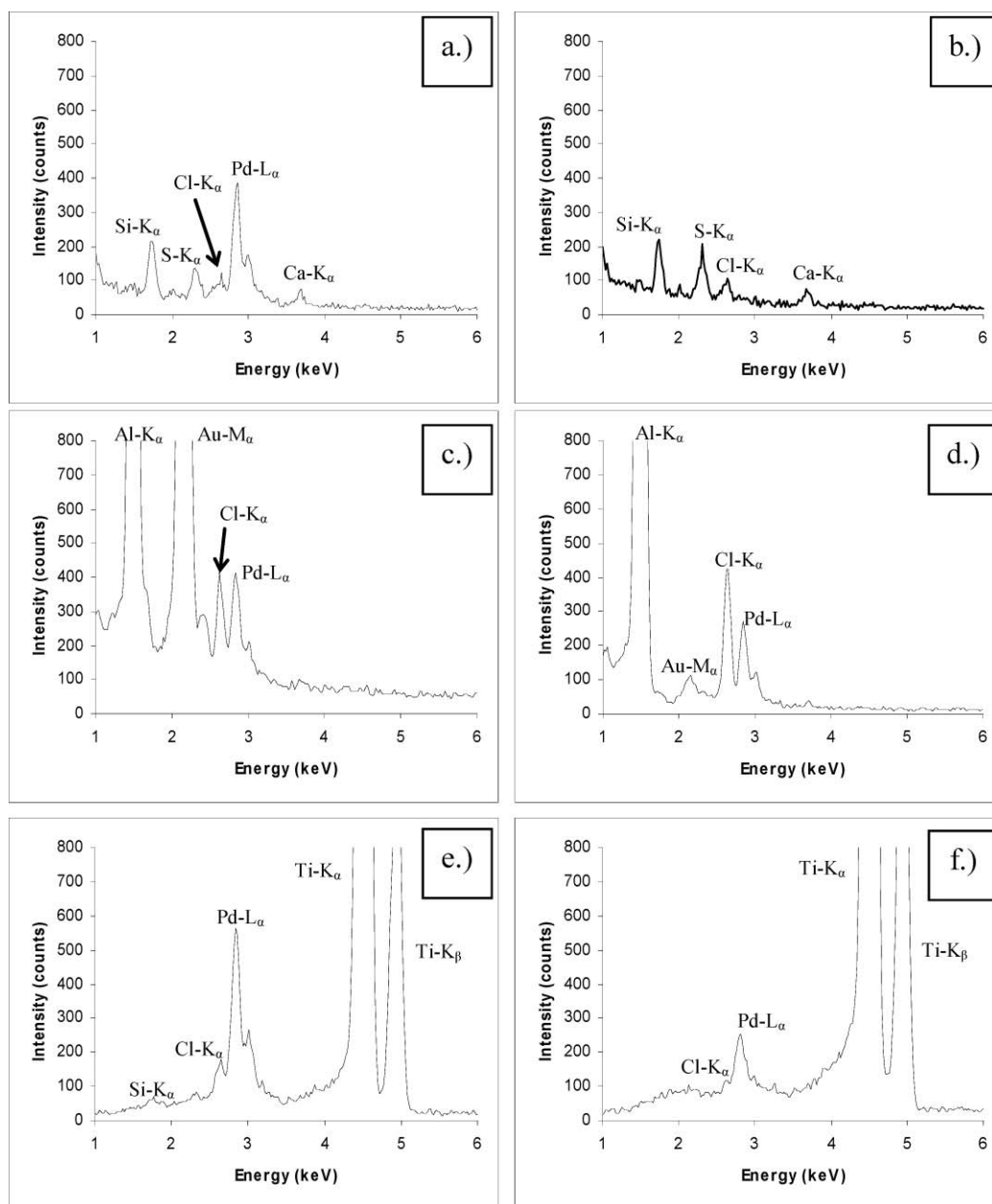


Fig. 5 STEM-ADF image (a) and corresponding Pd  $L\alpha$  (b) and Cl  $K\alpha$  (c) XEDS elemental maps of 2.5wt.%Au–2.5wt.%Pd/C catalyst.



**Fig. 6** Spectra extracted and summed from more than 500 pixels of STEM-XEDS data cubes corresponding to bimetallic particles (a,c,e) and the underlying support (b,d,f) acquired from 2.5wt.%Au–2.5wt.%Pd catalysts supported on carbon (a,b), Al<sub>2</sub>O<sub>3</sub> (c,d), and TiO<sub>2</sub> (e,f).

contribute to the observed trends in hydrogen peroxide synthesis, hydrogenation and decomposition, we have observed that the major parameter is the isoelectric point of the support, and supports with low isoelectronic points (*e.g.* carbon and silica) give catalysts with the highest rates for the synthesis of hydrogen peroxide. This observation is in line with previous data for Pd-only catalysts where acid has to be added to achieve appreciable selectivities for hydrogen utilisation. The isoelectronic point of the support controls the surface charge and clearly basic supports lead to the catalysis of non-desired sequential hydrogenation and decomposition of hydrogen peroxide. Having identified this major catalyst design parameter future studies should now concentrate on optimising the dispersion of the

Au–Pd bimetallic particles and the identification of the optimal particle size that is associated with high synthesis activity.

### Acknowledgements

This work formed part of the EU AURICAT project (Contract HPRN-CT-2002-00174) and an EPSRC funded project and we thank them for funding this research. We also thank the World Gold Council (through the GROW scheme), and Cardiff University (AA Reed studentship) for providing support for JKE. CJK and RT would also like to acknowledge the financial support of the NSF Nanomanufacturing program under contract # CMMI-0457602.

## References

- 1 H. T. Hess, in *Kirk-Othmer Encyclopaedia of Chemical Engineering*, ed. I. Kroschwitz and M. Howe-Grant, Wiley, New York, 1995, vol. 13, p. 961.
- 2 H. Henkel and W. Weber, *US Pat.*, 1108752, 1914.
- 3 G. A. Cook, *US Pat.*, 2368640, 1945.
- 4 Y. Izumi, H. Miyazaki and S. Kawahara, *US Pat.*, 4009252, 1977.
- 5 Y. Izumi, H. Miyazaki and S. Kawahara, *US Pat.*, 4279883, 1981.
- 6 H. Sun, J. J. Leonard and H. Shalit, *US Pat.*, 4393038, 1981.
- 7 L. W. Gosser and J.-A. T. Schwartz, *US Pat.*, 4772458, 1988.
- 8 L. W. Gosser, *US Pat.*, 4889705, 1989.
- 9 C. Pralins and J.-P. Schirmann, *US Pat.*, 4996039, 1991.
- 10 T. Kanada, K. Nagai and T. Nawata, *US Pat.*, 5104635, 1992.
- 11 J. Van Weynbergh, J.-P. Schoebrechts and J.-C. Colery, *US Pat.*, 5447706, 1995.
- 12 S.-E. Park, J. W. Yoo, W. J. Lee, J.-S. Chang, U. K. Park and C. W. Lee, *US Pat.*, 5972305, 1999.
- 13 G. Papparatto, R. d'Aloisio, G. De Alberti, P. Furlan, V. Arca, R. Buzzoni and L. Meda, *EP Pat.*, 0978316A1, 1999.
- 14 B. Zhou, L.-K. Lee, *US Pat.*, 6168775, 2001.
- 15 M. Nystrom, J. Wangard and W. Herrmann, *US Pat.*, 6210651, 2001.
- 16 G. J. Hutchings, *Chem. Commun.*, 2008, 1148.
- 17 Degussa Headwaters builds peroxide demonstrator, in *The Chemical Engineer*, 2005, vol. 766, p. 16.
- 18 J. H. Lunsford, *J. Catal.*, 2003, **216**, 455.
- 19 D. P. Dissanayake and J. H. Lunsford, *J. Catal.*, 2002, **206**, 173.
- 20 D. P. Dissanayake and J. H. Lunsford, *J. Catal.*, 2003, **214**, 113.
- 21 V. R. Choudhary, C. Samanta and A. G. Gaikwad, *Chem. Commun.*, 2004, 2054.
- 22 P. Landon, P. J. Collier, A. J. Papworth, C. J. Kiely and G. J. Hutchings, *Chem. Commun.*, 2002, 2058.
- 23 P. Landon, P. J. Collier, A. F. Carley, D. Chadwick, A. J. Papworth, A. Burrows, C. J. Kiely and G. J. Hutchings, *Phys. Chem. Chem. Phys.*, 2003, **5**, 1917.
- 24 B. E. Solsona, J. K. Edwards, P. Landon, A. F. Carley, A. Herzing, C. J. Kiely and G. J. Hutchings, *Chem. Mater.*, 2006, **18**, 2689.
- 25 J. K. Edwards, B. Solsona, P. Landon, A. F. Carley, A. Herzing, M. Watanabe, C. J. Kiely and G. J. Hutchings, *J. Mater. Chem.*, 2005, **15**, 4595.
- 26 J. K. Edwards, B. Solsona, P. Landon, A. F. Carley, A. Herzing, C. J. Kiely and G. J. Hutchings, *J. Catal.*, 2005, **236**, 69.
- 27 J. K. Edwards, A. F. Carley, A. Herzing, C. J. Kiely and G. J. Hutchings, *Faraday Discuss.*, 2007, **138**, 225.
- 28 G. Li, J. K. Edwards, A. F. Carley and G. J. Hutchings, *Catal. Today*, 2007, **122**, 361.
- 29 J. K. Edwards, A. Thomas, A. F. Carley, A. Herzing, C. J. Kiely and G. J. Hutchings, *Green Chem.*, 2008, **10**, 388.
- 30 [www.bic.com/zeta\\_Theory.html](http://www.bic.com/zeta_Theory.html).
- 31 M. Kosmulski, *Chemical Properties of Material Surfaces*, Marcel Dekker, 2001.
- 32 H.-S. Lee, T. Hur, S. Kim, J. Kim and H.-I. Lee, *Catal. Today*, 2003, **84**, 173.
- 33 P. P. Olivera, E. M. Patrino and H. Sellers, *Surf. Sci.*, 1994, **313**, 25.
- 34 F. Wang, D. Zhang, H. Sun and Y. Ding, *J. Phys. Chem. C*, 2007, **111**, 11590.
- 35 S. Abate, G. Centi, S. Melada, S. Perathoner, F. Pinna and G. Strukul, *Catal. Today*, 2005, **104**, 323.
- 36 Y. Voloshin, R. Halder and A. Lawal, *Catal. Today*, 2007, **125**, 40.
- 37 V. R. Choudhary, C. Samanta and P. Jana, *Appl. Catal., A*, 2007, **332**, 70.
- 38 F. Kapteijn, G. Marban, J. Rodriguez Mirasol and J. A. Moulijn, *J. Catal.*, 1997, **167**, 256.
- 39 G. J. Hutchings, *Faraday Discuss.*, 2007, **138**, 321.



# Evaluating the greenness of alternative reaction media

Denise Reinhardt,<sup>\*a</sup> Florian Ilgen,<sup>b</sup> Dana Kralisch,<sup>a</sup> Burkhard König<sup>b</sup> and Günter Kreisel<sup>a</sup>

Received 30th April 2008, Accepted 28th July 2008

First published as an Advance Article on the web 26th September 2008

DOI: 10.1039/b807379a

The solvent performances and ecological (dis)advantages of different solvent systems for the Diels–Alder reaction of cyclopentadiene and methyl acrylate were investigated. Promising solvent alternatives, especially [C<sub>6</sub>MIM][BF<sub>4</sub>](1-hexyl-3-methylimidazolium tetrafluoroborate), citric acid/*N,N'*-dimethyl urea as well as a solvent-free alternative were compared to the conventional solvent systems methanol, cyclohexane, acetone and methanol/water. By means of the ECO (Ecological and Economic Optimisation) method these solvent alternatives were evaluated already during an R&D (Research and Development) stage in a holistic approach. This method is a screening tool that employs a Simplified Life Cycle Assessment (SLCA) approach in combination with an optimisation procedure. All life cycle stages from the production of reactants, solvents *etc.*, synthesis and workup, recycling and disposal are considered within this methodology. With the help of the ECO method, some significant environmental issues depending on the solvent selection are compared in order to make a contribution to the assessment of the greenness of chemical processes and products during R&D.

## Introduction

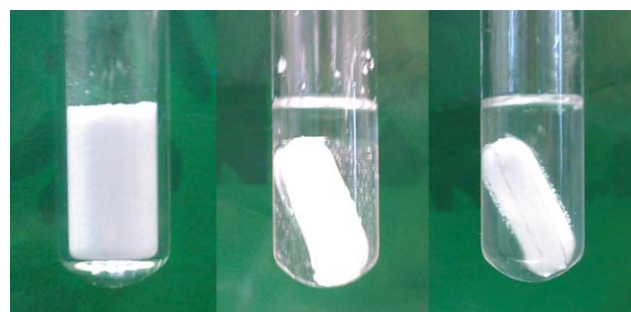
Much effort has already been made to replace toxic and hazardous substances, *e.g.* solvents, auxiliaries or catalysts, by non-volatile, less hazardous and non-toxic alternatives, respectively. However, most organic solvents still used in chemistry are volatile and often hazardous both to humans and the environment. In order to substitute them and to create more environmentally benign chemical processes, solvent alternatives such as supercritical fluids,<sup>1</sup> water,<sup>2</sup> ionic liquids<sup>3</sup> or solvent-free processes<sup>4</sup> have been receiving growing interest.

As an example, the supercritical fluid scCO<sub>2</sub> benefits from the fact that it has a comparatively low toxicity due to the high concentrations needed for acute toxicity. Furthermore, it is relatively inert, easily removable and recyclable. The nature of this reaction medium benefits from both liquid and gaseous properties. The facilitated diffusion of the substrate to the catalyst and rapid dissociation after the chemical conversion, results in a positive effect on catalytic reactions. The drawback of supercritical fluids, however, is the demand for sophisticated equipment, exceeding the standard lab equipment, and thus resulting in a still limited use during R&D.

Furthermore, water is considered to be the ideal solvent, being non-toxic, cheap and easily available. This solvent, however, has also some limitations due to the insolubility of nonpolar organic compounds and the instability of reactive reagents or

substrates in this medium. A neglected topic in the context of water-chemistry is the effort of removing the reactants during the workup procedure, consuming usually a large amount of organic solvent and energy, respectively. The extraction volume can exceed the volume of water by factors of up to 30.<sup>5</sup>

Further, new reaction media consisting of carbohydrates and urea were investigated as solvents for organic reactions, *e.g.* Diels–Alder or Stille reactions.<sup>6</sup> Stable and clear melts can easily be obtained by reaching the melting points between 65 °C and 92 °C (depending on the composition). Fig. 1 shows a citric acid/*N,N'*-dimethyl urea (DMU) melt in the case of a Diels–Alder reaction.



**Fig. 1** left: citric acid/DMU mixture (rt); middle: citric acid/DMU melt (65 °C) with methyl acrylate/cyclopentadiene loading (separation); right: homogeneous melt with starting material after stirring for 5 min.

These mixtures benefit from the advantages of having a very low toxicity, being non-volatile and consisting of compounds from readily available resources, being in line with the majority of the 12 principles of green chemistry.<sup>7</sup> At first glance, these media seem to be a green alternative to conventional solvents.

Ionic liquids have been discussed as an alternative to conventional organic solvents as well, since they offer *e.g.* significant

<sup>a</sup>Institute of Technical Chemistry and Environmental Chemistry, Friedrich-Schiller University of Jena, Lessingstr. 12, 07743, Jena, Germany. E-mail: D.Reinhardt@uni-jena.de; Fax: +49 3641 948402; Tel: +49 3641 948434

<sup>b</sup>Institute of Organic Chemistry, University of Regensburg, Universitätsstr. 31, 93040, Regensburg, Germany. E-mail: Florian.Ilgen@chemie.uni-regensburg.de; Fax: +49 941 9434566; Tel: +49 941 9434575

chemical advantages and have no relevant vapour pressure. However, results on their potential environmental impact, e.g. toxicity and environmental degradation, as well as the production effort required have been led to a more differentiated point of view.

Nowadays, it is widely accepted that no solvent is *a priori* green; its greenness rather strongly depends on the specific application, its toxicological properties and on the environmental impact resulting not only from the production process but also from the whole life cycle.

While choosing a suitable solvent for a process or searching for alternative technologies, environmental, health and safety criteria should be considered in addition to physical and chemical properties of a solvent. With this in mind, the efforts to eliminate, replace, recycle or minimise the use of solvents should commence in the earliest stage of the product/process development. A number of scientific groups have already published solvent selection/replacement tools in order to support this decision-making process.<sup>8</sup> These tools range from merely qualitative, semi-quantitative (e.g. ABC/XYZ-valuation<sup>9</sup>), to complex life cycle approaches. Some well-known computer aided methodologies and software tools, e.g. by Gani *et al.*,<sup>10</sup> EPA's SAGE (Environmental Protection Agency; Solvent Alternatives Guide) for surface cleaning processes<sup>11</sup> and PARIS II (Program for Assisting the Replacement of Industrial Solvents), reflecting solvent properties and environmental issues,<sup>12</sup> were developed.

In recent activities solvent selection tools were developed allowing for environmental, health and safety aspects at the R&D stage, partly under consideration of life cycle aspects/LCA (life cycle assessment),<sup>13</sup> as well as economic criteria.<sup>14</sup> For instance, the solvent selection guide by Capello *et al.*<sup>13</sup> integrates the life cycle assessment method as well as the EHS (environment, health, safety) method developed by Hungerbühler and coworkers.<sup>15</sup> Further, the Ecosolvent-Tool<sup>13</sup> is used as a life cycle assessment tool that facilitates the quantification of the environmental impact of waste-solvent treatment. For example, it is a useful tool to decide between "incineration versus distillation". Moreover, it contains life cycle inventories of the petrochemical production of the integrated solvents based on theecoinvent database.<sup>16</sup> Kralisch *et al.*<sup>17</sup> suggested a holistic evaluation and optimisation approach considering ecological and economic aspects. The ECO (ecological and economic optimisation) method was in particular designed by the authors to accompany and optimise early stage development work in chemical R&D regarding the principles of ecological and economic sustainability. The ECO method uses a Simplified Life Cycle Assessment (SLCA) approach,<sup>18</sup> integrating all life cycle stages from the production of reactants, solvents *etc.*, synthesis, workup, recycling and disposal. To evaluate the greenness of a product or process, the method uses three main criteria: the energy factor EF, the environmental and human health factor EHF and the cost factor CF, describing the energy demand, toxicity and cost of e.g. chemicals, auxiliaries, energies and equipment used during the life cycle stages of a product or process.

In this paper, ionic liquids and carbohydrate-urea mixtures are investigated regarding their ecological and economic sustainability for a typical organic reaction with the help of the ECO method. The Diels-Alder reaction was chosen as an exemplary

application, since the solvent effect on the reaction rate and selectivity has been widely examined and discussed, also in the case of the alternative solvents ionic liquids and carbohydrate-urea mixtures. Both media are compared to an assortment of conventional organic solvents as well as a solvent-free version (*i.e.* with no additional solvent within the Diels-Alder reaction), in order to demonstrate the process advantages, e.g. concerning product separation and catalyst recycling, but also to accentuate disadvantages and challenges, respectively.

## Diels-Alder reaction

To perform a comprehensive assessment of solvent alternatives for a given chemical synthesis, starting material, auxiliaries and the energy demand for synthesis and workup procedure have to be taken into account besides the solvent and its performance. Otherwise challenges and weak spots of processes/products during the whole life cycle can not be detected and improved. For our investigations, the Diels-Alder cycloaddition was chosen as a model reaction. The [4 + 2]-cycloaddition between a conjugated diene and a dienophile represents a widely used reaction to obtain fine chemicals, pharmaceuticals and bioactive molecules, respectively.<sup>19</sup> The pericyclic reaction proceeds *via* an aromatic transition state, typically resulting in the preferential formation of the *endo* diastereomer under kinetic control.

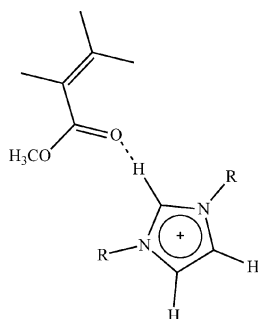
Both, efficiency and selectivity are significantly influenced by the acidity of the reaction medium. Up to now, Diels-Alder reactions have been investigated in several reaction media, like water,<sup>20</sup> LiClO<sub>4</sub>/ether,<sup>21</sup> lithium amides,<sup>22</sup> as well as surfactants.<sup>23</sup> Studies reviewing the solvent effects, the polarity of the solvent or solvent mixtures focused predominantly on the stereoselectivity and reaction rate.<sup>24</sup> In this context, Cativiela *et al.* found out that with increasing polarity both the reaction rate and the *endo/exo* ratio increase. Experiments in aqueous solution<sup>25</sup> showed an even higher reaction rate enhancement due to "enforced hydrophobic interactions between diene and dienophile". Engberts *et al.*<sup>25</sup> found out that relatively nonpolar reactants are "forced" to perform a solvophobic binding process, and that this is more favoured in water or aqueous, polar media, than in conventional organic solvents. As early as 1980, Rideout and Breslow demonstrated that Diels-Alder reactions were dramatically accelerated in water due to the "hydrophobic effect".<sup>20</sup>

In a comprehensive review, Cativiela *et al.* compared the theoretical and experimental results for solvent effects of diverse Diels-Alder reactions.<sup>26</sup> In this context, different solvents with polarities ranging from that of cyclohexane to acetic acid were tested in terms of reaction rate and three kinds of selectivity (*endo/exo*, regio- and diastereofacial). Experimental studies showed that the solvent polarity only has a marginal influence on the rate of some Diels-Alder reactions, whereas theoretical results pointed out that the activation barrier increases or decreases depending on the dienophile. However, solvent polarity enhanced the *endo/exo* selectivity, and, in agreement with theoretical calculations, the diastereofacial selectivity as well. In conclusion, solvent solvophobicity was established to be the main factor influencing reaction rate, accounting for the acceleration in aqueous media, and also the *endo/exo* selectivity of some Diels-Alder reactions.

In spite of many advantages, water is not always the solvent of choice, as discussed above. One disadvantage can be *e.g.* the stability of the catalyst. As an example in the context of Diels–Alder reactions, Lewis acids as catalysts are, with a few exceptions like  $\text{Sc}(\text{OTf})_3$  and  $\text{Ce}(\text{OTf})_3$ ,<sup>27</sup> rather problematic in use because of their immediate reaction with water.

The above mentioned carbohydrate–urea mixtures were tested to be very polar reaction media<sup>6</sup> with polarities between dimethyl sulfoxide and ethylene glycol and are therefore suitable for organic reactions proceeding *via* polar or ionic intermediates or transition states. Such polar reactions are promoted by polar solvents like carbohydrate–urea melts due to a strong stabilisation by solvation of polar intermediates. The hydrogenation with a Wilkinson catalyst, the Suzuki reaction and the Stille cross-coupling are examples for the applicability of carbohydrate–urea melts facilitating organic transformations in very high yields.<sup>6</sup> Apart from the efficient reaction procedure this alternative reaction medium has the advantage of consisting of mainly renewable components, which are vastly abundant and have a low impact on the environment and human health. Considering the risk for humans and the environment these melts should benefit from their very low (eco)toxicity compared with ionic liquids and conventional solvents.

Further, ionic liquids as reaction media and (acidic) catalysts for Diels–Alder reactions have also been the topic of numerous studies.<sup>28</sup> Aggarwal *et al.*<sup>29</sup> investigated the effect of possible hydrogen bonds between starting material and solvent molecules (ionic liquid) in terms of selectivity and reaction rate. The C2 imidazolium-proton shows a significant Lewis acid character and is able to coordinate the carbonyl oxygen in the methyl acrylate molecule during the reaction. The hydrogen bond formation between the cation of the ionic liquid and the dienophile, as a Lewis acid–base interaction, stabilises the transition state of the cycloadduct and leads to the preferential formation of the *endo* product (Scheme 1). By introducing sterically demanding residues (R), the preferred transition structure can be energetically disturbed, leading to a decrease in selectivity.

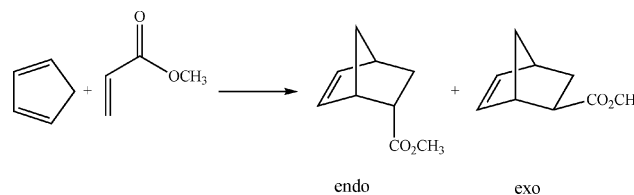


**Scheme 1** Activated complex with the help of hydrogen bond interactions of an imidazolium cation with methyl acrylate. (in accordance to ref. 29).

In order to maximise the product yield, in some cases ionic liquids have the advantage that products can be simply removed by decanting the organic layer and the extraction phase, respectively, without time and energy consuming steps. Further, the performance of ionic liquid-based processes is improved significantly if the catalyst remains in the ionic liquid phase after separation (see *e.g.* ref. 30).

## Sample reaction

To compare the performance of alternative solvents the reaction of cyclopentadiene and methyl acrylate (Scheme 2) was investigated, leading to a mixture of *endo*- and *exo*-bicyclo[2.2.1]hept-5-en-2-carboxylic acid methyl esters. We assumed the *endo* molecule as the desired product of the synthesis. The reaction is typically performed at room temperature with stirring. Herein we compare different solvent systems in terms of their overall performance in the Diels–Alder cycloaddition, taking into account an ecological and economic assessment. For this purpose, ionic liquids were tested as solvents for Diels–Alder reactions and compared with the results obtained in solvent-free systems and conventional organic media. As a representative ionic liquid, 1-hexyl-3-methylimidazolium tetrafluoroborate,  $[\text{C}_6\text{MIM}][\text{BF}_4]$ , was chosen. This ionic liquid does not show any Lewis acid character and hence does not interfere with a potentially used catalyst, shows moisture compatibility, is stable under air and thus simplifies the handling. Furthermore, 1-hexyl-3-methylimidazolium tetrafluoroborate allows for facile recycling of solvents, products and catalysts, and is easily accessible.<sup>31</sup> In addition, carbohydrate–urea mixtures as novel alternative solvents based on renewable components were compared regarding their performance, ecological and economic impact. Therefore, a melt consisting of citric acid/DMU (% w/w 40/60) was used. The conventional solvent systems evaluated in this work were acetone, methanol/deionised water, methanol, cyclohexane and a solvent-free reaction, respectively.



**Scheme 2** Diels–Alder reaction of cyclopentadiene and methyl acrylate.

## Experimental

$[\text{C}_6\text{MIM}]\text{Cl}$  was synthesised *via* the Menshutkin reaction. This synthesis of  $[\text{C}_6\text{MIM}]\text{Cl}$  was part of an optimisation study in earlier work.<sup>17</sup> It was performed in a 250 mL round bottom flask, fitted with a reflux condenser. The mixture of 0.21 mol *N*-methylimidazole and 0.21 mol *n*-hexyl chloride (1.0 mol equivalents) was stirred for 30 h (100 °C, oil bath) and cooled down to room-temperature afterwards. The workup procedure was carried out by dissolving the crude reaction mixture in water, followed by the extraction of the remaining *N*-methylimidazole content with diethyl ether. The yield of 98% was determined after removing of all volatiles *in vacuo* (rotary evaporator, water bath  $T = 80$  °C,  $t = 1.5$  h,  $p = 10$  mbar). The purity was checked by <sup>1</sup>H-NMR-spectroscopy.

$[\text{C}_6\text{MIM}][\text{BF}_4]$  was synthesised *via* reaction of  $[\text{C}_6\text{MIM}]\text{Cl}$  with  $\text{HBF}_4$ : 1 mol  $[\text{C}_6\text{MIM}]\text{Cl}$  was dissolved in 150 mL of water and stirred at rt for 3 h together with 1 mol  $\text{HBF}_4$  (48% aqueous solution). After the synthesis, the crude mixture was dissolved in methylene chloride, followed by an aqueous extraction. The

yield of 80% was determined after removal of all volatiles *in vacuo* (rotary evaporator, water bath  $T = 80\text{ }^{\circ}\text{C}$ ,  $t = 1.5\text{ h}$ ,  $p = 10\text{ mbar}$ ). The purity was verified by  $^1\text{H-NMR}$ -spectroscopy and the water content by means of Karl Fischer titration. By  $\text{AgNO}_3$  test and halide titration with  $0.1\text{ M AgNO}_3$ , using  $1\text{ g}$  of the ionic liquid (automated Mettler Toledo titration), no chloride content could be detected (halide  $< 200\text{ ppm}$ , water  $0.02\%$  by mass). The resulting ionic liquid was dried *in vacuo* immediately prior to use. Compared to commercially available  $[\text{C}_6\text{MIM}][\text{BF}_4]$ , e.g. from Merck (specification: high purity; halide  $< 200\text{ ppm}$ , water  $0.05\%$  by mass), no changing in performance properties concerning the Diels–Alder reaction of methyl acrylate and cyclopentadiene could be detected.

With regard to the citric acid/DMU mixture,  $10.5\text{ g DMU}$  and  $7\text{ g}$  citric acid were blended and led to a stable melt at  $65\text{ }^{\circ}\text{C}$ .

For a typical Diels–Alder reaction,  $15\text{ mL}$  of solvent (acetone, cyclohexane, methanol, methanol/water (% v/v 50/50),  $[\text{C}_6\text{MIM}][\text{BF}_4]$ , citric acid/DMU (% w/w 40/60)), cyclohexanone ( $1\text{ mL}$ ) as internal standard, methyl acrylate ( $5.34\text{ mL}$ ,  $59\text{ mmol}$ ) and freshly cracked cold cyclopentadiene ( $5.85\text{ mL}$ ,  $71\text{ mmol}$ ) were added into a Schlenk flask containing a small stirring bar. The reaction took place at  $25\text{ }^{\circ}\text{C}$  (controlled by a cryostat) and at  $65\text{ }^{\circ}\text{C}$ , respectively (see Table 1). The progress of the reaction was monitored at appropriate time intervals by extraction of aliquots with cyclohexane (for  $[\text{C}_6\text{MIM}][\text{BF}_4]$  and citric acid/DMU), appropriate dilution and GC analysis (conditions below). The yield of products and *endo/exo* ratios were calculated based on the GC analysis.

In the case of recycling experiments ( $[\text{C}_6\text{MIM}][\text{BF}_4]$ ), cyclohexane or diethyl ether (*ca.*  $5 \times 30\text{ mL}$ ) were added to extract non-reacted starting material and products. Afterwards, the cyclohexane phase including impurities was decanted. The purity of the cyclohexane phase was tested *via* GC. Before each run, the ionic liquid was dried *in vacuo*. Mass losses and performance properties can be seen in Table 2. In the case of citric acid/DMU, the same assumptions were made. For the conventional solvents, a solvent loss of  $10\%$  for each run was assumed. In general, the workup was performed by distillation steps to remove solvents and starting material from the product phase.

GC-measurements were performed using a Hewlett Packard, 8890 Series II apparatus; column HP 5 (Chrompack), length  $30\text{ m}$ , diameter  $0.32\text{ mm}$ ,  $0.25\text{ }\mu\text{m}$  film thickness. The following conditions were used: column pressure  $5\text{ psi}$ , flow rate

**Table 2** Reaction conversions and *endo/exo* ratios with recycled  $[\text{C}_6\text{MIM}][\text{BF}_4]$

Run	Mass loss/g	Mass loss (%)	<i>endo/exo</i> ratio <sup>a</sup>	Conversion of methyl acrylate <sup>a</sup> (%)
1			3.8	92
2	0.52	3.1	3.7	96
3	0.72	4.3	3.7	97
4	0.84	5	3.7	98

<sup>a</sup> Determined by gas chromatography.

$75\text{ mL min}^{-1}$  of hydrogen; inlet temperature:  $200\text{ }^{\circ}\text{C}$ , detector temperature:  $250\text{ }^{\circ}\text{C}$ ; oven conditions:  $50\text{ }^{\circ}\text{C}$  for  $6\text{ min}$ , then ramped at  $15\text{ }^{\circ}\text{C min}^{-1}$  to  $110\text{ }^{\circ}\text{C}$ , maintained for  $10\text{ min}$ , then ramped at  $25\text{ }^{\circ}\text{C min}^{-1}$  to  $250\text{ }^{\circ}\text{C}$ , maintained for  $2\text{ min}$ . Total run time:  $27.6\text{ min}$ . FID-detector.

The energy demand for heating, stirring and distillation for the Diels–Alder reaction was determined using an energy monitoring socket (Energy Monitor 3000, Voltcraft), and in the case of the ionic liquid synthesis calculated with the help of thermochemical data.

## Evaluation

### Assessment of the solvent performance

Table 1 summarises the results of the Diels–Alder reactions that were performed in different solvents (catalyst-free, without recycling). These experiments were carried out twice with no significant change neither in conversion nor selectivity. The evaluation was performed for reaction times of  $8\text{ h}$  and  $48\text{ h}$ , respectively, as can be seen in Table 1. These reaction times, yields and selectivities represent the basis for the evaluation, since in all cases similar and nearly quantitative conversion and high product yields were reached. Further, the conversions and yields reached a plateau during this time (see also Fig. 2).

Fig. 2 shows the time-dependent synthesis of *endo*-bicyclo[2.2.1]-hept-5-en-2-carboxylic acid methyl ester.

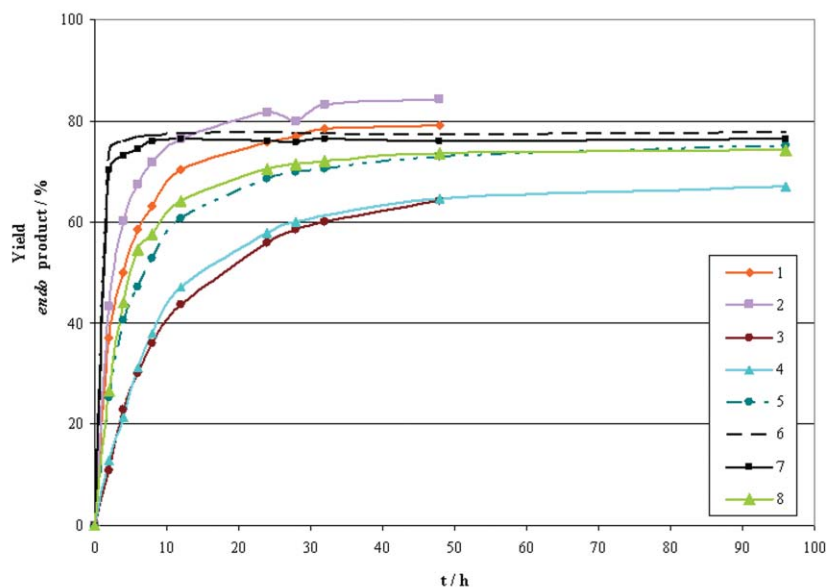
In general, the ionic liquid  $[\text{C}_6\text{MIM}][\text{BF}_4]$  showed a similar performance in the Diels–Alder reaction compared to conventional solvent systems at room temperature. The solvents methanol and methanol/water, respectively, appear to be the best choice among the tested solvents for the Diels–Alder reaction at room temperature (in accordance to the literature).

**Table 1** Solvents used in the Diels–Alder reaction and their performances

Exp. number	Solvent	Temp./ $^{\circ}\text{C}$	Conversion of methyl acrylate <sup>a</sup>		<i>endo/exo</i> ratio <sup>a</sup>
			Time/h	%	
1	Methanol	25	48	95	4.9
2	Methanol/water % v/v, 50/50	25	48	98	5.5
3	Acetone	25	48	83	3.3
4	Cyclohexane	25	48	90	2.6
5	$[\text{C}_6\text{MIM}][\text{BF}_4]$	25	48	92	3.8
6	Citric acid/DMU % w/w, 40/60	65	8	99	3.7
7	$[\text{C}_6\text{MIM}][\text{BF}_4]$	65	8	98	3.3
8	Solvent-free	25	48	98	2.9

<sup>a</sup> Determined by gas chromatography.





**Fig. 2** Yield of *endo*-bicyclo[2.2.1]-hept-5-en-2-carboxylic acid methyl ester in dependence of the time and solvent system (see Table 1).

Further, the citric acid/DMU mixture would be a good choice, if accepting a higher energy demand for heating and a slightly reduced *endo/exo* ratio. In the case of  $[\text{C}_6\text{MIM}][\text{BF}_4]$ , with increasing temperature higher conversion rates, but decreasing *endo/exo* ratios were observed.

In the case of the solvent-free route, good results were obtained too, even if the *endo/exo* ratio is lower than for the reactions with added solvents.

### Ecological assessment

The experimental work was accompanied by the application of the ECO method in order to compare the solvent performances in a holistic approach and to identify improvements regarding the objectives EF, EHF and CF.† The data obtained during the assessment procedure are very extensive and thus, only selected and significant findings will be discussed in detail below.

### Evaluation of the energy factor EF

The energy factor EF sums up the cumulative energy demand (CED)<sup>32</sup> resulting from the supply of the reactants, solvents and auxiliaries ( $E^S$ ), the performance of the reaction ( $E^R$ ), the energy demand necessary for the workup ( $E^W$ ), the application of the products ( $E^A$ ) and the disposal of waste ( $E^D$ ), related to a product-based benefit *e.g.* the product molarity (eqn (1)) or the product mass.

$$\text{EF} = \frac{\sum_{i=1}^{x_S} E_i^S + \sum_{i=1}^{x_R} E_i^R + \sum_{i=1}^{x_W} E_i^W + \sum_{i=1}^{x_A} E_i^A + \sum_{i=1}^{x_D} E_i^D}{n_{\text{product}}} \quad (1)$$

The EF was determined using the Life Cycle Assessment software Umberto,<sup>33</sup> incorporating the database Ecoinvent,<sup>16</sup> which contains literature references as well as a pool of data concerning the supply of organic and inorganic chemicals, electrical energy, inert gases *etc.*, starting from their primary sources. If specific data were not available, the energy demand for the supply of structurally similar compounds available from the database was used as an approximation.‡

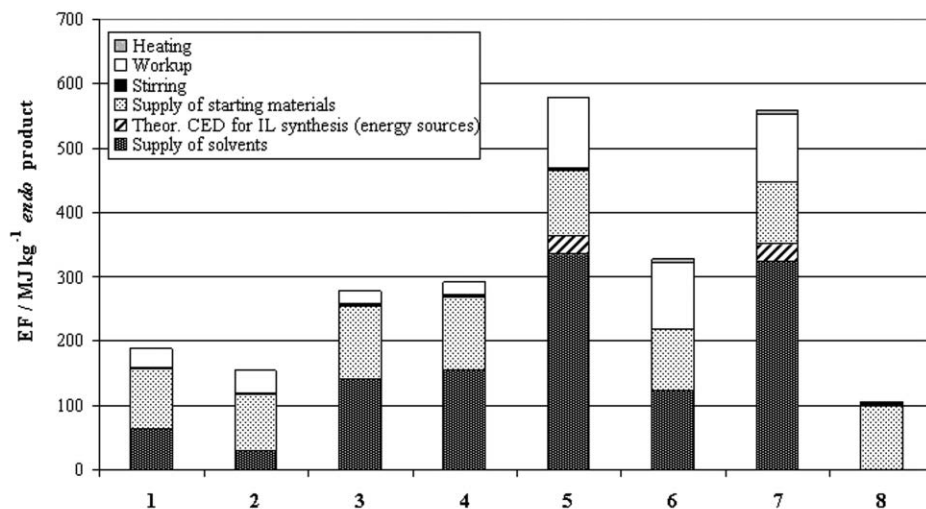
Fig. 3 demonstrates the EF for the synthesis of 1 mol *endo*-bicyclo[2.2.1]-hept-5-en-2-carboxylic acid methyl ester. The best results were obtained for methanol, methanol/water and for the solvent-free system. On the one hand, this can be explained by the comparatively low energy demand for the supply of the solvents and on the other hand by the solvent performance during the Diels–Alder reaction. Due to the low *endo/exo* selectivity, the EF for the supply of the reactants for the solvent-free route is higher than for methanol and methanol/water. In spite of this, the EF per kg *endo* product is comparably low, since no additional energy demand for the solvent supply is necessary. Further, the workup procedure involves no additional solvent distillation steps increasing the EF.

In the case of acetone, cyclohexane§ and DMU, the CEDs for solvent supply are generally higher than for methanol or water. In addition, the reaction in acetone and cyclohexane gave lower yields and selectivities, which results in higher EF values. For citric acid/DMU, a lower EF for the supply of

† For this study, the disposal of the ionic liquid was not included, due to lack of data concerning the end of life information. Since this study represents a screening of all solvent alternatives, only the upstream chains, the Diels–Alder reaction, the recycling considerations and workup were part of the calculation. To demonstrate the influence of  $[\text{C}_6\text{MIM}][\text{BF}_4]$  when released into the environment, a qualitative (Fig. 5) and quantitative assessment (environmental and human health factor) was made.

‡ The CED for cyclopentadiene was determined using the inventory data of “chemicals organic, at plant” (ecoinvent v. 1.3).

§ The CED for cyclohexane was determined using the ecoinvent database v. 2.0, 2007.



**Fig. 3** Dependence of EF on the choice of solvent for the Diels–Alder reaction of methyl acrylate and cyclopentadiene ( $T = 25\text{ }^{\circ}\text{C}$  and  $65\text{ }^{\circ}\text{C}$ ,  $t = 48\text{ h}$  and  $8\text{ h}$ , solvent systems methanol, methanol/water, acetone, cyclohexane,  $[\text{C}_6\text{MIM}][\text{BF}_4]$ , citric acid/DMU, solvent-free, see Table 1).

starting material can be expected. However, for the synthesis at  $65\text{ }^{\circ}\text{C}$ , the higher energy demand for heating has to be taken into account. Further, the workup procedure of the media citric acid/DMU and  $[\text{C}_6\text{MIM}][\text{BF}_4]$  is more complex and results in a higher EF, since additional organic solvents become necessary to extract the product from the stationary phase having no relevant vapour pressure. However, in some cases the organic phase can be removed from the stationary phase by decanting, resulting in a lower energy demand.

**Comparability of upstream processes for solvent supply.** One of the main requirements for a well-founded comparison is to ensure comparability. In this case, a direct comparison of the alternative solvents was difficult, since the same scale of production data for all solvents considered is necessary. The supply of acetone, methanol, deionised water, cyclohexane as well as of carbohydrates and urea derivatives can be evaluated on industrial production scale using the Ecoinvent-database, while such data were not available for the supply of  $[\text{C}_6\text{MIM}][\text{BF}_4]$ . The energy demand for a lab scale synthesis (batchwise) of the ionic liquid, known from our experiments, allows no energetic comparison to the supply of the other solvent systems. Whereas, especially the alkylation step of *N*-methylimidazole and *n*-hexyl chloride is exceedingly energy demanding. To guarantee comparability, the energy requirements for heating, stirring and distillation processes within upstream chains were theoretically calculated by means of thermochemical data. The amount of energy which is theoretically required (calculated by means of heat capacity, enthalpy of vaporisation, standard enthalpy change of formation, standard enthalpy change of reaction; assumed efficiency for heating: 80%) amounts to less than 10% of the overall result (Fig. 3).

Against this background, the approach seems to be sufficient regarding the task of our investigations.

The results presented in Fig. 3 point out that the energy demand for the supply of both reaction media, the melt system as well as the ionic liquid, is higher than that for the supply of the conventional solvents. In order to become an ener-

getically favourable alternative, further synthesis optimisation, new synthetic strategies and/or other techniques, *e.g.* process intensification *via* microreactors, as studied in the case of  $[\text{C}_4\text{MIM}]\text{Br}$ ,<sup>34</sup> have to be considered.

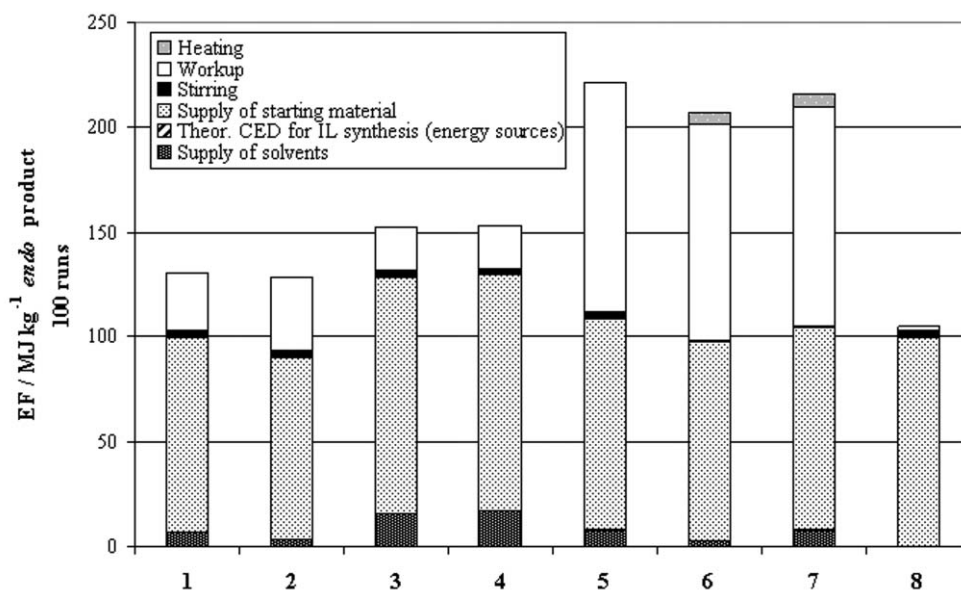
Another promising possibility of increasing the energy efficiency of the Diels–Alder synthesis could be an appropriate solvent recycling strategy. This aspect will be discussed in the following.

**Effects of solvent recycling.** To investigate a particular process advantage of ionic liquids,  $[\text{C}_6\text{MIM}][\text{BF}_4]$  was recycled and reused for 3 times. After three recycling steps, a mass loss of 5% was determined, while the solvent performance seems to remain unchanged (Table 2).

If ionic liquids (or carbohydrate–urea melts) should represent an ecological and further economic alternative to conventional solvent systems, their process advantages like solvent recovery or catalyst recycling are of particular importance. Therefore, we assumed a 100-fold use in order to demonstrate the impact on ecological and economic criteria.

For the determination of EF including recycling, the assumption was made, that the solvent performance does not diminish within 100 runs and the mass loss of 5% per 4 runs does not increase. Carbohydrate–urea mixtures benefit from their simple workup by adding water to the still warm melt, upon which the water soluble carbohydrates and urea derivatives are dissolved, leaving behind a supernatant of products and starting material, which can be decanted. However, the energy demand for the supply of the melt components is higher than for conventional solvents, and therefore recycling is desired. For the calculation, we assumed that the changes in solvent performance and mass loss are equal to the results obtained in the ionic liquid. In the case of the conventional solvents, a mass loss of 10% per run was assumed.

Fig. 4 shows a significant improvement in energy efficiency concerning the supply of  $[\text{C}_6\text{MIM}][\text{BF}_4]$ , resulting in a lower EF (reduction of approx. 98%) and in a better comparison to the other solvent systems in the case of a hundred-fold solvent



**Fig. 4** Dependence of EF on the choice of solvent for the Diels–Alder reaction of methyl acrylate and cyclopentadiene ( $T = 25\text{ }^{\circ}\text{C}$  and  $65\text{ }^{\circ}\text{C}$ ,  $t = 48\text{ h}$  and  $8\text{ h}$ , solvent systems methanol, methanol/water, acetone, cyclohexane,  $[\text{C}_6\text{MIM}][\text{BF}_4]$ , citric acid/DMU, solvent-free, see Table 1), per 100 cycles.

use. The EF for the supply of the  $[\text{C}_6\text{MIM}][\text{BF}_4]$  and of the citric acid/DMU melt is nearly equal to the energy demand for the supply of the conventional solvents. With the possibility of recycling the reaction medium easily, ionic liquids as well as carbohydrate–urea mixtures become a suitable alternative to conventional solvents (compare the black bars in Fig. 4).

However, a disadvantage for media having no relevant vapour pressure or being non-volatile became clear for the workup procedure, where additional solvents are needed to extract the organic reaction products and non-reacted reactants.

Although the workup procedure has not been optimised yet, we tried to estimate the additional energy demand for the supply of an extraction solvent and distillation steps. As shown in Fig. 4 (white bars), additional workup steps—to extract starting material and products from the stationary phase ( $[\text{C}_6\text{MIM}][\text{BF}_4]$ , citric acid/DMU) before reuse—decrease the energy efficiency of the Diels–Alder reaction. Although these alternative media feature non-volatility and therefore contribute to safety aspects, the workup regarding the Diels–Alder reaction seems to be the bottle-neck and accentuate the need for an assessment *via* a life cycle approach.

#### Evaluation of the environmental and human health factor EHF

We started our investigations addressing toxicological aspects of the solvent choice by means of qualitative criteria concerning aspects of mobility, acute toxicity and chronic toxicity for humans, acute toxicity for aquatic organisms, persistency in the environment and bioaccumulation, using the data given in safety data sheets.<sup>35</sup> These results are demonstrated in Fig. 5.

Against this background, water seems to be an environmentally benign solvent alternative, followed by the melt components DMU<sup>36</sup> and citric acid, which are harmless to human health and the environment. The classification of  $[\text{C}_6\text{MIM}][\text{BF}_4]$  turned out to be difficult, since quantitative data regarding toxicity for

humans, ecological effects, information about accumulation and biodegradability of this product are hardly or not available at all. Since  $[\text{C}_6\text{MIM}][\text{BF}_4]$  is classified by a water hazard class (WGK) of 3, the acute toxicity for aquatic organisms was assumed to be “high”.

To quantify the environmental effects and to integrate the quantity of the solvents used under consideration of technical constraints (*e.g.* safety issues), the environmental and health factor EHF was used. The EHF allows a comparison of different chemical substances used, *e.g.* as reactants, solvents or auxiliaries regarding the resulting risks for human and environment during their supply ( $\text{RPoD}^{\text{S}}$ ), product synthesis ( $\text{RPoD}^{\text{R}}$ ), product workup ( $\text{RPoD}^{\text{W}}$ ), product application ( $\text{RPoD}^{\text{A}}$ ) and disposal ( $\text{RPoD}^{\text{D}}$ ). EHF sums up the  $\text{RPoD}_{ij}$ , calculated according to Koller *et al.*,<sup>15</sup> and relates this input to the molarity (or mass) of the product. The EHF is divided into three sub-objectives: EHF(AcT), EHF(ChT) and EHF(WmE), referring to the categories acute toxicity, chronic toxicity and water-mediated effects. Their calculation is demonstrated using the example of EHF(AcT) (eqn (2)).

$$\text{EHF}(\text{AcT}) = \frac{\sum_{i=1}^{x_{\text{S}}} \text{RPoD}(\text{AcT})_i^{\text{S}} + \sum_{i=1}^{x_{\text{R}}} \text{RPoD}(\text{AcT})_i^{\text{R}}}{n_{\text{product}}} + \frac{\sum_{i=1}^{x_{\text{W}}} \text{RPoD}(\text{AcT})_i^{\text{W}} + \sum_{i=1}^{x_{\text{A}}} \text{RPoD}(\text{AcT})_i^{\text{A}} + \sum_{i=1}^{x_{\text{D}}} \text{RPoD}(\text{AcT})_i^{\text{D}}}{n_{\text{product}}} \quad (2)$$

As mentioned in safety data sheets, hazardous properties of  $[\text{C}_6\text{MIM}][\text{BF}_4]$  can not be excluded. In the absence of bioaccumulation and persistency data we assumed the risk as high as possible.

Solvent	Acetone	Cyclohexane	Methanol	Water	[C <sub>6</sub> mim][BF <sub>4</sub> ]	DMU	Citric acid
<b>Environmental effects</b>							
Mobility	Orange	Light green	Yellow	Dark green	Dark green	Dark green	Dark green
Acute toxicity for humans	Light green	Yellow	Orange	Dark green	Grey	Light green	Light green
Chronic toxicity for humans	Dark green	Light green	Yellow	Dark green	Grey	Dark green	Dark green
Acute toxicity for aquatic organisms	Light green	Orange	Light green	Dark green	Red	Light green	Light green
Persistency in environment	Light green	Orange	Light green	Dark green	Grey	Dark green	Dark green
Bioaccumulation	Dark green	Yellow	Dark green	Dark green	Grey	Dark green	Dark green
<b>Colour definition (qualitative)</b>							
<b>Effect</b>							
<b>Data base</b>							
Mobility	boiling point, temperature diff. betw. boiling point and process temperature, vapour pressure						
Acute toxicity for humans	EC classification (Xn, T, T+), GK, R-codes, LD50 (inhal., oral, dermal)						
Chronic toxicity for humans	carcinogenicity, mutagenicity <i>etc.</i> , R-codes, MAK, EC classification (Xn, T, T+)						
Acute toxicity for aquatic organisms	WGK (German water hazard class), R-codes, EC50/LC50						
Persistence in environment	OECD, EU classification (readily, inherent, no)						
Bioaccumulation	log <i>k</i> <sub>ow</sub> , qualitative info						

Fig. 5 Qualitative assessment of the ecological impact of the used solvents (database: safety data sheets).

Fig. 6 demonstrates the criteria EHF in the special case of acute toxicity regarding the alternative solvents used. Methanol is classified as a toxic substance and has therefore a significant impact on the human health. Although the risk is assumed to be high in the case of [C<sub>6</sub>MIM][BF<sub>4</sub>], the resulting acute toxicity for humans is lower than for methanol-systems, since [C<sub>6</sub>MIM][BF<sub>4</sub>] has no relevant vapour pressure and thus represents a low imminent hazard. Further, Fig. 6 gives an in-depth view into the toxicological impact of the starting-materials used as well. In the case of cyclopentadiene, the resulting EHF is about in

the same order of magnitude compared to the influence of the solvents. A possible negative effect resulting from the release potential of cyclopentadiene and methyl acrylate at  $T = 65\text{ }^{\circ}\text{C}$  was avoided by working under reflux to minimise the hazard potential.

Fig. 7 demonstrates the EHF for water mediated effects. The EHF(WmE) for [C<sub>6</sub>MIM][BF<sub>4</sub>] is extremely high in comparison to the other solvent systems. This effect is a result of its high classification in the German water hazard class as well as the low biological degradation<sup>37</sup> and has to be regarded as

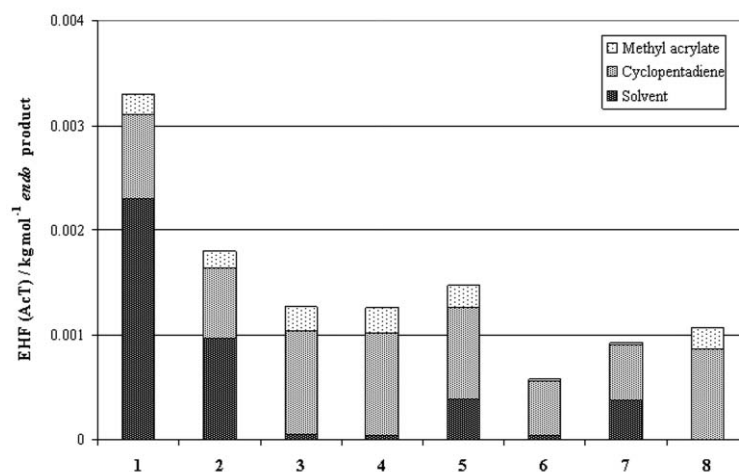
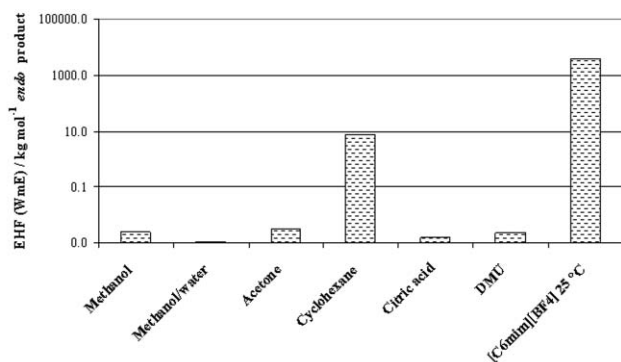


Fig. 6 Dependence of EHF(AcT) on the choice of the solvent for the Diels-Alder reaction of methyl acrylate and cyclopentadiene ( $T = 25\text{ }^{\circ}\text{C}$  and  $65\text{ }^{\circ}\text{C}$ ,  $t = 48\text{ h}$  and  $8\text{ h}$ , solvent systems methanol, methanol/water, acetone, cyclohexane, [C<sub>6</sub>MIM][BF<sub>4</sub>], citric acid/DMU, solvent-free, see Table 1).





**Fig. 7** Dependence of EHF(WmE) on the choice of the solvent for the Diels–Alder reaction of methyl acrylate and cyclopentadiene (see Table 1).

worst case scenario. Cyclohexane is classified as N-substance, *i.e.* environmentally dangerous substance. Further, cyclohexane is specified with R-codes 50/53, indicating a substance as very toxic to aquatic organism, and may cause long-term adverse effects in the aquatic environment. Acetone, methanol,

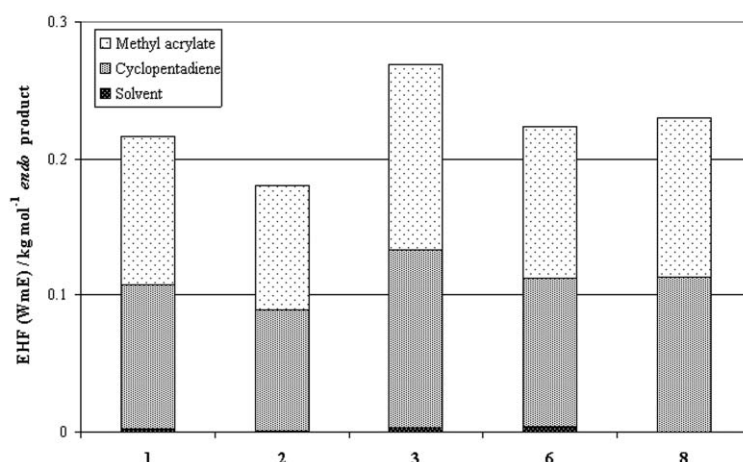
methanol/water and citric acid/DMU have no significant influence on aquatic organisms, since the systems are classified with WGK 1. For the latter solvent systems and the solvent-free alternative, respectively, Fig. 8 shows the resulting EHF(WmE). Here the environmental impact is significantly affected by the performance of the solvent.

In general, reactions in the citric acid/DMU melt are well suited regarding toxicological aspects, since their low impact on the environment and human health as well as their solvent performance. For the solvent-free experiment, reduced *endo/exo* ratios and yields were obtained, resulting in a slightly higher consumption of starting material and therefore higher EHF values.

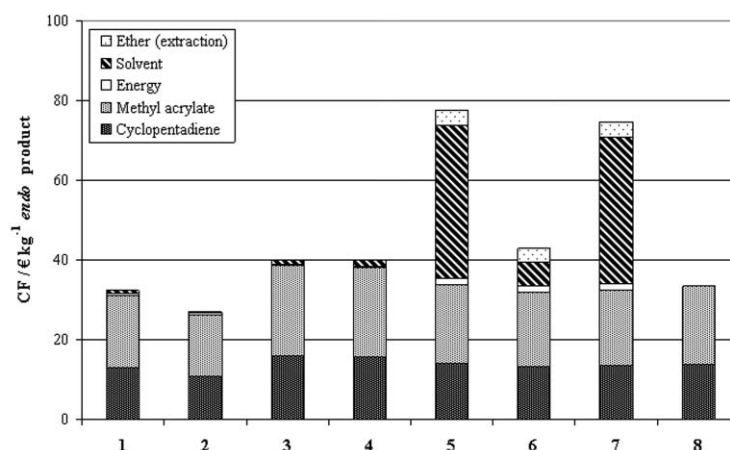
### Evaluation of the cost factor CF

The cost factor CF is determined in analogy to EF and EHF and sums up all occurring costs, *i.e.* the prices of the chemicals, energy, disposal, equipment and personnel as well as process expenditure *etc.*, related to the molarity (or mass) of the product.

Fig. 9 represents the cost factor CF for the synthesis of 1 kg *endo*-bicyclo[2.2.1]hept-5-en-2-carboxylic acid methyl ester



**Fig. 8** Dependence of EHF(WmE) on the choice of the solvent system for the Diels–Alder reaction ( $T = 25\text{ °C}$  and  $65\text{ °C}$ ,  $t = 48\text{ h}$  and  $8\text{ h}$ , solvent systems methanol, methanol/water, acetone, cyclohexane,  $[C_6MIM][BF_4]$ , citric acid/DMU, solvent-free, see Table 1).



**Fig. 9** Dependence of CF on the choice of the solvent for the Diels–Alder reaction of methyl acrylate and cyclopentadiene ( $T = 25\text{ °C}$  and  $65\text{ °C}$ ,  $t = 48\text{ h}$  and  $8\text{ h}$ , solvent systems methanol, methanol/water, acetone, cyclohexane,  $[C_6MIM][BF_4]$ , citric acid/DMU, solvent-free, see Table 1).

under consideration of a 100-fold use strategy.<sup>38</sup> Therein, the costs for starting-materials, solvents for reaction and workup as well as energy costs were considered. Personnel costs were not included yet, since their calculation on laboratory scale would not be representative.

The conventional solvents are easily available and relatively cheap, that is why the cost factor is mainly defined by the supply of the starting materials. Therefore, in case of a 100-fold use, CF mainly depends on the performance of the different reaction media. In the case of the ionic liquid as well as the carbohydrate–urea melt, the additional solvent demand for extraction and further higher costs for the supply of these media, lead to a comparably higher CF than for the reactions in conventional solvents and the solvent-free synthesis route. Taking into account the specific application for ionic liquids discussed herein, the price for [C<sub>6</sub>MIM][BF<sub>4</sub>] should not exceed 22 € kg<sup>-1</sup> in order to be in the range with the conventional solvents (40 € kg<sup>-1</sup> *endo* product). This is in accordance with Hilgers and Wasserscheid. They expected that a range of ionic liquids will become commercially available for €25–50 L<sup>-1</sup> at a ton scale.<sup>39</sup>

## Conclusions

Within this study, new, potentially green, solvent alternatives for the Diels–Alder reaction between methyl acrylate and cyclopentadiene were compared to conventional solvents and a solvent-free version, too. The ionic liquid [C<sub>6</sub>MIM][BF<sub>4</sub>] and carbohydrate–urea melt citric acid/DMU were chosen as two representative examples for those alternative reaction media. They were investigated regarding their performance and their ecological as well as economic sustainability.

One major disadvantage of the melt system can be its relatively low thermal and pressure stability compared to the other solvents used, since *N,N'*-dimethyl urea and carbohydrate components like glucose tend to decompose at high temperatures. However, within our investigations the system showed no thermal decay since the reactions and workup procedures were performed well below the decomposition temperature. In addition, the melt components feature very low (eco)toxicity, simplifying the handling.

Further, ionic liquids and carbohydrate–urea melts can become attractive alternatives to conventional solvents, if their separation efficiency and recyclability are high. The production stage of ionic liquids turns out to be disadvantageous in most cases and further research work has to be done in this context.

In the case of the investigated reaction, the solvent system methanol/water or the solvent-free synthesis seem to be the most ecological sustainable alternatives, yet. This has been proven within a decision support software. With the help of the outranking procedure PROMETHEE,<sup>40</sup> the different reaction media have been compared in an objective way under consideration of EF, EHF and CF. The outranking of the different solution candidates under consideration of a 100-fold reuse resulted in the following order of preference: solvent-free ≥ methanol/water > methanol > acetone > cyclohexane > citric acid/DMU > [C<sub>6</sub>MIM][BF<sub>4</sub>]. This result is valid under the following regulations: minimise EF, EHF(AcT), EHF(ChT), EHF(WmE), CF, weight: 33 : 11 : 11 : 11 : 33, preference

function: linear, threshold unit: percent, and was determined using the software Decision Lab 2000.<sup>41</sup>

The use of ionic liquids or carbohydrate–urea melts within the Diels–Alder reaction instead of water containing systems may be preferred, since these media allow the use of moisture sensitive reagents, and organic materials can be removed *in vacuo*. In addition, the use of Lewis acid catalysts, like Sc(OTf)<sub>3</sub>, in these media is advantageous compared to conventional solvents, if the catalyst remains in the reaction medium after workup. Addressing these issues, processes based on non- or low-volatile solvents can be improved significantly regarding their environmental and reaction performance. However, reactions in media with no relevant vapour pressure often require additional solvents during workup, which might affect environmental aspects adversely. Therefore, multiphasic systems, which often can be established in ionic liquid processes, probably provide more efficient pathways for practical applications.

If the costs of producing bulk ionic liquids remain at their current level, difficulties in adopting ionic liquids in industrial processes in order to replace volatile organic solvents can not be overcome.<sup>42</sup> The carbohydrates and urea components are easily available, but purity specifications for organic synthesis actually inhibit their cheap disposal.

The considered ionic liquid [C<sub>6</sub>MIM][BF<sub>4</sub>] presents only one example of the huge class of ionic liquids, and there is, for instance regarding the factor of human and environment, great potential for further optimisation by changing the solvent and using other synthesis strategies (see *e.g.* review by Stark and Seddon<sup>3</sup>). Nevertheless, the ECO method was used to accentuate the need for the assessment of alternative reaction media in a more holistic approach and to demonstrate the opportunities and challenges of these alternative media.

The presented results are part of a long-term investigation regarding the optimisation of synthesis pathways and assessment of applications of ionic liquids *via* life cycle approach.

## List of abbreviations

CED	Cumulative energy demand
CF	Cost factor
[C <sub>4</sub> MIM]Br	1-Butyl-3-methylimidazolium bromide
[C <sub>6</sub> MIM][BF <sub>4</sub> ]	1-Hexyl-3-methylimidazolium tetrafluoroborate
[C <sub>6</sub> MIM]Cl	1-Hexyl-3-methylimidazolium chloride
DMU	<i>N,N'</i> -Dimethyl urea
EC50	Half maximal effective concentration
ECO	Ecological and economic optimisation
EF	Energy factor
EHF	Environmental and human health factor
EHF(AcT)	Environmental and human health factor regarding acute toxicity risks
EHF(ChT)	Environmental and human health factor regarding chronic toxicity risks
EHF(WmE)	Environmental and human health factor regarding risks resulting from water-mediated effects
EHS	Environment, health and safety
GC	Gas chromatography
GK	Swiss poison class (Giftklasse)
LC50	Median lethal concentration
LCA	Life cycle assessment

LCC	Life cycle cost
LD50	Median lethal dose
Log $k_{ow}$	Log octanol–water partitioning coefficient
MAK	Workplace threshold value (Maximale Arbeitsplatzkonzentration)
OECD	Biodegradability after 28 days (standardised test)
R&D	Research and development
RPoD	Remaining potential of danger
rt	Room-temperature
SLCA	Simplified life cycle assessment
WGK	German water hazard class (Wassergefährdungsklasse)

## Acknowledgements

Denise Reinhardt and Florian Ilgen thank the German Federal Environmental Foundation (DBU) for graduate scholarships. Furthermore, the authors thank R. Grunert for her dedicated cooperation.

## Notes and references

- P. G. Jessop, T. Ikariya and R. Noyori, *Chem. Rev.*, 1999, **99**, 475; W. H. Hauthal, *Chemosphere*, 2001, **43**, 123; C. M. Gordon and W. Leitner, *Chim. Oggi*, 2004, **22**, 39.
- R. Breslow, in *Green Chemistry*, ed. P. T. Anastas and T. C. Williamson, Oxford University Press, New York, 1998, p. 225; B. Cornils and W. A. Herrmann, in *Aqueous Phase Organometallic Catalysis—concepts and applications*, ed. B. Cornils and W. A. Herrmann, Wiley-VCH, Weinheim, Germany, 1998; K. Manabe and S. Kobayashi, *Chem.–Eur. J.*, 2002, **8**, 4094; D. Sinou, *Adv. Synth. Catal.*, 2002, **344**, 221; F. Joo, *Acc. Chem. Res.*, 2002, **35**, 738.
- P. Wasserscheid and W. Keim, *Angew. Chem., Int. Ed.*, 2000, **39**, 3772; R. Sheldon, *Chem. Commun.*, 2001, 2399; D. Zhao, M. Wu, Y. Kou and E. Min, *Catal. Today*, 2002, **74**, 157; J. D. Holbrey, M. B. Turner and R. D. Rogers, *ACS Symp. Ser.*, 2003, **856**, 2; A. Stark, and K. R. Seddon, in *Kirk-Othmer Encyclopaedia of Chemical Technology*, ed. A. Seidel, John Wiley & Sons, Inc., Hoboken, New Jersey, 5th edn, 2007, p. 836.
- K. Tanaka and F. Toda, *Chem. Rev.*, 2000, **100**, 1025.
- D. G. Blackmond, A. Armstrong, V. Coombe and A. Wells, *Angew. Chem., Int. Ed.*, 2007, **46**, 3798.
- G. Imperato, E. Eibler, J. Niedermaier and B. König, *Chem. Commun.*, 2005, 1170; G. Imperato, R. Vasold and B. König, *Adv. Synth. Catal.*, 2006, **348**, 2243; G. Imperato, S. Höger, D. Lenoir and B. König, *Green Chem.*, 2006, **8**, 1051.
- P. T. Anastas and J. C. Warner, *Green Chemistry: Theory and Practice*, Oxford University Press, New York, 1998.
- A. D. Curzons, D. J. C. Constable and V. L. Cunningham, *Clean Prod. Processes*, 1999, **1**, 82; K. Alfonsi, J. Colberg, P. J. Dunn, T. Fevig, S. Jennings, T. A. Johnson, H. P. Kleine, C. Knight, M. A. Nagy, D. A. Perry and M. Stefaniak, *Green Chem.*, 2008, **10**, 31.
- G. Fleischer and W.-P. Schmidt, *Int. J. Life Cycle Assess.*, 1997, **2**, 20.
- R. Gani, *Comput. Chem. Eng.*, 2004, **28**, 2441; R. Gani, C. Jimenez-Gonzalez and D. J. C. Constable, *Comput. Chem. Eng.*, 2005, **29**, 1661.
- C. H. Darwin and K. Monroe, *Met. Finish.*, 1997, **95**, 24.
- H. Cabezas, R. Zhao, J. C. Bare and S. R. Nishtala, *NATO Science Series, 2: Environmental Security*, 1999, **62**, 317; H. Cabezas, P. F. Harten and M. R. Green, *Chem. Eng.*, 2000, **107**, 107; M. Li, P. F. Harten and H. Cabezas, *Ind. Eng. Chem. Res.*, 2002, **41**, 5867.
- C. Jimenez-Gonzales, A. D. Curzons, D. J. C. Constable and V. L. Cunningham, *Clean Technol. Environ. Policy*, 2005, **7**, 42; C. Capello, S. Hellweg and K. Hungerbühler, *The Ecosolvent Tool*, ETH Zurich, Safety & Environmental Technology Group, Zurich, 2006, <http://www.sust-chem.ethz.ch/tools/ecosolvent>; C. Capello, U. Fischer and K. Hungerbühler, *Green Chem.*, 2007, **9**, 927.
- S. Elgue, L. Prat, P. Cognet, M. Cabassud, J. M. Le Lann and J. Cezerac, *Sep. Purif. Technol.*, 2004, **34**, 273–281; S. Elgue, L. Prat, M. Cabassud and J. Cezerac, *Chem. Eng. J.*, 2006, **117**, 169.
- G. Koller, U. Fischer and K. Hungerbühler, *Ind. Eng. Chem. Res.*, 2000, **39**, 960; H. Sugiyama, U. Fischer and K. Hungerbühler, *The EHS Tool*, ETH Zurich, Safety & Environmental Technology Group, Zurich, 2006, <http://sust-chem.ethz.ch/tools/EHS>.
- Ecoinvent database by Frischknecht, *et al.*, v.1.3, 2006, Swiss Centre for Life Cycle Inventories, Switzerland.
- D. Kralisch, A. Stark, S. Körsten, B. Ondruschka and G. Kreisel, *Green Chem.*, 2005, **7**, 301; D. Kralisch, D. Reinhardt and G. Kreisel, *Green Chem.*, 2007, **9**, 1308.
- Simplifying LCA: just a cut?—Final report of the SETAC–Europe Screening and Streamlining Working-Group*, Society of Environmental Chemistry and Toxicology (SETAC), Brussels, Belgium, 1997.
- O. Diels and K. Alder, *Justus Liebigs Ann. Chem.*, 1928, **460**, 98.
- D. C. Rideout and R. Breslow, *J. Am. Chem. Soc.*, 1980, **102**, 7816.
- P. A. Grieco, J. J. Nunes and M. D. Gaul, *J. Am. Chem. Soc.*, 1990, **112**, 4595; P. A. Grieco, J. L. Collins and S. T. Handy, *Synlett*, 1995, **11**, 1155.
- S. T. Handy, P. A. Grieco, C. Mineur and L. Ghosez, *Synlett*, 1995, 565.
- M. J. Diego-Castro and H. C. Hailes, *Tetrahedron Lett.*, 1998, **39**, 2211.
- C. Cativiela, J. I. Garcia, J. Gil, R. M. Martinez, J. A. Mayoral, L. Salvatella, J. S. Urieta, A. M. Mainar and M. H. Abraham, *J. Chem. Soc., Perkin Trans. 2: Phys. Org. Chem.*, 1997, 653; C. Cativiela, J. I. Garcia, J. A. Mayoral, A. Avenzoza, J. M. Peregrina and M. A. Roy, *J. Phys. Org. Chem.*, 1991, **4**, 48; C. Cativiela, J. I. Garcia, J. A. Mayoral, A. J. Royo, L. Salvatella, X. Assfeld and M. F. Ruiz-Lopez, *J. Phys. Org. Chem.*, 1992, **5**, 230; J. A. Berson, Z. Hamlet and W. A. Mueller, *J. Am. Chem. Soc.*, 1962, **84**, 297.
- R. Breslow, *Acc. Chem. Res.*, 1991, **24**, 159; W. Blokzijl, M. J. Blandamer and J. B. F. N. Engberts, *J. Am. Chem. Soc.*, 1991, **113**, 4241; S. Otto and J. B. F. N. Engberts, *Pure Appl. Chem.*, 2000, **72**, 1365; A. Meijer, S. Otto and J. B. F. N. Engberts, *J. Org. Chem.*, 1998, **63**, 8989.
- C. Cativiela, J. I. Garcia, J. A. Mayoral and L. Salvatella, *Chem. Soc. Rev.*, 1996, **25**, 209.
- S. Kobayashi and C. Ogawa, *Chem.–Eur. J.*, 2006, **12**, 5954.
- T. Fischer, A. Sethi, T. Welton and J. Woolf, *Tetrahedron Lett.*, 1999, **40**, 793; M. J. Earle, P. B. McCormac and K. R. Seddon, *Green Chem.*, 1999, **1**, 23; I. Meracz and T. Oh, *Tetrahedron Lett.*, 2003, **44**, 6465; J. K. Park, P. Sreekanth and B. M. Kim, *Adv. Synth. Catal.*, 2004, **346**, 49; A. Vidis, C. A. Ohlin, G. Laurenczy, E. Kuesters, G. Sedelmeier and P. J. Dyson, *Adv. Synth. Catal.*, 2005, **347**, 266; G. Silvero, M. J. Arevalo, J. L. Bravo, M. Avalos, J. L. Jimenez and I. Lopez, *Tetrahedron*, 2005, **61**, 7105; E. Janus, I. Goc-Maciejewska, M. Lozynski and J. Pernak, *Tetrahedron Lett.*, 2006, **47**, 4079; R. A. Bartsch and S. V. Dzyuba, *ACS Symp. Ser.*, 2003, **856**, 289.
- A. Aggarwal, N. L. Lancaster, A. R. Sethi and T. Welton, *Green Chem.*, 2002, **4**, 517.
- P. Wasserscheid and M. Haumann, *Catalysis by Metal Complexes*, 2006, **30**, 183; S. L. Jain, J. K. Joseph and B. Sain, *Catal. Lett.*, 2007, **115**, 52.
- G. Silvero, M. J. Arevalo, J. L. Bravo, M. Avalos, J. L. Jimenez and I. Lopez, *Tetrahedron*, 2005, **61**, 7105.
- Cumulative Energy Demand—Terms, Definitions, Methods of Calculation*, in *VDI-Richtlinien 4600*, Verein Deutscher Ingenieure, Düsseldorf, 1997.
- Umberto, v. 5.0, 2005. ifu Institut für Umweltinformatik, Hamburg; ifeu Institut für Energie- und Umweltforschung, Heidelberg; Germany.
- D. A. Waterkamp, M. Heiland, M. Schlüter, J. C. Sauvageau, T. Beyersdorff and J. Thöming, *Green Chem.*, 2007, **9**, 1084.
- e.g. Merck KGaA, Safety data sheets, 2008.
- DMU is mentioned in teratogen lists to have teratogenic properties. Von Kreybig *et al.* as well as Teramoto *et al.* showed that teratogenic activity is enhanced by the increasing number of methyl groups in the urea system. In their investigations, 1,3-dimethyl urea seems to be

- unlikely to be teratogenic. Mostly, teratogenic effects are not included in safety data sheets. T. von Kreybig, R. Preussmann and I. von Kreybig, *Arzneim.-Forsch.*, 1969, **19**, 1073; S. Teramoto, M. Kaneda, H. Aoyama and Y. Shirasu, *Teratology*, 1981, **23**, 335.
- 37 S. Stolte, S. Abdulkarim, J. Arning, A. K. Blomeyer-Nienstedt, U. Bottin-Weber, M. Matzke, J. Ranke, B. Jastorff and J. Thöming, *Green Chem.*, 2008, **10**, 214.
- 38 Chemical prices: online quote request ([www.merck.de](http://www.merck.de), February 2008); in the case of [C<sub>6</sub>MIM][BF<sub>4</sub>] online quote request ([www.solvent-innovation.com](http://www.solvent-innovation.com), April 2008). The energy-related costs are influenced by the energy required for the synthesis (stirring, reaction temperature), the workup effort and by the refeeding of the solvent. Costs of 0.20 € (kW h)<sup>-1</sup> were assumed to calculate the share of this cost source.
- 39 C. Hilgers, P. Wasserscheid, in *Ionic Liquids in Synthesis*, ed. P. Wasserscheid and T. Welton, Wiley-VCH, Weinheim, Germany, 2003, p. 21.
- 40 J. P. Brans, P. Vincke and B. Mareschal, *Eur. J. Operat. Res.*, 1986, **24**, 228.
- 41 Decision Lab 2000. v. 1.01.0386, 2005. Visual Decision Inc.
- 42 Accelerating ionic liquid commercialization—Research Needs to Advance New Technology. Technical report, BCS Incorporated, 2004. [www.chemicalvision2020.org/pdfs/ionicliquid\\_commercialization.pdf](http://www.chemicalvision2020.org/pdfs/ionicliquid_commercialization.pdf).



# Synthesis of dialkyl ethers by decarboxylation of dialkyl carbonates

Pietro Tundo,\*<sup>a,b</sup> Fabio Aricò,<sup>a</sup> Anthony E. Rosamilia<sup>a</sup> and Sofia Memoli<sup>a</sup>

Received 2nd June 2008, Accepted 1st August 2008

First published as an Advance Article on the web 1st October 2008

DOI: 10.1039/b809271k

The decarboxylation reaction of dialkyl carbonates to give their related ethers was investigated. The reaction was carried out at atmospheric pressure and in the presence of hydrotalcite or basic alumina as catalysts without any solvent. The influence of several reaction parameters on the selectivity was studied (e.g. temperature, amount of catalyst, substrate concentration, solvent). The stability of the catalyst was also investigated. The experimental data for the decarboxylation confirmed that this reaction is complicated by competitive processes, such as *dismutation* and, in one case, pyrolysis. The results obtained show that in the presence of hydrotalcite as a catalyst, symmetrical dialkyl ethers can be synthesised with yields up to 80%. Dissymmetrical ethers (*i.e.* methyl alkyl ethers) can be produced with yields up to 80% at high temperature (250 °C). The catalyst proved to be fully recyclable in all cases studied, except for the carbonate containing *n*-octyl moiety.

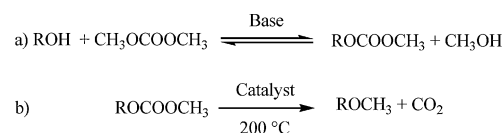
## 1. Introduction

Methylations are extremely important reactions in synthetic organic chemistry. Typically methylations are carried out using methyl halides or dimethyl sulfate. Both reagents are toxic and corrosive chemicals. Moreover the reaction requires a stoichiometric amount of a base as catalyst and produces a stoichiometric amount of inorganic salts that need to be disposed of. Dimethyl carbonate (DMC) is an environmentally benign substitute for dimethyl sulfate and methyl halides.<sup>1-4</sup> In fact, at temperatures higher than 150 °C, it acts as a methylating agent, producing CO<sub>2</sub> and methanol as the only by-products. DMC reacts in the presence of a base with nucleophiles, such as anilines,<sup>1</sup> phenols<sup>2</sup> and methylene-active compounds,<sup>3</sup> to yield, at reflux temperature, their mono-methyl derivatives, according to a B<sub>Al</sub>2 mechanism.<sup>4</sup> Under similar conditions, the reaction of alcohols with DMC gives only the transesterification product (B<sub>Ac</sub>2 attack).<sup>5</sup>

Recently we reported the synthesis of methyl ethers in high yield from the reaction of their parent alcohols with DMC by operating in the presence of catalysts (such as hydrotalcite or basic alumina) at 200 °C.<sup>6</sup>

Scheme 1 reports a possible reaction mechanism for the reaction. Presumably, under basic catalysis the carbonate derivative forms first and would then decarboxylate to the corresponding methyl ether.

This methylation procedure requires a large excess of DMC, which is used as solvent and reagent, and produces dimethyl ether as by-product. In this paper, we aim to investigate the two step synthesis of dialkyl ethers and in particular of alkyl methyl ethers, from their parent alcohols. Thus, according to



Scheme 1 Methylation of alcohols with DMC.

Scheme 1, a selection of dialkyl carbonates (Fig. 1) has been synthesised using only stoichiometric amounts of DMC. Then the decarboxylation reaction of the isolated products was investigated in the presence of catalysts and without any solvent. The influence of several reaction parameters on the selectivity was studied.

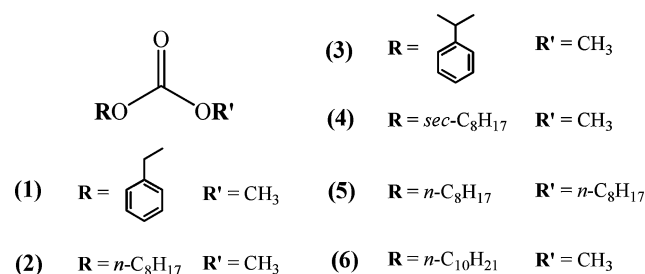


Fig. 1 Investigated dialkyl carbonates.

The advantages of this approach is that DMC is employed only in stoichiometric amounts and the catalyst of the decarboxylation reaction can be recycled.

## 2. Result and discussion

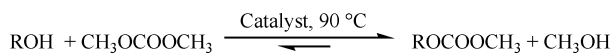
### 2.1 Decarboxylation of primary alkyl derivatives: benzyl methyl carbonate (1) and 1-octyl methyl carbonate (2)

Benzyl methyl carbonate (1) and 1-octyl methyl carbonate (2) were synthesised by transesterification with DMC from their

<sup>a</sup>Interuniversity Consortium "Chemistry for the Environment", Via delle Industrie 21/8, 30175, Marghera, Venice, Italy

<sup>b</sup>Ca' Foscari Università di Venezia, Dipartimento Scienze Ambientali, Dorsoduro 2137, 30123, Venice, Italy. E-mail: tundop@unive.it; Fax: +39-041-2348620; Tel: +39-041-2348642

parent alcohols (benzyl alcohol and 1-octanol, respectively) under reflux conditions (90 °C), in the presence of hydrotalcite KW2000 ( $\text{Mg}_{0.7}\text{Al}_{0.3}\text{O}_{1.15}$ )<sup>7</sup> or  $\text{K}_2\text{CO}_3$  as catalyst (Scheme 2), according to the procedure already reported in the literature<sup>5a</sup> or described in the Experimental.



**Scheme 2** Synthesis of alkyl methyl carbonates.

The isolated carbonates **1** and **2** were then subjected to decarboxylation. In a typical experiment the alkyl methyl carbonate was added through a funnel to the catalyst pre-heated at the given reaction temperature without any solvent present. Either basic alumina or activated hydrotalcite KW2000 was used as the catalyst.

The results obtained at 180 °C and 200 °C are reported in Table 1 for compound **1** and in Table 2 for compound **2**.  $\text{K}_2\text{CO}_3$ -catalysed reactions were also performed for comparison. When the reaction was catalysed by alumina or hydrotalcite, the two carbonates **1** and **2** were converted into their methyl and dialkyl ethers (entries 1–4, Tables 1 and 2).

For benzyl methyl carbonate, the KW2000-catalysed reaction was complete at 180 °C after 30 minutes (entry 3, Table 1), while the alumina-catalysed reaction needed higher temperature (200 °C) to achieve an almost quantitative conversion (entry 2, Table 1). For the benzyl methyl carbonate **1**, KW2000 was more effective as a catalyst than alumina in the synthesis of symmetrical ethers. For both the substrates **1** and **2**, temperature seemed to have just a little effect on the outcome of the reactions.

As expected, no methylether products were observed for the  $\text{K}_2\text{CO}_3$ -catalysed reactions (entries 5 and 6, Tables 1 and 2).

## 2.2 Decarboxylation of secondary alkyl derivatives: 1-phenylethyl methyl carbonate (**3**) and 2-octyl methyl carbonate (**4**)

In order to study the reactivity of secondary alcohol derivatives and to investigate the related reaction mechanism, 1-phenylethyl methyl carbonate **3** and 2-octyl methyl carbonate **4** were synthesised by a transesterification reaction with DMC from their parent alcohols (1-phenylethanol and 2-octanol, respectively) and then they were decarboxylated under the same conditions employed for the compounds **1** and **2**.

The results are shown in the Tables 3 and 4, respectively.

Also in this case, when the reaction was catalysed by alumina or hydrotalcite, the two secondary carbonates were converted into the methylether products (entries 1–4, Tables 3 and 4). For 1-phenylethyl methyl carbonate **3**, the KW2000-catalysed reaction was complete at 180 °C (entries 3, Table 3), while the alumina-catalysed reaction required a higher temperature (200 °C) to achieve an almost quantitative conversion (entry 2, Table 3). However, in all the experiments a considerable amount of symmetrical ethers was also observed. Methylether products were not observed for the  $\text{K}_2\text{CO}_3$ -catalysed reactions (entries 5 and 6, Table 3 and 4).

In the decarboxylation of 1-phenylethyl methyl carbonate (Table 3) styrene was also formed as by-product. In this regard, two possible reaction pathways leading to the olefin may be envisaged: (i) the base-promoted elimination of methyl carbonate  $\text{CH}_3\text{OCOO}^-$  from the reagent carbonate, and (ii) the pyrolysis of the methyl carbonate (Tschugaev's reaction) with

**Table 1** Decarboxylation of benzyl methyl carbonate **1**; Scheme 3<sup>a</sup>

	Catalyst	<i>T</i> /°C	Conv. (%)	Product distribution (GC-MS %) R = PhCH <sub>2</sub>			
				ROME	ROR	ROCOOR	ROH
1	Al <sub>2</sub> O <sub>3</sub> (10%) <sup>b</sup>	180	71	22	38	26	10
2	Al <sub>2</sub> O <sub>3</sub> (10%) <sup>b</sup>	200	92	31	48	13	4
3	KW2000 (10%) <sup>b</sup>	180	100	31	66	—	—
4	KW2000 (10%) <sup>b</sup>	200	100	29	71	—	—
5	K <sub>2</sub> CO <sub>3</sub> (1.2 eq.)	180	47	—	—	67	26
6	K <sub>2</sub> CO <sub>3</sub> (1.2 eq.)	200	59	—	—	74	26

<sup>a</sup> Reaction conditions: Reaction time: 30 min. <sup>b</sup> **1**/catalyst 1.0 : 0.1 (w/w).

**Table 2** Decarboxylation of 1-octyl methyl carbonate **2**; Scheme 3<sup>a</sup>

	Catalyst	<i>T</i> /°C	Conv. (%)	Product distribution (%) R = CH <sub>3</sub> (CH <sub>2</sub> ) <sub>7</sub>			
				ROME	ROR	ROCOOR	ROH
1	Al <sub>2</sub> O <sub>3</sub> (10%) <sup>b</sup>	180	80	20	3	67	11
2	Al <sub>2</sub> O <sub>3</sub> (10%) <sup>b</sup>	200	81	24	4	62	9
3	KW2000 (10%) <sup>b</sup>	180	92	21	5	63	11
4	KW2000 (10%) <sup>b</sup>	200	100	23	23	45	9
5	K <sub>2</sub> CO <sub>3</sub> (1.2 eq.)	180	14	—	—	100	—
6	K <sub>2</sub> CO <sub>3</sub> (1.2 eq.)	200	49	—	—	100	—

<sup>a</sup> Reaction conditions: Reaction time 30 min. <sup>b</sup> **2**/catalyst 1.0 : 0.1 (w/w).

**Table 3** Decarboxylation of 1-phenylethyl methyl carbonate **3**; Scheme 3<sup>a</sup>

	Catalyst	T/°C	Conv. (%)	Product distribution (%) R = Ph (Me)CH				
				ROME	ROR	ROCOOR	ROH	Styrene
1	Al <sub>2</sub> O <sub>3</sub> (10%) <sup>b</sup>	180	74	37	12	3	17	29
2	Al <sub>2</sub> O <sub>3</sub> (10%) <sup>b</sup>	200	96	34	12	—	11	38
3	KW2000 (10%) <sup>b</sup>	180	98	23	25	9	19	24
4	KW2000 (10%) <sup>b</sup>	200	100	24	32	—	19	25
5	K <sub>2</sub> CO <sub>3</sub> (1.2 eq.)	200	63	—	—	80	10	10

<sup>a</sup> Reaction conditions: Reaction time 30 min. <sup>b</sup> **3**/catalyst 1.0 : 0.1 (w/w).

**Table 4** Decarboxylation of 2-octyl methyl carbonate **4**; Scheme 3<sup>a</sup>

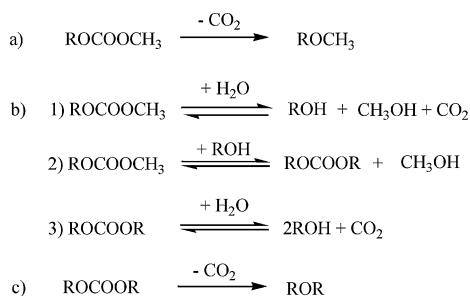
	Catalyst	T/°C	Conv. (%)	Product distribution (%) R = CH <sub>3</sub> (CH <sub>2</sub> ) <sub>5</sub> CHCH <sub>3</sub>			
				ROME	ROR	ROCOOR	ROH
1	Al <sub>2</sub> O <sub>3</sub> (10%) <sup>b</sup>	180	19	21	—	33	42
2	Al <sub>2</sub> O <sub>3</sub> (10%) <sup>b</sup>	200	24	28	—	28	39
3	KW2000 (10%) <sup>b</sup>	180	85	24	—	73	3
4	KW2000 (10%) <sup>b</sup>	200	100	35	4	53	7
5	K <sub>2</sub> CO <sub>3</sub> (1.2 eq.)	180	15	—	—	3	53
6	K <sub>2</sub> CO <sub>3</sub> (1.2 eq.)	200	10	—	—	100	—

<sup>a</sup> Reaction conditions: Reaction time 30 min. <sup>b</sup> **4**/catalyst 1.00:0.10 (w/w).

elimination of methylcarbonic acid; both rapidly decompose in CO<sub>2</sub> and methanol. However the formation of 1- or 2-octene was never observed (Table 2 and 4) in the reactions where **2** and **4** were used as substrates. The absence of any elimination by-product in these reactions demonstrates that the elimination reaction is not base-promoted, thus the styrene production is probably due only to pyrolysis reaction.

### 2.3 The reaction pathway

These preliminary results show that different and competitive processes might be involved in the decarboxylation of methylcarbonates: Scheme 3 reports a possible reaction pathway. According to the proposed mechanism, the presence of the symmetric ethers in the reaction mixture might be due to a



**Scheme 3** Competitive processes involved in the decarboxylation of alkyl methyl carbonates: (a) decarboxylation of methyl carbonates; (b) *dismutation* via transesterification (trace of methanol, due to the presence of a small amount of water, or other Brønsted acids catalyse the reaction); (c) decarboxylation of the dialkyl carbonates. Steps b1, b2 and b3 are equilibrium reactions; steps a and c are not equilibrium reactions.

*“dismutation reaction”*. In this case, the term *dismutation* is not used in the conventional redox sense; it is used instead to indicate the transformation of an alkyl methyl carbonate into dimethylcarbonate and the corresponding dialkylcarbonate.

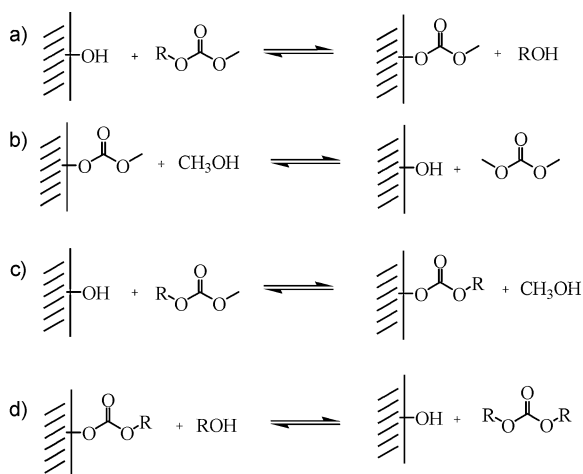
Scheme 4 describes some possible reaction pathways for the *“dismutation”* reaction catalysed by the surface hydroxyls of the catalyst. In fact, transesterification, which leads to the symmetrical carbonate, might be due to the presence of acidic hydroxyl moieties in the catalyst: hydrolysis or methanolysis of the methyl carbonates gives the alcohol, which reacts with the initial carbonate to form the symmetrical carbonates.

The acidic hydroxyl moieties of the catalyst might play a crucial role, since they are the catalysts for the transesterification reaction, too. Catalytic amounts of methanol (or water) might be sufficient to initiate these side processes since the methanol produced can react once again with the carbonate in a self-sustaining process. These acidic hydroxyls, being real catalysts, do not enter into the stoichiometry of the overall reaction.

The driving force for this *dismutation* reaction, which produces the symmetrical ethers as the final products, might be the formation of DMC (always present in significant amounts in the distillate, see Experimental) or methanol, both removed by evaporation from the reaction mixture at the given temperatures.

In order to understand the correlation between the acidic hydrogen of the catalyst hydrotalcite and the observed transesterification behavior which yields symmetrical ethers, IR analysis was performed on the catalyst after different heating activation methods.

The IR spectrum of untreated hydrotalcite (KBr pellet) showed the broad absorption band for the OH stretching around 3400 cm<sup>-1</sup> and the corresponding HOH bending at 1630 cm<sup>-1</sup>, along with the typical band at 1363 cm<sup>-1</sup> attributable to the



Total reaction (*dismutation*):



**Scheme 4** Dismutation of methyl alkyl carbonates. Due the presence of acidic hydroxyls on the surface of the catalyst, transesterification reactions occur: methanol and alcohol are released which, in turn, produce, through a series of equilibria reactions, DMC and the symmetrical dialkyl carbonate. The overall reaction (addition of routes *a*, *b*, *c* and *d*) is shown.

interlayer anions  $\text{CO}_3^{2-}$ . By heating the pellet at 200 °C for two hours under vacuum, interlayer water was removed from the hydrotalcite, as shown by the lost of the band at 1630  $\text{cm}^{-1}$  and the decrease in the intensity of the band at 3400  $\text{cm}^{-1}$ . However, after a few seconds in the air, the intensity of the latter band rapidly increased.

In a separate experiment, the pellet was heated under vacuum at 450 °C for 1.5 hours in a quartz tube, equipped with a  $\text{CaF}_2$  window, which allowed recording of the IR spectrum without opening the system. The spectrum shows that this treatment completely removed not only the interlayer water and carbonate groups, but also surface hydroxyl groups. However, a very short exposure to air by opening the tube immediately restored the lost water. Such results showed that, if the decarboxylation reaction is performed under atmospheric air, heat activation may not ensure the complete absence of water on the catalyst surface. And, even when the interlayer water is completely removed, hydrolysis and transesterification reactions may also occur, due to the hydroxyl groups which are not affected by the treatment at 200 °C.

#### 2.4 Effect of the temperature and of the amount of catalyst

In order to improve the yield of the decarboxylation over the other competing pathways, the influence of some reaction parameters was investigated. In a first set of experiments, the decarboxylation of 1-octyl methyl carbonate **2** was performed using varying amounts of catalyst. In particular, the reaction was carried out using an amount of KW2000 ranging from 10% to 50% w/w. Results reported in Table 5 show that no relevant improvement was obtained increasing the catalyst/substrate ratio. On the contrary, higher ratio of catalyst increased the viscosity of the reaction, strongly impairing the stirring.

**Table 5** Decarboxylation of 1-octyl methyl carbonate **2** with different substrate/catalyst ratio

	KW2000 (%) <sup>a</sup>	Conv. (%)	Product distribution (%) R = $\text{CH}_3(\text{CH}_2)_7$			
			ROME	ROR	ROCOOR	ROH
1	10	100	23	32	34	9
2	25	100	27	63	1	6
3	50	100	33	54	2	9

<sup>a</sup> Reaction time: 30 min.  $T = 220$  °C.

In addition, the decarboxylation reactions on 1-octyl methyl carbonate **2** and 2-octyl methyl carbonate **4** were performed varying the temperature from 180 °C to 250 °C. In all cases the reaction time was 30 minutes and KW2000 was used as a catalyst.

The results, reported in Table 6, showed that performing the reaction at different temperatures did not affect the conversion, which is complete in every case, except when the reaction was carried out at 180 °C. There is, however, a little effect on the selectivity to 1-octyl methyl ether.

The yield of 1-octyl methyl ether increased at high reaction temperatures, although not significantly. The most important effect observed was the complete decarboxylation of the intermediate dioctyl carbonate into dioctyl ether.

Table 7 reports the results of the decarboxylation of 2-octyl methyl carbonate **4**. Also in this case, no major differences in the reaction outcome were observed. However, the yields of the methyl and dialkyl ether are slightly increased, whilst the yield of dialkyl carbonate decreased.

**Table 6** Decarboxylation of 1-octyl methyl carbonate **3** at different temperatures<sup>a</sup>

	$T/^\circ\text{C}$	Conv. (%)	Product distribution (%) R = $\text{CH}_3(\text{CH}_2)_7$			
			ROME	ROR	ROCOOR	ROH
1	180	92	21	5	63	11
2	200	100	23	23	45	9
3	220	100	23	32	34	9
4	240	99	27	68	0	1
5	250	100	28	70	0	2

<sup>a</sup> **3**/KW2000 1.00 : 0.10 (w/w). Reaction time: 30 min.

**Table 7** Decarboxylation of 2-octyl methyl carbonate **4** at different temperatures<sup>a</sup>

	$T/^\circ\text{C}$	Conv. (%)	Product distribution (%) R = $\text{CH}_3(\text{CH}_2)_5\text{CHCH}_3$			
			ROME	ROR	ROCOOR	ROH
1	180	85	24	0	73	3
2	200	100	35	4	53	7
3	220	100	44	13	27	13
4	240	100	53	24	0	21
5	250	100	53	31	0	14

<sup>a</sup> **4**/KW2000 1.00 : 0.10 (w/w). Reaction time: 30 min.



**Table 8** Decarboxylation of *n*-decyl methyl carbonate at different concentrations<sup>a</sup>

	Solvent	Substrate conc.	Conv. (%)	Product distribution (%) R = CH <sub>3</sub> (CH <sub>2</sub> ) <sub>9</sub>			
				ROME	ROR	ROCOOR	ROH
1	no solvent	—	100	55	27	10	7
2	<i>n</i> -dodecane	1.2 M	100	45	42	0	13
3	<i>n</i> -dodecane	0.015 M	98	52	10	14	22

<sup>a</sup> *T* = 216 °C; KW2000 10%; reaction time: 30 minutes.

## 2.5 Effect of the substrate concentration

*n*-Dodecane was chosen as a non-polar solvent to explore the effect of the substrate concentration (if any); the decarboxylation of *n*-decyl methyl carbonate **6**, chosen as a test reaction, was carried out at the reflux temperature of the solvent, 216 °C. The results obtained for the two studied concentrations (1.2 and 0.015 M) are reported in Table 8. Entry 1 reports, for comparison, the result obtained from the reaction performed at 216 °C in the absence of solvent.

Table 8 shows that dilution does not considerably influence the yield of 1-decyl methyl ether, which is formed in about 50% yield in all cases.

## 2.6 Effect of the solvent

Because solvent polarity very often affects the reaction outcome, the decarboxylation was carried out in different solvents. In this case, a standard procedure using different solvents was used (see Experimental): the decarboxylation reaction was carried out by slow dropwise addition of the *n*-decyl methyl carbonate to the refluxing solvent. Accordingly, experiments were conducted using different solvents at their respective refluxing temperature. Table 9 reports that the selectivity to the methyl ether dramatically increased with respect to the same reaction performed by the bulk addition of the substrate (compare Table 8 to entry 2 of Table 9).

Using *n*-dodecane as the solvent at 1.2 M substrate concentration, the yield of *n*-decyl methyl ether increased from 45% (Table 8, entry 2) to 78% (Table 9, entry 2). The yield of the methyl ether was even higher (80%, entry 3, Table 9) in refluxing *n*-tetradecane (b.p. 252 °C), while slightly lower (67%, entry 1) in refluxing *trans*-decaline (b.p. 190 °C). No reaction was observed with polar aprotic solvents, such as polyethyleneglycol dimethylether (PEG 250 DME) and tri-

ethyleneglycol dimethylether (triglime). Probably, such polar solvents inhibit the absorption of the polar compounds on the catalyst, preventing the reaction from occurring. *Vice versa*, the non polar solvents, by allowing the absorption on the catalyst, promote the reaction.

Since all the non polar solvents used have a similar hydrocarbon structure, the different yields observed may be attributed to the temperature. This might indicate that the activation energy of the decarboxylation reaction is higher than that of the transesterification, since increasing the temperature (from 190 to 252 °C), increased the yield of the methyl ether (from 67 to 80%).

## 2.7 Decarboxylation of di-1-octylcarbonate (5)

Finally, in order to avoid the production of undesired by-products *via* the *dismutation* pathway, the decarboxylation of a symmetrical dialkyl carbonate was also carried out. The reaction was performed in the absence of solvent; this should give the corresponding ether only. Thus, a set of experiments was performed using di-1-octyl carbonate as the substrate at different temperatures (Table 10).

The effect of temperature on the conversion was evident. Conversion reached a plateau at 240 °C. As expected, the yield of dioctyl ether increases by increasing temperature, while the yield of 1-octanol dramatically decreases. The results support the idea that decarboxylation is highly dependent on the temperature, due to its high activation energy.

## 2.8 Catalyst stability and recycling

The stability of the catalyst is also an important parameter. Fig. 2 shows the data obtained performing the decarboxylation reaction of di-1-octyl carbonate **5** at different reaction times. After two hours the reaction shows no significant improvement

**Table 9** Decarboxylation of *n*-decyl methyl carbonate **6** by dropwise addition to refluxing solvents containing the catalyst<sup>a</sup>

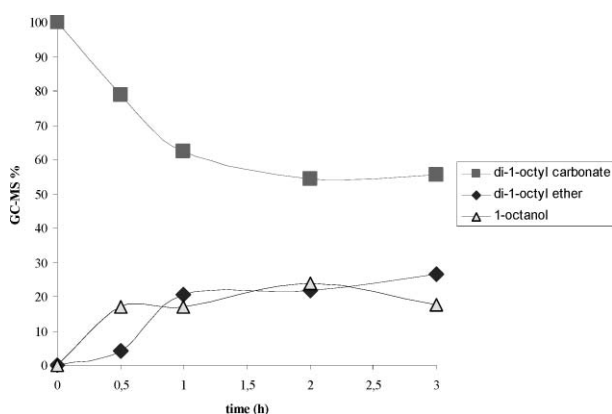
	Solvent	Reflux <i>T</i> /°C	Conv. (%)	Product distribution (%) R = CH <sub>3</sub> (CH <sub>2</sub> ) <sub>9</sub>			
				ROME	ROR	ROCOOR	ROH
1	<i>trans</i> -decaline	190	98	67	21	—	10
2	<i>n</i> -dodecane	216	100	78	21	—	1
3	<i>n</i> -tetra decane	252	100	80	20	—	—
4	PEG 250 DME <sup>b</sup>	220	4	—	1	—	1
5	Triglime	216	9	—	—	—	9

<sup>a</sup> 1.2 M *n*-decyl methyl carbonate added dropwise; KW2000 10%; reaction time: 30 minutes after complete addition. <sup>b</sup> Poly(ethylene glycol) dimethyl ether, average *M<sub>n</sub>* ~ 250; b.p > 250 °C.

**Table 10** Decarboxylation of di-1-octyl carbonate **5** at different temperatures<sup>a</sup>

	<i>T</i> /°C	Conv. (%)	Product distribution (%) R = CH <sub>3</sub> (CH <sub>2</sub> ) <sub>7</sub>	
			ROR	ROH
1	180	21	20	80
2	200	57	63	35
3	220	71	79	21
4	240	98	84	14
5	250	94	82	18

<sup>a</sup> Reaction condition: **5**/KW2000 1.00 : 0.10 (w/w). For other reaction conditions see footnotes of Table 6.

**Fig. 2** Decarboxylation of dioctyl carbonate **5** with time. Reaction conditions: dioctyl carbonate/KW2000 1.00 : 0.10 (w/w). *T* = 180 °C.

on conversion; this can be attributed to possible deactivation of the catalyst.

In order to investigate the origin of such a deactivation, a few tests for the re-use of the catalyst were carried out. After the reaction, KW2000 was regenerated by washing with diethyl ether and then dehydrated in an oven at 100 °C or in a muffle oven at 500 °C; the latter treatment is the general condition used to activate the catalyst in all the experiments so far reported (see Experimental). In Table 11, the results obtained with some of the carbonates previously investigated: an aliphatic substrate **2**, an aromatic substrate **3**, and a secondary aliphatic substrate

**4**, are shown. The recovered catalyst was reused with the same carbonate for which it was originally tested.

The tests show that the catalyst is not regenerated completely when treated at 100 °C (entries 6 and 9), while it is regenerated by treatment at 500 °C (entries 7 and 10), except in the case of octyl methyl carbonate **3** (entries 2 and 4). The structure and the texture of hydrotalcite is not affected by the treatment, and its activity remains unaffected.

The results given by the C<sub>8</sub> moiety are quite interesting. In fact, after 100 °C treatment (entry 2) while the conversion is not significantly changed, the efficiency of the catalyst dramatically decreased. Visible changes (from white to dark black) were observed after treatment at 500 °C, due to carbon formation.

This behaviour might show that the cavities of hydrotalcite are particularly suited to the 1-octanol generated in the reaction, which is difficult to remove by washing and cracks during heat treatment. The affinity of 1-octanol for the catalyst cavities might also be the cause of its deactivation depicted in Fig. 2.

The only method possible for the removal of the 1-octanol from the KW2000 cavities was to wash the catalyst in diethylether using a sonicator bath.

### 3. Conclusions

The synthesis of ethers from the parent carbonates has been reported utilizing basic alumina and hydrotalcite as catalysts; the latter proved to be the best catalyst. Dimethyl carbonate was used only in a stoichiometric amount for the conversion of the alcohols to carbonates. The reaction can be carried out at atmospheric pressure and with no solvent.

In such a two step procedure, and starting from alkyl methyl carbonates, the reaction becomes complicated by the presence of symmetrical dialkyl carbonates and the corresponding dialkyl ethers as by-products.

This is due to the presence of acidic hydrogens (water, alcohols, and surface hydroxyls) which allow the organic carbonates to give transesterified compounds which produce the symmetrical ethers; this process is controlled also by the boiling points of the alkyl carbonates involved, since DMC is removed by distillation from the reaction mixture.

Dissymmetrical ethers (*i.e.* methyl alkyl ethers) can be obtained in good yield if the reactions are carried out at high

**Table 11** Recycling test. Decarboxylation of compound **2**, **3** and **4**, for each carbonate the reaction with both recycled and new catalyst<sup>a</sup>

	Substrate	Catalyst origin	Conv. (%)	Product distribution (%)				
				ROME	ROR	ROCOOR	ROH	Styrene
1	<b>2</b>	new <sup>b</sup>	92	21	5	63	11	NA
2	<b>2</b>	recycled (100 °C)	89	0	0	100	0	NA
3	<b>2</b>	new (100 °C)	77	0	0	83	17	NA
4 <sup>c</sup>	<b>2</b>	recycled (500 °C)	—	—	—	—	—	—
5	<b>3</b>	new <sup>d</sup>	98	23	25	9	19	24
6	<b>3</b>	recycled (100 °C)	54	14	4	54	21	8
7	<b>3</b>	recycled (500 °C)	96	24	18	28	16	13
8	<b>4</b>	new <sup>e</sup>	85	24	0	73	3	NA
9	<b>4</b>	recycled (100 °C)	58	14	7	71	10	NA
10	<b>4</b>	recycled (500 °C)	82	21	0	57	9	NA

<sup>a</sup> Reaction conditions: *T* = 180 °C. Reaction time: 30 min; carbonate/catalyst 1.00 : 0.10 (w/w). Data given as GC%. NA: not applicable. <sup>b</sup> Entry 3 Table 2. <sup>c</sup> The reaction was not performed due to blackening of the catalyst. <sup>d</sup> Entry 3 Table 3. <sup>e</sup> Entry 3 Table 4.

temperature. High temperature favours the decarboxylation over the “*dismutation*” reaction and methyl ethers can be obtained in high yield.

A possible reason for this temperature effect is that entropic factors facilitate the elimination of CO<sub>2</sub> at high temperatures, as a consequence of the higher activation energy of the decarboxylation process. The catalyst proved to be fully recyclable in all cases, except with the compound containing the *n*-octyl moiety.

## 4. Experimental

### 4.1 General information

All compounds used were ACS grade and were used without further purification. Al<sub>2</sub>O<sub>3</sub> was from Merck, type 5016A basic standard grade, 150 mesh, no activation. KW2000 was from Kyowa Chemical Industry Co. Tokyo, Mg<sub>0.7</sub>Al<sub>0.3</sub>O<sub>1.15</sub>, specific surface area 202 m<sup>2</sup> g<sup>-1</sup>, activated at 500 °C for 4 hours.

GC-MS analyses were performed at 70 eV (MS) with a 30 m HP 5 capillary GC column.

Infrared spectra were recorded on a Nicolet Magna 750 FT-IR spectrophotometer. NMR spectra (<sup>1</sup>H, <sup>13</sup>C) were obtained on AVANCE 300 Bruker spectrometers at 25 °C and referred to internal tetramethylsilane.

Basic alumina type 5016A basic standard grade, 150 mesh, was purchased from Merck, and hydrotalcite was a kind gift from Cognis Company.

If not otherwise specified, all the reactions were performed in batch conditions and at atmospheric pressure.

### 4.2 Preparation of methyl carbonates: general procedure, Scheme 2

In a three-necked flask equipped with a dephlegmator, alcohol (30 g), DMC (100 g) and KW2000 (Mg<sub>0.7</sub>Al<sub>0.3</sub>O<sub>1.15</sub>) (30 g) were heated at refluxing conditions (90 °C) under magnetic stirring. Continuous removal of methanol as an azeotropic mixture with DMC (3 : 1 w/w) boiling at 64 °C pushed the equilibrium toward the carbonate. The reaction was followed by GC-MS analysis of the reaction mixture. At complete conversion of the substrate (usually after 24 hours), the mixture was filtered over Gooch no. 4 to remove the solid catalyst, and the solid was washed three times with 100 ml of diethylether. After removal of diethylether, methanol and unreacted DMC by evaporation under vacuum, alkyl methyl carbonate was obtained as a colourless oil.

**1:** 39 g obtained; yield: 85%; b.p.: 68–70 °C/7 torr (lit.<sup>8</sup> 125–127 °C/20 torr); <sup>1</sup>H NMR (300 MHz, CDCl<sub>3</sub>, lit.<sup>8</sup>): δ 3.81 (s, 3H); δ 5.19 (s, 2H); δ 7.37–7.41 (m, 5H)

**2:** 33 g obtained; yield: 75%; b.p.: 238 °C/760 torr (lit.<sup>9</sup> 73 °C/1 torr); <sup>1</sup>H NMR (300 MHz, CDCl<sub>3</sub>, lit.<sup>10a</sup>): δ 1.62–1.64 (d, 3H); δ 3.77 (s, 3H); δ 5.73–5.80 (m, 1H); δ 7.32–7.40 (m, 5H)

**3:** 38 g obtained; yield: 88%; b.p. 70 °C/7 torr; <sup>1</sup>H NMR (300 MHz, CDCl<sub>3</sub>, lit.<sup>10b</sup>): δ 0.86–0.90 (t, 3H); δ 1.27 (m, 10H); δ 1.62–1.70 (m, 2H); δ 3.78 (s, 3H); δ 4.11–4.16 (t, 2H)

**4:** 39 g obtained; yield: 90%; b.p. 45 °C/7 torr; <sup>1</sup>H NMR (300 MHz, CDCl<sub>3</sub>): δ 0.89 (t, 3H), δ 1.27–1.29 (m, 8H), δ 1.46–1.55 (m, 2H), δ 1.60–1.65 (m, 2H), δ 3.77 (s, 3H) δ 4.71–4.81 (m, 1H)

**6:** 36 g obtained; yield: 89%; b.p. 75 °C/7 torr; <sup>1</sup>H NMR (300 MHz, CDCl<sub>3</sub>): δ 0.86–0.90 (t, 3H); δ 1.27 (m, 14H); δ 1.62–1.70 (m, 2H); δ 3.78 (s, 3H); δ 4.11–4.16 (t, 2H)

### 4.3 Preparation of di-1-octyl carbonate (5)

In a three-necked flask equipped with a dephlegmator, 1-octanol (85 g), 1-octyl methyl carbonate (30 g) and KW2000 (30 g) were heated at 110 °C with magnetic stirrer. The reaction was followed by GC-MS analysis of the reaction mixture. At complete conversion of the substrate, which took place after 5 hours, the mixture was filtered over Gooch no. 4 to remove the catalyst and the solid was washed three times with 100 ml of diethylether. After removal of diethylether and unreacted 1-octanol by distillation under vacuum, the symmetrical carbonate was obtained as colourless oil.

**5:** 37 g obtained; yield: 82%; b.p. 165 °C/7 torr (lit.<sup>11</sup> 168–170 °C/5 torr); <sup>1</sup>H NMR (300 MHz, CDCl<sub>3</sub>, lit.<sup>12</sup>): δ 0.87–0.91 (t, 6H); δ 1.28 (m, 20H); δ 1.62–1.72 (m, 4H); δ 4.10–4.15 (t, 4H)

### 4.4 Decarboxylation reactions (Tables 1–7 and Tables 9 and 10)

All the decarboxylation reactions were carried out in a three neck round bottom flask at atmospheric pressure. The flask was equipped with a condenser and a dropping funnel. The reactor was heated using a heating jacket and the temperature was controlled by a thermocouple dipped in the reaction mixture through the side neck.

The reactions were carried out in the absence of solvent. The methylcarbonate (2 g) was added dropwise over a 1 minute period through the funnel to the catalyst pre-heated at the reaction temperature (typically at 180 or 200 °C). Basic alumina (0.2 g) or hydrotalcite KW2000 (0.2 g) or K<sub>2</sub>CO<sub>3</sub> (1.2 eq) were used as the catalysts.

Addition of the methylcarbonate substrates to the catalyst produced, in every case, vigorous foaming, due to the rapid evolution of CO<sub>2</sub>. The results obtained performing the decarboxylation reaction on the carbonates **1–6** at 180 °C and 200 °C are reported in Tables 1–7 and Tables 9 and 10, leaving out the value for DMC; however, it was always present in the chromatograms as 15% of total compounds.

### 4.5 Substrate concentration analysis (Table 8)

A round bottom flask was equipped with condenser and two dropping funnels. After heating the catalyst (1.8 g or 0.02 g) at 220 °C, *n*-dodecane (75 mL) was added from the first funnel. When the refluxing temperature of *n*-dodecane was reached (*T* = 216 °C), *n*-decyl methyl carbonate, according to the chosen concentration (18 g or 0.24 g), was quickly added from the second funnel.

### 4.6 Catalyst recycling (Table 11)

After a typical decarboxylation reaction, KW2000 was separated by a paper filter, washed with diethyl ether and submitted to 2 different treatments: dehydration in an oven at 100 °C (entries 2, 5 and 9, Table 11) and reactivation in a muffle oven up to 500 °C (entries 3, 7 and 10, Table 11). The so-treated catalyst

was then re-used performing a reaction exactly as the one from which the catalyst was taken.

## Acknowledgements

This work was supported by the Interuniversity Consortium "La Chimica per l'Ambiente" (Chemistry for the Environment) INCA, and Università "Ca' Foscari" di Venezia.

## Notes and references

- 1 M. Selva, A. Bomben and P. Tundo, *J. Chem. Soc., Perkin Trans. 1*, 1997, 1041.
- 2 A. Bomben, M. Selva and P. Tundo, *Ind. Eng. Chem. Res.*, 1999, **38**, 2075.
- 3 (a) P. Tundo, G. Moraglio and F. Trotta, *Ind. Eng. Chem. Res.*, 1989, **28**, 881; (b) A. Bomben, C. A. Marques, M. Selva and P. Tundo, *Tetrahedron*, 1995, **51**, 11573; (c) A. Bomben, M. Selva and P. Tundo, *J. Chem. Res. (S)*, 1997, 448.
- 4 (a) P. Tundo, M. Selva, A. Perosa and S. Memoli, *J. Org. Chem.*, 2002, **67**, 1071; (b) S. Memoli, M. Selva and P. Tundo, *Chemosphere*, 2001, **43**, 115; (c) P. Tundo, L. Rossi and A. Loris, *J. Org. Chem.*, 2005, **70**(6), 2219–2224.
- 5 (a) P. Tundo, F. Trotta, G. Moraglio and F. Ligorati, *Ind. Eng. Chem. Res.*, 1988, **27**, 1565; (b) P. Tundo, S. Bassanello, A. Loris and G. Sathicq, *Pure Appl. Chem.*, 2005, **77**(10), 1719.
- 6 P. Tundo, S. Memoli, D. Héroult and K. Hill, *Green Chem.*, 2004, **6**, 609.
- 7 As is well known, hydrotalcite is a synthetic aluminium-magnesium-hydroxycarbonate. Hydrotalcite-like anionic clays are a family of interesting materials with many practical applications as catalysts, catalyst supports, ion exchangers, and composite materials. Natural hydrotalcite,  $Mg_6Al_2(OH)_{16}CO_3 \cdot 4H_2O$ , structurally similar to brucite,  $Mg(OH)_2$ , is composed of sheets of edge-sharing  $Mg(OH)_6$  and  $Al(OH)_6$  octahedra. Due to isomorphous substitution of  $Al^{3+}$  for  $Mg^{2+}$ , the sheets are positively charged and stacked on top of each other and held together by charge-balancing anions, normally  $CO_3^{2-}$ , and/or hydrogen bonding. The  $Mg^{2+}$  and  $Al^{3+}$  in the sheets can also be isomorphously substituted by other metal ions having two or three positive charges and the  $CO_3^{2-}$  in the interlayer space by other inorganic and organic anions, forming new hydrotalcite-like materials. The general formula can be described as  $[M_{1-x}^{2+}M_x^{3+}(OH)_2]^{+}A_{x/n}^{n-} \cdot mH_2O$ , where M denotes metal ions, A denotes exchangeable anions with valence  $n$ , and  $x$  is within 0.17–0.33.
- 8 M. Selva, F. Trotta and P. Tundo, *J. Chem. Soc., Perkin Trans. 1*, 1992, **2**(4), 519.
- 9 Taylor, *J. Chem. Soc. B*, 1971, 622.
- 10 (a) M. Verdecchia, M. Feroci, L. Palombi and L. Rossi, *J. Org. Chem.*, 2002, **67**(23), 828; (b) C. Yu, B. Zhou, W. Su and Z. Xu, *Synth. Commun.*, 2007, **37**(4), 647.
- 11 Fukui *et al.*, *Chem. Abstr.*, 1963, **58**, 2366.
- 12 S. Sakai, Y. Kobayashi and Y. Ishii, *J. Org. Chem.*, 1971, **36**, 1176.



# Synthesis of biobased epoxy and curing agents using rosin and the study of cure reactions

Honghua Wang,<sup>a,b</sup> Bo Liu,<sup>a</sup> Xiaoqing Liu,<sup>a,b</sup> Jinwen Zhang<sup>\*a</sup> and Ming Xian<sup>\*b</sup>

Received 26th February 2008, Accepted 11th August 2008

First published as an Advance Article on the web 19th September 2008

DOI: 10.1039/b803295e

Rosin is an abundantly available natural product. Rosin is a mixture of acidic (*ca.* 90%) and neutral (*ca.* 10%) compounds. The characteristic fused ring structure of rosin acids is analogous to that of some aromatic compounds in rigidity, and makes rosin and its derivatives potential substitutes for those aromatic compounds in polymers. In this study, the synthesis of biobased epoxy and curing agent using rosin and the cure reaction were investigated. Abietyl glycidyl ether and methyl maleopimarate were synthesized from one of the rosin acids. Abietyl glycidyl ether was used as a model compound representing rosin-based epoxies, while methyl maleopimarate was used as a model compound representing rosin-based anhydride curing agents. The synthesis methods of the model compounds were examined and the chemical structures were confirmed by <sup>1</sup>H NMR, <sup>13</sup>C NMR, FT-IR and ESI-MS. Curing of abietyl glycidyl ether with aniline and curing of methyl maleopimarate with phenyl glycidyl ether were investigated separately. Nonisothermal curing of the model systems was studied by DSC, and the cured products were characterized by <sup>1</sup>H NMR.

## Introduction

Rosin is an abundantly available natural product. Rosin is mainly obtained from the exudation of pines and conifers. It is also obtained by the distillation of crude tall oil, which is a byproduct in the Kraft pulp process, or from aged pine stumps. Total world production of rosin is approximately 1.2 million tons annually.<sup>1</sup> Rosin is a mixture of acidic (*ca.* 90%) and neutral (*ca.* 10%) compounds.<sup>2</sup> The acidic components, generally named rosin (or resin) acids, are also a mixture containing mainly isomeric abietic-type acids (40–60%) and pimaric-type (9–27%) acids on the basis of total rosin weight.<sup>1</sup> The exact composition of rosin acids varies, depending on the tree species and production location. Rosin and its derivatives have long been used as adhesive tackifiers, and are still mainly used in that market. In addition, rosin and its derivatives have also found other niche applications in printing, varnishes, paints, sealing wax, some soaps, paper sizing, soldering, plasters, *etc.*<sup>2</sup>

In recent years, the drive for obtaining chemicals and materials from renewable resources has also prompted the research of new applications for rosin. Rosin acids, owing to their characteristic fused ring structure, are analogous to many aromatic compounds in rigidity. Therefore, rosin and its derivatives could become important alternatives to current fossil carbon-based aromatic monomer compounds in polymers. The chemical reactivity of rosin resides in its monocarboxylic acid and the unsaturated carbon–carbon double bonds. The Diels–Alder

adduct of levopimaric acid (one of the isomeric rosin acids) and maleic anhydride, the maleopimaric acid, for example, was used for polyesterimide<sup>3</sup> and polyamideimide.<sup>4,5</sup> Rosin-based polyols were also prepared and applied to polyurethane synthesis.<sup>6–8</sup> The adduct of levopimaric acid and acrylic acid was used to synthesize polyesters and polyamides.<sup>9</sup> Maleopimaric acid was also used as a rigid building block in aliphatic copolyesters to regulate molecular rigidity.<sup>10,11</sup> On the other hand, there have been only a few studies using rosin for epoxy resin applications. In one study, rosin-based polyamides were synthesized and used as hardeners for epoxy resins.<sup>12</sup> In another study, glycidyl esters of maleopimaric acid were prepared and then the resulting epoxides were cured with 1,2-cyclohexanedicarboxylic anhydride.<sup>13</sup> However, the relatively low hydrolysis resistance and thermal stability of the ester linkages in the epoxy resin may limit its application in uses such as electronics packaging.

It is known that anhydride-type curing agents are widely used for epoxy coating resins. Maleopimaric acid has similarities in rigid structure and functionality to trimellitic acid which is an important building block for anhydride-type curing agents. Since the conjugated carbon–carbon double bond in levopimaric acid can easily undergo Diels–Alder reaction with maleic anhydride, we are more interested in using maleopimaric acid derivatives as curing agents. Although only levopimaric acid possesses the optimum cyclic diene structure for Diels–Alder addition, the other isomeric rosin acids can undergo isomerization to levopimaric acid at elevated temperatures, preferably in the presence of a strong acid.<sup>3</sup> Considering that the ether group is more hydrolytically and thermally stable than the ester group, derivatives of rosin-based glycidyl ether are preferred for the preparation of rosin-based epoxies.

In this study, two model compounds, which represented rosin-based anhydride type curing agents and rosin-based glycidyl

<sup>a</sup>Wood Materials and Engineering Laboratory & Materials Science Program, Washington State University, Pullman, Washington, 99164, USA. E-mail: jwzhang@wsu.edu; Tel: +1 509-335-8723

<sup>b</sup>Department of Chemistry, Washington State University, Pullman, Washington, 99164, USA. E-mail: mxian@wsu.edu; Tel: +1 509-335-6073

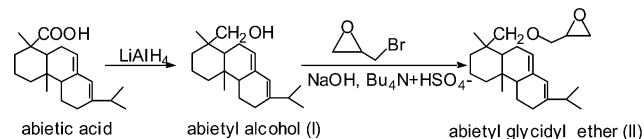
ether type epoxies, respectively, were prepared. The respective curing reactions of the epoxide with aniline and the anhydride with phenyl glycidyl ether and cure kinetics were also investigated. To the best of our knowledge, there has not been a similar study using glycidyl ether of rosin analogs as epoxies and maleated rosin analogs as hardeners in the literature. This study is part of the results from our recent investigation utilizing rosin acids as building blocks for epoxies and hardeners. The major aim of this study is to provide some synthesis methods for rosin-based anhydride and glycidyl ether and to investigate their curing and cure reactions in potential epoxy applications.

## Results and discussion

### Synthesis of model compounds

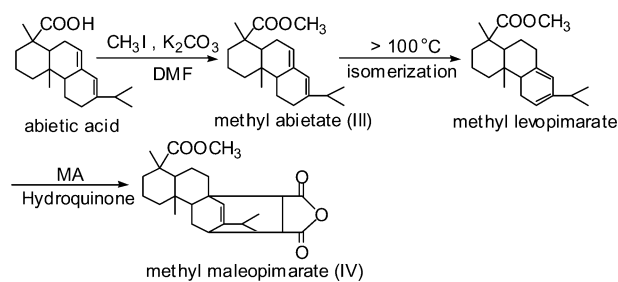
Maiti *et al.*<sup>2</sup> and Vandenberg<sup>14</sup> reported the preparation of epoxy resins based on glycidyl esters of rosin or rosin derivatives in the literature. Those epoxides were prepared by the reaction between the carboxyl groups of rosin or the anhydride groups of maleated rosin with epihalohydrin. However, those epoxies contained ester linkages rather than ether linkages between the rosin moiety and the glycidyl groups. Considering that the ether linkage is more resistant to hydrolysis and thermolysis than the ester group, the glycidyl ether type of rosin-based epoxies is more advantageous. In this study, the glycidyl ether of abietic alcohol was synthesized as an analog to rosin-based epoxies. The carboxyl group of rosin acid was first reduced to a hydroxyl group which was then reacted with epihalohydrin to achieve the glycidyl ether.

To reduce the carboxyl group of rosin to a hydroxyl group,  $\text{LiAlH}_4$  was used as the reducing agent (Scheme 1). The resulting abietyl alcohol intermediate (**I**) was then reacted with epibromohydrin to form abietyl glycidyl ether (**II**) in the presence of a phase transferring catalyst  $\text{Bu}_4\text{N}^+\text{HSO}_4^-$ . Because of the steric hindrance effect of the fused ring on the hydroxyl methyl group of abietyl alcohol, using epichlorohydrin only resulted in a very low yield of the glycidyl ether. By using the more reactive epibromohydrin, the etherification was able to proceed with a better yield. The yield and recovery yield of the epoxide from the two-step reaction were 29% and 87%, respectively.



**Scheme 1** Synthesis route of abietic glycidyl ether.

For the preparation of an analog to the rosin-based anhydride hardeners, the free carboxyl groups of rosin were first blocked by esterification (Scheme 2) with  $\text{CH}_3\text{I}$  in DMF, using  $\text{K}_2\text{CO}_3$  as the catalyst. Similar to the above etherification, the fused ring also had a significant steric hindrance effect on the reaction of the carboxyl group. Employing other reagents, such as methanol/*p*-toluenesulfonic acid, methanol/ $\text{KOH}$ , and methanol/*N,N'*-dicyclohexyl-carbodiimide, did not yield satisfactory results. Maleic anhydride was added onto the methyl ester of abietic acid (**III**) through Diels–Alder reaction, using hydroquinone as the catalyst. It was known that levopimaric acid was the only



**Scheme 2** Synthesis route of methyl maleopimarate.

rosin acid which could undergo Diels–Alder adduction, and the other isomeric rosin acids experienced the isomerization to levopimaric acid at elevated temperatures during the reaction.<sup>2,3</sup> The yield of rosin-based anhydride (**IV**, methyl maleopimarate) from the two-step reaction was 66%. Using  $\text{H}_3\text{PO}_4$  as a catalyst in the Diels–Alder reaction could also achieve the final product, but resulted in a lower yield (54%) from the two-step reaction. The structures of the intermediate and final products were identified by  $^1\text{H}$  NMR. Fig. 1 gives the  $^1\text{H}$  NMR spectra of abietic acid, abietyl glycidyl ether and methyl maleopimarate. Chemical shift peaks from  $\delta$  0.6 to 2.2 were attributed to the protons of six-member fused rings of rosin.

### Curing and cure kinetics

Similar to the isothermal curing of many other epoxy systems, a reaction was noted to take place during heating to the selected cure temperatures in this study. Although approaches such as dropping the cold sample into a preheated DSC or curve fitting could be adopted to compensate for the lost signal,<sup>15</sup> in this study we selected the simple nonisothermal method for the curing study. It has been concluded that there is no fundamental contradiction between kinetic parameters determined from isothermal and nonisothermal experiments,<sup>16,17</sup> though the inconsistency in Arrhenius parameters between these two methods persists.<sup>18,19</sup> Fig. 2 shows the exothermic heat flows of nonisothermal curing of the model compounds in the DSC experiment. The DSC experiment results are summarized in Tables 1 and 2. As the heating rate ( $\beta$ ) increased, initial curing temperature ( $T_i$ ), peak exothermic temperature ( $T_p$ ) and temperature at curing end ( $T_c$ ) all shifted to higher temperatures, and the range of curing temperature widened. However, the curing time actually decreased with heating rate increase. The enthalpy of cure reaction generally increased with heating rate up to  $10^\circ\text{C min}^{-1}$ , then showed a significant decrease at  $20^\circ\text{C min}^{-1}$ .

While the shift in the cure temperature of the cure reaction with heating rate is more probably methodological, the dependence of the cure reaction enthalpy on heating rate is supposed to have a chemical nature.<sup>20</sup> Epoxy curing involves a sequence of elementary reactions; these elementary steps and reaction pathway are temperature dependent. The relatively low enthalpy at heating rate  $20^\circ\text{C min}^{-1}$  for both curing systems is likely related to the different reaction pathways involved at the higher cure temperature. DSC analysis measures the overall reaction enthalpy. Without a comprehensive analysis of the possible elementary reactions, DSC results can only provide very limited information on the cure mechanism. Nevertheless,

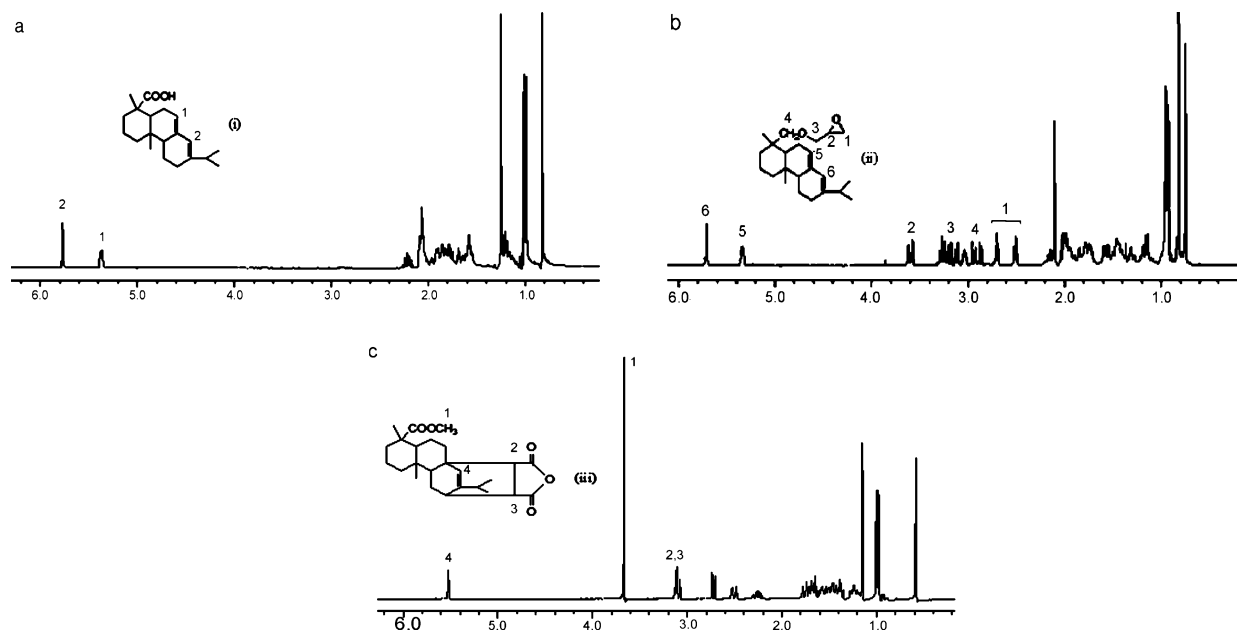


Fig. 1  $^1\text{H}$  NMR spectra of (a) abietic acid, (b) abietyl glycidyl ether, (c) methyl maleopimarate.

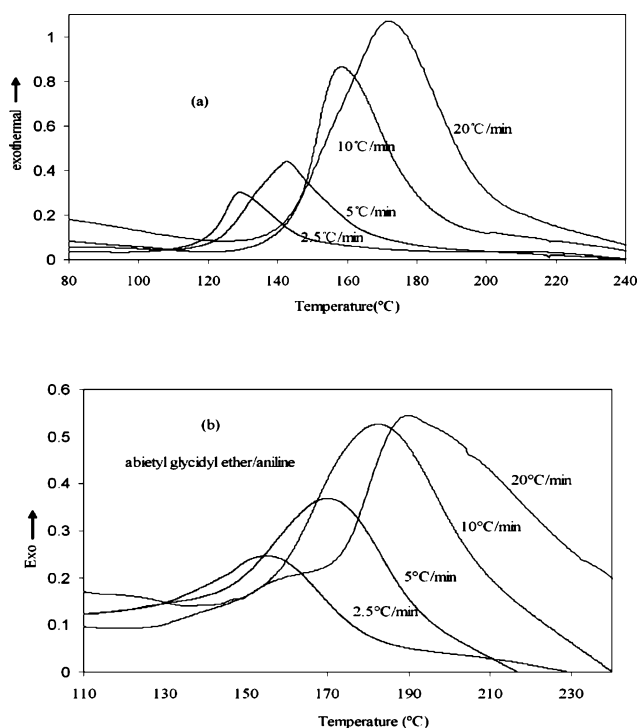


Fig. 2 DSC thermograms of curing of model compounds at different heating rates.

the dependence of cure kinetics on heating rate could be eliminated by extrapolating the results to infinitely slow heating rates (isothermal conditions), therefore “true” cure reaction temperature and Arrhenius parameters can be determined.<sup>18</sup> The values of these curing reaction parameters at the zero heating rate were estimated from linear extrapolation and are also given in Tables 1 and 2, ranging from 119 to 149 °C for maleopimarate/EPP and from 124 to 175 °C for abietyl glycidyl ether/aniline, respectively. If the initial curing, peak

Table 1 DSC results of nonisothermal curing of the methyl maleopimarate/phenyl glycidyl ether system

20	112.4	80.4	411.8	444.2	499.5
10	151.8	108.5	406.7	430.8	505.8
5	128.4	91.8	390.1	415.3	457.8
2.5	139.6	99.8	380.9	402.1	451.4
0 <sup>b</sup>	127.9 <sup>c</sup>	91.5 <sup>c</sup>	392	402	422

<sup>a</sup> On the basis of per mole of epoxide. <sup>b</sup> Linear extrapolation at  $dT/dt = 0$ . <sup>c</sup> Enthalpy was extrapolated by excluding the result at a heating rate of 20 °C min<sup>-1</sup>.

Table 2 DSC results of nonisothermal curing of the abietyl glycidyl ether/aniline system

$\beta/\text{K min}^{-1}$	$\Delta H/\text{J g}^{-1}$	$\Delta H/\text{kJ mol}^{-1a}$	$T_i/\text{K}$	$T_p/\text{K}$	$T_e/\text{K}$
20	55.4	21.6	423.0	463.2	516.6
10	105.5	41.2	408.7	455.1	491.8
5	93.5	36.5	394.5	443.9	463.5
2.5	90.3	35.3	382.7	429.2	444.6
0 <sup>b</sup>	105 <sup>c</sup>	41 <sup>c</sup>	397	431	448

<sup>a</sup> On the basis of per mole of epoxide. <sup>b</sup> Linear extrapolation at  $dT/dt = 0$ . <sup>c</sup> Enthalpy was extrapolated by excluding the result at a heating rate of 20 °C min<sup>-1</sup>.

and curing end temperatures at the zero heating rate can be used as references for the selection of temperatures in the isothermal curing study,<sup>20,22</sup> then these temperatures fell within the conventional epoxy curing temperature range. By comparing the enthalpy of the cure reaction on the basis of per mole of epoxide, it was interesting to note that the molar enthalpy of curing of abietyl glycidyl ether by aniline (~33 kJ mol<sup>-1</sup>) was less than half of that of the curing of the phenyl glycidyl ether system. The latter showed a molar enthalpy of reaction (~91 kJ mol<sup>-1</sup>) close to that of diglycidyl ether of bisphenol A cured with *m*-phenylene diamine.<sup>20,21</sup> This result suggests that

rosin-based epoxy tends to yield significantly lower enthalpy of reaction than the conventional epoxies.

Fig. 3 shows the progress of reaction conversion with curing temperature. The s-shaped curves of degree of conversion ( $\alpha$ ) versus temperature indicate that the cure reaction was autocatalytic.<sup>23</sup> The slope reached a maximum in the range of low to medium conversions. This is a clear indication that the reaction intermediates accelerated the cure reaction. At higher conversions, the linearity is lost, indicating the decrease in reaction rate. Since there was no network structure formed in the model reaction systems, the slowdown of reaction in this region was probably due to the decrease in the reactant concentrations. Fig. 4 shows the cure rate as a function of curing temperature. It indicates that the maximum reaction rate occurred around the peak exothermic temperature, and increased with heating rate.

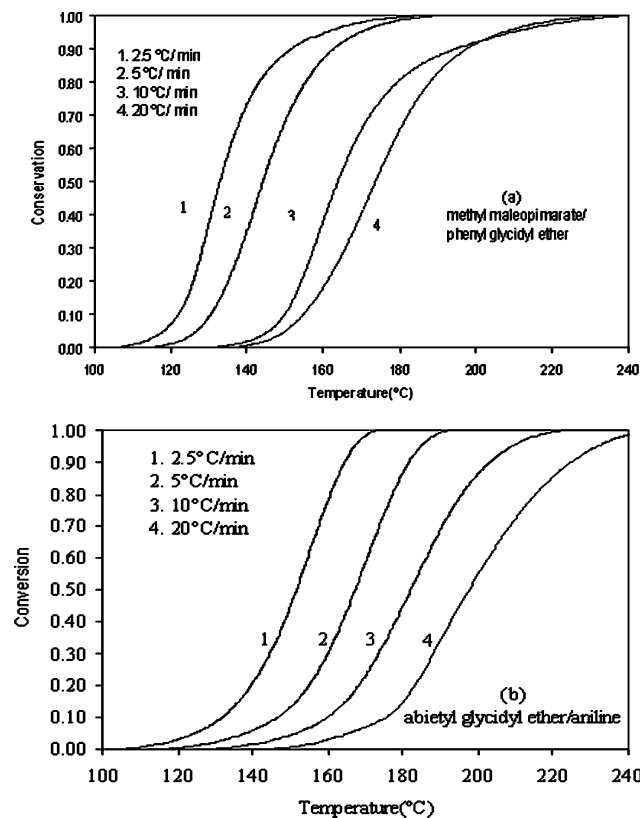


Fig. 3 Degree of conversion versus temperature at different heating rates.

Activation energy was measured following the Kissinger's method:<sup>24</sup>

$$E_a = -R \left[ \frac{d(\ln \frac{\beta}{T_p^2})}{d(1/T_p)} \right]$$

where  $\beta$  = heating rate;  $T_p$  = peak exothermic temperature (K);  $E_a$  = kinetic activation energy; and  $R$  = gas constant ( $1.987 \text{ cal K}^{-1} \text{ mol}^{-1}$ ). The plot of  $\ln(\beta/T_p^2)$  against  $1/T_p$  fell in a good linear relationship (curves not shown), and the slope was equal to  $-E_a/R$ . The calculated value of  $E_a$  was  $65.3 \pm 4.8 \text{ kJ mol}^{-1}$  for

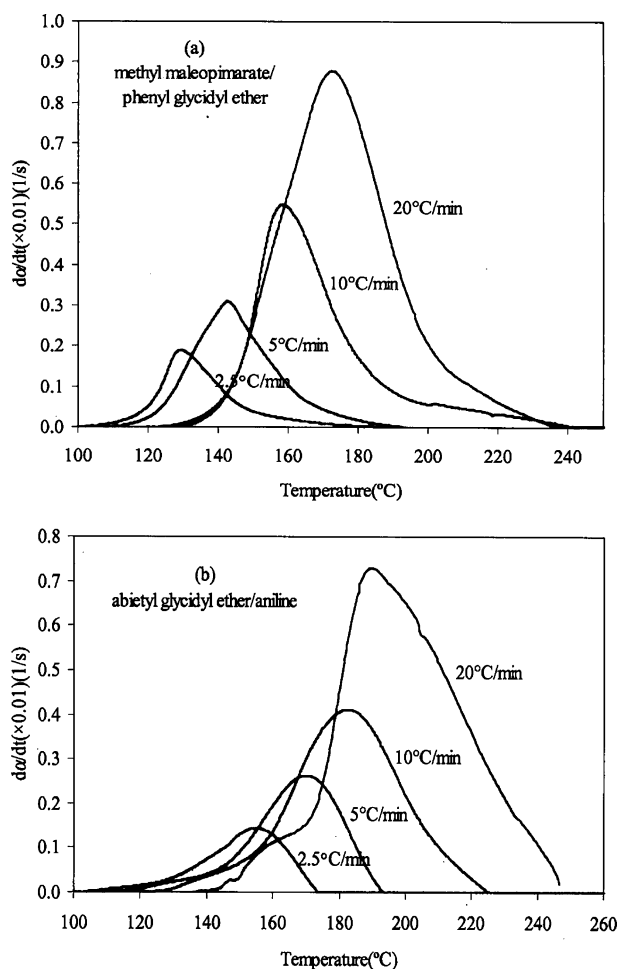


Fig. 4 Effect of heating rate on reaction rate.

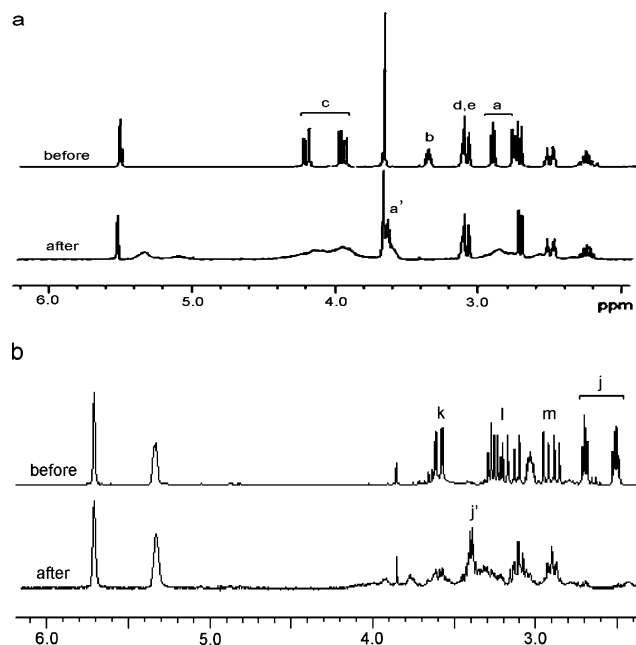
the methyl maleopimarate/1,2-epoxy-3-phenyl propane system and  $91.6 \pm 5.2 \text{ kJ mol}^{-1}$  for the abietyl glycidyl ether/aniline system, respectively.

### Cure reactions and curing mechanism

The reactant mixture before curing and the product after curing were analyzed by  $^1\text{H NMR}$ . Fig. 5 shows  $^1\text{H NMR}$  spectra of the above two reaction systems before and after curing. The cured products in Fig. 5 were from the above nonisothermal DSC curing study at a heating rate at  $2.5 \text{ °C min}^{-1}$ . The assignments of the chemical shifts correspond to those labels in Scheme 3. The chemical shifts of the oxirane in phenyl glycidyl ether at  $\delta$  2.77, 2.91 and 3.36 (Fig. 5a) basically disappeared after the cure reaction with methyl maleopimarate; instead, new peaks at  $\delta$  3.65 and  $\delta$  5.35, which were attributed to the methylene and methenyl groups connected with the newly formed ester and hydroxyl groups (Scheme 3a), respectively, were observed. The peaks at  $\delta$  3.97 and  $\delta$  4.16 were attributed to the diastereomeric protons of the methylene connecting with the oxirane, and disappeared after curing. Chemical shifts of the double bond ( $\delta$  5.53), methyl group ( $\delta$  3.67) of the rosin ester and other protons in the rosin moiety did not show any observable changes.

In the abietyl glycidyl ether/aniline reaction system (Fig. 5b), the peaks at  $\delta$  2.57, 2.76 and 3.65, which were attributed to





**Fig. 5**  $^1\text{H}$  NMR spectra before and after curing reaction. a: methyl maleopimarate/1,2-epoxy-3phenoxy propane; b: abietyl glycidyl ether/aniline.

the oxirane, disappeared after reaction. A new peak at 3.40 attributed to the methylene group connected with aniline was noted. Similarly, the chemical shifts at  $\delta$  5.71 and 5.32, which belonged to the two protons of the two double bonds in the rosin structure, and the chemical shifts of other protons in the rosin moiety did not change after curing.

Based on the  $^1\text{H}$  NMR results of cure reactions, the curing mechanisms for the two epoxy systems in this study can be suggested as in Scheme 3. In the presence of a base catalyst (2-ethyl-4-methylimidazole), rosin-based anhydride curing of epoxide selectively resulted in the formation of diester (Scheme 3a), and this result was consistent with the well established epoxy curing mechanisms using anhydride.<sup>25</sup> Initially the catalyst activated the reaction by attacking the oxirane, forming a hydroxyl-containing intermediate (I).<sup>26</sup> This intermediate reacted with the rosin-based anhydride to yield a monoester with a free carboxyl group, which then reacted with an epoxide to form a diester with a hydroxyl. The reaction continued in the same cycle. The cure reactions of rosin-based epoxy with aniline were also suggested as in Scheme 3b. According to Shechter *et al.*,<sup>27,28</sup> a primary and a secondary amine reacted with epoxide to give a secondary and a tertiary amine, respectively. Without more evidence, the involvement of the catalyst in the curing of the abietyl glycidyl ether/aniline system was not discussed in this study. There was no evidence of reaction (etherification) between epoxide and the newly formed hydroxyl groups noted. This was probably due to the equivalent stoichiometric amount of reactants used in the reaction system, where excess epoxide was not available for favorable etherification. In this study, under the condition of 1 : 1 epoxy/anhydride (or 1 : 1 epoxy/amine) equivalent stoichiometry, the reaction selectively resulted in a hydroxyl ester or tertiary amine rather than polyether. In addition, according to Shechter *et al.*,<sup>25</sup> the esterification is the preferred reaction in a base-catalyzed system.

## Conclusions

Rosin acid derivatives, glycidyl abietyl ether and methyl maleopimarate, were successfully synthesized as analogs for rosin-based epoxies and anhydride curing agents, respectively. The synthesis methods for the products and intermediates were examined in detail. The maleation of methyl abietate was relatively easy and gave a good yield, while the etherification of the abietic alcohol showed steric hindrance as reflected in the relatively low yield. The nonisothermal curing study by DSC suggested that both the curing reaction of epoxide with the rosin anhydride compound and the curing reaction of rosin epoxide with aniline were autocatalytic, and the cure reactions were similar to the respective conventional epoxy resin systems. In the presence of 2-methyl-4-ethyl-imidazole catalyst and under the equivalent stoichiometric amount of epoxy and curing agent, the curing of rosin-based anhydride with 1,2-epoxy-3phenoxy-propane selectively yielded a diester, and the curing of rosin-based epoxy cured with aniline selectively yielded a tertiary amine. There was no etherification noted in the cure reactions.

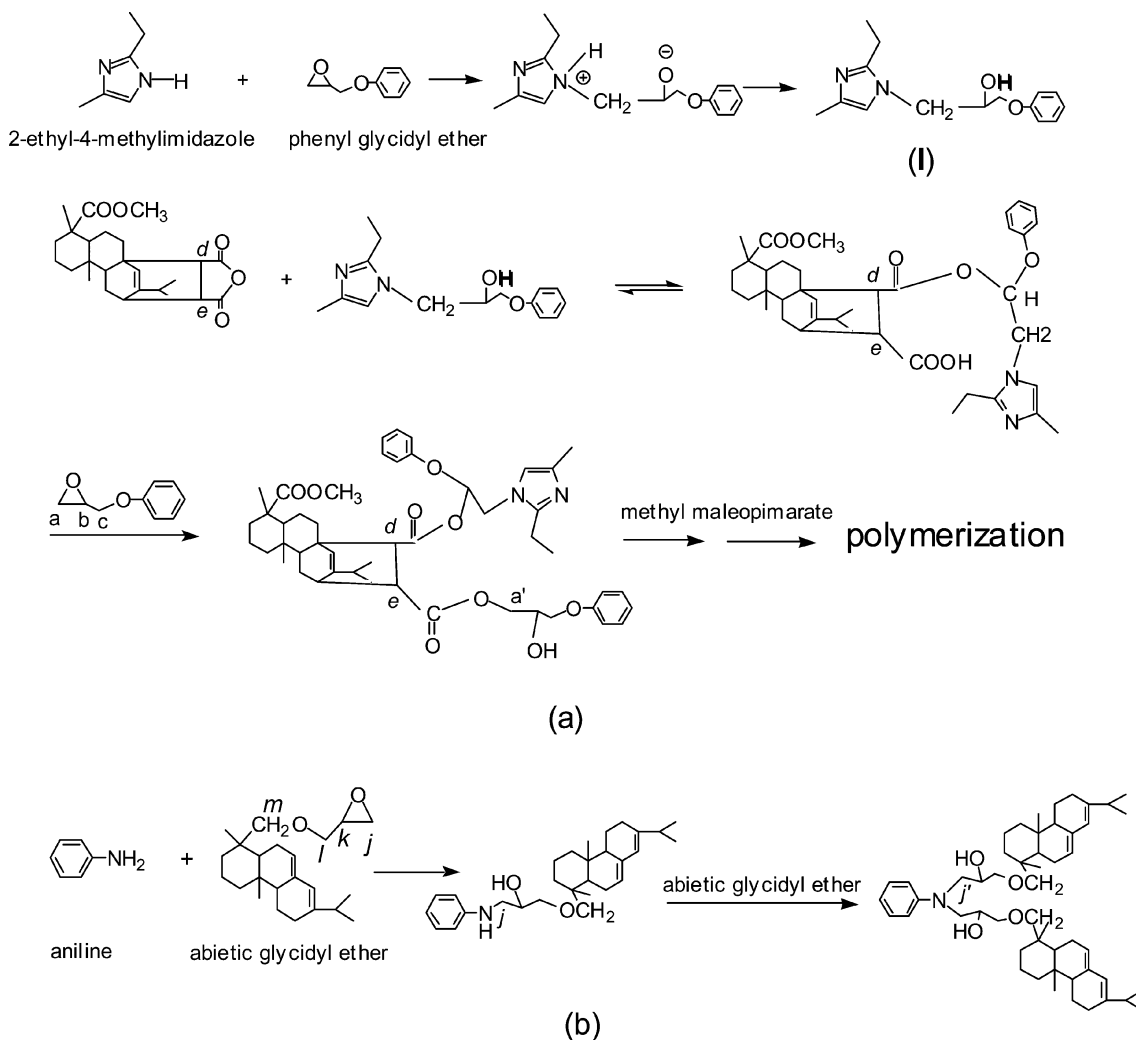
## Experimental

### General

Abietic acid (75% by HPLC) was obtained from Aldrich and used as received. It was actually a mixture of abietic acid and other rosin acids with the most neutral rosin compounds removed. Maleic anhydride (powder, 95%), iodomethane (99.5%), epibromohydrin (98%), hydroquinone (99%), phenyl glycidyl ether (99%) and 2-ethyl-4-methylimidazole (95%), aniline (99.5%) were also obtained from Aldrich. Lithium aluminum hydride (95%) was obtained from ACROS. Tetra-n-butylammonium hydrogen sulfate (97%) was obtained from Lancaster. Sodium hydroxide (99%, pellet), potassium carbonate (99%, anhydrous, granular) were obtained from B.T. Baker. Magnesium sulfate (anhydrous, reagent grade) was obtained from Fisher, as were all organic solvents (analytical grade). Solvents for synthesis (methanol, xylene, toluene, THF, DMF) were dried with 5 Å molecular sieves before use; the others (ethyl ether, chloroform) were used as received. TLC was performed on silica gel/UV<sub>254</sub> (0.25 mm, Sorbent Technology) plates. Column chromatography was carried out with Merck Kieselgel 60 (0.040–0.063 mm).  $^1\text{H}$  NMR and  $^{13}\text{C}$  NMR spectra were recorded with a Bruker 300 MHz spectrometer at room temperature in deuterated chloroform ( $\text{CDCl}_3$ ). Chemical shifts are reported relative to chloroform ( $\delta$  7.26) for  $^1\text{H}$  NMR and chloroform ( $\delta$  77.28) for  $^{13}\text{C}$  NMR. FTIR spectra were recorded with NEXUS 670 FT-IR, KBr pellet, wavelength from 4000 to 400  $\text{cm}^{-1}$ . Mass spectrum was recorded with a LCQ Advantage ESI mass spectrometer.

### Synthesis of model compounds

**Abietyl alcohol (I).** Abietic acid (2.00 g, 75% purity, 5 mmol) in dry THF (60 mL) was added dropwise to a suspension of powdered  $\text{LiAlH}_4$  (1.12 g, 29.4 mmol) in dry THF (30 mL) at room temperature. The reaction mixture was stirred overnight at room temperature. To this mixture was added 60 mL water and 50 mL  $\text{H}_2\text{SO}_4$  (1 M), stirring for 1 h. The mixture was extracted



**Scheme 3** Curing reactions of methyl maleopimarate/phenyl glycidyl ether (a), and abietyl glycidyl ether/aniline (b).

with ethyl ether (60 mL  $\times$  3). After drying with anhydrous  $\text{MgSO}_4$  and evaporating the solvent, the residue was purified by silica gel column chromatography (AcOEt : hexane = 13 : 87) to yield the product (**I**, 1.38 g, yield 96.5%).  $^1\text{H NMR}$   $\delta$  5.77 (s,1H), 5.40 (s,1H), 3.36 (m,1H), 3.13 (m,1H), 2.17–1.83 (m,9H), 1.37–1.22 (m,5H), 1.03–1.01 (m,7H), 0.75–0.41 (m,7H).  $^{13}\text{C NMR}$   $\delta$  145.47, 135.77, 122.60, 121.13, 72.35, 50.99, 43.88, 39.09, 37.72, 35.93, 35.11, 34.86, 27.75, 24.05, 22.90, 21.66, 21.10, 18.40, 17.93, 14.47. FT-IR  $\nu$  889, 1050, 1300, 1380, 1470, 2960, 3390  $\text{cm}^{-1}$ . ESI-MS  $m/z$  289.2,  $[\text{M} + \text{H}^+]$ .

**Abietyl glycidyl ether (II).** Abietic alcohol (**I**) (527 mg, 1.8 mmol) was dissolved in toluene (10 mL) at room temperature. To this solution were added powdered NaOH (146 mg, 3.6 mmol) and  $\text{Bu}_4\text{N}^+\text{HSO}_4^-$  (186 mg, 0.5 mmol). The mixture was stirred for 0.5 h at room temperature and then epibromohydrin (600 mg, 4.4 mmol) was dropped in. The mixture was further stirred overnight at 60  $^\circ\text{C}$  and cooled to room temperature. The reaction was quenched with  $\text{H}_2\text{O}$  (20 mL) and the mixture was extracted with ethyl ether (30 mL  $\times$  3). After drying with anhydrous  $\text{MgSO}_4$  and removing the solvent under reduced pressure, the product was purified by silica gel column

chromatography (AcOEt : hexane = 1 : 9). [**II**, 200 mg, yield 30% (yield based on recovering start material 90%)].  $^1\text{H NMR}$   $\delta$  5.77 (s,1H), 5.40 (s,1H), 3.65 (m,1H), 3.36–2.92 (m,4H), 2.76 (m,1H), 2.57 (m,1H), 2.21–1.20 (m,12H), 1.02–0.98 (m,8H), 0.88–0.81 (m,7H).  $^{13}\text{C NMR}$   $\delta$  145.16, 135.42, 122.44, 121.24, 80.92, 72.03, 51.08, 50.69, 44.24, 43.89, 38.80, 37.25, 36.37, 34.88, 34.63, 27.54, 23.99, 22.66, 21.42, 20.86, 18.22, 18.03, 14.23. FT-IR  $\nu$  768, 883, 893, 922, 1110, 1260, 1380, 1470, 1740, 2960  $\text{cm}^{-1}$ . ESI-MS  $m/z$  345.2,  $[\text{M} + \text{H}^+]$ ; 367.2,  $[\text{M} + \text{Na}^+]$ .

**Methyl abietate (III).** Powdered  $\text{K}_2\text{CO}_3$  (5.75 g, 42 mmol) was added to anhydrous DMF (60 mL) and the mixture was stirred for 5 min at 25  $^\circ\text{C}$ . To this mixture was added abietic acid (5.00 g, 75% purity, 12 mmol) and then iodomethane (11.40 g, 60 mmol). The reaction was stirred for 4 h at 25  $^\circ\text{C}$  and the solid precipitate was removed *via* filtration. The filtrate was diluted with 300 mL ethyl ether, and then washed with water (3  $\times$  100 mL). The ethyl ether layer was then dried with anhydrous  $\text{MgSO}_4$  and concentrated in vacuum. Purification was carried out by silica-gel column chromatography (EtOAc : hexane = 1 : 9) to provide methyl abietate (**III**, 3.00 g, yield 77%).  $^1\text{H NMR}$   $\delta$  5.77 (s,1H), 5.36 (s,1H), 3.62 (s,3H), 2.23–1.56 (m,11H),

1.25–1.18 (m,6H), 1.02–1.00 (m,7H), 0.80 (s,3H).  $^{13}\text{C}$  NMR  $\delta$  179.20, 145.52, 135.74, 122.56, 120.84, 52.06, 51.15, 46.81, 45.32, 38.55, 37.33, 35.11, 34.75, 27.70, 25.90, 22.69, 21.64, 21.08, 18.36, 17.24, 14.26. FT-IR  $\nu$  897, 1150, 1230, 1250, 1390, 1460, 1730, 2960  $\text{cm}^{-1}$ . ESI-MS  $m/z$  317.6,  $[\text{M} + \text{H}^+]$ ; 339.6,  $[\text{M} + \text{Na}^+]$ .

**Methyl maleopimarate (IV).** Methyl abietate (III) (3.00 g, 9 mmol), maleic anhydride (1.76 g, 18 mmol) and hydroquinone (0.02 g, 0.18 mmol) were mixed in a sealed tube in dry xylene (10 mL). The mixture was stirred at 220 °C for 5 h under Ar protection. The reaction was cooled to 80 °C, and the reaction solution was transferred into a beaker. Most of the product precipitated itself as crystals with the cooling down of the solution and was collected with a funnel. The residual product in the filtrate was precipitated with ethyl ether (50 mL) and collected by filtration. Then the two solid parts were combined and washed with 200 mL ethyl ether, dried to obtain the pure product (IV, 3.2 g, yield 86%).  $^1\text{H}$  NMR  $\delta$  5.53(s,1H), 3.67 (s,3H), 3.11 (m,2H), 2.72 (d,1H), 2.50 (m,1H), 2.25 (m,1H), 1.78–1.24 (m,13H), 1.15 (s,3H), 1.00–0.98 (d,6H), 0.59 (s,3H).  $^{13}\text{C}$  NMR  $\delta$  179.32, 172.97, 171.26, 148.31, 125.34, 53.51, 53.47, 52.27, 49.64, 47.30, 45.87, 40.67, 38.21, 37.89, 36.90, 35.88, 35.00, 32.99, 27.42, 21.85, 20.79, 20.17, 17.20, 16.95, 15.76. FT-IR  $\nu$  795, 850, 922, 945, 1000, 1090, 1140, 1240, 1390, 1470, 1720, 1790, 1860, 2880, 2960  $\text{cm}^{-1}$ . ESI-MS  $m/z$  415.4,  $[\text{M} + \text{H}^+]$ .

### Sample preparation for curing study

To study the curing activity of methyl maleopimarate (MMAP), phenyl glycidyl ether (PGE) was used as the epoxide. In order to achieve a good mixing of the reactants, MMAP/PGE in molar ratio 1 : 2 together with the catalyst were first dissolved in  $\text{CHCl}_3$ , and then the solvent was removed in a vacuum at room temperature. To study the curing activity of abietyl glycidyl ether (AGLE), aniline was used as the curing agent. Similarly, an equivalent stoichiometric amount of AGLE and aniline (AGLE/aniline in molar ratio 2 : 1) together with a catalyst were first dissolved in ethyl ether, and then the solvent was removed in vacuum at room temperature. For both epoxy systems, 2-ethyl-4-methylimidazole was added as a catalyst during preparation at the level of 0.5 wt% of the total weight of epoxide and curing agent. The mixtures were sealed in glass vials and were kept in dry ice for a maximum of 48 h while waiting for curing tests.

### Curing study by DSC and $^1\text{H}$ NMR

Nonisothermal curing of the epoxy systems was performed on a Mettler-Toledo 822e DSC in a nitrogen atmosphere. Heat scan ranging from –50 to 250 °C was performed at heating rates of 2.5, 5, 10, and 20 °C  $\text{min}^{-1}$ , respectively. Approximate 5 mg of each of the above prepared samples was weighed and sealed in an aluminium DSC sample pan, and the curing was conducted immediately. The degree of conversion of the epoxy group at any instantaneous temperature (or time) during the curing reaction,  $\alpha$ , was calculated from the area under the DSC exothermic peak:

$$\alpha = \frac{Q_t}{Q_{\text{tot}}}$$

where  $Q_t$  was given by the fraction peak area at time  $t$  (or corresponding temperature  $T$ ) and  $Q_{\text{tot}}$  by the total peak area.

The cure reactions were studied by  $^1\text{H}$  NMR analysis of the reaction products. The reacted sample after curing on DSC and unreacted samples were examined using  $^1\text{H}$  NMR in  $\text{CDCl}_3$ .

### Acknowledgements

This activity was funded, in part, with an Emerging Research Issues Internal Competitive Grant from the Washington State University, College of Agricultural, Human and Natural Resource Sciences, Agricultural Research Center.

### References

- 1 J. J. W. Coppen and G. A. Hone, *Gum naval stores: Turpentine and rosin from pine resin*, Food and Agriculture Organization of the United Nations, 1995, ch. 1.
- 2 S. Maiti, S. S. Ray and A. K. Kundu, *Prog. Polym. Sci.*, 1989, **14**, 297–338.
- 3 S. Das and S. Maiti, *J. Macromol. Sci., Chem.*, 1982, **A17**, 1177–1192.
- 4 S. S. Ray, A. K. Kundu, M. Ghosh and S. Maiti, *Eur. Polym. J.*, 1985, **21**, 131–133.
- 5 S. S. Ray, A. K. Kundu and S. Maiti, *J. Appl. Polym. Sci.*, 1988, **36**, 1283–1293.
- 6 J. B. Lewis and G. W. Hederick, *Ind. Eng. Chem. Prod. Res. Dev.*, 1970, **9**, 304–310.
- 7 Y. Zhang and D. J. Hourston, *J. Appl. Polym. Sci.*, 1998, **69**, 271–291.
- 8 J. F. Jin, Y. L. Chen, D. N. Wang, C. P. Hu, S. Zhu, L. Vanoverloop and D. Randall, *J. Appl. Polym. Sci.*, 2002, **84**, 598–604.
- 9 S. S. Roy, A. A. Kundu and S. Maiti, *Eur. Polym. J.*, 1990, **26**, 471–474.
- 10 X. Liu, C. Li, D. Zhang, Y. Xiao and G. Guan, *Polym. Int.*, 2006, **55**, 545–551.
- 11 X. Liu, C. Li, D. Zhang and Y. Xiao, *J. Polym. Sci., Part B: Phys.*, 2006, **44**, 900–913.
- 12 A. M. Atta, R. Mansour, M. I. Abdou and A. M. Sayed, *Polym. Adv. Technol.*, 2004, **15**, 514–522.
- 13 T. Matynia, *J. Appl. Polym. Sci.*, 1980, **25**, 1–13.
- 14 E. J. Vandenberg, *US Pat.*, 3 285 870, 1966.
- 15 R. B. Prime, in *Thermal characterization of polymer Materials*, ed. E. Turi, Academic Press, San Francisco, 1997, vol. 2, ch. 6, pp. 1389–1400.
- 16 H. J. Flammersheim, *Thermochim. Acta*, 2000, **361**, 21–29.
- 17 J. Sestak, in *Comprehensive analytical chemistry*, ed. G. Svehla, Elsevier, Amsterdam, 1976, vol. 12D, ch. 9, pp. 212–217.
- 18 S. Vyazovkin and C. A. Wight, *Annu. Rev. Phys. Chem.*, 1997, **48**, 125–49.
- 19 S. Vyazovkin and N. Sbirrazzuoli, *Macromol. Chem. Phys.*, 1999, **200**, 2294–2303.
- 20 V. L. Zvetkov, *Polymer*, 2001, **42**, 6687–6697.
- 21 Z. Dai, Y. Li, S. Yang, C. Zong, X. Lu and J. Xu, *J. Appl. Polym. Sci.*, 2007, **106**, 1476–481.
- 22 S. Sourour and M. R. Kamal, *Thermochim. Acta*, 1976, **14**, 41–59.
- 23 D. K. Hadad, in *Epoxy resins chemistry and technology*, ed. C. A. May, Marcel Dekker, Inc., New York and Basel, 2nd edn, 1988, ch. 14, pp. 1127–1133.
- 24 H. E. Kissinger, *J. Res. Natl. Bur. Stand.*, 1956, **57**, 217–221.
- 25 L. Shechter and J. Wynstra, *J. Ind. Eng. Chem.*, 1956, **48**, 86–93.
- 26 T. Dearlove, *J. Appl. Polym. Sci.*, 1970, **14**, 1615–1626.
- 27 L. Shechter, J. Wynstra and R. P. Kurkky, *J. Ind. Eng. Chem.*, 1956, **48**, 94–97.
- 28 L. Shechter, J. Wynstra and R. P. Kurkky, *J. Ind. Eng. Chem.*, 1957, **49**, 1107–1109.

# Thermoregulated aqueous biphasic catalysis of Heck reactions using an amphiphilic dipyridyl-based ligand

Hicham Azoui, Krystyna Baczek, Stéphanie Cassel and Chantal Larpent\*

Received 20th March 2008, Accepted 11th August 2008

First published as an Advance Article on the web 7th October 2008

DOI: 10.1039/b804828b

A neat water-based thermoregulated system for Pd-catalyzed Heck reactions is described. It uses a thermo-responsive ligand **L** that enables (1) the transfer of the catalyst in the organic phase upon heating thus allowing the reaction to take place in one phase, and (2) the separation/recovery of the catalyst in the water phase upon cooling and hence catalyst reuse. The amphiphilic ligand **L** with an inverse temperature-dependent solubility in water is prepared by covalent attachment of 2,2'-dipyridylamine to the tip of a nonionic polyoxyethylene surfactant (decyloctaethyleneglycol C<sub>10</sub>E<sub>8</sub>). Spectroscopic studies reveal that the amphiphilic dipyridyl-based ligand **L** forms a 1 : 1 Pd complex (PdLCl<sub>2</sub>) in organic solvent and a 1 : 2 Pd complex in water. Cross-coupling reactions of iodobenzene with ethyl acrylate and styrene are achieved, without any organic solvent, at 100–120 °C with sodium carbonate as a base using 0.1 to 0.5 mol% of Pd catalyst generated in water from **L** and Na<sub>2</sub>PdCl<sub>4</sub>. The reaction products, trans-cinnamic acid and stilbene, are readily isolated at room temperature, and the catalyst is recovered in the aqueous phase, without the need to add any organic solvent. The aqueous phase can be used in three catalytic runs with an almost constant catalytic activity for the coupling of iodobenzene with ethyl acrylate.

## Introduction

The development of reactions in water, which is a cheap, safe and non toxic solvent or in aqueous-based systems is attracting nowadays a growing interest in response to environmental concerns and increased restrictions on the use of hazardous organic solvents.<sup>1</sup> Water-based catalytic systems, that permit the catalyst separation and recycling, have many potential advantages and meet several goals of green chemistry. Liquid–liquid biphasic catalysis using homogeneous water-soluble catalysts has been widely studied.<sup>1–6</sup> However, while biphasic conditions facilitate catalyst/product separation and catalyst reuse, multiple phases introduce kinetic barriers and mass transfer limitations, which are sometimes overcome by adding an organic co-solvent or a phase transfer agent.<sup>2,3</sup> Thermomorphic systems offer an alternative approach to facilitate the catalyst separation while preserving the benefits of homogeneous catalysis and are therefore attracting widespread attention.<sup>1,2,7–9</sup> One of the unique features of thermoregulated biphasic catalysis is that it provides a mean to perform monophasic catalysis at one temperature with biphasic catalyst–product separation at another temperature. Numerous thermomorphic catalytic systems have been reported during the last decades. Fluorous biphasic catalysis as well as thermomorphic light fluorinated catalysts have provided some elegant solutions, with, however, the main drawback of using perfluorinated or organic solvents.<sup>1,2,7,10</sup> Thermomorphic systems based on polymer-supported catalysts in properly

chosen organic solvent mixtures have been shown to perform homogeneous catalytic reactions at one temperature and to permit the catalyst recovery by cooling, heating or addition of a solvent or a perturbing agent.<sup>7–9,11,12</sup>

A limited number of water-based thermoregulated biphasic catalytic reactions have been reported. Phosphine and phosphite ligands containing polyethylene glycol (PEG) moieties have been used in rhodium-catalyzed hydroformylation or hydrogenation of alkenes in water–organic solvent thermoregulated phase transfer catalysis.<sup>1,2,7,13</sup> These thermoregulated systems are based on the inverse temperature dependent solubility of PEG residues in water that allows the transfer of the catalyst in the organic phase during the reaction at high temperature and the subsequent separation of the catalyst in the aqueous phase, and further reuse, upon cooling.

In this paper, we report the use of a thermo-responsive amphiphilic dipyridyl ligand in the thermoregulated biphasic water-based, organic solvent-free, palladium-catalyzed Heck reaction. The Heck reaction, a carbon–carbon coupling reaction of major relevance in synthetic organic chemistry,<sup>2–5</sup> is usually performed at elevated temperatures and is therefore particularly suitable for the conception of thermoregulated catalytic processes. Various thermomorphic systems based on polymer-supported catalysts, as well as water–organic biphasic systems using water-soluble phosphine ligands, have been used to perform Heck reactions and to facilitate the catalyst–product separation and catalyst reuse.<sup>2–5,8,9,11,12</sup> However, to the best of our knowledge, there is no previous report of water-based thermoregulated biphasic catalysis of Heck reactions.

Non-ionic alkylpolyoxyethylene surfactants, usually referred as C<sub>i</sub>E<sub>j</sub>, exhibit a temperature-dependent behaviour, with a

Institut Lavoisier UMR-CNRS 8180, Université de Versailles-Saint-Quentin-en-Yvelines, 45 Avenue des Etats-Unis, 78035, Versailles Cedex, France. E-mail: Larpent@chimie.uvsq.fr; Fax: +33 139254452; Tel: +33 139254413



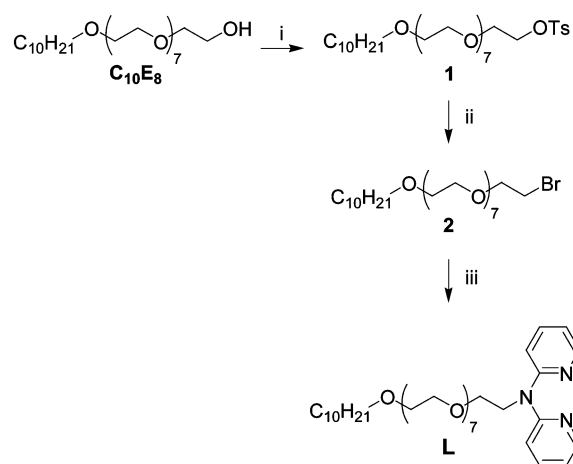
separation into two phases when an aqueous micellar solution is heated above a certain temperature, referred to as the cloud point (CP).<sup>14,15</sup> The driving force for clouding and phase separation of aqueous solutions of non-ionic surfactants is the dehydration of the polyoxyethylene (POE) polar headgroup upon heating.<sup>14</sup> Consequently, the CPs depend on the surfactants molecular structure with known relationships<sup>15</sup> and can be easily adjusted. This property makes non-ionic surfactants useful potential building blocks for the design of thermo-responsive ligands. In previous studies, we have shown that the covalent attachment of metal-binding units to surfactant blocks is a versatile, modular, synthetic approach that gives access to functional surfactants with controlled predictable properties.<sup>16,17</sup> Recently, we used this strategy to design thermo-responsive nonionic surfactants tethered with a diamide chelating group having adjustable CPs which were successfully used for the solvent-free thermoregulated separation of uranyle.<sup>17</sup>

Bidentate dipyridyl ligands have proven to be efficient ligands for palladium catalyzed C–C bond forming reactions in organic or aqueous solvents.<sup>18–22</sup> Pd (II) complexes with aminodipyridyl-based ligands immobilized on polymer or inorganic supports have also been used as recoverable heterogenized catalysts for C–C cross coupling reactions.<sup>19–22</sup> Considering the stability and the catalytic activity of Pd complexes with dipyridylamine based ligands, we chose to design an amphiphilic thermo-responsive ligand by tethering a  $C_{10}E_8$  surfactant with a 2,2'-dipyridyl amine residue. We describe here the synthesis of this amphiphilic ligand and its ability to form Pd complexes as well as first results on model catalytic Heck reactions that illustrate the potentialities of functional nonionic surfactants for performing thermoregulated aqueous biphasic cross coupling catalysis without any added organic solvent.

## Results and discussion

### Synthesis of the amphiphilic ligand **L** and formation Pd complexes

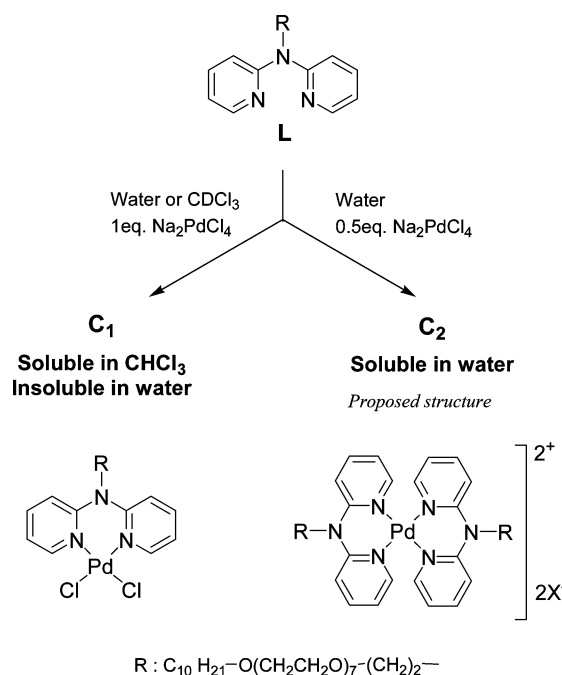
The amphiphilic ligand **L** was synthesized by covalent attachment of *N,N'*-di-2-pyridylamine (DPA) to the tip of decyloxyethylene glycol ( $C_{10}E_8$ ) in three steps, as depicted in Scheme 1, with a good overall yield (88%).  $C_{10}E_8$  was first quantitatively converted to tosylate **1** using standard procedures.<sup>23</sup> The bromo derivative **2** was then obtained through nucleophilic substitution with lithium bromide in an almost quantitative yield. Finally, the alkylation of DPA with **2** in the presence of sodium hydride afforded the amphiphilic ligand **L** which was isolated and purified by column chromatography. Elemental analysis, NMR and MS spectra confirm the structure and purity of **L**. The ESI-MS spectrum shows the sodium adduct  $[LNa]^+$  as the base peak at  $m/z$  686.5. The <sup>1</sup>H and <sup>13</sup>C NMR spectra indicate the presence of pyridyl groups, oxyethylene units and alkyl chain; the resonance of the methylene protons  $CH_2N$  as a triplet at 4.40 ppm confirms the covalent linkage of DPA to the tip of the POE group. It is worth noting that this synthetic approach is general and could be extended to the functionalization of other nonionic polyethylene glycol based surfactants and may therefore allow one to prepare a series of amphiphilic ligands with modulable properties.



i : TsCl, Py,  $CH_2Cl_2$ , 4°C; ii : LiBr, DMF, 110°C; iii : DPA, NaH, DMF, 60°C

**Scheme 1** Synthesis of the amphiphilic dipyridyl ligand **L**.

The formation of Pd complexes with the amphiphilic ligand **L** in organic solvent and in water has been studied by NMR and ESI-MS analyses (Scheme 2). The <sup>1</sup>H NMR spectrum of a 1/1 mixture of ligand **L** and  $Na_2PdCl_4$  in  $CDCl_3$  is indicative of a complete instantaneous complexation and shows downfield signals for the pyridyl nuclei in agreement with a coordination to Pd: the <sup>1</sup>H and <sup>13</sup>C NMR spectra are consistent with an  $LPdCl_2$  structure for the complex **C**<sub>1</sub> formed in organic solvent, as was observed for *N*-methylbenzyl- and *N*-acyl-aminodipyridine derivatives.<sup>22,24</sup> The observation of 1 : 1  $LPd$  ions in the electrospray mass spectrum with a base peak corresponding to  $LPdCl_2Na^+$  confirms the formation of a 1 : 1 complex **C**<sub>1</sub> in  $CDCl_3$ . The same complex **C**<sub>1</sub> is formed from equimolar amounts of ligand and Pd salt in aqueous solution. Nevertheless,



**Scheme 2** Pd complexes formed with the amphiphilic ligand **L**.

complex  $C_1$  is not soluble in water and precipitates quantitatively and instantaneously.

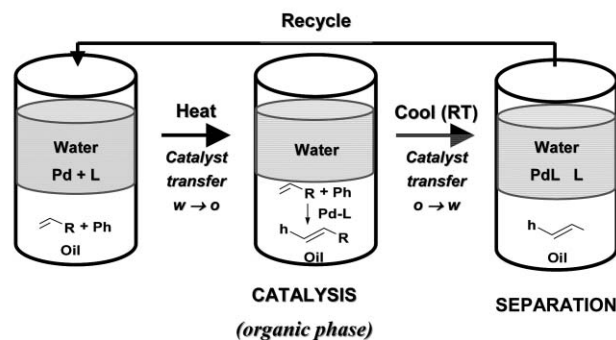
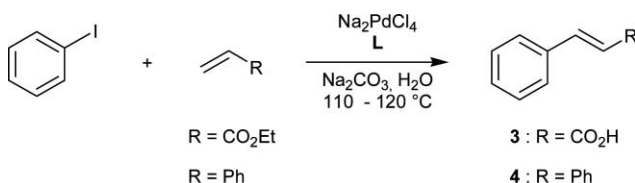
On the other hand, a water-soluble Pd complex  $C_2$  is formed when the ligand  $L$  is reacted with 0.5 equivalent of  $Na_2PdCl_4$  in water. The ESI-MS is indicative of the formation of a 1 : 2 complex  $PdL_2^{2+}$  in water and shows a base and unique peak, with the expected isotopic pattern, at  $m/z$  716.8 for  $PdL_2^{2+}$ . The  $^1H$  NMR spectrum in  $D_2O$  shows downfield signals for the nuclei  $H_\beta$ ,  $H_\gamma$ ,  $H_\delta$  of the coordinated pyridyl groups and methylene  $CH_2-N$  ( $\Delta\delta = 0.2$  to  $0.7$  ppm relative to the free ligand) while the pyridyl ortho proton ( $H_\alpha$ ) is slightly upfield shifted. It is worth noting that this 1 : 2 complex is not observed in organic solvents and that the NMR spectrum of a 2/1 mixture of ligand and Pd salt in  $CDCl_3$  reveals the presence of the characteristic signals for 1 : 1 complex  $C_1$  ( $LPdCl_2$ ) and free ligand. Although further studies are required to determine the exact structure of complex  $C_2$ , the formation of a dicationic complex  $PdL_2^{2+}$  in water may be rationalized by the following reasons: (1) the displacement of chlorine by pyridyl ligand is favoured in polar solvent as was observed in the study of the equilibrium between  $[Pd(Py)_4]^{2+}$  and  $[Pd(Py)_2(OAc)_2]^{2+}$ ; (2) the close proximity of the bipyridyl groups at the surface of the surfactant micellar aggregates should favour the coordination of two ligands to the metal, as was already observed with other functional metal-binding surfactants.<sup>26</sup>

Catalytic experiments were therefore performed in the presence of an excess of ligand  $L$  relative to Pd, with  $L/Pd$  molar ratio of 2 or 10, in order to generate *in situ* the Pd complex ( $C_2$ ) soluble in water at room temperature. Aqueous solutions of amphiphilic ligand  $L$  and  $Na_2PdCl_4$  exhibit a temperature-dependent behaviour with clouding and phase separation when heated. The cloud points vary with the Pd-to-ligand molar ratio: the CPs for 1 wt% solutions of ligand in water are respectively 16, 34 and 100 °C for Pd-to-ligand ratios of 0.1, 0.25 and 0.5, respectively. The formation of a cationic Pd complex  $C_2$  ( $PdL_2^{2+}$ ) in aqueous micellar solutions may account for the observed increase of the cloud point when the Pd content is increased, in a similar manner to what is observed in mixtures of non-ionic surfactants with ionic surfactants.<sup>27</sup>

### Biphasic aqueous thermoregulated catalysis of Heck reactions

Biphasic aqueous thermoregulated catalysis was tested in two model Heck cross coupling reactions of iodobenzene with ethyl acrylate and styrene (Scheme 3). The catalyst was pre-formed by mixing the amphiphilic ligand  $L$  and  $Na_2PdCl_4$  in water in a 1/2 or 1/10 Pd-to-ligand molar ratio before adding the other reactants and further heating. The reactions were carried out, without any added organic solvent, at 110–120 °C with sodium carbonate as a base. The main results are summarized in Table 1. It is important to note that no precautions against catalyst oxidation need to be taken: all the reactions and separations were run in air.

The coupling of iodobenzene with ethyl acrylate proceeds smoothly at low Pd content (0.1 mol%) with quantitative conversion after 20 h and leads to *trans*-cinnamic acid **3**, which results from the *in situ* saponification of the acrylic ester (Table 1, entries 1–3). Interestingly, under the experimental conditions used here, the reaction product precipitates as a sodium salt upon cooling to room temperature and is easily separated



**Scheme 3** Schematic of the biphasic aqueous thermoregulated system and Heck reactions tested with the amphiphilic Pd/L catalyst.

from the aqueous catalytic phase by a simple filtration without the need of any treatment or extraction with organic solvent. Whatever the ligand-to-metal ratio, pure cinnamic acid **3** is isolated with good yields of about 90% after crystallization in acidic water. The aqueous phase retains its catalytic activity and can be reused for further experiments. The catalytic activity of the recycled phase was found to depend dramatically on the ligand-to-palladium ratio: for  $L/Pd$  ratio of 2, a significant loss of the catalytic activity is observed for the second and third runs (Table 1, entry 2). Similar yields are obtained in blank experiments performed without ligand (Table 1, entry 3). On the other hand, when an excess of ligand is used ( $L/Pd = 10$ ), the aqueous phase can be used for three catalytic runs with a good conservation of activity (Table 1, entry 1). In this case, the amount of ligand is large enough to retain Pd as a 1 : 2 complex  $C_2$ , soluble in the water phase at room temperature, and hence enable the transfer of the Pd catalyst in the aqueous phase upon cooling. However, a significant loss of activity is observed at the 4th catalytic run. Although the loss of Pd as colloidal particles should not be excluded, the increase of the ionic strength in the aqueous phase after multiple uses may account for this observed diminution of activity. As already pointed out by Berbreiter,<sup>9</sup> this is a potential limitation for the multiple recyclings in thermoregulated biphasic catalysis of a reaction that produces a salt as by-product (NaI in the present case), since the clouding and phase behaviour of nonionic surfactants is known to be influenced by the presence of inorganic salts. The facile separation of the product, just filtered off, without the need of any added solvent, and the multiple uses of the catalyst show the advantages of using a thermosensitive ligand compared to other syntheses of cinnamic acid by ligand-free or conventional soluble ligands based Heck processes in neat water.<sup>18b,28</sup> Considering the reaction yields and the separation and re-use of the catalyst, the thermoregulated aqueous biphasic system appears comparable to supported Pd catalysts based systems.<sup>29,30</sup>

**Table 1** Pd-catalyzed Heck reactions under biphasic aqueous thermoregulated conditions

Entry	R	Conditions <sup>a</sup>	Pd (mol%)	L/Pd	Product	Run	Yield (%) <sup>b</sup>
1	CO <sub>2</sub> Et	<b>A</b> <i>R<sub>w</sub></i> = 6.6	0.1	10	<b>3</b>	1	89
						2	93
						3	85
						4	10
2	CO <sub>2</sub> Et	<b>A</b> <i>R<sub>w</sub></i> = 5.9	0.1	2	<b>3</b>	1	88
						2	42
						3	10
3	CO <sub>2</sub> Et	<b>A</b> <i>R<sub>w</sub></i> = 6.6	0.1	0	<b>3</b>	1	91
						2	40
						3	0
4	Ph	<b>B</b> <i>R<sub>w</sub></i> = 21.8	0.5	10	<b>4</b>	1 <sup>c</sup>	93
						2 <sup>d</sup>	42
						3	13 <sup>e</sup>
5 <sup>f</sup>	Ph	<b>B</b> <i>R<sub>w</sub></i> = 5.9	0.5	10	<b>4</b>	1 <sup>g</sup>	65
						2 <sup>h</sup>	23
6	Ph	<b>B</b> <i>R<sub>w</sub></i> = 4	0.5	2	<b>4</b>	1	55
						2	11
7 <sup>i</sup>	Ph	<b>B</b> <i>R<sub>w</sub></i> = 1.3	0.1	10	<b>4</b>	1	48

<sup>a</sup> Conditions A: ethyl acrylate (1.1 mol/PhI), Na<sub>2</sub>CO<sub>3</sub> (1.1 mol/PhI), water (9.5 mL), 120 °C, 20 h; Conditions B: styrene (2 mol/PhI), Na<sub>2</sub>CO<sub>3</sub> (1.5 mol/PhI), water (2.5 to 9.5 mL), 110 °C, 40 h; *R<sub>w</sub>* = volume of water/volume of organic reactants (PhI + alkene). <sup>b</sup> Isolated yields of pure products **3** and **4**: **3** was recrystallized in acidic water and **4** was purified by flash column chromatography. <sup>c</sup> 25% of the ligand initially introduced was recovered in the organic phase. <sup>d</sup> 62% of the ligand initially introduced was recovered in the organic phase. <sup>e</sup> After 64 h. <sup>f</sup> Same yields for the first and second runs were obtained with 0.75 mol Na<sub>2</sub>CO<sub>3</sub>/PhI. <sup>g</sup> 80% of the ligand initially introduced was recovered in the organic phase. <sup>h</sup> 15% of the ligand initially introduced was recovered in the organic phase. <sup>i</sup> 1 mol styrene/PhI was used.

This all-water based catalytic process was also found to be successful for the coupling of iodobenzene with styrene, with, however, lower activities (Table 1, entries 4–7). The reaction product is readily isolated, without the need for adding any organic solvent, after separation of the organic and aqueous phases upon cooling to room temperature. Catalytic reactions performed with a 0.5 mol% Pd load and a ligand-to-Pd ratio of 10 give *trans*-stilbene **4** in more than 90% isolated yield after 40 h (Table 1, entry 4). Lower yields (50–55%) are obtained at lower Pd loads (0.1 mol%) or ligand-to-Pd ratio (L/Pd = 2) (Table 1, entries 6–7). The absence of coupling products in a blank experiment conducted without ligand confirms the role of the amphiphilic Pd complex in the catalytic cycles. The aqueous phases can be reused for a second catalytic run, with, however, a significant decrease of activity (Table 1, entries 4–6). Remarkably, the reaction yields of the first runs and recycled phases are found to be tremendously dependent on the volume of water: as shown in entries 4 and 5, for a given Pd load (0.5 mol%) and ligand-to-Pd ratio (L/Pd = 10), the yield increases from 65% to 93% when the volume of water is increased by a factor 4. The increase of the volume of aqueous phase also ensures a better conservation of activity in a second use, with about 55% of remaining activity (Table 1, entries 4 and 5). A significant leakage of the amphiphilic ligand and Pd-complex in the organic phase accounts for the loss of efficiency during recycling. The amount of ligand lost in the organic phase depends on the volume of water: about 80% after the first catalytic run at low water/reactants ratio *R<sub>w</sub>* (Table 1, entry 5) and 25% for experiments performed with a larger volume of water (*R<sub>w</sub>* > 20, Table 1, entry 4). These results indicate that in this aqueous biphasic thermoregulated catalytic process, the catalyst recycling could be optimized by adjusting the water-to-organics volume ratio. However, the partition of the ligand and its Pd-complex

is clearly a severe limitation with the particular ligand used in this study. For this Pd-catalyzed coupling reaction, the use of a more hydrophilic ligand, with a larger POE group, should be highly profitable in order to favour the partition of the Pd-complex towards the aqueous phase during the separation at room temperature and hence multiple catalyst re-uses.

## Conclusion

In conclusion, we described an environmentally friendly neat water-based catalytic system for C–C coupling reactions that allows the product/catalyst separation by a simple variation of temperature without the need of organic solvent. The amphiphilic alkylpolyoxyethylene aminodipyridyl ligand engenders a thermo-responsive, air-stable, Pd-catalyst for Heck reaction. Multiple uses of the aqueous phase reveal, however, that the remaining catalytic activity is affected by the increase of salt concentration and by the ligand partition. Using the modular synthetic approach reported here, the design of more hydrophilic dipyrindyl ligands with larger POE polar groups that will facilitate the transfer in the aqueous phase during the separation step and impart a less pronounced sensitivity to the ionic strength is currently under investigation.

## Experimental

### General

High purity monodisperse octaethyleneglycol *n*-decyl ether (C<sub>10</sub>E<sub>8</sub>) was obtained from Nikko and used as received. All other products were purchased from current commercial sources. Solvents were distilled by conventional methods. Reactions were monitored by TLC on plates coated with 0.25 mm silica gel

60 F<sub>254</sub>, using UV (254 nm), sulfuric acid (15%) or ninhydrin (0.2%) in ethanol as revealing agents. Silica gel Merck Gerduran SI60 (40–63 μm) was used for column chromatography. The <sup>1</sup>H and <sup>13</sup>C NMR spectra were recorded on a Bruker AC 300. The chemical shifts δ are reported in ppm and coupling constant in Hz, referenced to internal solvent CDCl<sub>3</sub> (7.27 and 77.00 ppm). Mass spectra were obtained in the electrospray positive mode (ESI+) on a MS-Engine HP5989B, samples were diluted in methanol. Elemental analyses were obtained from the Service de Microanalyse ICSN-CNRS (Gif-sur-Yvette, France).

### Synthesis of the amphiphilic ligand L

**Toluene-4-sulfonic acid, 23-decyloxy-3,6,9,12,15,18,21-hepta-oxa-tricosyl ester 1.** A solution of tosyl chloride (4.5 g, 23.6 mmol) in a mixture of CH<sub>2</sub>Cl<sub>2</sub> (70 mL) and pyridine (2 mL) was added dropwise to C<sub>10</sub>E<sub>8</sub> (10 g, 19.6 mmol) in 10 mL of pyridine at 0 °C. The reaction mixture was stirred at 4 °C for 24 h and then poured in 75 mL of ice-cooled water, acidified to pH 2 with conc. HCl and extracted with CH<sub>2</sub>Cl<sub>2</sub> (3 × 50 mL). The combined organic layers were washed with brine, dried over anhydrous MgSO<sub>4</sub>. The crude tosylate **1** (13.5 g, quantitative yield) was obtained as a colourless oil after removal of the solvent. (Found: C, 58.81; H, 9.13. C<sub>33</sub>H<sub>61</sub>O<sub>11.5</sub>S (H<sub>2</sub>O)<sub>0.5</sub> requires C, 58.8; H, 9.1%; R<sub>f</sub> 0.66 (AcOEt/MeOH 9/1); δ<sub>H</sub> (300 MHz, CDCl<sub>3</sub>) 7.80 (2 H, d, J<sub>1,3</sub> 8.2 Hz, Ar–H), 7.35 (2 H, d, J<sub>1,3</sub> 8.2 Hz, Ar–H), 4.16 (2 H, t, J<sub>1,3</sub> 4.8 Hz, CH<sub>2</sub>OTs), 3.64 (30 H, m, OCH<sub>2</sub>CH<sub>2</sub>O), 3.44 (2 H, t, J<sub>1,3</sub> 6.8 Hz, OCH<sub>2</sub>CH<sub>2</sub>CH<sub>2</sub>), 2.45 (3 H, s, CH<sub>3</sub>Ph), 1.57 (2 H, m, OCH<sub>2</sub>CH<sub>2</sub>CH<sub>2</sub>), 1.26 (14 H, m, CH<sub>2</sub>), 0.88 (3 H, t, J<sub>1,3</sub> 5.8 Hz, CH<sub>2</sub>CH<sub>3</sub>); δ<sub>C</sub> (75 MHz, CDCl<sub>3</sub>) 144.74 (C<sub>ipso-S</sub>), 132.96 (C<sub>ipso-C</sub>), 129.78, 127.95 (C<sub>arom</sub>), 71.51, 70.70, 70.53, 70.00, 69.20, 68.63 (OCH<sub>2</sub>), 31.85, 29.59, 29.57, 29.53, 26.45, 29.28, 26.05, 22.63 (CH<sub>2</sub>), 21.06 (CH<sub>3</sub>–Ar), 14.08 (CH<sub>3</sub>); m/z (ESI) 687.5 (MNa<sup>+</sup>, 100%), 704.2 (MK<sup>+</sup>, 56).

**1-Bromo-23-decyloxy-3,6,9,12,15,18,21-hepta-oxa-tricosane 2.** Lithium bromide (0.2 g, 2.3 mmol) was added to a solution of crude tosylate **1** (1.0 g, 1.5 mmol) in 12 mL of dry DMF (previously distilled over CaH<sub>2</sub>). The reaction mixture was heated at 110 °C for 3 h and stirred at room temperature overnight. After removal of the excess of LiBr by filtration, the filtrate was co-evaporated with toluene and the residue was purified by column chromatography on silica gel using AcOEt/MeOH 4/1 as eluent to give **2** (0.99 g, 98%) as a colourless oil (Found: C, 54.78; H, 9.34. C<sub>26</sub>H<sub>53</sub>O<sub>8</sub>Br requires C, 54.4; H, 9.3%; R<sub>f</sub> 0.81 (AcOEt/MeOH 4/1); δ<sub>H</sub> (300 MHz, CDCl<sub>3</sub>) 3.82 (2 H, t, J<sub>1,3</sub> 6.4 Hz, OCH<sub>2</sub>CH<sub>2</sub>Br), 3.58 (m, 28 H, OCH<sub>2</sub>CH<sub>2</sub>O), 3.48 (2 H, t, J<sub>1,3</sub> 6.4 Hz, OCH<sub>2</sub>CH<sub>2</sub>Br), 3.45 (2 H, t, J<sub>1,3</sub> 6.8 Hz, OCH<sub>2</sub>CH<sub>2</sub>CH<sub>2</sub>), 1.56 (2 H, m, OCH<sub>2</sub>CH<sub>2</sub>CH<sub>2</sub>), 1.27 (14 H, m, CH<sub>2</sub>), 0.89 (3 H, t, J<sub>1,3</sub> 6.6 Hz, CH<sub>3</sub>); δ<sub>C</sub> (75 MHz, CDCl<sub>3</sub>) 71.61, 71.24, 70.68, 70.60, 70.07 (OCH<sub>2</sub>), 31.94, 29.65, 29.61, 29.53, 26.36, 26.12, 22.72 (CH<sub>2</sub>), 14.17 (CH<sub>3</sub>); m/z (ESI) 595.4 and 597.4 (MNa<sup>+</sup>, 100%), 611.4 and 613.4 (MK<sup>+</sup>, 13).

**(23-decyloxy-3,6,9,12,15,18,21-hepta-oxa-tricosyl)-dipyrid-2-yl amine L.** A solution of 2,2'-dipyridylamine (0.45 g 2.6 mmol) in dry DMF (10 mL) was added under N<sub>2</sub> to a suspension of sodium hydride (60% in mineral oil, previously washed with hexane, 0.3 g, 5.2 mmol) in dry DMF (10 mL). After stirring for 30 min, a solution of bromide **2** (1 g, 1.7 mmol) in dry

DMF (10 mL) was progressively added over 0.5 hour. After stirring for 16 hours at 60 °C, the reaction mixture was quenched with MeOH at 0 °C. The solvent was evaporated under reduced pressure and the residue solubilized in diethyl ether and filtered. The filtrate was concentrated and the mixture purified by column chromatography on silica gel using AcOEt/MeOH 10/1 as eluent to give **L** (1 g, 90%) as a yellow oil (Found: C, 65.06; H, 9.36; N, 6.33. C<sub>36</sub>H<sub>61</sub>N<sub>3</sub>O<sub>8</sub> requires C, 65.1; H, 9.3; N, 6.3%; R<sub>f</sub> 0.60 (AcOEt/MeOH 4/1); δ<sub>H</sub> (300 MHz, CDCl<sub>3</sub>) 8.32 (2 H, dd, J<sub>1,3</sub> 5.0 Hz, J<sub>1,4</sub> 1.5 Hz, Py-H<sub>α</sub>), 7.52 (2 H, dt, J<sub>1,3</sub> 8.2 Hz, J<sub>1,3</sub> 7.3 Hz, J<sub>1,4</sub> 1.5 Hz, Py-H<sub>γ</sub>), 7.17 (2 H, br d, J<sub>1,3</sub> 8.2 Hz, Py-H<sub>δ</sub>), 6.86 (2 H, ddd, J<sub>1,3</sub> 7.3 Hz, J<sub>1,3</sub> 5.0 Hz, J<sub>1,4</sub> 0.8 Hz, Py-H<sub>β</sub>), 4.40 (2 H, t, J<sub>1,3</sub> 6.3 Hz, NCH<sub>2</sub>CH<sub>2</sub>O), 3.79 (2 H, t, J<sub>1,3</sub> 6.3 Hz, NCH<sub>2</sub>CH<sub>2</sub>O), 3.58 (m, 28 H, OCH<sub>2</sub>CH<sub>2</sub>O), 3.44 (2 H, t, J<sub>1,3</sub> 6.3 Hz, OCH<sub>2</sub>CH<sub>2</sub>CH<sub>2</sub>), 1.58 (2 H, m, OCH<sub>2</sub>CH<sub>2</sub>CH<sub>2</sub>), 1.27 (14 H, m, CH<sub>2</sub>), 0.88 (3 H, t, J<sub>1,3</sub> 6.3 Hz, CH<sub>3</sub>); δ<sub>C</sub> (75 MHz, CDCl<sub>3</sub>) 157.42 (Py-C<sub>ipso</sub>), 148.12 (Py-C<sub>α</sub>), 137.24, 117.08, 114.99 (Py), 71.59, 70.66, 70.60, 70.00, 70.42, 70.09, 69.37 (OCH<sub>2</sub>), 48.06 (NCH<sub>2</sub>), 31.93, 29.67, 29.64, 29.61, 29.53, 29.36, 26.13, 22.71 (CH<sub>2</sub>), 14.16 (CH<sub>3</sub>); m/z (ESI) 664.5 (MH<sup>+</sup>, 8%), 686.5 (MNa<sup>+</sup>, 100), 702.5 (MK<sup>+</sup>, 9).

### Formation of palladium complexes with ligand L

**Formation of complex C<sub>1</sub> (LPdCl<sub>2</sub>) in CDCl<sub>3</sub>.** 9 mg Na<sub>2</sub>PdCl<sub>4</sub> (0.031 mmol) was added to a solution of ligand **L** (18 mg, 0.027 mmol) in 1.5 mL of CDCl<sub>3</sub> and the mixture was allowed to stir for 10 min. The <sup>1</sup>H and <sup>13</sup>C NMR spectra were recorded after removal of the excess of salt by filtration. The ESI mass spectrum was acquired after dilution in MeOH. δ<sub>H</sub> (300 MHz, CDCl<sub>3</sub>) 8.91 (2 H, dd, J<sub>1,3</sub> 6.0 Hz, J<sub>1,4</sub> 1.5 Hz, Py-H<sub>α</sub>), 7.93 (2 H, dt, J<sub>1,3</sub> 7.7 Hz, J<sub>1,4</sub> 1.5 Hz, Py-H<sub>γ</sub>), 7.46 (2 H, br d, J<sub>1,3</sub> 8.4 Hz, Py-H<sub>δ</sub>), 7.18 (2 H, br t, J<sub>1,3</sub> 6.6 Hz, Py-H<sub>β</sub>), 4.45 (2 H, br t, NCH<sub>2</sub>CH<sub>2</sub>O), 3.98 (2 H, t, J<sub>1,3</sub> 5.6 Hz, NCH<sub>2</sub>CH<sub>2</sub>O), 3.79 (2 H, m, OCH<sub>2</sub>CH<sub>2</sub>O), 3.71–3.55 (m, 26 H, OCH<sub>2</sub>CH<sub>2</sub>O), 3.44 (2 H, t, J<sub>1,3</sub> 6.8 Hz, OCH<sub>2</sub>CH<sub>2</sub>CH<sub>2</sub>), 1.55 (2 H, m, OCH<sub>2</sub>CH<sub>2</sub>CH<sub>2</sub>), 1.25 (14 H, m, CH<sub>2</sub>), 0.87 (3 H, t, J<sub>1,3</sub> 6.6 Hz, CH<sub>3</sub>); δ<sub>C</sub> (75 MHz, CDCl<sub>3</sub>) 152.75 (Py-C<sub>ipso</sub>), 152.46 (Py-C<sub>α</sub>), 140.77 (Py-C<sub>γ</sub>), 120.95 (Py-C<sub>β</sub>), 116.25 (Py-C<sub>δ</sub>), 71.58 (OCH<sub>2</sub>R), 70.65, 70.59, 70.49, 70.07 (OCH<sub>2</sub>CH<sub>2</sub>O), 68.64 (OCH<sub>2</sub>CH<sub>2</sub>N), 51.58 (NCH<sub>2</sub>), 31.92, 29.66, 29.63, 29.60, 29.52, 29.35, 26.12, 22.70 (CH<sub>2</sub>), 14.16 (CH<sub>3</sub>); m/z (ESI) 489.5 (C<sub>10</sub>E<sub>7</sub>Na<sup>+</sup>, 30%), 805.4 (LPdCl<sup>+</sup>, 30), 863.8 (LPdCl<sub>2</sub>Na<sup>+</sup>, 100), 880.6 (LPdCl<sub>2</sub>K<sup>+</sup>, 22).

The <sup>1</sup>H NMR spectrum of a 1/2 Pd/L mixture in CDCl<sub>3</sub> prepared as described above shows the presence of the 1 : 1 Pd-complex PdLCl<sub>2</sub> (C<sub>1</sub>) and free ligand **L** in an equimolar ratio.

**Formation of complex C<sub>1</sub> (LPdCl<sub>2</sub>) in water.** Addition of 250 μL 0.125 M solution of Na<sub>2</sub>PdCl<sub>4</sub> (0.03 mmol) in D<sub>2</sub>O to a solution of ligand **L** (18.6 mg, 0.028 mmol) in 1.35 mL D<sub>2</sub>O leads to the instantaneous and quantitative formation of a yellow precipitate. The <sup>1</sup>H and <sup>13</sup>C NMR spectra of the solid separated by centrifugation, recorded in CDCl<sub>3</sub>, are identical to the spectra of complex PdLCl<sub>2</sub> (C<sub>1</sub>) formed in CDCl<sub>3</sub> described above.

**Formation of complex C<sub>2</sub> (PdL<sub>2</sub><sup>2+</sup>) in water.** 112 μL of a 0.125 M solution of Na<sub>2</sub>PdCl<sub>4</sub> in D<sub>2</sub>O (0.014 mmol) was added to a solution of ligand **L** (18.6 mg, 0.028 mmol) in 1.35 mL D<sub>2</sub>O. The mixture was allowed to stir for 5 min and the <sup>1</sup>H and



$^{13}\text{C}$  NMR spectra were recorded. The ESI mass spectrum was recorded after dilution in MeOH. The NMR spectra show the characteristic signals for a Pd complex  $\text{C}_2$  together with traces of free ligand (less than 15%).  $\delta_{\text{H}}$  (300 MHz,  $\text{D}_2\text{O}$ ) Pd complex  $\text{C}_2$  (Major) 8.06 (2 H, td,  $J_{1,3}$  8 Hz,  $J_{1,4}$  1.7 Hz, Py-H $_{\gamma}$ ), 7.71 (2 H, dd,  $J_{1,3}$  6 Hz,  $J_{1,4}$  1.4 Hz, Py-H $_{\alpha}$ ), 7.64 (2 H, br d,  $J_{1,3}$  8.3 Hz, Py-H $_{\delta}$ ), 7.18 (2 H, br t,  $J_{1,3}$  6.7 Hz, Py-H $_{\beta}$ ), 4.46 (2 H, br t,  $\text{NCH}_2\text{CH}_2\text{O}$ ), 3.95 (2 H, br t,  $\text{NCH}_2\text{CH}_2\text{O}$ ), 3.66 (2 H, m,  $\text{OCH}_2\text{CH}_2\text{O}$ ), 3.49–3.34 (26 H, m,  $\text{OCH}_2\text{CH}_2\text{O}$ ), 3.27 (2 H, t br,  $\text{OCH}_2\text{CH}_2\text{CH}_2$ ), 1.39 (2 H, m,  $\text{OCH}_2\text{CH}_2\text{CH}_2$ ), 1.11 (14 H, m,  $\text{CH}_2$ ), 0.71 (3 H, t,  $J_{1,3}$  6.7 Hz,  $\text{CH}_3$ );  $\delta_{\text{C}}$  (75 MHz,  $\text{D}_2\text{O}$ ) 153.30 (Py-C $_{\text{ipso}}$ ), 149.94 (Py-C $_{\alpha}$ ), 143.28 (Py-C $_{\gamma}$ ), 122.95 (Py-C $_{\beta}$ ), 118.32 (Py-C $_{\delta}$ ), 71.00, 70.09, 69.91, 69.79, 69.69, 69.60, 69.56, 69.51, 69.42, 68.87 ( $\text{OCH}_2\text{CH}_2\text{O}$ ), 67.29 ( $\text{OCH}_2\text{CH}_2\text{N}$ ), 50.12 ( $\text{NCH}_2$ ), 31.92, 29.77, 29.70, 29.58, 29.41, 26.03, 22.59 ( $\text{CH}_2$ ), 13.85 ( $\text{CH}_3$ );  $m/z$  (ESI) 716.8 ( $\text{PdL}_2^{2+}$ , 100%).

### General procedures for Heck reactions

**Typical procedure for the coupling of iodobenzene with ethyl acrylate (Table 1, entry 1).** 108  $\mu\text{L}$  of a freshly prepared 0.063 M aqueous solution of  $\text{Na}_2\text{PdCl}_4$  (0.0068 mmol) was added to a solution of ligand **L** (45 mg, 0.068 mmol) in  $\text{H}_2\text{O}$  (9.5 mL) and the mixture stirred at room temperature for few minutes.  $\text{Na}_2\text{CO}_3$  (0.8 g, 7.5 mmol), iodobenzene (0.77 mL, 6.9 mmol) and ethyl acrylate (0.77 mL, 7.1 mmol) were then successively added and the reaction mixture was heated in an oil bath at 120  $^{\circ}\text{C}$  for 20 hours with magnetic stirring. After cooling to room temperature, the product precipitates as well as carbonate in excess. The resulting viscous mixture was filtered and the aqueous filtrate retained for a second catalytic run. *trans*-cinnamic acid **3** was isolated by crystallization after solubilization of the solid residue in water followed by acidification to pH 2 with conc. HCl. White solid (0.9 g, 89%); mp 125  $^{\circ}\text{C}$  (lit.,<sup>31</sup> 124–125  $^{\circ}\text{C}$ );  $\delta_{\text{H}}$  (300 MHz,  $\text{CDCl}_3$ ) 11.00 (1H, br s,  $\text{CO}_2\text{H}$ ), 7.81 (1H, d,  $J_{1,3}$  16 Hz,  $\text{PhCH}=\text{C}$ ), 7.57 (2 H, m,  $\text{H}_o$ ), 7.44 (3 H, m,  $\text{H}_{m,p}$ ), 6.48 (1H, d,  $J_{1,3}$  16 Hz,  $=\text{CHCO}_2\text{H}$ ).

**Recycling.**  $\text{Na}_2\text{CO}_3$  (0.8 g, 7.5 mmol), iodobenzene (0.77 mL, 6.9 mmol) and ethyl acrylate (0.77 mL, 7.1 mmol) were added to the aqueous phase separated from the previous catalytic run. The coupling reaction performed as described above (20 h, 120  $^{\circ}\text{C}$ ) yielded 0.94 g (93%) of *trans*-cinnamic acid **3**.

**Typical procedure for the coupling of iodobenzene with styrene (Table 1, entry 4).** 123  $\mu\text{L}$  of a freshly prepared 0.049 M aqueous solution of  $\text{Na}_2\text{PdCl}_4$  (0.006 mmol) was added to a solution of ligand **L** (40 mg, 0.06 mmol) in  $\text{H}_2\text{O}$  (9.5 mL) and the mixture stirred at room temperature for few minutes.  $\text{Na}_2\text{CO}_3$  (0.2 g, 1.9 mmol), iodobenzene (0.14 mL, 1.2 mmol) and styrene (0.3 mL, 2.4 mmol) were then successively added and the reaction mixture was heated in an oil bath at 110  $^{\circ}\text{C}$  for 40 hours with magnetic stirring. After cooling to room temperature, the organic and aqueous phases were separated by centrifugation. The organic layer was concentrated under reduced pressure and pure *trans*-stilbene **4** (0.20 g, 93%) was isolated by flash column chromatography on silica gel with AcOEt as eluent; mp 134  $^{\circ}\text{C}$  (lit.,<sup>31</sup> 135–136  $^{\circ}\text{C}$ );  $R_f$  0.89 (AcOEt);  $\delta_{\text{H}}$  (300 MHz,  $\text{CDCl}_3$ ) 7.57 (4 H, m,  $\text{H}_o$ ), 7.41 (6 H, m,  $\text{H}_{m,p}$ ), 7.16 (2 H, s,  $\text{CH}=\text{C}$ ). The

ligand lost in the organic phase was isolated and quantified after elution with methanol.

**Recycling.** The aqueous phase was reused, as separated, for a second catalytic run after addition of iodobenzene (0.14 mL, 1.2 mmol) and styrene (0.3 mL, 2.4 mmol) using the procedure described above yielding to 0.09 g, (42%) of *trans*-stilbene **4**.

### References

- R. A. Sheldon, *Green Chem.*, 2005, **7**, 267.
- S. Liu and J. Xiao, *J. Mol. Catal. A: Chem.*, 2007, **270**, 1.
- C. J. Li, *Chem. Rev.*, 2005, **105**, 3095.
- F. Alonso, I. P. Beletskaya and M. Yus, *Tetrahedron*, 2005, **61**, 11771.
- J. P. Genet and M. Savignac, *J. Organomet. Chem.*, 1999, **576**, 305.
- N. Pinault and D. W. Bruce, *Coord. Chem. Rev.*, 2003, **241**, 1.
- A. Behr, G. Henze and R. Schomäcker, *Adv. Synth. Catal.*, 2006, **348**, 1485.
- D. E. Bergbreiter, *Chem. Rev.*, 2002, **102**, 3345.
- P. L. Osburn and D. E. Bergbreiter, *Prog. Polym. Sci.*, 2001, **26**, 2015.
- (a) *Handbook of Fluorous Chemistry*, ed. J. A. Gladysz, D. P. Curran and I. T. Horváth, Wiley-VCH, Weinheim, 2004; (b) I. T. Horváth, *Acc. Chem. Res.*, 1998, **31**, 641; (c) M. Wende and J. A. Gladysz, *J. Am. Chem. Soc.*, 2003, **125**, 5861.
- D. E. Bergbreiter and S. Furryk, *Green Chem.*, 2004, **6**, 280.
- (a) D. E. Bergbreiter, P. L. Osburn, T. Smith, C. Li and J. D. Frels, *J. Am. Chem. Soc.*, 2003, **125**, 6254; (b) D. E. Bergbreiter, P. L. Osburn, T. Smith and J. D. Frels, *J. Am. Chem. Soc.*, 2001, **123**, 11105; (c) D. E. Bergbreiter, P. L. Osburn and C. Li, *Org. Lett.*, 2002, **4**, 737.
- (a) C. Feng, Y. Wang, J. Jiang, Y. Yang and Z. Jin, *J. Mol. Catal. A: Chem.*, 2007, **268**, 201; (b) X. Liu, F. Kong, X. Zheng and Z. Jin, *Catal. Commun.*, 2003, **4**, 129; (c) C. Liu, J. Jiang, Y. Wang, F. Cheng and Z. Jin, *J. Mol. Catal. A: Chem.*, 2003, **198**, 23; (d) J. Jiang, Y. Wang, C. Liu, Q. Xiao and Z. Jin, *J. Mol. Catal. A: Chem.*, 2001, **171**, 85; (e) Y. Wang, J. Jiang, R. Zhang, X. Liu and Z. Jin, *J. Mol. Catal. A: Chem.*, 2000, **157**, 111; (f) R. Chen, J. Jiang, Y. Wang and Z. Jin, *J. Mol. Catal. A: Chem.*, 1999, **149**, 113; (g) J. Jiang, Y. Wang, C. Liu, F. Han and Z. Jin, *J. Mol. Catal. A: Chem.*, 1999, **147**, 131; (h) Z. Jin, X. Zheng and B. Fell, *J. Mol. Catal. A: Chem.*, 1997, **116**, 55.
- (a) A. Blom, G. G. Warr and E. J. Wanless, *Langmuir*, 2005, **21**, 11850 and references therein.
- (a) A. Berthod, S. Tomer and J. G. Dorsey, *Talanta*, 2001, **55**, 69; (b) P. D. T. Huibers, D. O. Shah and A. R. Katritzky, *J. Colloid Interface Sci.*, 1997, **193**, 132; (c) M. J. Rosen, A. W. Cohen, M. Dahanayake and X. Y. Hua, *J. Phys. Chem.*, 1982, **86**, 541.
- (a) C. Larpent, A. Laplace and T. Zemb, *Angew. Chem., Int. Ed.*, 2004, **43**, 3163; (b) L. Arleth, D. Posselt, D. Gazeau, C. Larpent, T. Zemb, K. Mortensen and J. S. Pedersen, *Langmuir*, 1997, **13**, 1887; (c) H. Coulombeau, F. Testard, T. Zemb and C. Larpent, *Langmuir*, 2004, **20**, 4840.
- C. Larpent, S. Prevost, L. Berthon, T. Zemb and F. Testard, *New J. Chem.*, 2007, **31**, 1424.
- (a) C. Najera, J. Gil-Molto and S. Karlstrom, *Adv. Synth. Catal.*, 2004, **346**, 1798; (b) C. Najera, J. Gil-Molto, S. Karlstrom and L. R. Falvello, *Org. Lett.*, 2003, **5**, 1451.
- J. Gil-Molto, S. Karlstrom and C. Najera, *Tetrahedron*, 2005, **61**, 12168.
- M. Trilla, R. Pleixats, M. W. C. Man, C. Bied and J. J. E. Moreau, *Tetrahedron Lett.*, 2006, **47**, 2399.
- (a) M. R. Buchmeiser, S. Lubbad, M. Mayr and K. Wurst, *Inorg. Chim. Acta*, 2003, **345**, 145; (b) M. R. Buchmeiser, T. Schareina, R. Kempe and K. Wurst, *J. Organomet. Chem.*, 2001, **634**, 39.
- M. R. Buchmeiser and K. Wurst, *J. Am. Chem. Soc.*, 1999, **121**, 11101.
- (a) B. T. Holmes and A. W. Snow, *Tetrahedron Lett.*, 2007, **48**, 4813; (b) I. Hamachi, K. Nakamura, A. Fujita and T. Kunitake, *J. Am. Chem. Soc.*, 1993, **115**, 4966.

- 24 T. Schareina, G. Hillebrand, H. Fuhrmann and R. Kempe, *Eur. J. Inorg. Chem.*, 2001, 2421.
- 25 L. Ma, R. C. Smith and J. D. Protasiewicz, *Inorg. Chim. Acta*, 2005, **358**, 3478.
- 26 (a) X. Huang, M. Cao, J. Wang and Y. Wang, *J. Phys. Chem. B*, 2006, **110**, 19479; (b) X. Luo, S. Wu and Y. Liang, *Chem. Commun.*, 2002, 492; (c) N. A. J. M. Sommerdijk, K. J. Booy, A. M. A. Pistorius, M. C. Feiters, R. J. M. Nolte and B. Zwanenburg, *Langmuir*, 1999, **15**, 7008.
- 27 (a) K. Glenn, A. van Bommel, S. C. Bhattacharya and R. M. Palepu, *Colloid Polym. Sci.*, 2005, **283**, 845; (b) T. Gu and P. A. Galera-Gomez, *Colloids Surf. A*, 1995, **104**, 307.
- 28 (a) N. A. Bumagin, P. G. More and I. P. Beletskaya, *J. Organomet. Chem.*, 1989, **371**, 397; (b) Z. Zhang, Z. Zha, C. Gan, C. Pan, Y. Zhou, Z. Wang and M. Zhou, *J. Org. Chem.*, 2006, **71**, 4339.
- 29 (a) Z. Wang, B. Shen, A. Zou and N. He, *Chem. Eng. J.*, 2005, **113**, 27; (b) S. F. Zhao, R. X. Zhou and X. M. Zheng, *J. Mol. Catal. A: Chem.*, 2004, **211**, 139.
- 30 (a) Y. Uozumi and T. Kimura, *Synlett*, 2002, 2045; (b) Y. Uozumi and T. Watanabe, *J. Org. Chem.*, 1999, **64**, 6921; (c) Y. M. A. Yamada, K. Takeda, H. Takahashi and S. Ikegami, *Tetrahedron*, 2004, **60**, 4097.
- 31 *Handbook of Chemistry and Physics*, CRC Press, 74th edn, 1993–1994.

# Hydrothermal carbon from biomass: a comparison of the local structure from poly- to monosaccharides and pentoses/hexoses†

Maria-Magdalena Titirici, Markus Antonietti and Niki Baccile\*

Received 24th April 2008, Accepted 22nd July 2008

First published as an Advance Article on the web 7th October 2008

DOI: 10.1039/b807009a

Carbon particles are synthesized under hydrothermal conditions using different biomass (glucose, xylose, maltose, sucrose, amylopectin, starch) and biomass derivatives (5-hydroxymethyl-furfural-1-aldehyde (HMF) and furfural) as carbon sources. Carbons obtained from mono- and polysaccharides, hexose and pentose sugars, and from the biomass derivatives, HMF and furfural, are compared from the particle morphology, chemical composition and structural point of view. A clear structural and morphological difference can be observed in carbons from pentoses and hexoses, but in the latter case, irrespective of the nature of the hexose sugar, all carbon materials showed astonishing similarities, opening the way for the use of renewable biomass in the synthesis of such carbon materials.

## Introduction

Research on materials usually gives the priority to increase the performance-to-cost ratio, disregarding the sustainability of the methods, techniques and processes involved in the conception and synthesis of the material itself. In the field of carbon-based materials, activated charcoals are usually made under high-energy conditions. Recently developed routes to obtain a periodic porous carbon network<sup>1–4</sup> were successful but again did not take into account any criteria of sustainability. In this case, it involves: indirect impregnation techniques (mesoporous silica is generally used as the template), hydrogen fluoride etching,<sup>1,2</sup> and finally high carbonization temperatures.<sup>1</sup> Even direct templating of resins (phenol/formaldehyde)<sup>4</sup> are still far from following sustainable principles such as energy and atom economy, low toxicological impact of materials and processes and use of renewable resources.

The problem of carbon synthesis under sustainable conditions was recently revisited and implemented by several research teams,<sup>5–8</sup> where hydrothermal treatment of biomass in water under relatively mild conditions provided bulk, mesoporous, or nanostructured carbon materials. This technique has been known for a long time,<sup>9</sup> but the need for exploring cheap and sustainable ways to obtain chemicals<sup>10</sup> and carbons from raw materials other than crude oil or natural gas (for soot generation) led to a re-exploration of this field. In addition, the implementation of a low-cost pathway to recycle byproducts of farmed biomass would additionally represent a way to sequester significant amounts of CO<sub>2</sub>,<sup>5</sup> creating a materials benefit at the same time.

The use of hydrothermal synthesis between 180 °C and 220 °C allowed one to obtain carbon-based powders, nanofibers,<sup>11,12</sup> or sponge-like mesoporous carbons that were potentially useful as soil conditioners, ion exchange resins or sorption coals.<sup>7</sup> The synthesis proved to be feasible when glucose<sup>6</sup> is used or even when side products from raw biomass materials like oak leaves and orange peels are taken.<sup>7</sup> In the first case, the surface chemistry could also be modified by means of hydrophilic or hydrophobic coupling agents.<sup>13</sup> Along similar lines, the group of Clark showed that a slightly different approach using expanded starch treated with sulfuric acid instead of pure hydrothermal conditions could provide functional materials with disordered mesoporosity which proved to be satisfactory as catalysts in the esterification of succinic acid.<sup>14,15</sup> In spite of the undoubted usefulness of the recent re-discovery of the hydrothermal process to obtain carbonaceous material, some basic work is still lacking as far as process of formation and final structure are concerned.

Some groups tried to investigate, directly or indirectly, the reaction mechanisms which transform glucose first into 5-hydroxymethyl-furfural-1-aldehyde (HMF), the dehydrated intermediate,<sup>16,17</sup> and then from here to the carbonaceous structure,<sup>18,19</sup> but a clear reaction path is still missing and the chemistry of furans and furan-derived compounds is far too large to easily forecast any possible result.<sup>20</sup> Even less is known about the final material structure mainly because of its intrinsic complexity and lack of a technique allowing discrimination among all carbon sites with satisfactory resolution. In general, FT-IR, and in some cases FT-Raman, is the main, easily accessible technique used to discriminate between various functional groups (C=O, C=C, aliphatic carbons).<sup>7,18,19</sup> XPS was also used to identify the main carbon sites but resolution here is worse than in vibrational-based spectroscopies.<sup>13</sup> <sup>13</sup>C solid-state NMR has also been already attempted<sup>8,18</sup> but its use was as a complement to other techniques. Even if exploitation of solid state NMR data on these materials was in its very beginnings, the authors have found that hydrothermal carbon materials give very

MPI campus, Am Muehlenberg, 1 D-14476, Golm (Potsdam), Germany.  
E-mail: pape@mpikg.mpg.de, niki.baccile@mpikg.mpg.de; Fax: +49 331 567 9502; Tel: +49 331 567 9508

† Electronic supplementary information (ESI) available: Fig. S1. GC experiments of residual liquors from C-glucose, C-HMF, C-xylose and C-furfural. See DOI: 10.1039/b807009a

nicely resolved  $^{13}\text{C}$  spectra which have deserved recent deeper investigations.<sup>21</sup> So far, several studies<sup>7,8,22,23</sup> have proved that different types of biomass could be used to obtain carbon under hydrothermal conditions but in no case has a clear comparison analyzing the local structure been made.

In this study we will attribute the chemical and structural fingerprint of hydrothermal carbons obtained from hexose and pentose sugars as well as from their corresponding main dehydration intermediates, HMF and furfural reactions.<sup>24,25</sup> The aim of this work is to lead a comparative structural study of hydrothermally synthesized carbon materials obtained from different saccharides classified according to their number of carbons (pentoses vs. hexoses) and growing complexity (mono- vs. di- vs. polysaccharides).

We will show that all materials obtained from hexoses-based mono- (glucose, HMF), di- (maltose, sucrose) and polysaccharides (amylopectin, starch) have the same chemical nature in terms of atom percentage and functional groups, as verified by  $^{13}\text{C}$  solid-state cross polarization (CP) NMR analysis and scanning electron microscopy (SEM) images. On the other hand, pentose-based (xylose, furfural) carbonaceous materials clearly showed interesting morphological and chemical differences with respect to hexose-based ones.

This work also clearly underlines that no substantial difference exists between monosaccharide- and polysaccharide-derived carbons, suggesting that the complexity of sugar-containing biomass (not including cellulose) hardly has any influence on the material-forming mechanisms. This is important as it indicates that basic studies performed on simple test molecules, like glucose,<sup>21</sup> have broader validity and that irrespective of the complexity of the saccharide source, the final materials have very similar local functionalities and connection patterns.

## Experimental

### Materials

For all samples, about 13.5 ml of a deionized water solution containing 1.5 g in mass of carbohydrate biomass was used. D(+)-Glucose, D(+)-xylose, D(+)-maltose monohydrate, sucrose, amylopectin from potato starch, starch from potatoes or carbohydrate-dehydrated derivatives, HMF and furfural, were used as received (Sigma Aldrich). In order to prevent any contamination from multiple experiments, the mixture was sealed into an open-end glass vial (~25 ml) inside a typical PTFE-lined autoclave system (~45 ml) and hydrothermally reacted in a pre-heated oven at 180 °C for 24 h. After reaction, the autoclave is cooled down in a water bath at room temperature. The obtained black solid powder is then separated from the remaining aqueous solution by centrifugation (7000 rpm for 20 min) and put into an oven at 80 °C under vacuum overnight for drying. Sample notation for carbon material introduces an italic-styled capital "C" before each carbonized material; e.g., if glucose is the starting product, then *C*-glucose is its corresponding carbon sample obtained from hydrothermal treatment. In some cases, the terms *C*-hexose or *C*-pentose are used referring to all carbons from hexose and pentose sugars.

### Characterization

Gas chromatography (GC) coupled to mass spectroscopy (MS) was used to separate and identify the main molecular species by mean of the NIST database included in the instrument software package (Enhanced Chemstation, MSD Chemstation D.03.00.611, © Agilent Technologies 1989–2006). The instrument used is an Agilent Technologies (GC= 6890N; MS= 5975) apparatus.

**Solid-state NMR.**  $^1\text{H}$  and  $^{13}\text{C}$  solid-state magic angle spinning (MAS) NMR experiments have been acquired on a Bruker Avance 300 MHz (7 T) spectrometer using the 4 mm zirconia rotors as sample holders spinning at MAS rate  $\nu_{\text{MAS}} = 14$  kHz. The chemical shift reference was tetramethylsilane (TMS;  $\delta = 0$  ppm). Proton-to-carbon CP MAS was used to enhance carbon sensitivity: the recycle delay for all CP experiments is 3 s and TPPM decoupling is applied during signal acquisition. Cross-polarization transfers were performed under adiabatic tangential ramps<sup>26,27</sup> to enhance the signal with respect to other known methods<sup>28</sup> and the CP time  $t_{\text{CP}} = 3$  ms was found to be a good compromise in order to have a good overview of all carbon species. The number of transients is 1840 (*C*-glucose, *C*-xylose) and 1200 for all other carbon samples. The peak attribution was done following ref. 29–32 and 33.

Elemental chemical analysis was performed on a (C, N, O, S, H) Elementar Vario Micro Cube. SEM images were acquired on a LEO 1550/LEO GmbH Oberkochen provided with a Everhard Thornley secondary electron and In-lens detectors.  $\text{N}_2$  adsorption and desorption isotherms were performed at 77 K with a Quadrachrome Adsorption Instrument and the BET method was used for specific surface area determination.

## Results and discussion

### Monosaccharide-derived carbons

Particle dispersions of carbonaceous materials were prepared from saccharides at 180 °C in water in a closed autoclave.

Fig. 1 and Fig. 2 show, respectively, SEM pictures and  $^{13}\text{C}$  solid state CP-MAS NMR spectra of *C*-glucose and *C*-xylose (highlighted in gray for convenience) carbon materials. Despite the similar chemical nature of the employed sugars, the first being a hexose and the second a pentose, the final materials have remarkably different shapes. The decomposition of xylose leads to separated carbon spheres with a diameter between 100 and 500 nm (Table 1) while glucose-based carbon is characterized by a mixture of spheres whose size varies between 500 nm and 1  $\mu\text{m}$ , randomly dispersed inside an interconnected matrix of smaller particles (<200 nm).

$^{13}\text{C}$  NMR spectra present some common peaks at 208 ppm (though a difference in 4 ppm at higher fields is observed for *C*-xylose), 175 ppm, 150 ppm and 40 ppm. On the other side, significant differences occur in the regions between 130 and 110 ppm, at 75 ppm and between 40 and 20 ppm. These observations show that similarities can be related to a comparable amount of carbonyl groups (aldehydes, ketones and carboxylic acids at chemical shifts between 210 and 170 ppm) as well as to the presence of oxygen-substituted protonated and non-protonated C=C bonds resonating at 150 ppm.



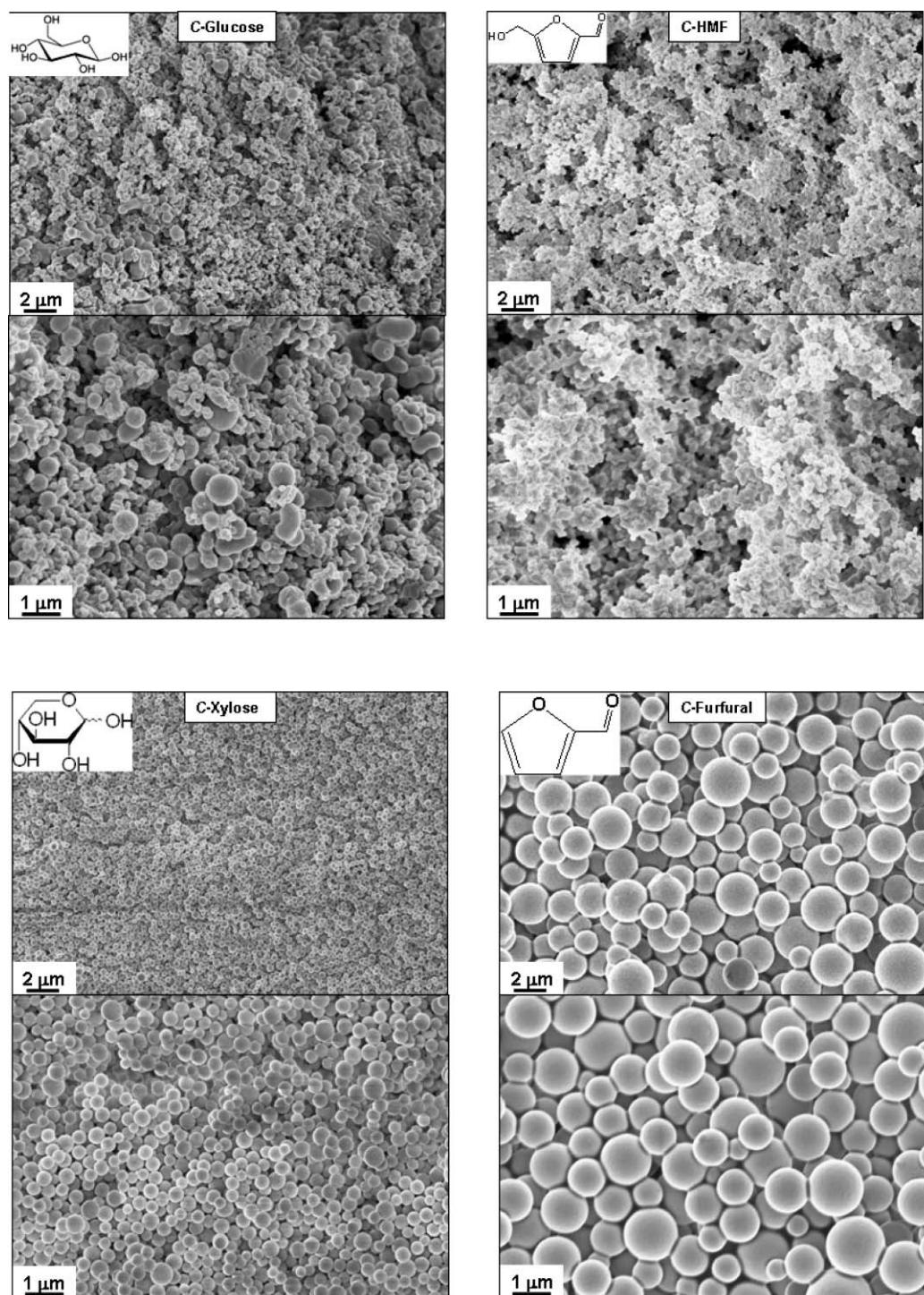
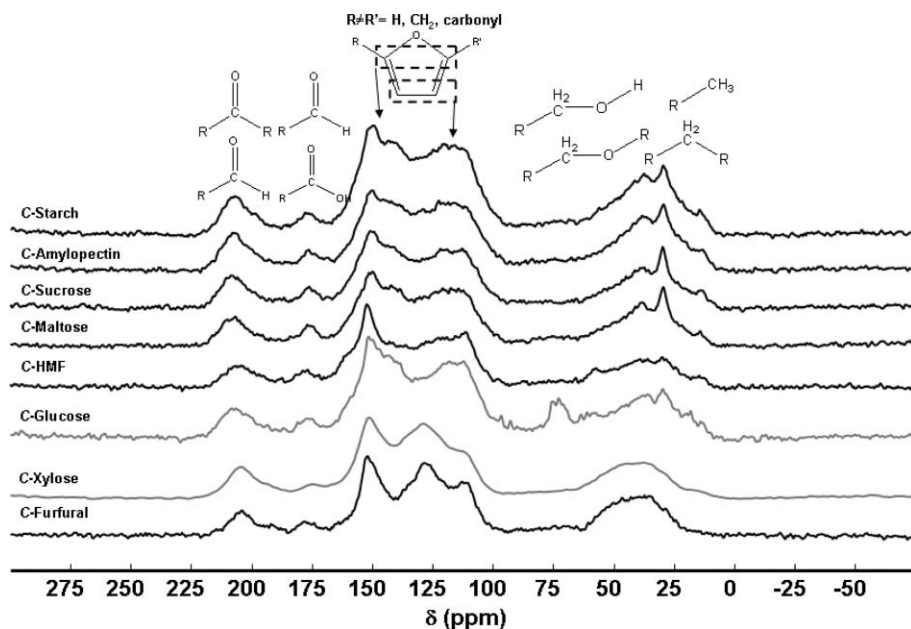


Fig. 1 SEM images of samples C-glucose, C-HMF, C-xylose and C-furfural.

By contrast, the peak at 129 ppm, which is generally attributed to aromatic carbons, as it is typical for graphitic structures or long-range conjugated double bonds, indicates the higher aromatic character of C-xylose carbon with respect to C-glucose. The peak at 75 ppm is indicative of the presence of hydroxylated methylene groups, which constitute an important part of C-glucose, while almost no hint of such groups is observed in C-xylose. Finally, at low chemical shifts, C-xylose

seems to be dominated by aliphatic groups resonating in the 40–50 ppm region while C-glucose shows an additional contribution of methylene between 20 and 40 ppm.

Overall, it seems that carbon material obtained from xylose has a higher aromatic character than C-glucose, and its higher carbon content (68.5%) supports this view (Table 2). Nonetheless, the oxygen level remains quite high even in C-xylose (27.3%) meaning that the conjugated C=C network



**Fig. 2**  $^{13}\text{C}$  solid-state CP-MAS NMR spectra ( $t_{\text{CP}} = 3$  ms) of *C*-starch, *C*-amylopectin, *C*-sucrose and *C*-maltose, *C*-HMF, *C*-glucose, *C*-xylose and *C*-furfural.

**Table 1** Morphological and dimensional aspect of carbon powders, as observed from SEM images

Sample	Morphology	Size/nm
Hexoses		
<i>C</i> -Glucose	Interconnected particles	<200
	Spheres	500–1000
<i>C</i> -HMF	Interconnected particles	<200
	Interconnected particles	200–500
<i>C</i> -Maltose	Agglomerated particles	200–500
	Spheres	2000
<i>C</i> -Sucrose	Interconnected spheres	700–2000
<i>C</i> -Amylopectin	Interconnected spheres	1000–2000
<i>C</i> -Starch	Interconnected spheres	300–1000
Pentoses		
<i>C</i> -Furfural	Dispersed spheres	500–3000
<i>C</i> -Xylose	Dispersed spheres	100–1000

**Table 2** Elemental analysis of carbon materials

Sample	Elemental analysis		
	C wt%	H wt%	O wt% <sup>a</sup>
Hexoses			
<i>C</i> -Glucose	64.47	4.69	30.85
<i>C</i> -HMF	65.63	4.15	30.22
<i>C</i> -Maltose	64.70	4.54	30.76
<i>C</i> -Sucrose	64.15	4.77	31.09
<i>C</i> -Amylopectin	65.76	4.56	29.69
<i>C</i> -Starch	64.47	4.57	30.97
Pentoses			
<i>C</i> -Xylose	68.58	4.11	27.31
<i>C</i> -Furfural	68.60	3.90	27.50

<sup>a</sup> Calculated value.

is always accompanied by larger quantities of functional groups (CHO, CC=CO, COOH), furan rings and ethers.

To reveal further details of this difference, we also tried to carbonize the known intermediates of dehydration, HMF

and furfural under the same carbonization conditions. SEM images and  $^{13}\text{C}$  NMR spectra of carbons obtained from HMF and furfural are also presented in Fig. 1 and Fig. 2. The *C*-HMF microstructure is composed of small particles (<200 nm) which forms an interconnected network, and the similarities to *C*-glucose are obvious. Interestingly, furfural produces larger polydispersed spherical carbon particles whose size ranges between 500 nm and 3  $\mu\text{m}$  (Table 1). The analysis of local chemical environments around carbon atoms probed by  $^{13}\text{C}$  NMR also reveals some astonishing similarities between *C*-glucose and *C*-HMF and between *C*-xylose and *C*-furfural, respectively. The characteristic aromatic peak at 129 ppm is clearly prominent only in the pentose-derived carbon samples. Elemental analysis (Table 2) reveals, first of all, a high oxygen content, which undoubtedly makes these materials different from coal; secondly, carbon content in *C*-HMF (65.6%) is lower than in *C*-furfural (68.6%), and those values are coherent with values detected for *C*-glucose and *C*-xylose, discussed above. Mechanistic implications will be discussed later. Isothermal nitrogen adsorption/desorption experiments (results not shown) indicate them as non-porous materials (BET specific surface areas < 10  $\text{m}^2 \text{g}^{-1}$ ).

### Polysaccharide-derived carbons

SEM micrographs of carbon materials from disaccharides (maltose, sucrose) and polysaccharides (amylopectin, starch) are depicted in Fig. 3. *C*-maltose and *C*-sucrose are composed of interconnected particles, in coexistence with domains (larger in *C*-maltose) where aggregation occurs. Differences in morphology and size are summarized in Table 1: *C*-maltose is composed of a larger number of small (200–500 nm) particles in coexistence with larger spheres (2  $\mu\text{m}$ ). By contrast, *C*-sucrose is composed of spherical particles whose size vary between 700 nm and 2  $\mu\text{m}$ . Strong similarities are found for *C*-maltose and *C*-glucose materials, both characterized by isolated large spherical



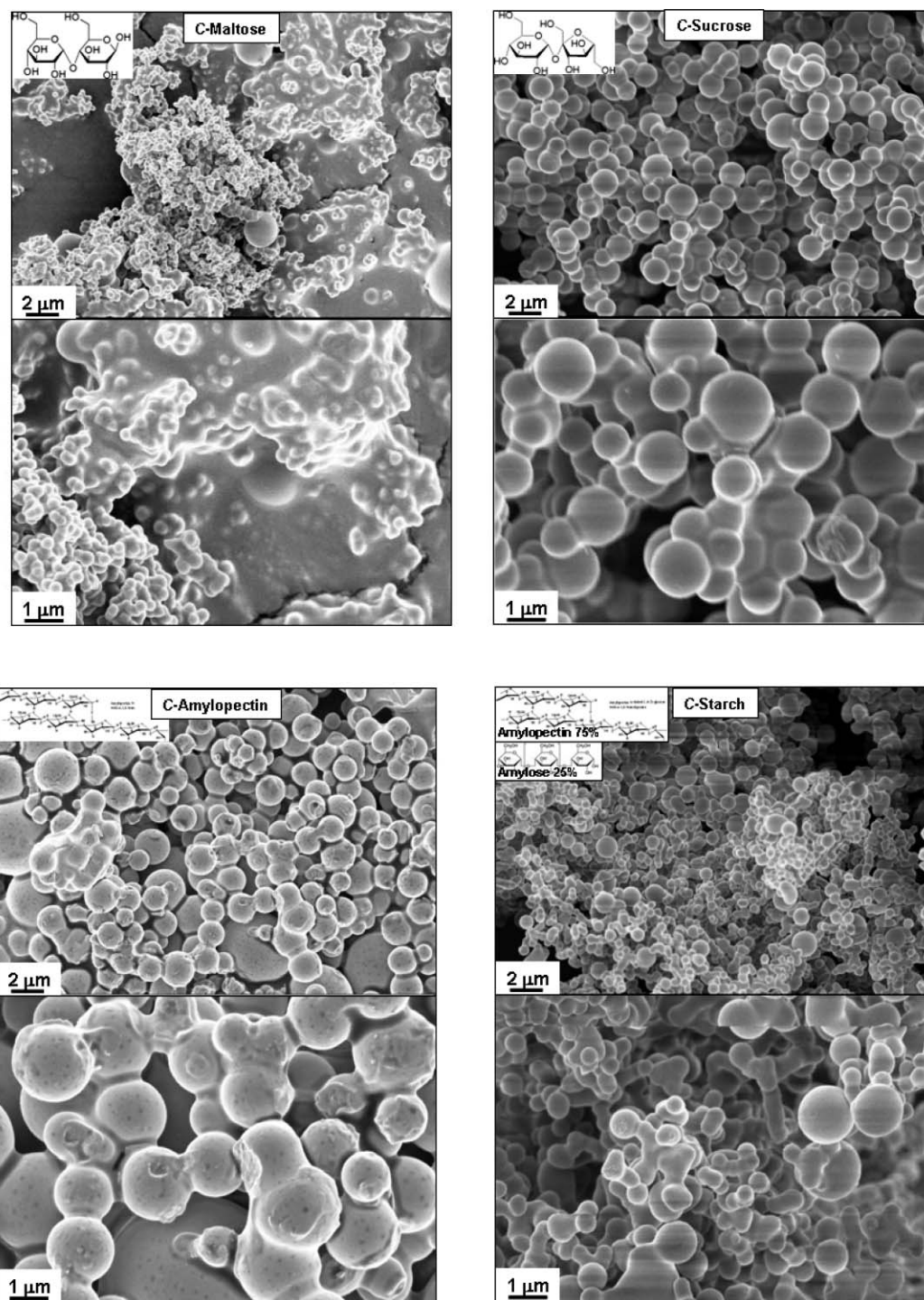


Fig. 3 SEM images of samples C-sucrose, C-maltose, C-starch and C-amylopectin.

particles within a large matrix of interconnected small particles with ill-defined shape. Polysaccharides including amylopectin and starch, whose SEM images (Fig. 1) show interconnected spherical particles ranging from 700 nm to 2 μm, provide very similar dispersion patterns despite their low solubility in water at room temperature.

When one compares SEM structures of final carbons to original saccharides (examples from pure glucose, xylose,

amylopectin and starch powders are provided in Fig. 4), the destructuring process which took place during carbonization and transformed the original disordered bulky materials into micrometer-sized particles and/or spheres is self-evident. The chemical composition also largely changed during the hydrothermal process: saccharides turn into dark brown or black powders with a carbon content increasing from the original 40 wt% to 64–70 wt% (Table 2); meanwhile, the oxygen presence

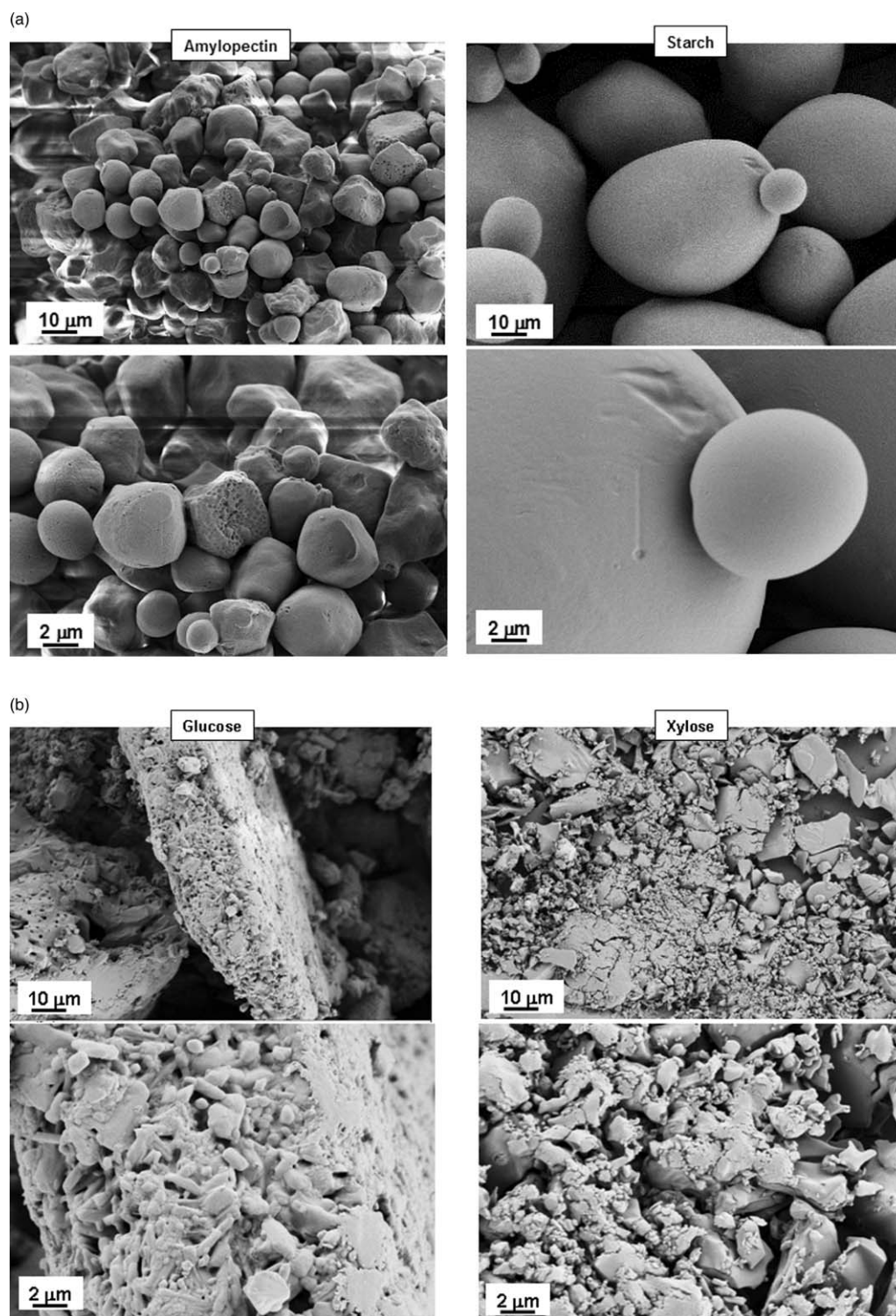


Fig. 4 SEM images of pure glucose, xylose, amylopectin and starch solid powders.

is reduced from 53 wt%, as found in, *e.g.*, glucose, to 27–30 wt% for carbon powders.

$^{13}\text{C}$  solid-state NMR (Fig. 2) spectra from *C*-maltose, *C*-sucrose, *C*-amylopectin and *C*-starch show exactly the same characteristics already observed for *C*-glucose and *C*-HMF. The materials can be considered as chemically equivalent, in good agreement with the elemental analysis shown in Table 2,

where the carbon content for all hexose-based carbons is  $64\% \pm 1\%$ .

#### Mechanistic considerations

As we pointed out earlier in the discussion, it is generally assumed that dehydration of pentoses and hexoses leads to



the formation of furfural and HMF as a first and main dehydration product. Our experiments strongly suggest that these furans are also the reacting species for carbon material. In fact, the morphologies and chemical structures of carbons obtained from saccharides are directly related to those of carbons obtained from pure furans according to the following parallelism: *C*-hexoses ~ *C*-HMF and *C*-pentoses ~ *C*-furfural. Additionally, intermediate molecules derived from saccharide dehydration (levulinic acid, dihydroxyacetone, formic acid, acetic acid, formaldehyde, pyruvaldehyde, etc. . .)<sup>25</sup> coexist with furans and they can probably be responsible for particle size, powder texture and aggregation discrepancies. The striking similarities of NMR fingerprint spectra between all hexose-based carbons and *C*-HMF, or between *C*-xylose and *C*-furfural clearly prove that chemical complexity, the usual problem of raw biomass as an educt for materials chemistry, is indeed essentially resolved throughout hydrothermal carbonization by driving all saccharides only through two main reaction pathways: from sugar to furan-based (furfural or HMF) intermediate and from the furan to carbon. This is supported by GC-MS analysis (Fig. S1†) of the side products in the remaining product waters, where in all cases the nature and amount of the unreacted by-products is very similar for the hexoses, e.g. *C*-glucose and *C*-HMF, and pentoses, *C*-xylose and *C*-furfural. These side-product molecules mainly come either from the dehydration of carbohydrates or from the re-hydration of the furans, plus the hydrolytic splitting of those intermediates. Table 3 shows the normalized integrated intensity of HMF, furfural and 4-oxo-pentanoic acid detected by GC in the final liquors of the indicated final materials as well as for pure furfural and HMF solutions at three different concentrations, used as reference for quantification. Errors are estimated to 10% of the indicated values and account for possible discrepancies in manual simulation of each GC peak. When only monosaccharides and furans values are compared, one observes that: (1) the carbonization process from glucose seems slightly more efficient if compared to the xylose one, since HMF concentration in solution for *C*-glucose after reaction is less

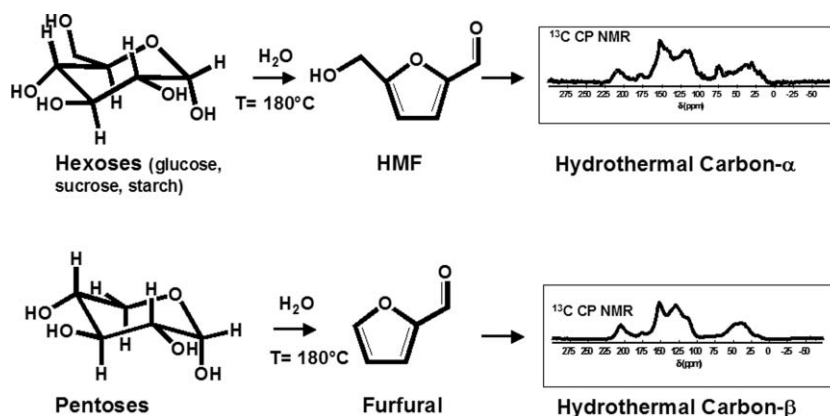
than half with respect to remaining furfural concentration from *C*-xylose; additionally, the amount of final carbon powder from glucose is about 1.5 times higher than carbon obtained from xylose. This is probably not a big surprise as it is known from furan chemistry that furfural, the dehydration product of xylose, is a low reactive compound due to the joint stabilizing effects of furan aromatic ring and carbonyl function<sup>20</sup> with respect to polycondensation. On the other hand, even if general knowledge about the reactivity of HMF itself is smaller, its molecular similarity to furfuryl alcohol, a widely studied and highly reactive modified furan,<sup>20</sup> may justify its higher reactivity. (2) The reaction seems to be less efficient when starting from pure furans rather than from carbohydrates, especially when pure furfural is employed (concentration in solution after reaction is around 5 wt%). As pointed out earlier, reactivity of furfural is low and extremely condition dependent. In general, addition of proper co-monomers, like furfuryl alcohol, increase its reactivity.<sup>20</sup> Consequently, the heterogeneous medium composed of furans and dehydrated forms of saccharides (when sugars are used instead of pure HMF and furfural) may be highly favourable to the overall efficiency of the carbon-formation process. Reaction between HMF and de-hydrated glucose was recently used to obtain liquid alkanes.<sup>34</sup> (3) The higher the HMF content, the lower the 4-oxo-pentanoic acid content (also known as levulinic acid, it is a common side product of hexose dehydration, and it is expected to increase with decreasing hexose concentration<sup>25</sup>), indicating the competition of monomolecular decomposition reactions and the (at least) bimolecular carbonization reaction which is obviously promoted at higher concentrations.

Chemical reactions in the presence of a di- or polysaccharide do follow the same path, that is, dehydration of hexose units and formation of HMF, which then turns into hydrothermal carbon. As shown in Table 3, HMF residues do not exceed the 0.4 wt%, and the actual values for *C*-maltose (0.14 wt%) and *C*-sucrose (0.12 wt%) are almost as low as those registered for glucose (0.12 wt%). In the case of *C*-amylopectin and *C*-starch, residual HMF increases, respectively, to 0.26 wt% and 0.37 wt%. The

**Table 3** Relative integrated peak areas from GC-MS experiments and wt% concentration for residual HMF and furfural compounds<sup>a</sup>

Sample (solution)	*Oxopentanoic acid	HMF	HMF wt%	Furfural	Furfural wt%
Hexoses					
Pure HMF solution		0.20	0.50		
		0.50	1.00		
		1.00	2.00		
<i>C</i> -Glucose	0.12	0.01	0.12		
<i>C</i> -HMF	0.05	0.43	0.91		
<i>C</i> -Maltose	0.11	0.02	0.14		
<i>C</i> -Sucrose	1.00	0.05	0.19		
<i>C</i> -Amylopectin	0.66	0.09	0.26		
<i>C</i> -Starch	0.54	0.15	0.37		
Pentoses					
Pure furfural solution				0.31	0.50
				0.52	1.00
				1.00	2.00
<i>C</i> -Furfural				2.42	5.08
<i>C</i> -Xylose				0.21	0.29

<sup>a</sup> Experiments were performed on remaining liquor solutions of indicated samples after 24 h of hydrothermal treatment synthesis of indicated carbon materials. By contrast, pure HMF and furfural solution were freshly prepared for comparison purposes. Residual solution wt% values for HMF and furfural are calculated after a linear fit of recorded values for pure solutions. Errors, coming from the integration procedure, are estimated to be ±10% of indicated concentration values.



**Fig. 5** Reaction pathways encountered in the formation of hydrothermal carbons from hexose and pentose sources, leading to the differently structured and shaped materials.

slightly higher values are attributed to a delayed dehydration kinetics due to the required hydrolysis of the macromolecular structure towards the monosaccharides.

An additional aspect which constitutes a difference between hexoses and pentoses is the colloidal structure of the carbon powders: nicely dispersed, separated spherical particles are always found for *C*-xylose and *C*-furfural. Explanation for this may probably come from the limited water solubility of furfural (< 8.5 m/v%), which tends to emulsify in solution, and carbonization may only take place inside droplets. The intense peak at 129 ppm observed for these materials, typical for aromatic C=C sites, is most presumably indicative for a higher degree of self reaction between furfural molecules within the droplets *via* the unprotected, highly reactive, 5-position.<sup>20</sup>

By contrast, <sup>13</sup>C solid-state NMR spectra and elemental analysis data for *C*-hexoses and *C*-HMF are remarkably similar, thus indicating that the system most presumably has to pass the same reaction pathway *via* the hydroxymethylfurfural stage and before carbonization can take place. In addition, interconnected spherical particle networks are generally observed, especially for low-weight sugars-derived carbons. These results may appear in contrast with previous experiments, where relatively well separated particles from mono- and polysaccharides (glucose, starch or rice) under similar conditions were obtained.<sup>22,35,36</sup> Nevertheless, those experiments were undertaken in the presence of external pressure,<sup>22</sup> metal salts (Fe(II), Co(II), Cu(II), *etc.*) or metal nanoparticles (Fe<sub>2</sub>O<sub>3</sub>), which can act as external nucleators and stabilizers.<sup>37</sup> Since our experiments used pure sugar solutions, emulsion polymerization occurs in the absence of a stabilizer; hence, the dispersed spherical particles formed from pentoses should depend only on the hydrophobic character of furfural.

An important question may arise. Is hydrothermal carbon just a polymerization product of HMF and furfural? At the moment, a clear-cut answer cannot be provided but an insight into polyfuranes generally reveals the existence of cross-linked polymers which may appear as black and glassy materials<sup>20</sup> according to the polymerization mechanism and type of added co-monomers. Unfortunately, the number of examples provided in ref. 20 and references therein show that the chemistry of furans is very large and many possible reaction ways can simultaneously occur especially in an heterogeneous system like the one where

hydrothermal carbon is obtained. Hydrothermal carbon is by contrast a rather low-dense, dark brown powder which is not soluble in common solvents. So, even if during hydrothermal carbonization furfural and HMF are most likely the main reactive species, we cannot depict either the exact reaction mechanisms or the clear final structure yet. This last point will be dealt with in a further communication by means of highly advanced solid-state NMR techniques.<sup>21</sup>

Finally, the fact that no substantial difference exists between all hydrothermal hexose carbons also shows that glucose can be safely used as a model molecule for the understanding of the formation of these materials. Fig. 5 makes a summary of the main results of this communication, indicating that all hexoses (including their dehydration product, HMF) lead to the same type of material, called carbon-α for convenience, while pentoses lead to a different type of carbon, called arbitrarily carbon-β.

## Conclusions

In this work, we compared hydrothermal carbons synthesized from diverse biomass (glucose, xylose, maltose, sucrose, amylopectin, starch) and biomass derivatives (HMF and furfural) under hydrothermal conditions at 180 °C with respect to their chemical and morphological structures. SEM, <sup>13</sup>C solid-state NMR and elemental analysis on final powders combined with GC-MS experiments on residual liquor solutions were the main tools which allowed us demonstrate that all sugars in their hexose form, no matter their complexity, degradate into hydroxymethyl furfural, which finally condenses to a carbon-like material having morphological similarities and the same chemical and structural composition. By contrast, xylose dehydrate into furfural, which in turn reacts to provide very similar carbon materials as obtained from pure furfural. <sup>13</sup>C solid-state NMR shows that the local structure of these two families of carbons, from hexoses and pentoses, are relatively different.

Contrary to simple expectations, starting from more complex biomass instead of clean sugars does not harm the outcome of the hydrothermal carbonization reaction, and remarkable similarities between the products of homologous series do occur, both with respect to morphology and local structural connectivity. This is a positive outcome concerning the green chemistry aspects of this process, as even complex waste biomass

can be used without too much influence on the final carbonized structure: biological diversity is simply reduced by the elemental steps of the carbonization reaction.

## Acknowledgements

We acknowledge Dr F. Babonneau and G. Laurent (Laboratoire de Chimie de la Matière Condensée de Paris, CNRS-Univ. Pierre et Marie Curie, Paris, France) for providing access to solid-state NMR facilities.

## Notes and References

- 1 R. Ryoo, S. H. Joo and S. Kun, *J. Phys. Chem. B*, 1999, **103**, 7743.
- 2 B. Sakintuna and Y. Yürüm, *Ind. Eng. Chem. Res.*, 2005, **44**, 2893.
- 3 F. Zhang, Y. Meng, D. Gu, Y. Yan, C. Yu, B. Tu and D. Zhao, *J. Am. Chem. Soc.*, 2005, **127**, 13508.
- 4 Y. Meng, D. Gu, F. Zhang, Y. Shi, H. Yang, Z. Li, C. Yu, B. Tu and D. Zhao, *Angew. Chem., Int. Ed.*, 2005, **44**, 7053.
- 5 M.-M. Titirici, A. Thomas and M. Antonietti, *New J. Chem.*, 2007, **31**, 787.
- 6 M.-M. Titirici, A. Thomas and M. Antonietti, *Adv. Funct. Mater.*, 2007, **17**, 1010.
- 7 M.-M. Titirici, A. Thomas, S.-H. Yu, J.-O. Muller and M. Antonietti, *Chem. Mater.*, 2007, **19**, 4205.
- 8 V. Budarin, J. H. Clark, J. J. E. Hardy, R. Luque, K. Milkowski, S. J. Tavener and A. J. Wilson, *Angew. Chem., Int. Ed.*, 2006, **45**, 3782.
- 9 E. Berl and A. Schmidt, *Justus Liebigs Ann. Chem.*, 1932, **45**, 97.
- 10 A. Corma, S. Iborra and A. Velty, *Chem. Rev.*, 2007, **107**, 2411.
- 11 H.-S. Qian, S.-H. Yu, L.-B. Luo, J.-Y. Gong, L.-F. Fei and X.-M. Liu, *Chem. Mater.*, 2006, **18**, 2102.
- 12 S.-H. Yu, X. Cui, L. Li, K. Li, B. Yu, M. Antonietti and H. Coelfen, *Adv. Mater.*, 2004, **16**, 1636.
- 13 M.-M. Titirici, A. Thomas and M. Antonietti, *J. Mater. Chem.*, 2007, **17**, 3412.
- 14 V. L. Budarin, R. Luque, D. J. Macquarrie and J. H. Clark, *Chem.–Eur. J.*, 2007, **13**, 6914.
- 15 V. L. Budarin, J. H. Clark, R. Luque and D. J. Macquarrie, *Chem. Commun.*, 2007, 634.
- 16 K. Lourvanij and G. L. Rorrer, *Appl. Catal. A*, 1994, **109**, 147.
- 17 K. Lourvanij and G. L. Rorrer, *Ind. Eng. Chem. Res.*, 1993, **32**, 11.
- 18 C. Yao, Y. Shin, L.-Q. Wang, C. F. Windisch, Jr., W. D. Samuels, B. W. Arey, C. Wang, W. M. Risen, Jr. and G. J. Exarhos, *J. Phys. Chem. C*, 2007, **111**, 15141.
- 19 X. Sun and Y. Li, *Angew. Chem.*, 2004, **116**, 607.
- 20 A. Gandini and M. N. Belgacem, *Prog. Polym. Sci.*, 1997, **22**, 1203.
- 21 N. Baccile, G. Laurent, F. Babonneau, M.-M. Titirici and M. Antonietti, 2008, in preparation.
- 22 C. Yao, Y. Shin, L.-Q. Wang, C. F. Windisch, Jr., W. D. Samuels, B. W. Arey, C. Wang, W. M. Risen, Jr. and G. J. Exarhos, *J. Phys. Chem. C*, 2007, **111**, 15141.
- 23 F. Cheng, J. Liang, J. Zhao, Z. Tao and J. Chen, *Chem. Mater.*, 2008, DOI: 10.1021/cm702816x.
- 24 B. Sain, A. Chaudhuri, J. N. Borgohain, B. P. Baruah and J. L. Ghose, *J. Sci. Ind. Res.*, 1982, **41**, 431.
- 25 R. J. Ulbricht, S. J. Northup and J. A. Thomas, *Fundam. Appl. Toxicol.*, 1984, **4**, 843; M. J. Antal, W. S. L. Mok and G. N. Richards, *Carbohydr. Res.*, 1990, **199**, 91; F. S. Asghari and H. Yoshida, *Ind. Eng. Chem. Res.*, 2006, **45**, 2163.
- 26 S. Hediger, B. H. Meier, N. D. Kurur, G. Bodenhausen and R. R. Ernst, *Chem. Phys. Lett.*, 1994, **223**, 283.
- 27 S. Hediger, B. H. Meier and R. R. Ernst, *Chem. Phys. Lett.*, 1995, **240**, 449.
- 28 S. C. Christiansen, N. Hedin, J. D. Epping, M. T. Janicke, Y. del Amo, M. Demarest, M. Brzezinski and B. F. Chmelka, *Solid State Nucl. Magn. Reson.*, 2006, **29**, 170.
- 29 P. F. Barron and M. A. Wilson, *Nature*, 1981, **289**, 275.
- 30 M. J. Sullivan and G. E. Maciel, *Anal. Chem.*, 1982, **54**, 1608.
- 31 R. K. Sharma, J. B. Wooten, V. L. Baliga, P. A. Martoglio-Smith and M. R. Hajaligol, *J. Agric. Food Chem.*, 2002, **50**, 771.
- 32 K. M. Holtman, H.-M. Chang, H. Jameel and J. F. Kadla, *J. Wood Chem. Technol.*, 2006, **26**, 21.
- 33 *Carbon-13 NMR Spectroscopy*, ed. E. Breitmaier and W. Voelter, VCH, New York, 3rd edn, 1990.
- 34 G. W. Huber, J. N. Chheda, C. J. Barret and J. A. Dumesic, *Science*, 2005, **308**, 1446.
- 35 X. Cui, M. Antonietti and S.-H. Yu, *Small*, 2006, **2**, 756.
- 36 M.-M. Titirici, M. Antonietti and A. Thomas, *Chem. Mater.*, 2006, **18**, 3808.
- 37 *Fine Particles: Synthesis, Characterization and Mechanisms of Growth (Surfactant Science)*, ed. T. Sugimoto, CRC, New York, 2000, vol. 92, ch. 11.

# Developmental toxicity assessment of the ionic liquid 1-butyl-3-methylimidazolium chloride in CD-1 mice

Melissa M. Bailey,<sup>a,b</sup> Megan B. Townsend,<sup>a</sup> Peter L. Jernigan,<sup>a</sup> John Sturdivant,<sup>a</sup> Whitney L. Hough-Troutman,<sup>c</sup> Jane F. Rasco,<sup>a</sup> Richard P. Swatloski,<sup>c,d</sup> Robin D. Rogers<sup>\*c,d</sup> and Ronald D. Hood<sup>a,e</sup>

Received 25th April 2008, Accepted 13th August 2008

First published as an Advance Article on the web 7th October 2008

DOI: 10.1039/b807019a

The effects of prenatal exposure of mice to the ionic liquid (IL) 1-butyl-3-methylimidazolium chloride ([C<sub>4</sub>mim]Cl) were studied because of the potential for human exposure as a result of water or soil contamination from industrial effluent or accidental spills. After exposure to the IL, fetal weight was significantly decreased at the two highest dosages ( $P \leq 0.01$ ). Malformations were also somewhat more numerous at the highest dosage, suggesting that [C<sub>4</sub>mim]Cl may be teratogenic, although the apparent increase was not statistically significant. Maternal toxicity was also present, as shown by a dose-dependent increase in maternal morbidity and mortality during the course of treatment. Therefore from these results, [C<sub>4</sub>mim]Cl appears to be developmentally toxic at maternally toxic dosages, although the mechanism is unknown.

## Introduction

Ionic liquids (ILs) are salts composed solely of ions that melt below 100 °C and possess unique properties, such as a wide liquidus range and low or negligible vapor pressure.<sup>1-4</sup> Additionally, the properties of ILs can be customized for specific applications by altering either of the ions,<sup>5</sup> and thus a tremendous number of new ILs have become known, with many more possible combinations yet to be made.<sup>6</sup> Unique property sets, nearly unlimited choices, and tuneability have led to a broad range of applications in synthesis, coatings, high refractive index materials, metal plating, fuel cells, catalysis, chromatography columns, biomass processing, and drug delivery.<sup>7,8</sup> This has also led to difficulties in assessing the safety and toxicity of ILs recommended for major industrial processes. With so many different classes of ILs with widely variant biological properties, it has not been possible to study a 'representative' IL. This lack of specific information has allowed both advocates and opponents of the field to make gross overgeneralizations regarding the safety or lack thereof of ILs. This underscores the need to continue testing as many different classes of ILs as possible while focusing on those most likely to see bulk industrial use.

One such cation class that has received much attention and has been considered for commercialization includes the

1-alkyl-3-methylimidazolium [C<sub>n</sub>mim]<sup>+</sup> ions. One of the most popular and well-known members of this class is 1-butyl-3-methylimidazolium chloride ([C<sub>4</sub>mim]Cl), a hygroscopic, water soluble salt<sup>9</sup> (Fig. 1), which when dissolved in water yields fully hydrated ions.<sup>10</sup> [C<sub>4</sub>mim]Cl is also commonly used as an intermediate to other ILs.<sup>11</sup>

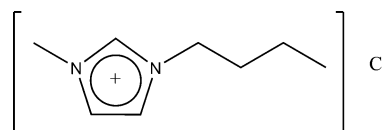


Fig. 1 Chemical structure of 1-butyl-3-methylimidazolium chloride.

The [C<sub>n</sub>mim]<sup>+</sup> cations are a source of concern for both environmental and aquatic toxicologists as they are not readily biodegradable, are water soluble, and have the potential for transport through groundwater.<sup>12-14</sup> Therefore, the majority of toxicity studies of imidazolium-based ILs have focused on aquatic life, utilizing a variety of model systems, such as algae,<sup>5,15-17</sup> marine bacteria,<sup>15,16,18-21</sup> zebrafish,<sup>20-23</sup> and snails.<sup>24</sup> But other model systems, including Fisher 344 rats,<sup>10</sup> human (HeLa,<sup>25,26</sup> CaCo-2,<sup>27</sup> HT-29,<sup>27</sup> and MCF7<sup>28</sup>) and rat (ICP-81 and C<sub>6</sub> glioma<sup>29</sup>) cell lines, and bacteria<sup>30-32</sup> have been used to better assess the overall toxicity of these ILs.

Results from toxicity studies have concluded that the cation is primarily responsible for the toxicity of the resulting ILs,<sup>15,29,31</sup> although this may be a result of the reliance on the current simple inorganic anions. The reported toxicity resulted, at least in part, from the ability to intercalate with the lipid bilayer membrane, thus increasing membrane permeability.<sup>33</sup> Alkyl chain length has been reported to be the major variable that increases toxicity, with toxicity increasing as chain length increases.<sup>12,26,32</sup> Generally, the ILs studied based on ammonium, pyridinium, imidazolium, or pyrrolidonium cations were found to be less

<sup>a</sup>Department of Biological Sciences, The University of Alabama, Tuscaloosa, AL, 35487, USA

<sup>b</sup>Department of Biological Sciences, Emporia State University, Emporia, KS, 66801, USA

<sup>c</sup>Department of Chemistry and Center for Green Manufacturing, The University of Alabama, Tuscaloosa, AL, 35487, USA

<sup>d</sup>QUILL and School of Chemistry & Chemical Engineering, The Queen's University of Belfast, Belfast, BT9 5AG, Northern Ireland, UK

<sup>e</sup>R. D. Hood & Associates, Toxicology Consultants, Tuscaloosa, AL, 35487, USA



toxic than traditional solvents, such as ether and benzene, but the ILs were more toxic than acetonitrile, acetone, and methanol.<sup>18,22</sup>

Based on current toxicity results, it is not unreasonable to hypothesize that exposure to some ILs during organism development may be a cause for concern. A previous study<sup>22</sup> found that exposure to [C<sub>4</sub>mim]Cl at various concentrations adversely affected reproductive parameters in zebrafish, causing a significant reduction in the number of total fry, first-brood fry, and average number of fry. However, no one has yet studied the effects of ILs on development in a mammalian species. Here we report on our investigation which focused on the effects of exposure to [C<sub>4</sub>mim]Cl on the development of CD-1 mice.

## Experimental

### Chemicals

The salt, 1-butyl-3-methylimidazolium chloride, was prepared following standard procedures,<sup>34</sup> in which equal molar amounts of 1-methylimidazole and chlorobutane were reacted to form the IL which yielded a white crystalline solid. The absence of starting materials was confirmed utilizing <sup>1</sup>H and <sup>13</sup>C NMR.

Samples for testing on mice were prepared as aqueous solutions of this water soluble salt. Residual water, determined by Karl–Fisher (2.34 wt% H<sub>2</sub>O), was noted before diluting 34.144 g of [C<sub>4</sub>mim]Cl with 100 mL deionized water to achieve a concentration of 341.44 mg mL<sup>-1</sup> of the test compound.

### Animals and husbandry

Male and female CD-1 mice, obtained from Charles River Breeding Laboratories International (Wilmington, MA, USA), were housed in an AAALAC (Association for Assessment and Accreditation of Laboratory Animal Care International)-approved animal facility in rooms maintained at 22 ± 2 °C, with 40–60% humidity and a 12 h photoperiod. Animals were bred naturally, two females with one male. Observation of a copulation plug designated gestation day 0 (GD 0). Mated females were individually housed in shoebox type cages with hardwood bedding and were given Teklad LM-485 rodent diet (Harlan Teklad, Madison, WI, USA) and tap water *ad libitum*. All procedures performed on these animals were in accordance with established guidelines and were reviewed and approved by The University of Alabama's Institutional Animal Care and Use Committee.

### Treatments

Prior to the definitive study, a preliminary range-finding study was conducted at [C<sub>4</sub>mim]Cl dosages of 0, 250, 500, or 1000 mg kg<sup>-1</sup> d<sup>-1</sup>, with five females in each dosage group. All mice in the 500 and 1000 mg kg<sup>-1</sup> d<sup>-1</sup> treatment groups became moribund and were subsequently euthanized by CO<sub>2</sub> overdose approximately 8 h after the initial dose. The mice in this group displayed ataxia, hypoactivity, and labored breathing. Two out of five mice in the 250 mg kg<sup>-1</sup> d<sup>-1</sup> treatment group appeared sluggish after the initial dose, but recovered within 24 h and survived multiple doses. For the definitive study, mated females were randomly assigned to one of four treatments administered by gavage from GD 6–16: (1) vehicle control, (2) 113 mg kg<sup>-1</sup> d<sup>-1</sup>

[C<sub>4</sub>mim]Cl, (3) 169 mg kg<sup>-1</sup> d<sup>-1</sup> [C<sub>4</sub>mim]Cl, or (4) 225 mg kg<sup>-1</sup> d<sup>-1</sup> [C<sub>4</sub>mim]Cl. The dosage volume was 0.01 mL g<sup>-1</sup> body weight. Clinical signs were recorded daily, and females were weighed on GD 0 as well as prior to each dosing.

### Data collection

On GD 17, mated females were euthanized by CO<sub>2</sub> overdose, their uteri were exposed, and the numbers of resorptions and dead or live fetuses were recorded. Live fetuses were removed from the uterus, weighed individually, and examined for gross malformations. Maternal body weight, minus the gravid uterine weight, was then obtained. Fetuses were initially fixed in 70% ethanol and then cleared and stained by the double-staining technique described by Webb and Byrd.<sup>35</sup> All fetuses were subsequently examined for skeletal abnormalities.

### Data analysis

The litter was used as the experimental unit for statistical analysis. This study was performed in three replicates. The data from each study replicate were calculated independently, tested for homogeneity of variance by the Levene statistic using SPSS (SPSS, Inc., Chicago, IL), and then pooled and analyzed to give the results reported. All tabular data are presented as the mean ± standard error of the mean (SEM). Data were analyzed by one-way analysis of variance (ANOVA) followed by a least significant difference (LSD) post-hoc test to determine specific significant differences ( $P \leq 0.05$ ) or by a Pearson chi-square test ( $P \leq 0.05$ ).

## Results and discussion

In this study, mated female CD-1 mice were gavaged from GD 6–16 with one of four treatments: (1) vehicle control, (2) 113 mg kg<sup>-1</sup> d<sup>-1</sup> [C<sub>4</sub>mim]Cl, (3) 169 mg kg<sup>-1</sup> d<sup>-1</sup> [C<sub>4</sub>mim]Cl, or (4) 225 mg kg<sup>-1</sup> d<sup>-1</sup> [C<sub>4</sub>mim]Cl. Clinical signs were recorded daily, dams were euthanized on GD 17, and the fetuses were removed and examined for gross morphological and skeletal defects. Litter parameters (including the average number of implantations, average fetal weight, *etc.*) and maternal data are presented in Table 1 and discussed below. A number of unusual gross morphological defects were found in fetuses from [C<sub>4</sub>mim]Cl-treated dams, and these data are presented in Table 2.

### Maternal data

There was an apparent treatment effect on maternal weight gain in the highest [C<sub>4</sub>mim]Cl dosage group (225 mg kg<sup>-1</sup> d<sup>-1</sup>), although the difference from the control value was not statistically significant (Table 1). There was also evidence of dosage-dependent maternal morbidity/mortality (Fig. 2). The percentage of animals either dying or becoming moribund and necessitating euthanization prior to the completion of treatment was significantly greater in the 225 mg kg<sup>-1</sup> d<sup>-1</sup> treatment group as compared to controls or either of the other dosage groups. However, some dams were affected even at the lowest [C<sub>4</sub>mim]Cl dosage.

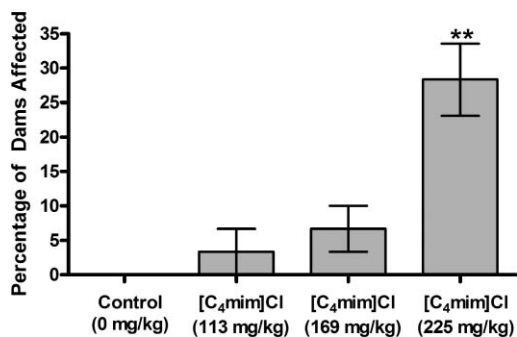
**Table 1** Maternal weight gain and litter parameters of CD-1 mice exposed to [C<sub>4</sub>mim]Cl *in utero*

	Treatment and dose/mg kg <sup>-1</sup> d <sup>-1</sup>			
	Vehicle Control	[C <sub>4</sub> mim]Cl (113)	[C <sub>4</sub> mim]Cl (169)	[C <sub>4</sub> mim]Cl (225)
Fetuses/litters examined	489/36	288/23	319/26	314/23
Maternal weight gain/g ± SEM	10.67 ± 0.39	10.29 ± 0.44	10.38 ± 0.42	9.28 ± 0.64
Implantations/mean ± SEM	13.97 ± 0.36	12.78 ± 0.55	13.40 ± 0.36	13.91 ± 0.44
Resorbed or dead fetuses (No. ± SEM)	2.77 ± 0.84	2.24 ± 0.88	6.20 ± 2.82	3.24 ± 0.98
Litters with resorbed or dead fetuses (No./%)	10/27.8	6/26.1	8/30.8	9/39.1
Fetal weight/g ± SEM	0.99 ± 0.02	1.00 ± 0.03	0.91 ± 0.03 <sup>a</sup>	0.84 ± 0.03 <sup>a</sup>
Malformed fetuses <sup>b,c</sup> (% ± SEM)	0.91 ± 0.44	1.09 ± 0.60	1.56 ± 0.76	2.47 ± 0.93
Malformed fetuses (% affected litters) <sup>b</sup>	11.1	13.0	15.4	26.1

<sup>a</sup> Significantly different from control and [C<sub>4</sub>mim]Cl 113 mg kg<sup>-1</sup> d<sup>-1</sup> values ( $P \leq 0.01$ ). <sup>b</sup> Fetuses displaying any gross malformation. <sup>c</sup> Grand mean of litter mean percentages.

**Table 2** Gross malformations in CD-1 mouse fetuses from dams orally dosed with [C<sub>4</sub>mim]Cl

Malformation	Treatment and dose/mg kg <sup>-1</sup> d <sup>-1</sup>			
	Vehicle Control	[C <sub>4</sub> mim]Cl (113)	[C <sub>4</sub> mim]Cl (169)	[C <sub>4</sub> mim]Cl (225)
Fetuses examined (No.)	489	288	319	314
Bent tail	2	3	4	3
Talipes	0	0	1	0
Hemimelia	0	0	0	2
Ablepharia	2	0	1	1
Exencephaly	0	0	1	1
Craniorachischisis	0	0	0	1
Cleft palate	0	0	2	0
Total	4	3	9	8



**Fig. 2** Effects of [C<sub>4</sub>mim]Cl on the incidence of morbidity/mortality prior to treatment completion. \*\*225 mg kg<sup>-1</sup> d<sup>-1</sup> results are significantly different from the control, 113 mg kg<sup>-1</sup> d<sup>-1</sup>, and 169 mg kg<sup>-1</sup> d<sup>-1</sup> values ( $P \leq 0.01$ ).

### Fetal data

The numbers of implantations and the percentages of resorbed or dead fetuses did not differ significantly among treatment groups, nor did the percentage of litters that had resorbed or dead fetuses (Table 1). However, fetal weight was significantly affected by treatment with [C<sub>4</sub>mim]Cl in a dosage-dependent manner (Table 1). Fetuses from both the 169 mg kg<sup>-1</sup> d<sup>-1</sup> and the 225 mg kg<sup>-1</sup> d<sup>-1</sup> treatment groups, weighed significantly less than fetuses from the control or 113 mg kg<sup>-1</sup> d<sup>-1</sup> treatment groups.

Several gross malformations were observed in the treated groups: ablepharia, bent tail, hemimelia, exencephaly, cleft

palate, craniorachischisis and talipes. The mean litter percentage of fetuses and the per litter incidence of any specific malformation was not significantly greater in the offspring of the treated dams. However, both the fetal and litter incidences of total malformations increased in an apparently dosage-dependent manner, and the percentage of grossly malformed fetuses in the highest treatment group was more than double that of the controls (Table 2).

Fetal skeletons were examined for malformations, and the incidence of supernumerary ribs did not differ significantly among treatment groups (Table 3). There was a significant reduction in the incidence of rudimentary ribs in the highest dosage group (225 mg kg<sup>-1</sup> d<sup>-1</sup>) compared to values from control fetuses or from fetuses of dams treated with 113 mg kg<sup>-1</sup> d<sup>-1</sup> [C<sub>4</sub>mim]Cl. There was a significant reduction in rudimentary ribs in fetuses from the 169 mg kg<sup>-1</sup> d<sup>-1</sup> group as well, but the reduction was only in comparison with the 113 mg kg<sup>-1</sup> d<sup>-1</sup> treatment group, and not in comparison to the controls (Table 3).

The present study did not find significant differences in implantations, number of viable fetuses, or resorbed/dead fetuses among treatment groups. It did, however, reveal an adverse effect on fetal weight and an apparent teratogenic effect, with only the offspring of treated mice exhibiting certain uncommon morphological defects, such as craniorachischisis and hemimelia.

Although the numbers of malformed fetuses observed in the treated groups were relatively modest, it must be kept in mind that the multiple dosing regimen employed is relatively inefficient at producing malformed offspring, even if the test compound is capable of doing so. It should also be noted that the positive fetal findings all occurred at maternal dosages associated with at least some maternal morbidity or mortality. In the range of dosages tested, the apparent NOAEL (no observed adverse effect level) for fetal effects was 113 mg kg<sup>-1</sup> d<sup>-1</sup>, while the LOAEL (lowest observed adverse effect level) was 169 mg kg<sup>-1</sup> d<sup>-1</sup>. However, these values may have been lower if visceral defects had been evaluated. Comparison of the toxicity of [C<sub>4</sub>mim]Cl relative to other common solvents is difficult, primarily because of the different routes of administration or different species used in previous studies. Generally, however, solvents such as benzene, toluene, acetonitrile, xylene, and commercial polychlorinated biphenyl mixtures tended to produce effects similar to those

**Table 3** Skeletal malformations of CD-1 mice exposed to [C<sub>4</sub>mim]Cl *in utero*

	Treatment and dose/mg kg <sup>-1</sup> d <sup>-1</sup>			
	Vehicle Control	[C <sub>4</sub> mim]Cl (113)	[C <sub>4</sub> mim]Cl (169)	[C <sub>4</sub> mim]Cl (225)
Fetuses/litters examined	489/36	288/23	319/26	314/23
Supernumerary ribs (% ± SEM)	24.53 ± 4.16	16.49 ± 4.42	16.97 ± 4.17	18.10 ± 5.28
Rudimentary ribs (% ± SEM)	18.85 ± 2.70	21.47 ± 4.50	12.72 ± 2.16 <sup>a</sup>	7.92 ± 2.35 <sup>b</sup>
Supernumerary ribs (% litters affected)	28	14	16	14
Rudimentary ribs (% litters affected)	28	18	19	12 <sup>c</sup>

<sup>a</sup> Significantly different from [C<sub>4</sub>mim]Cl 113 mg kg<sup>-1</sup> d<sup>-1</sup> value ( $P \leq 0.05$ ). <sup>b</sup> Significantly different from control and [C<sub>4</sub>mim]Cl 113 mg kg<sup>-1</sup> d<sup>-1</sup> values ( $P \leq 0.05$ ). <sup>c</sup> Significantly different from control value ( $P \leq 0.05$ ).

observed in this study, including reduced fetal weight and fetal anomalies, particularly at high maternal exposures.<sup>36–39</sup>

The mechanism for the developmental toxicity of [C<sub>4</sub>mim]Cl remains unknown, although it is known that imidazolium-based ILs can act as cationic surfactants, which have the potential to disrupt the lipid bilayer and increase membrane permeability. This might negatively affect embryonic development and viability. Enzyme inhibition is another possible means of toxicity, as several imidazolium- and pyridinium-based ILs, including [C<sub>4</sub>mim]Cl, have been shown to inhibit enzymes, such as acetylcholinesterase, *in vitro*. ILs have also been shown to inhibit the P450 enzyme CYP3A4 to a degree comparable to the effects of organic cosolvents such as acetonitrile.<sup>40</sup> Further investigation to elucidate the mechanisms of developmental toxicity of ILs is needed, as the current data are only observational.

## Conclusions

ILs may offer a viable (and in some cases preferential) alternative to traditional organic solvents, as a result of their unique property sets, unparalleled customizability, and potential to be used and recycled, while eliminating the emission of VOCs. However, while air exposure is not likely, the possibility of water or soil contamination *via* accidental spills or effluent release exists. Furthermore, there have been suggestions that ILs could be used as tissue preservatives in place of formaldehyde<sup>41</sup> or as pharmaceuticals and disinfectants,<sup>42</sup> thus considerably increasing the likelihood of human exposure. The present study indicates that even simple representatives, such as [C<sub>4</sub>mim]Cl, commonly used as a 'standard' IL solvent or precursor, may possibly have adverse effects on development, at least at high maternal exposures. It is incumbent on all users or potential users of *any* IL at industrial scale to thoroughly understand the toxicity, fate, and transport of these chemicals, despite the continued overuse of the term 'green solvents'.

## Acknowledgements

This work was supported in part by a Howard Hughes Medical Institute Undergraduate Biological Sciences Program grant to The University of Alabama and by the Alabama Institute for Manufacturing Excellence. We would also like to thank Whitney Swatloski for contributing to the creative aspect of this work.

## References

- 1 P. Walden, *Bull. Acad. Sci. St. Petersburg*, 1914, 405.
- 2 H. Olivier-Bourbigou and L. Magna, *J. Mol. Catal. A: Chem.*, 2002, **182–183**, 419.
- 3 T. Welton, *Chem. Rev.*, 1999, **99**, 2071.
- 4 R. D. Rogers and K. Seddon, *Science*, 2003, **302**, 792.
- 5 A. Latala, P. Stepnowski, M. Nedzi and W. Mroziak, *Aquat. Toxicol.*, 2005, **73**, 91.
- 6 K. Seddon, in *The International George Patheodorou Symposium: Proceedings*, ed. S. Boghosian, 1999, pp. 131–135.
- 7 N. V. Plechkova and K. R. Seddon, *Chem. Soc. Rev.*, 2008, **37**, 123.
- 8 H. G. Joglekar, I. Rahman and B. D. Kulkarni, *Chem. Eng. Technol.*, 2007, **30**, 819.
- 9 J. Pernak, K. Sobaszekiewicz and J. Foksowicz-Flaczyk, *Chem.–Eur. J.*, 2004, **10**, 3479.
- 10 T. Landry, K. Brooks, D. Poche and M. Woolhiser, *Bull. Environ. Contam. Toxicol.*, 2005, **74**, 559.
- 11 A. Bosmann, L. Datsevich, A. Jess, A. Lauter, C. Schmitz and P. Wasserscheid, *Chem. Commun.*, 2001, **23**, 2794.
- 12 D. Couling, R. Bernot, K. Docherty, J. Dixon and E. Maginn, *Green Chem.*, 2006, **8**, 82.
- 13 D. Gorman-Lewis and J. Fein, *Environ. Sci. Technol.*, 2004, **38**, 2491.
- 14 D. Zhao, Y. Liao and Z. Zhang, *Clean*, 2007, **35**, 42.
- 15 S. Stolte, M. Matzke, J. Arning, A. Boeschen, W-R. Pitner, U. Welz-Biernann, B. Jastorff and J. Ranke, *Green Chem.*, 2007, **9**, 1170.
- 16 M. Matzke, S. Stolte, K. Thiele, T. Juffernholz, J. Arning, J. Ranke, U. Welz-Biermann and B. Jastorff, *Green Chem.*, 2007, **9**, 1198.
- 17 C.-W. Cho, T. Pham, Y.-C. Jeon, K. Vijayaraghavan, W.-S. Choe and Y.-S. Yun, *Chemosphere*, 2007, **69**, 1003.
- 18 D. Couling, R. Bernot, K. Docherty, J. Dixon and E. Maginn, *Green Chem.*, 2006, **8**, 82.
- 19 P. Luis, I. Ortiz, R. Aldaco and A. Irabien, *Ecotoxicol. Environ. Saf.*, 2007, **67**, 423.
- 20 C. Samori, A. Pasteris, P. Galletti, E. Tagliavini and Environ, *Toxicol. Chem.*, 2007, **26**, 2379.
- 21 K. Docherty and C. Kulpa Jr., *Green Chem.*, 2005, **7**, 185.
- 22 C. Pretti, C. Chiappe, D. Pieraccini, M. Gregori, F. Abramo, G. Monni and L. Intorre, *Green Chem.*, 2006, **8**, 238.
- 23 R. Bernot, M. Brueske, M. Evans-White and G. Lamberth, *Environ. Toxicol. Chem.*, 2005, **24**, 87.
- 24 R. Bernot, E. Kennedy and G. Lamberti, *Environ. Toxicol. Chem.*, 2005, **24**, 1759.
- 25 X. Wang, C. A. Ohlin, Q. Lu, Z. Fei, J. Hu and P. J. Dyson, *Green Chem.*, 2007, **9**, 1191.
- 26 P. Stepnowski, A. Skladanowski, A. Ludwiczak and E. Laczynska, *Hum. Exp. Toxicol.*, 2004, **23**, 513.
- 27 R. Frade, A. Matias, L. Branco, C. Afonso and C. Duarte, *Green Chem.*, 2007, **9**, 873.
- 28 J. Salminen, N. Papaiconomou, R. A. Kumar, J.-M. Lee, J. Kerr, J. Newman and J. M. Prausnitz, *Fluid Phase Equil.*, 2007, **261**, 421.
- 29 A. Chefson and K. Auclair, *ChemBioChem*, 2007, **8**, 1189.
- 30 F. Ganske and U. Bornscheuer, *Biotechnol. Lett.*, 2006, **28**, 465.

- 31 S.-M. Lee, W.-J. Chang, A.-R. Choi and Y.-M. Koo, *Kor. J. Chem. Eng.*, 2005, **22**, 687.
- 32 M. Matsumoto, K. Mochiduki and K. Kondo, *J. Biosci. Bioeng.*, 2004, **98**, 334.
- 33 J. Ranke, K. Molter, F. Stock, U. Bottin-Weber, J. Poczobutt, J. Hoffmann, B. Ondruschka, J. Filser and B. Jastorff, *Ecotoxicol. Environ. Safe.*, 2004, **58**, 396.
- 34 J. G. Huddleston, H. W. Willauer, R. P. Swatloski, A. E. Visser and R. D. Rogers, *Chem. Commun.*, 1998, **16**, 1765.
- 35 G. Webb and R. Byrd, *Biotechnol. Histochem.*, 1994, **69**, 181.
- 36 A. Hudak and G. Ungvary, *Toxicology*, 1978, **11**, 55.
- 37 International Research and Development Corporation, unpublished study sponsored by Monsanto Company, 1981, Acetonitrile IR-79-162.
- 38 P. E. Berteau, G. J. Levinskas and D. E. Rodwell, *Toxicol. Sci.*, 1982, **2**, 118.
- 39 M. S. Golub, J. M. Donald and J. A. Reyes, *Environ. Health Perspect.*, 1991, **94**, 245.
- 40 A. Chefson and K. Auclair, *ChemBioChem*, 2007, **8**, 1189.
- 41 P. Majewski, A. Pernak, M. Grzymislawski, K. Iwanik and J. Pernak, *Acta Histochem.*, 2003, **105**, 135.
- 42 W. L. Hough, *et al.*, *New J. Chem.*, 2007, **31**, 1429.



# A CO<sub>2</sub>/H<sub>2</sub>O<sub>2</sub>-tunable reaction: direct conversion of styrene into styrene carbonate catalyzed by sodium phosphotungstate/*n*-Bu<sub>4</sub>NBr†

Jing-Lun Wang, Jin-Quan Wang, Liang-Nian He,\* Xiao-Yong Dou and Fang Wu

Received 28th April 2008, Accepted 28th July 2008

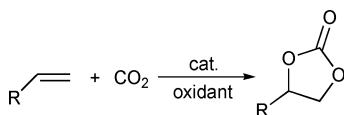
First published as an Advance Article on the web 26th September 2008

DOI: 10.1039/b807108j

Inspired by biomimetic oxybromination, a binary catalyst system composed of sodium phosphotungstate and *n*-Bu<sub>4</sub>NBr (TBAB) was developed for facile synthesis of styrene carbonate in a single operation from styrene and CO<sub>2</sub> using 30% H<sub>2</sub>O<sub>2</sub> as an oxidant. Notably, the presence of a base like NaHCO<sub>3</sub> markedly improved the formation of styrene carbonate. Interestingly, an oxidized product, *i.e.* phenacyl benzoate, could be obtained exclusively in good yield directly from styrene in the absence of CO<sub>2</sub> under the appropriate reaction conditions.

## Introduction

Nowadays, chemical transformation of CO<sub>2</sub> into useful organic chemicals has attracted ever-increasing attention from the point of view of environment protection and resource utilization.<sup>1</sup> One of the most promising methodologies of CO<sub>2</sub> chemical fixation is the synthesis of five-membered cyclic carbonates *via* the cycloaddition of epoxide to CO<sub>2</sub>. The cyclic carbonates have been widely used for various purposes, such as polar aprotic solvents, intermediates for organic and polymeric synthesis, chemical intermediates for pharmaceutical/fine chemicals in biomedical applications, and ingredients for electrolytic elements of lithium secondary batteries.<sup>2</sup> Therefore, numerous catalysts have been devised to synthesize cyclic carbonates utilizing CO<sub>2</sub> as a building block.<sup>3–10</sup> However, such a cycloaddition generally requires the initial synthesis of an epoxide, which involves toxic or costly reagents and requires a tedious workup for separation. Therefore, a promising approach would be the direct synthesis of cyclic carbonates from olefins instead of epoxides, a so-called one-pot “oxidative carboxylation” of olefin utilizing CO<sub>2</sub> as a building block (Scheme 1). It has been known for over four decades,<sup>10</sup> but only a few efficient methods have been exploited up to now. There are three typical methodologies to produce cyclic carbonates directly from olefins and CO<sub>2</sub>.



**Scheme 1** Direct synthesis of cyclic carbonate (**1a**) from alkenes and CO<sub>2</sub>.

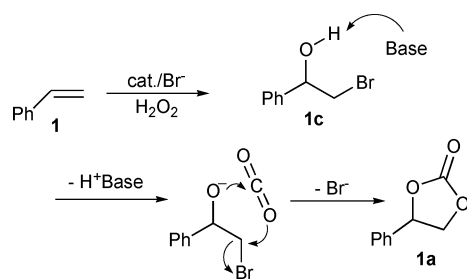
Aresta *et al.* reported an approach involving CO<sub>2</sub> insertion into the metal–oxygen bond in the presence of a noble metal

oxide using dioxygen as the oxidant;<sup>7</sup> the method of Arai and co-workers combined two sequential reactions, epoxidation of olefins and cycloaddition of CO<sub>2</sub> to epoxides, into a one-pot process without the need for separation of the epoxides;<sup>8b–c</sup> and it is the more effective one to date developed by Eghbali and Li,<sup>9a</sup> that olefins can be directly converted into cyclic carbonates through a “bromohydrin” species formed *in-situ* using *N*-bromosuccinimide (NBS) or Br<sup>−</sup>/H<sub>2</sub>O<sub>2</sub> as the bromination reagent in the presence of 1,8-diazabicyclo[5.4.0]undec-7-ene (DBU). Although quite good progress has been made in this respect, ongoing issues such as low yield and selectivity toward the desired products, long reaction time, complicated separation processes, and the requirement of a hazardous or expensive “halohydrination reagent”, or an organic base, need to be addressed.

Based on mechanistic considerations,<sup>9a</sup> bromohydrin would be assumed to be a crucial intermediate from an olefin, thereby leading to the formation of styrene carbonate. The biohalogenation performed by haloperoxidase enzyme draws our attention.<sup>11</sup> Those biomimetic catalyst systems have been used in the oxybromination of alkenes or aromatics, bromide-assisted epoxidation of alkenes and the oxidation of alcohol.<sup>12</sup> Inspired by the biomimetic process, we reasoned that traditional oxybromination methods using molecular bromine or other expensive organic oxybromination reagents could be replaced by a more cost-effective and environmentally benign one comprising a bromide salt and aqueous H<sub>2</sub>O<sub>2</sub>,<sup>13,14</sup> which would likely work in a mode similar to the bio-process. In this work, the direct synthesis of cyclic carbonate would be operated from styrene through the “bromohydrin” intermediate generated *in-situ* in the presence of TBAB and H<sub>2</sub>O<sub>2</sub> catalyzed by phosphotungstate, followed by its subsequent reaction with CO<sub>2</sub> in the presence of a “deprotonation reagent” as outlined in Scheme 2. We would like to demonstrate herein a facile synthesis of styrene carbonate in a single operation directly from styrene and CO<sub>2</sub> in an environmentally benign manner with an inorganic base as the “deprotonation reagent”, and a recyclable catalyst system comprising sodium phosphotungstate and TBAB, and mild reaction conditions (at 50 °C, 350 psig and in aqueous medium). Interestingly, a useful compound, phenacyl benzoate, could also

State Key Laboratory and Institute of Elemento-Organic Chemistry, Nankai University, Tianjin, 300071, P. R. China. E-mail: hehn@nankai.edu.cn; Fax: +86 22 2350 4216; Tel: +86 22-2350 4216

† Electronic supplementary information (ESI) available: Copies of the NMR spectra for products and the typical GC–MS chart for the reaction mixture. See DOI: 10.1039/b807108j



**Scheme 2** Direct synthesis of styrene carbonate (**1a**) from styrene (**1**) and CO<sub>2</sub> through “oxybromination” *in-situ* generated.

be preferentially obtained directly from styrene by subtly varying the quantities of CO<sub>2</sub> and H<sub>2</sub>O<sub>2</sub>.

## Results and discussion

### Direct formation of styrene carbonate

As envisioned, a binary catalyst comprising Na<sub>2</sub>H<sub>5</sub>P(W<sub>2</sub>O<sub>7</sub>)<sub>6</sub>/TBAB was initially tested for the direct synthesis of styrene carbonate (**1a**) from styrene and CO<sub>2</sub> using 30% H<sub>2</sub>O<sub>2</sub> as an oxidant. The results are summarized in Table 1. The reaction proceeded smoothly under the reaction conditions and afforded **1a** and phenacyl benzoate (**1b**) (entry 1, Table 1), concomitantly in 5% of benzaldehyde and (1,2-dibromoethyl)benzene, being detected by GC–MS.<sup>15</sup> No styrene carbonate was detected without TBAB (entry 2). Moreover, sodium bromide was not a good bromide source for the formation of either product **1a** or **1b** (entry 3). Accordingly, TBAB able to provide bromide species would be indispensable for such a biphasic reaction, where TBAB could serve as a phase transferable

**Table 1** Direct conversion of styrene into styrene carbonate (**1a**) catalyzed by Na<sub>2</sub>H<sub>5</sub>P(W<sub>2</sub>O<sub>7</sub>)<sub>6</sub><sup>a</sup>

Entry	Cat. <sup>b</sup> (mol%)	Conv. (%)	Yield <sup>c</sup> (%)	
			<b>1a</b>	<b>1b</b>
1	2	98	65	28
2 <sup>d</sup>	2	0	0	0
3 <sup>e</sup>	2	6	5	0
4 <sup>f</sup>	0	0	0	0
5	0	40	16	13
6	1	94	66	18
7 <sup>g</sup>	1	80	56	10
8 <sup>h</sup>	2	72	50	14
9 <sup>i</sup>	2	70	48	16
10 <sup>j</sup>	9	81	56	13

<sup>a</sup> Unless stated otherwise, all reactions were performed using styrene (0.25 mL, 2.2 mmol), TBAB (0.25 g, 0.78 mmol), Na<sub>2</sub>H<sub>5</sub>P(W<sub>2</sub>O<sub>7</sub>)<sub>6</sub> (0.125 g, 0.0425 mmol), H<sub>2</sub>O<sub>2</sub> (1.5 mL, 6 equiv.), H<sub>2</sub>O (0.5 mL) and NaHCO<sub>3</sub> (0.025 g, 0.3 mmol), at 50 °C and 350 psig, for 12 h. <sup>b</sup> Based on styrene. <sup>c</sup> Determined by GC using biphenyl as an internal standard. <sup>d</sup> Without TBAB. <sup>e</sup> NaBr (0.78 mmol) was used as a bromide agent. <sup>f</sup> Without H<sub>2</sub>O<sub>2</sub>. <sup>g</sup> 1,5-Diazabicyclo[4.3.0]non-5-ene (DBN) was used in place of NaHCO<sub>3</sub>, 6 h, H<sub>2</sub>O<sub>2</sub> (4 equiv., 1.0 mL). <sup>h</sup> Cat. (NH<sub>4</sub>)<sub>3</sub>PW<sub>12</sub>O<sub>40</sub> (0.0425 mmol). <sup>i</sup> Cat. Cs<sub>2.5</sub>H<sub>0.5</sub>PW<sub>12</sub>O<sub>40</sub> (0.0425 mmol). <sup>j</sup> Cat. Na<sub>2</sub>WO<sub>4</sub> (0.2 mmol).

bromide-reagent. Without a catalyst and oxidant, the reaction did not occur at all (entry 4). It is worthwhile noticing that the presence of 1 mol% Na<sub>2</sub>H<sub>5</sub>P(W<sub>2</sub>O<sub>7</sub>)<sub>6</sub> significantly boosted the reaction (entries 5 vs. 6, 7). In this regard, ammonium and cesium salts of phosphotungstate and sodium tungstate were also shown to be active for this process (entries 8, 9, 10). Note that their somewhat low performance could be presumably owing to sparse transferability between the organic and aqueous phases in this biphasic system.<sup>16</sup>

### Dependence of the added base on the reaction

The key intermediate *i.e.* 2-bromo-1-phenylethanol (**1c**) would be generated in this protocol for the direct synthesis of cyclic carbonate as elaborated in Scheme 2. Indeed, **1c** was isolated in 16% yield in the absence of any base under the identical conditions (entry 1, Table 2). In this context, a hydroxyl anion as a deprotonating reagent could be assumed to be produced during the bromohydroxylation step of styrene under the given reaction conditions.<sup>12,14</sup> Whereas, the presence of a base able to render the 2-bromo-1-phenylethanol (**1c**) to be deprotonated, resulted in a considerable increase in **1a** yield (entry 1 vs. 2, Table 2). Accordingly, we reasoned that a base could have a remarkable effect on cyclic carbonate (**1a**) formation. As listed in Table 2, either organic or inorganic bases gave rise to a positive effect on the reaction (entries 2–9). Given the goal of the present work, we chose NaHCO<sub>3</sub> as a model base for further investigating the selective formation of **1a** and **1b** *via* the CO<sub>2</sub>/H<sub>2</sub>O<sub>2</sub>-tunable reaction in terms of availability, environmentally friendly and simple workup, as well as economical consideration.

### CO<sub>2</sub>/H<sub>2</sub>O<sub>2</sub>-tunable selective formation of **1b** and **1a**

Given the CO<sub>2</sub> pressure dependency of pH in the H<sub>2</sub>O/CO<sub>2</sub> biphasic system<sup>17</sup> and our hypothesis as shown in Scheme 2, we next investigated the effects of CO<sub>2</sub> pressure and H<sub>2</sub>O<sub>2</sub> amount on the reaction. As depicted in Table 3, it turned out to be that a lower CO<sub>2</sub> pressure within a range of 350–2000 psig would benefit the reaction, resulting in enhanced reactivity and improved selectivity towards cyclic carbonate **1a**. In other words, a low pressure is also sufficient to conduct the reaction, thereby

**Table 2** Effect of the added base<sup>a</sup>

Entry	Base	Conv. (%)	Yield (%) <sup>b</sup>	
			<b>1a</b>	<b>1b</b>
1 <sup>c</sup>	None	35	10	4
2	NaHCO <sub>3</sub>	66	43	7
3	Na <sub>2</sub> CO <sub>3</sub>	74	56	9
4	Cs <sub>2</sub> CO <sub>3</sub>	80	65	9
5	NaOH	76	52	10
6	Et <sub>3</sub> N	75	47	11
7	DBU	88	59	9
8	DBN	80	56	10
9	DMAP <sup>d</sup>	81	57	12

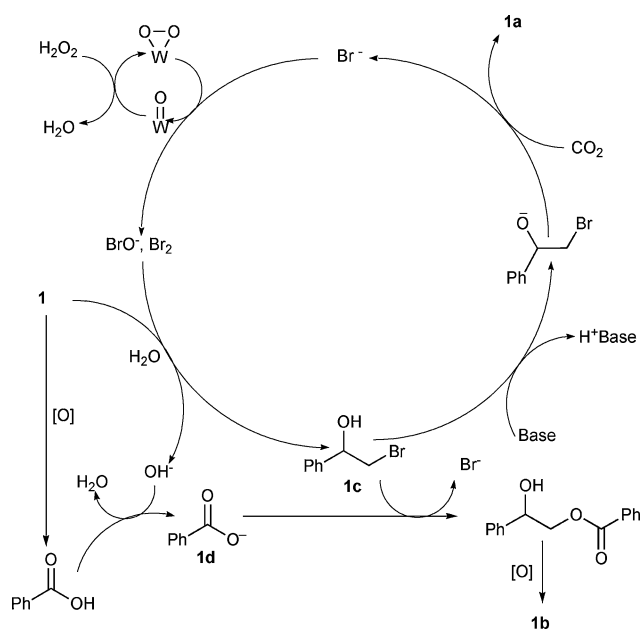
<sup>a</sup> Reaction conditions: styrene (0.25 mL, 2.2 mmol), TBAB (0.25 g, 0.78 mmol), Na<sub>2</sub>H<sub>5</sub>P(W<sub>2</sub>O<sub>7</sub>)<sub>6</sub> (0.0625 g, 0.0213 mmol), base (0.3 mmol), H<sub>2</sub>O<sub>2</sub> (1.0 mL, 4 equiv.), H<sub>2</sub>O (0.5 mL), at 50 °C, 6 h, 350 psig. <sup>b</sup> Determined by GC using biphenyl as an internal standard. <sup>c</sup> 2-Bromo-1-phenylethanol (**1c**) was also isolated in 16% yield. <sup>d</sup> DMAP: 4-(dimethylamino)pyridine.

**Table 3** CO<sub>2</sub>/H<sub>2</sub>O<sub>2</sub>-tunable selective formation of **1b** and **1a**<sup>a</sup>

Entry	P <sub>CO<sub>2</sub></sub> (psig)	H <sub>2</sub> O <sub>2</sub> (equiv.)	Conv. (%) <sup>b</sup>	Yield (%) <sup>b</sup>	
				<b>1a</b>	<b>1b</b>
1	2000	6	43	22	10
2	1500	6	59	40	13
3	1000	6	90	61	22
4	500	6	92	63	23
5	350	6	98	65	27
6	350	2	83	62	10
7	350	3	88	67	13
8	350	4	99	68	21
9 <sup>c</sup>	0	6	78	0	35
10 <sup>d</sup>	0	12	99	0	65

<sup>a</sup> Unless noted otherwise, all reactions were performed using styrene (0.25 mL, 2.2 mmol), TBAB (0.25 g, 0.78 mmol), Na<sub>2</sub>H<sub>5</sub>P(W<sub>2</sub>O<sub>7</sub>)<sub>6</sub> (0.125 g, 0.0425 mmol), NaHCO<sub>3</sub> (0.025 g, 0.3 mmol) and H<sub>2</sub>O (0.5 mL), at 50 °C for 12 h. <sup>b</sup> Determined by GC using biphenyl as an internal standard. <sup>c</sup> Without NaHCO<sub>3</sub>. **1c** was also isolated in a yield of 17%. <sup>d</sup> Without NaHCO<sub>3</sub>, isolated yield.

furnishing a predominant formation of cyclic carbonate **1a**, along with minor quantities of **1b** (entries 1–5). On the other hand, the excess of H<sub>2</sub>O<sub>2</sub> is likely to have an adverse effect on the production of **1a**, but is presumably to be favorable for the formation of **1b** (entries 5–8), being probably ascribed to the facile oxidation of styrene into benzoic acid<sup>18</sup> leading to generation of **1b** as elaborated in Scheme 3. Gratifyingly, **1b** as an exclusive product was isolated in 65% yield without the formation of **1a** after a rough optimization of the reaction conditions such as with 12 equiv. H<sub>2</sub>O<sub>2</sub> in the absence of CO<sub>2</sub> and NaHCO<sub>3</sub> (entry 9, 10). It is evident that the selective formation of **1b** and preferential production of **1a** could be achieved by subtly varying the quantities of CO<sub>2</sub> and H<sub>2</sub>O<sub>2</sub>.



**Scheme 3** Possible pathways to styrene carbonate (**1a**) and phenacyl benzoate (**1b**) directly from styrene (**1**).

The phenacyl benzoate is an important intermediate and reagent<sup>19a-d</sup> in organic synthesis. Current methods<sup>19d-g</sup> are

generally based on  $\alpha$ -bromoacetophenone as a starting material. To the best of our knowledge, the work presented herein is the first example of the synthesis of phenacyl benzoate from styrene in a single operation, and offers a practical and environmentally benign approach to the synthesis of benzoate derivatives in terms of simple workup, low toxic reagent used, and readily available materials as well as good yield of the desired product.

#### Formation of various cyclic carbonates from alkenes and CO<sub>2</sub>

To test the utility of this protocol, various *para*-substituted styrene derivatives were explored for the synthesis of cyclic carbonates as summarized in Table 4. This methodology is easily found to be applicable to several styrene derivatives, producing the corresponding cyclic carbonates. Note that the substrates with an electron-donating substituent at a *para* position gave higher reactivity and selectivity towards formation of product **a** than that bearing an electron-withdrawing counterpart (entries 2, 3 vs. 4). It is worth mentioning that 1*H*-indene (**5**) was also effective for uniquely producing **5a**; whereas, cyclohexene (**6**) gave 2-bromocyclohexanol<sup>20</sup> as a main product in 48% yield, but the desired product **6a** was isolated in just 7% yield (entries 5, 6).

A series of catalytic recycles<sup>21</sup> using 4-methoxystyrene (**3**) as a model substrate were also tested under the identical reaction conditions as indicated in Table 4. In each cycle, the products could be easily isolated *via* extraction with diethyl ether, and the aqueous phase containing the catalyst was reused for subsequent reaction. As a result, the catalyst could be reused for at least three times with retention of catalytic activity. Consequently, the efficacious reusability of the catalyst makes the process more economically and potentially viable for commercial application.

**Table 4** Formation of various cyclic carbonates from alkenes and CO<sub>2</sub> catalyzed by Na<sub>2</sub>H<sub>5</sub>P(W<sub>2</sub>O<sub>7</sub>)<sub>6</sub><sup>a</sup>

Entry	Substrate	Conv. (%) <sup>b</sup>	Yield (%) <sup>c</sup>	
			<b>a</b>	<b>b</b>
1	Styrene ( <b>1</b> )	79	57	14
2	4-Methylstyrene ( <b>2</b> )	97	81	11
3	4-Methoxystyrene ( <b>3</b> )	100	83	0
4	4-Chlorostyrene ( <b>4</b> )	46	34	5
5	1 <i>H</i> -Indene ( <b>5</b> )	98	82	0
6 <sup>d</sup>	Cyclohexene ( <b>6</b> )	89	7	0

<sup>a</sup> Reaction conditions: substrate (2.2 mmol), TBAB (0.25 g, 0.78 mmol), Na<sub>2</sub>H<sub>5</sub>P(W<sub>2</sub>O<sub>7</sub>)<sub>6</sub> (0.0625 g, 0.022 mmol), H<sub>2</sub>O<sub>2</sub> (1.0 mL, 4 equiv.), H<sub>2</sub>O (0.5 mL), at 50 °C, 12 h, 350 psig. <sup>b</sup> Determined by GC using biphenyl as an internal standard. <sup>c</sup> Isolated yield. <sup>d</sup> Reaction time: 24 h, 2-bromocyclohexanol was formed in 48% yield.

## Possible reaction mechanism

A plausible catalytic cycle for the present CO<sub>2</sub>/H<sub>2</sub>O<sub>2</sub>-tunable reaction is depicted in Scheme 3. The initial bromohydroxylation of styrene leading to **1c** is accomplished in the presence of TBAB and H<sub>2</sub>O<sub>2</sub> catalyzed by polyoxometalate. Subsequent deprotonation of **1c** promoted by a base, followed by a cycloaddition reaction with CO<sub>2</sub> leads to formation of the product **1a**. On the other hand, benzoic acid<sup>18</sup> is assumed to be formed *in-situ* under the reaction conditions, and further converts to the species like carboxylate anion **1d** prompted by either a base or hydroxyl anion generated *in-situ*. As envisioned, **1d** would likely react with **1c** in the absence of CO<sub>2</sub> to afford another product, *i.e.* phenacyl benzoate (**1b**). In particular, this tentative mechanism could account for the finding of this work that the selective formation of **1b** and **1a** could be realized by tuning the amounts of CO<sub>2</sub> and H<sub>2</sub>O<sub>2</sub>, as aforementioned and listed in Table 1–3. The in-depth mechanistic insight on this process is in progress.

## Conclusion

In summary, we developed a facile synthesis of styrene carbonate (**1a**) in a single operation from styrene and CO<sub>2</sub> catalyzed by sodium phosphotungstate/TBAB with the aid of an inorganic base as a “CO<sub>2</sub>-activator” or “deprotonation reagent”. Interestingly, the selective formation of **1b** and preferential production of **1a** could be controlled by subtly tuning the quantities of CO<sub>2</sub> and H<sub>2</sub>O<sub>2</sub>. This methodology is easily found to be applicable to several styrene derivatives, producing the corresponding cyclic carbonates. It is worth mentioning that the catalyst system can be recovered and reused with excellent activity. On the other hand, this finding represents a simpler and more cost-effective pathway for the environmentally benign chemical fixation of CO<sub>2</sub> to produce cyclic carbonates and also offers a practical methodology for the synthesis of benzoate derivatives. The scope and application of this method are under investigation in our laboratory.

## Experimental

### Caution

Experiments using the compressed gas CO<sub>2</sub> are potentially hazardous and must only be carried out by using the appropriate equipment and under rigorous safety precautions.

### General

Styrene was obtained from Tianjin Guangfu Chemical Company and distilled prior to use. Carbon dioxide with a purity of 99.99% was commercially available. All of the other reagents and catalysts used in this work were of analytical grade and were used as received without further purification. <sup>1</sup>H NMR and <sup>13</sup>C NMR spectra were recorded on a Varian Mercury Plus 400 MHz or Bruker 300 MHz, and at 100.4 or 75 MHz respectively in CDCl<sub>3</sub>. Chemical shifts (δ) are given in ppm relative to TMS. The solvent signals were used as references and the chemical shifts converted to the TMS scale (CDCl<sub>3</sub>: δ<sub>C</sub> 77.0 ppm; residual CHCl<sub>3</sub> in CDCl<sub>3</sub>: δ<sub>H</sub> 7.26 ppm). Column chromatography was performed by using silica gel 200–300 mesh and eluting as reported in

the following description. GC–MS analyses were carried out on a Finnigan HP G1800A. GC analyses were performed on a Shimadzu GC-2014, equipped with a capillary column (RTX-5, 30 m × 0.25 μm) using a flame ionization detector. Melting points were measured on an X4 apparatus and were uncorrected.

### General procedure for the synthesis of carbonates **a**

The reaction was carried out in a 50 mL stainless-steel autoclave reactor with an inner glass and a magnetic stirrer. A mixture of Na<sub>2</sub>H<sub>3</sub>P(W<sub>2</sub>O<sub>7</sub>)<sub>6</sub> (0.125 g, 0.0425 mmol), *n*-Bu<sub>4</sub>NBr (0.25 g, 0.78 mmol), and NaHCO<sub>3</sub> (0.025 g, 0.3 mmol) dissolved in 0.5 mL H<sub>2</sub>O was placed in the reactor. H<sub>2</sub>O<sub>2</sub> (1.0 mL, 4 equiv.) and substrate (2.2 mmol) were then added. The CO<sub>2</sub> was introduced into the autoclave with an initial pressure of *ca.* 300 psig at room temperature. The pressure was adjusted to 350 psig at 50 °C. The mixture was stirred for 12 h. After the reaction was completed, the reactor was quickly cooled to 0 °C in ice water. The excess of CO<sub>2</sub> was depressurized slowly. The resultant mixture was then extracted by diethyl ether (5 mL × 3), and dried over MgSO<sub>4</sub>. The solvent was removed, and the residue was subjected to column chromatography with ethyl acetate–petroleum (1 : 20) as the eluent to obtain the desired product **a**.

**Styrene carbonate (1a).** White solid; mp 53–54 °C (lit.<sup>22</sup> 56 °C); <sup>1</sup>H NMR (400 MHz, CDCl<sub>3</sub>): δ 4.33 (t, 1H, *J* = 8.0 Hz), 4.79 (t, 1H, *J* = 8.4 Hz), 5.67 (t, 1H, *J* = 8.0 Hz), 7.34–7.43 (m, 5H); <sup>13</sup>C{<sup>1</sup>H} NMR (75 MHz, CDCl<sub>3</sub>): δ 71.2, 78.0, 125.9, 129.2, 129.7, 135.9, 154.9; IR (KBr): 1779, 1162, 1046, 756, 688 cm<sup>-1</sup>; GC–MS (EI, 70 eV): *m/z* 164 (M<sup>+</sup>), 119, 105, 90, 78, 65, 51, 39, 29.

**4-Methylstyrene carbonate (2a).** White solid; mp 40–41 °C (lit.<sup>22</sup> 43–44 °C); <sup>1</sup>H NMR (300 MHz, CDCl<sub>3</sub>): δ 2.35 (s, 3H), 4.26–4.32 (m, 1H), 4.74 (t, 1H, *J* = 7.8 Hz), 5.61 (t, 1H, *J* = 7.8 Hz), 7.19–7.25 (m, 4H); <sup>13</sup>C{<sup>1</sup>H} NMR (75 MHz, CDCl<sub>3</sub>): δ 21.2, 71.2, 78.1, 126.1, 129.8, 132.9, 139.8, 155.0; IR (KBr): 1785, 1172, 1049, 896, 808 cm<sup>-1</sup>; GC–MS (EI, 70 eV): *m/z* 178 (M<sup>+</sup>), 163, 134, 119, 104, 91, 78, 65, 51, 39.

**4-Methoxystyrene carbonate (3a).** White solid; mp 43–44 °C (lit.<sup>23</sup> 71–72 °C); <sup>1</sup>H NMR (400 MHz, CDCl<sub>3</sub>): δ 3.83 (s, 3H), 4.35 (t, 1H, *J* = 8.0 Hz), 4.76 (t, 1H, *J* = 8.0 Hz), 5.63 (t, 1H, *J* = 8.0 Hz), 6.95 (d, 2H, *J* = 8.4 Hz), 7.31 (d, 2H, *J* = 8.4 Hz); <sup>13</sup>C{<sup>1</sup>H} NMR (75 MHz, CDCl<sub>3</sub>): δ 55.4, 71.1, 78.1, 114.6, 127.5, 127.8, 154.8, 160.8; IR (KBr): 1777, 1617, 1245, 1180, 1034, 823, 722 cm<sup>-1</sup>; GC–MS (EI, 70 eV): *m/z* 194 (M<sup>+</sup>), 163, 149, 135, 121, 108, 91, 77, 65, 51.

**4-Chlorostyrene carbonate (4a).** White solid; mp 69–70 °C (lit.<sup>22</sup> 68–69 °C); <sup>1</sup>H NMR (400 MHz, CDCl<sub>3</sub>): δ 4.31 (t, 1H, *J* = 8.0 Hz), 4.81 (t, 1H, *J* = 8.0 Hz), 5.66 (t, 1H), 7.28 (d, 2H, *J* = 8.4 Hz), 7.43 (d, 2H, *J* = 8.4 Hz); <sup>13</sup>C{<sup>1</sup>H} NMR (75 MHz, CDCl<sub>3</sub>): δ 70.9, 76.6, 127.2, 129.5, 134.4, 135.8, 154.5; IR (KBr): 1792, 1158, 1049, 823, 772 cm<sup>-1</sup>; GC–MS (EI, 70 eV): *m/z* 198 (M<sup>+</sup>), 163, 139, 124, 112, 112, 89, 75, 63, 51.

**1H-Indene carbonate (5a).** White solid; mp 78–79 °C (lit.<sup>24</sup> 73–74 °C); <sup>1</sup>H NMR (400 MHz, CDCl<sub>3</sub>): δ 3.40 (m, 2H), 5.44–5.47 (m, 1H), 6.01 (d, 1H, *J* = 6.8 Hz), 7.32–7.53 (m, 4H); <sup>13</sup>C{<sup>1</sup>H} NMR (75 MHz, CDCl<sub>3</sub>): δ 38.1, 79.7, 83.6, 125.6,



126.5, 128.3, 131.1, 136.5, 140.1, 154.7; IR (KBr): 1770, 1165, 1049, 1012, 764, 691  $\text{cm}^{-1}$ ; GC-MS (EI, 70 eV):  $m/z$  176 ( $\text{M}^+$ ), 132, 115, 104, 89, 78, 63, 51, 39.

**Cyclohexene carbonate (6a).** White solid; mp 31–35 °C (lit.<sup>25</sup> 40–41 °C);  $^1\text{H}$  NMR (300 MHz,  $\text{CDCl}_3$ ):  $\delta$  1.40–1.46 (m, 2H), 1.55–1.62 (m, 2H), 1.86–1.89 (m, 4H), 4.64–4.7 (m, 2H);  $^{13}\text{C}\{^1\text{H}\}$  NMR (75 MHz,  $\text{CDCl}_3$ ):  $\delta$  19.1, 26.8, 75.7, 155.3; IR (KBr): 1788, 1210, 1014  $\text{cm}^{-1}$ ; GC-MS (EI, 70 eV):  $m/z$  143 ( $\text{M}^+$ ), 97, 83, 79, 69, 55, 39.

### General procedure for the synthesis of phenacyl benzoate derivatives b

The reaction was carried out in a 50 mL stainless-steel autoclave reactor with an inner glass and a magnetic stirrer. The reactor was charged with  $\text{Na}_2\text{H}_2\text{P}(\text{W}_2\text{O}_7)_6$  (0.125 g, 0.0425 mmol),  $n\text{-Bu}_4\text{NBr}$  (0.25 g),  $\text{H}_2\text{O}_2$  (3.0 mL, 12 equiv.) and substrate (2.2 mmol). The reaction mixture was heated at 50 °C until the substrate was completely consumed. After cooling to ca. 0 °C with an ice-water bath, the reaction mixture was extracted with diethyl ether (5 mL  $\times$  3), then dried over  $\text{MgSO}_4$ . The solvent was removed, and the residue was chromatographed on silica gel using a 1 : 20 ethyl acetate–petroleum mixture as the eluent, which yielded the products b.

**Phenacyl benzoate (1b).** White solid; mp 118–119 °C (lit.<sup>26</sup> 118–120 °C);  $^1\text{H}$  NMR (400 MHz,  $\text{CDCl}_3$ ):  $\delta$  5.59 (s, 2H), 7.46–7.64 (m, 6H), 7.97 (d, 2H,  $J = 7.6$  Hz) 8.15 (d, 2H,  $J = 7.2$  Hz);  $^{13}\text{C}\{^1\text{H}\}$  NMR (75 MHz,  $\text{CDCl}_3$ ):  $\delta$  192.1, 166.0, 134.4, 133.9, 133.3, 130.0, 128.9, 128.4, 127.8, 66.4; IR (KBr): 1722, 1692, 1585, 1453, 1410, 1368, 1275, 1218, 1119, 948, 756, 688  $\text{cm}^{-1}$ ; GC-MS (EI, 70 eV):  $m/z$  240 ( $\text{M}^+$ ), 118, 105, 77, 51, 27, 15.

**4-Methylbenzoic acid-(4-methyl-phenacyl ester) (2b).** White solid; mp 141–142 °C (lit.<sup>27</sup> 145 °C);  $^1\text{H}$  NMR (300 MHz,  $\text{CDCl}_3$ ):  $\delta$  2.43 (s, 6H), 5.54 (s, 2H), 7.25–7.31 (m, 4H), 7.87 (d, 2H,  $J = 8.1$  Hz), 8.04 (d, 2H,  $J = 8.1$  Hz);  $^{13}\text{C}\{^1\text{H}\}$  NMR (75 MHz,  $\text{CDCl}_3$ ):  $\delta$  191.9, 166.1, 144.8, 144.1, 131.9, 130.0, 129.6, 129.2, 128.0, 126.7, 66.3, 21.8, 21.7; IR (KBr): 1719, 1690, 1595, 1442, 1406, 1362, 1274, 1223, 1172, 1107, 954, 801, 743  $\text{cm}^{-1}$ ; GC-MS (EI, 70 eV):  $m/z$  132, 119, 91, 65, 39.

**4-Chlorobenzoic acid-(4-chloro-phenacyl ester) (4b).** White solid; mp 119–120 °C;  $^1\text{H}$  NMR (300 MHz,  $\text{CDCl}_3$ ):  $\delta$  5.54 (s, 2H), 7.26–7.50 (m, 4H), 7.90 (d, 2H,  $J = 8.4$  Hz), 8.07 (d, 2H,  $J = 8.4$  Hz);  $^{13}\text{C}\{^1\text{H}\}$  NMR (75 MHz,  $\text{CDCl}_3$ ):  $\delta$  190.8, 165.2, 140.6, 140.0, 132.5, 131.4, 131.0, 129.3, 129.2, 129.1, 128.9, 128.8, 127.7, 66.4; IR (KBr): 1725, 1701, 1590, 1486, 1425, 1396, 1368, 1283, 1226, 1127, 1090, 1009, 820, 758  $\text{cm}^{-1}$ ; GC-MS (EI, 70 eV):  $m/z$  152, 139, 111, 75, 50.

### Acknowledgements

Support of this work from National Science Foundation of China (Grant 20872073, 20421202, and 20672054), the 111 project (B06005), and the Tianjin Natural Science Foundation is gratefully acknowledged. We also thank the referees for their valuable comments regarding revision.

### References and notes

- (a) J. H. Clark, *Green Chem.*, 1999, **1**, 1; (b) P. T. Anastas, *Green Chem.*, 2003, **5**, G29; (c) T. Sakakura, J. C. Choi and H. Yasuda, *Chem. Rev.*, 2007, **107**, 2365.
- (a) A. A. G. Shaikh and S. Sivaram, *Chem. Rev.*, 1996, **96**, 951; (b) K. Biggadike, R. M. Angell, C. M. Burgess, R. M. Farrel, A. P. Hancock, A. J. Harker, W. R. Irving, C. Ioannou, P. A. Procopiou, R. E. Shaw, Y. E. Solanke, O. M. P. Singh, M. A. Snowden, R. J. Stubbs, S. Walton and H. E. Weston, *J. Med. Chem.*, 2000, **43**, 19; (c) B. Ochiai and T. Endo, *Prog. Polym. Sci.*, 2005, **30**, 183.
- Typical examples on the synthesis of cyclic carbonates via cycloaddition epoxides with  $\text{CO}_2$ : (a) J. L. Jiang, F. X. Gao, R. M. Hua and X. Q. Qiu, *J. Org. Chem.*, 2005, **70**, 381; (b) J. W. Huang and M. Shi, *J. Org. Chem.*, 2003, **68**, 6705; (c) W. N. Sit, S. M. Ng, K. Y. Kwong and C. P. Lau, *J. Org. Chem.*, 2005, **70**, 8583; (d) H. Yasuda, L.-N. He, T. Sakakura and C.-W. Hu, *J. Catal.*, 2005, **233**, 119; (e) Y. Du, F. Cai, D.-L. Kong and L.-N. He, *Green Chem.*, 2005, **7**, 518; (f) C.-X. Miao, J.-Q. Wang, Y. Wu, Y. Du and L.-N. He, *ChemSusChem*, 2008, **1**, 236; (g) X.-Y. Dou, J.-Q. Wang, Y. Du, E. Wang and L.-N. He, *Synlett*, 2007, (19), 3058.
- Representative examples for the synthesis of cyclic carbonates from diols and  $\text{CO}_2$ : (a) K. Tomishige, H. Yasuda, Y. Yoshida, M. Nurunnabi, B. T. Li and K. Kunimori, *Green Chem.*, 2004, **6**, 206; (b) Y. Du, D. L. Kong, H. Y. Wang, F. Cai, J. S. Tian, J. Q. Wang and L. N. He, *J. Mol. Catal. A: Chem.*, 2005, **241**, 233; (c) Y. Du, L.-N. He and D.-L. Kong, *Catal. Commun.*, 2008, **9**, 1754.
- Synthesis of cyclic carbonates through the reaction of cyclic ketal with  $\text{CO}_2$ : M. Aresta, A. Dibenedetto, C. Dileo, I. Tommasi and E. Amodio, *J. Supercrit. Fluids*, 2003, **25**, 177.
- Other routes to cyclic carbonates starting from  $\text{CO}_2$ : (a) M. Yoshida, M. Fujita, T. Ishii and M. Ihara, *J. Am. Chem. Soc.*, 2003, **125**, 4874; (b) M. Yoshida and M. Ihara, *Chem.-Eur. J.*, 2004, **10**, 2886; (c) G. E. Greco, B. Gleason, T. A. Lowery, M. J. Kier, L. B. Hollander, S. A. Gibbs and A. D. Worthy, *Org. Lett.*, 2007, **9**, 3817; (d) Y. Kayaki, M. Yamamoto and T. Ikariya, *J. Org. Chem.*, 2007, **72**, 647.
- For the synthesis of cyclic carbonates from olefins and  $\text{CO}_2$  catalyzed by homogeneous catalysts and metal oxides, see: (a) M. Aresta and E. Quaranta, *J. Mol. Catal. A: Chem.*, 1987, **41**, 355; (b) M. Aresta, A. Dibenedetto and I. Tommasi, *Appl. Organomet. Chem.*, 2000, **14**, 799; (c) M. Aresta and A. Dibenedetto, *J. Mol. Catal. A: Chem.*, 2002, **182**, 399.
- One-pot synthesis of cyclic carbonates from olefins and  $\text{CO}_2$  via the “epoxides” intermediate: (a) S. Srivastava, D. Srinivas and P. Ratnasamy, *Catal. Lett.*, 2003, **91**, 133; (b) J. Sun, S. I. Fujika, B. M. Bhanage and M. Arai, *Catal. Commun.*, 2004, **5**, 83; (c) J. Sun, S. I. Fujika, B. M. Bhanage and M. Arai, *Catal. Today*, 2004, **93–95**, 383; (d) J. Sun, S. I. Fujika, F. Zhao, M. Hasegawa and M. Arai, *J. Catal.*, 2005, **230**, 398; (e) J. Sun, S. I. Fujika and M. Arai, *J. Organomet. Chem.*, 2005, **690**, 3490; (f) S. E. Jacobson and N. J. Morristown, *US Pat.*, 4 483 994, 1984.
- Cyclic carbonates direct from olefins and  $\text{CO}_2$  through a “halohydrins” species *in-situ* generated: (a) N. Eghbali and C. J. Li, *Green Chem.*, 2007, **9**, 213; (b) S. Carlo Fumagalli, M. Giuseppe Caprara and M. Paolo Roffia, *US Pat.*, 4 009 183, 1977; (c) S. E. Jacobson, *US Pat.*, 4 325 874, 1982; (d) J. L. Kao, G. A. Wheaton, H. Shalit and M. N. Sheng, *US Pat.*, 4 247 465, 1981.
- J. A. Verdol, *US Pat.*, 3 025 305, 1962.
- (a) M. C. R. Franssen and H. C. van der Plas, Haloperoxidases: their properties and their use in organic synthesis, *Adv. Appl. Microbiol.*, 1992, **93**, 1937; (b) A. Buttler, in *Bioinorganic Catalysis*, ed. J. Reedijk, Dekker, New York, 1993, ch. 13; (c) A. Butler and J. V. Walker, *Chem. Rev.*, 1993, **93**, 1937.
- (a) G. E. Meister and A. Butler, *Inorg. Chem.*, 1994, **33**, 3269; (b) R. I. De la Rosa, M. J. Clague and A. Butler, *J. Am. Chem. Soc.*, 1992, **114**, 760; (c) G. J. Colpas, B. J. Hamstra, J. W. Kampf and V. L. Pecoraro, *J. Am. Chem. Soc.*, 1996, **118**, 3469; (d) R. Neumann and I. Assael, *J. Am. Chem. Soc.*, 1989, **111**, 8410; (e) M. S. Reynolds, S. J. Morandi, J. W. Raebiger, S. P. Melican and S. P. E. Smith, *Inorg. Chem.*, 1994, **33**, 4977; (f) M. J. Clague and A. Butler, *J. Am. Chem. Soc.*, 1995, **117**, 3475; (g) J. R. Hanson, A. Opakunle and P. Petit, *J. Chem. Res. (S)*, 1995, 457; (h) J. E. Espenson, Z. Zhu and T. H. Zauche, *J. Org. Chem.*, 1999, **64**, 1191; (i) J. V. Walk, *J. Am. Chem. Soc.*, 1997, **119**, 6921; (j) B. F. Sels, D. V. Vos and P. A. Jacobs, *J. Am. Chem. Soc.*,

- 2001, **123**, 8350; (k) B. Sels, D. E. De Vos, M. Buntinx, F. Pierard, A. Kirsch-De Mesmaeker and P. A. Jacobs, *Nature*, 1999, **400**, 855.
- 13 (a) B. Ganchegui and W. Leitner, *Green Chem.*, 2007, **9**, 26; (b) U. Bora, G. Bose, M. K. Chaudhuri, S. S. Dhar, R. Gopinath, A. T. Khan and B. K. Patel, *Org. Lett.*, 2000, **2**, 247; (c) G. Rothenberg and J. H. Clark, *Org. Process Res. Dev.*, 2000, **4**, 270.
- 14 G. Rothenberg and J. H. Clark, *Green Chem.*, 2000, **2**, 248.
- 15 The GC-MS chart was given in the ESI†.
- 16 I. V. Kozhevnikov, *Appl. Catal., A*, 2003, **256**, 3.
- 17 C. Roosen, M. Ansorge-Schumacher, T. Mang, W. Leitner and L. Greiner, *Green Chem.*, 2007, **9**, 455.
- 18 The benzoic acid was detected by GC by comparing a retention time with that of an authentic sample.
- 19 (a) D. D. Tanner, J. J. Chen, L. Chen and C. Luelo, *J. Am. Chem. Soc.*, 1991, **113**, 8074; (b) Y. Tanabe, N. Matsumoto, T. Higashi, T. Misaki, T. Itoh, M. Yamamoto, K. Mitarai and Y. Nishii, *Tetrahedron*, 2002, **58**, 8269; (c) A. Banerjee and D. E. Falvey, *J. Org. Chem.*, 1997, **62**, 6245; (d) W. Huang, J. Pei, B. Chen, W. Pei and X. Ye, *Tetrahedron*, 1996, **52**, 10131; (e) S. J. Jagdale, S. V. Patil and M. M. Salunkhe, *Synth. Commun.*, 1996, **26**, 1747; (f) R. Ruzicka, M. Zabadal and P. Klan, *Synth. Commun.*, 2002, **32**, 2581; (g) Z. Liu, Z. C. Chen and Q. G. Zheng, *Synthesis*, 2004, **1**, 33.
- 20 2-Bromocyclohexanol was detected by GC-MS.
- 21 After extracting the products, we conducted further reaction by the addition of successive portions of the substrate **3**, H<sub>2</sub>O<sub>2</sub> and CO<sub>2</sub> to the aqueous phase containing the catalyst, which was concentrated prior to use. The result for catalyst recycling: yield of the cyclic carbonate **3a**, the first run: 83%, the second run: 81%; the third run: 81%.
- 22 T. Iwasaki, N. Kihara and T. Endo, *Bull. Chem. Soc. Jpn.*, 2000, **73**, 713.
- 23 K. Kawasaki and T. Katsuki, *Tetrahedron*, 1997, **53**(18), 6337.
- 24 R. C. White, P. Drew and R. Moorman, *J. Heterocycl. Chem.*, 1988, **25**, 1781.
- 25 B. Ochiai, M. Matsuki, T. Miyagawa, D. Nagai and T. Endo, *Tetrahedron*, 2005, **61**(7), 1835.
- 26 A. Banerjee and D. E. Falvey, *J. Org. Chem.*, 1997, **62**, 6245.
- 27 Karrer, *Helv. Chim. Acta*, 1952, **35**, 427.

# One-pot copper nanoparticle-catalyzed synthesis of S-aryl- and S-vinyl dithiocarbamates in water: high diastereoselectivity achieved for vinyl dithiocarbamates†

Sukalyan Bhadra, Amit Saha and Brindaban C. Ranu\*

Received 30th May 2008, Accepted 1st August 2008

First published as an Advance Article on the web 7th October 2008

DOI: 10.1039/b809200a

A convenient, green and efficient procedure for the synthesis of aryl and vinyl dithiocarbamates has been developed by a simple one-pot three component condensation of an amine, carbon disulfide, and an aryl iodide or a styrenyl bromide catalyzed by copper nanoparticles in water. Significantly, the (*E*)- and (*Z*)-styrenyl bromides provide the corresponding (*E*)- and (*Z*)-styrenyl dithiocarbamates in high diastereoselectivities. The catalyst is recycled.

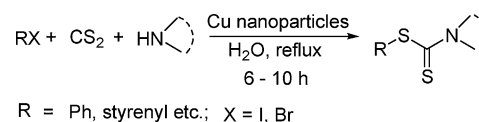
## 1. Introduction

Reactions in water have attracted considerable interest in recent times because of their environmental acceptability, abundance and low cost.<sup>1</sup> In addition, water often exhibits unique reactivity and selectivity that cannot be attained in conventional organic solvents.<sup>2</sup> Thus, development of an efficient procedure for an organic reaction using water as the reaction medium has received high priority in the design of a chemical process.

Organic dithiocarbamates are of much importance as versatile synthetic intermediates,<sup>3</sup> and linkers in solid phase organic synthesis.<sup>4</sup> Moreover, their occurrence in a variety of biologically active compounds,<sup>5</sup> their pivotal roles in agriculture,<sup>6</sup> and their medicinal and biological properties,<sup>7</sup> prompted interest in the development of convenient synthetic procedures for these compounds. Conventional methods involve reactions of amines with thiophosgene and its derivatives, which are not desirable for environmental concerns.<sup>8</sup> Several one-pot procedures by reaction of amines with carbon disulfide and alkyl halides or  $\alpha,\beta$ -unsaturated compounds have also been reported.<sup>9</sup> However, although these methods were satisfactory for the synthesis of alkyl dithiocarbamates, they were not effective for aryl or vinyl derivatives. The procedures for the synthesis of aryl and vinyl dithiocarbamates are rather limited and the available methods involved reaction of the sodium salt of dithiocarbamic acid with hypervalent iodine compounds<sup>10</sup> and the Wittig reaction of aldehydes with phosphonium ylides<sup>11</sup> among others.<sup>12</sup> Recently, a new protocol based on the Ullmann-type coupling of sodium dithiocarbamates with aryl iodides and vinyl bromides catalyzed by CuI in the presence of a ligand, *N,N*-dimethylglycine in DMF, has been reported.<sup>13</sup>

In recent times, interest in nanoparticle-catalysis has increased considerably because of its high efficiency under environmentally

benign reaction conditions in the context of green chemistry.<sup>14</sup> As a part of our continued activities<sup>15</sup> to explore catalysis by metal nanoparticles in water we report here a one-pot three-component condensation of an amine, carbon disulfide and an aryl iodide or styrenyl bromide catalyzed by copper nanoparticles in water under ligand- and base-free conditions leading to the synthesis of aryl or styrenyl dithiocarbamates (Scheme 1).



Scheme 1

## 2. Results and discussion

The experimental procedure is very simple. A mixture of aryl iodide or styrenyl bromide, carbon disulfide, amine was heated under reflux in water in the presence of copper nanoparticles for a required period of time (TLC). Standard work-up provided the product. The aqueous part containing Cu nanoparticles, remaining after work up, was recycled upto four times without appreciable loss of efficiency for a representative reaction of 2-(4-methylphenyl)vinyl bromide and pyrrolidine (entry 11, Table 1) (Fig. 1).

The best results in terms of yields were obtained using water as reaction medium compared to conventional organic solvents such as DMF, toluene and THF. The amount of Cu nanoparticles was optimized to 3.0 mol%. Use of base such as  $K_2CO_3$  and  $K_3PO_4$  in water fails to show any effect on reaction. Thus, contrary to several conventional procedures no base is used for this Cu-nanoparticles catalyzed reaction. Copper nanoparticles were prepared from copper sulfate by reduction with hydrazine hydrate in ethylene glycol.<sup>16</sup> The identity and size (2–6 nm) of Cu nanoparticles were established by transmission electron microscope (TEM) (Fig. 2), energy dispersive X-ray spectroscopy (EDS) (Fig. 3), and UV spectroscopy (Fig. 4).

Department of Organic Chemistry, Indian Association for the Cultivation of Science, Jadavpur, Kolkata, 700 032, India. E-mail: ocbcr@iacs.res.in

† Electronic supplementary information (ESI) available: <sup>1</sup>H and <sup>13</sup>C NMR spectra of all products in Table 1. CCDC reference number 684382. For ESI and crystallographic data in CIF or other electronic format see DOI: 10.1039/b809200a

**Table 1** Copper nanoparticles catalyzed coupling of aryl and vinyl halides with dithiocarbamate anion

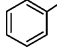
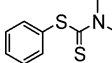
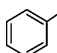
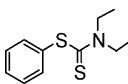
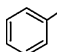
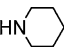
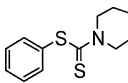
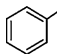
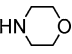
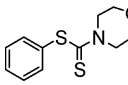
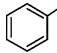
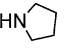
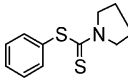
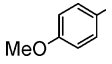
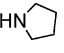
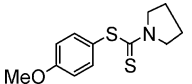
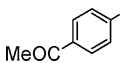
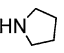
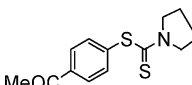
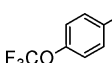
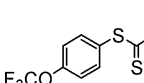
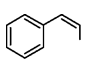
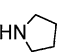
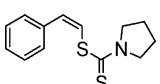
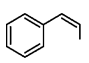
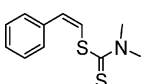
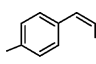
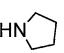
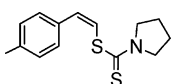
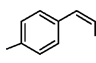
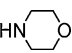
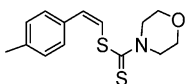
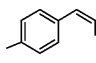
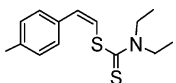
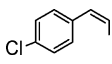
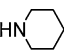
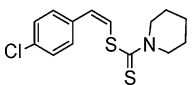
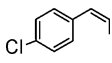
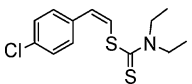
Entry	R	X	Amine	Time/h	Product	Yield (%) <sup>a</sup>	Ref.
1		I	HNMe <sub>2</sub>	8		94	10
2		I	HNEt <sub>2</sub>	8		91	10
3		I	HN 	8		92	10
4		I	HN 	8.2		88	18
5		I	HN 	8		87	19
6		I	HN 	9		75	
7		I	HN 	8.5		80	
8		I	HNMe <sub>2</sub>	8		85	
9		Br	HN 	6		92	
10		Br	HNMe <sub>2</sub>	6		95	13
11		Br	HN 	7		91	
12		Br	HN 	9		87	
13		Br	HNEt <sub>2</sub>	8		88	
14		Br	HN 	8.2		89	
15		Br	HNEt <sub>2</sub>	8		92	



Table 1 (Contd.)

Entry	R	X	Amine	Time/h	Product	Yield (%) <sup>a</sup>	Ref.
16		Br	HNEt <sub>2</sub>	10		76	
17		Br	HN(C <sub>6</sub> H <sub>11</sub> )	8.2		86 <sup>b</sup>	13
18		Br	HNMe <sub>2</sub>	8		89 <sup>b</sup>	13
19		Br	HN(C <sub>4</sub> H <sub>9</sub> )	8.5		84 <sup>b</sup>	
20		Br	HNEt <sub>2</sub>	8.4		92 <sup>b</sup>	
21		Br	HN(C <sub>6</sub> H <sub>11</sub> )	8		86	

<sup>a</sup> Isolated yields of pure products (<sup>1</sup>H and <sup>13</sup>C). <sup>b</sup> The substrates in entries 17–20 gave a trace amount (1–3%) of the corresponding Z-isomers as determined by <sup>1</sup>H NMR.

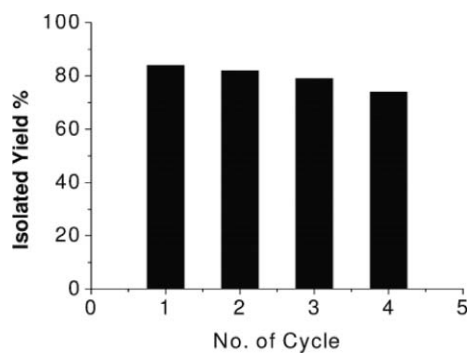


Fig. 1 Recyclability chart.

Several substituted aryl iodides and styrenyl bromides underwent coupling with the dithiocarbamate anion, generated *in situ* by the reaction of carbon disulfide and amine to provide the corresponding dithiocarbamate derivatives. The results are summarized in Table 1.

A variety of substituents in the aromatic ring, such as Cl, OCH<sub>3</sub>, OCF<sub>3</sub>, COCH<sub>3</sub> are compatible in this reaction. The open-chain as well as cyclic amines participated uniformly. Significantly, the reactions of vinyl bromides are highly stereoselective. The (Z)-vinyl bromides (Table 1, entries 9–16) provided the corresponding (Z)-vinyl dithiocarbamates (no E-isomer was detected/isolated), while the (E)-bromides (Table 1, entries

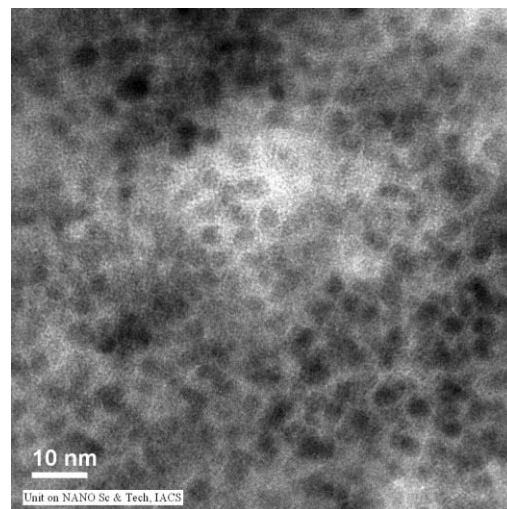


Fig. 2 TEM image of Cu nanoparticles.

17–21) furnished the (E)-dithiocarbamates predominantly with a trace amount (1–3%) of (Z)-isomers. The (E)- and (Z)-isomers were characterized by their <sup>1</sup>H and <sup>13</sup>C NMR spectroscopy. Our analysis was also confirmed by the X-ray structure<sup>17</sup> of one of the styrenyl dithiocarbamates (Table 1, entry 21) as shown in Fig. 5.

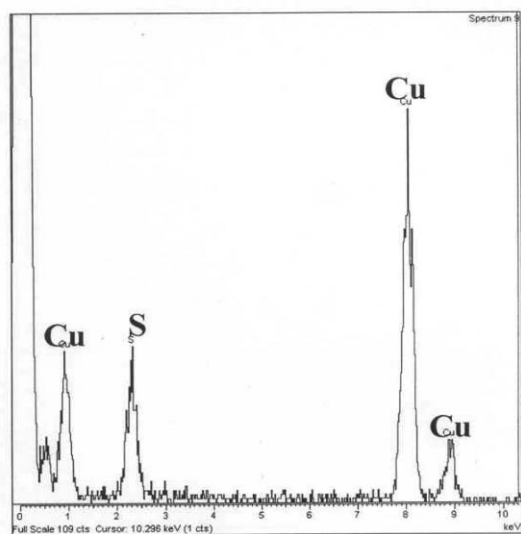


Fig. 3 EDS of Cu nanoparticles on a Cu grid.

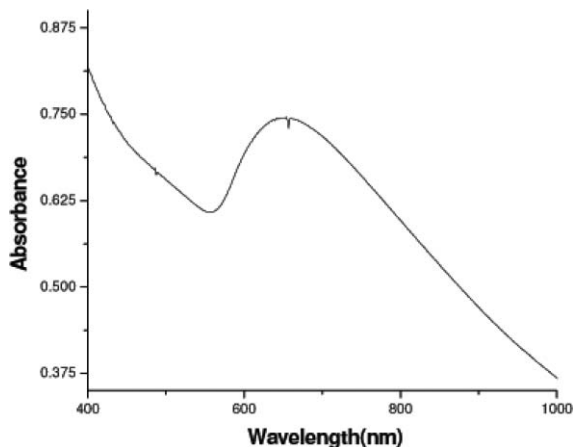


Fig. 4 UV spectrum of Cu nanoparticles.

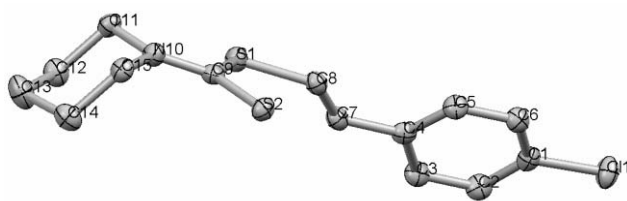
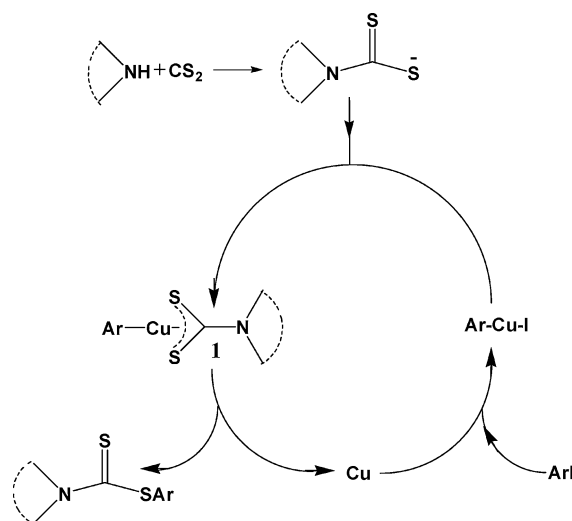


Fig. 5 ORTEP diagram of the dithiocarbamate (Table 1, entry 21).

We believe that the reaction proceeds in a catalytic cycle where the aryl/styrenyl halide undergoes oxidative addition to Cu to form ArCuI which combines with dithiocarbamate anion, generated *in situ* by the reaction of amine and carbon disulfide, to give an intermediate **1**, which leads to the product by subsequent reductive elimination. The liberated Cu(0) initiates a further reaction and propagates the cycle (Scheme 2). We believe that Cu nanoparticles facilitate oxidative coupling with aryl iodide because of their inherent character to transfer electrons<sup>20</sup> more easily than metallic Cu (Table 2). Presumably, use of water also makes this reaction more facile because of its amphoteric nature and thus not requiring any base.<sup>2b</sup>

Table 2 Comparison of results of reactions catalyzed by metallic Cu powder with Cu nanoparticles

Entry	Reaction	Yield (%) metallic Cu	Yield (%) Cu nanoparticles
1		12	91
2		20	87
3		35	92
4		23	95
5		21	89



Scheme 2

The reactions were very clean and high yielding and no side products were isolated. A comparison of results of reactions by Cu nanoparticles with those by metallic Cu (Table 2) distinctly demonstrates the superior efficiency of Cu nanoparticles compared to metallic Cu. Our procedure also offers significant improvements to that catalyzed by CuI<sup>13</sup> with regard to catalyst loading (3.0 vs. 15 mol%), reaction medium (H<sub>2</sub>O vs. DMF) and reaction time (6–10 h vs. 22 h). The present procedure provides a one-pot operation and avoids the use of sodio-salt of dithiocarbamic acid used in the CuI one. The preparation and purification of the sodio-salt is very tedious and is also commercially very expensive. In addition, our reaction did not require a ligand or a base, whereas the CuI-catalyzed one<sup>13</sup> did not proceed without ligand. The stereoselectivities achieved for vinyl dithiocarbamates by this Cu nanoparticle

catalyzed reaction are also better than those for the CuI-catalyzed ones. In fact, highly diastereoselective synthesis of vinyl dithiocarbamates was not addressed in earlier reports.<sup>8–12</sup>

### 3. Experimental section

#### Preparation of Cu nanoparticles

A solution of  $N_2H_4 \cdot H_2O$  (0.75 mL, 80% aqueous solution, 12 mmol) and NaOH (0.016 g, 0.4 mmol) in ethylene glycol (80 mL) was added to another solution of  $CuSO_4 \cdot 5H_2O$  (2.00 g, 8 mmol) in ethylene glycol (80 mL) with stirring at room temperature (30 °C). The mixture was then subjected to irradiation in a conventional microwave oven (BPL, India, 1080 Watt, working cycle of 19 s on and 6 s off) for 3.5 min. The solution turned black and was allowed to come to room temperature. Cu nanoparticles were centrifuged, washed with ethanol five times and dried under vacuum. The particles were characterized by TEM (4–6 nm), EDX and UV spectra (Fig. 2, 3 and 4). Cu nanoparticles can be preserved under an argon atmosphere for 3 weeks.

**General experimental procedure for the synthesis of dithiocarbamates. Representative experimental procedure for condensation of amine,  $CS_2$  and aryl/styrenyl halide (entry 9, Table 1).** To a well stirred mixture of *cis*-(2-bromovinyl)benzene (185 mg, 1 mmol) and carbon disulfide (190 mg, 2.5 mmol) in water (2 mL) was added pyrrolidine (84 mg, 1.2 mmol) drop by drop at 0–5 °C. After stirring for 5 min Cu nanoparticles (2 mg, 3.0 mol%) were added and the reaction mixture was heated under reflux for 6 h (TLC). The reaction mixture was extracted with ethyl acetate (3 × 7 mL) and the extract was washed with brine and dried ( $Na_2SO_4$ ). Evaporation of organic solvent left the crude product which was purified by column chromatography over silica gel (hexane–ether 85 : 15) to provide the corresponding dithiocarbamate, pyrrolidine-1-carbodithionic acid styryl ester as a white solid, mp 120 °C, IR (KBr): 2964, 2925, 2898, 1463, 1440, 1330, 1155, 1004, 958, 840, 783, 694  $cm^{-1}$ ;  $^1H$  NMR (300 MHz,  $CDCl_3$ )  $\delta$  1.85–1.94 (m, 2H), 1.95–2.04 (m, 2H), 3.65 (t,  $J = 6.65$ , 2H), 3.89 (t,  $J = 6.75$ , 2H), 6.70 (d,  $J = 11.06$ , 1H), 7.17 (t,  $J = 7.05$ , 1H), 7.28 (t,  $J = 7.33$ , 2H), 7.36 (d,  $J = 7.41$ , 2H), 7.45 (d,  $J = 11.12$ , 1H);  $^{13}C$  NMR (75 MHz,  $CDCl_3$ )  $\delta$  24.2, 26.0, 50.9, 55.4, 123.8, 127.5, 128.1, 128.4 (2C), 128.8 (2C), 136.5, 189.0; HRMS Calcd for  $C_{13}H_{15}NS_2$  [M + H]<sup>+</sup>: 250.0646; found: 250.0719. The aqueous part after organic extract containing Cu(0) nanoparticles was reused for subsequent reactions (no loss of efficiency up to four times).

This procedure was followed for all the reactions listed in Table 1. Although this procedure was described with a 1 mmol scale, 10 mmol scale reactions also provided uniform results. Several products are known compounds and were easily identified by comparison of their spectroscopic data and mp's with those reported (see refs in Table 1). The unknown compounds (entries 6–8, 11–17, 19–21, Table 1) were properly characterized by their spectroscopic (IR,  $^1H$  NMR,  $^{13}C$  NMR, HRMS) data which are provided below in order of their entries in Table 1.

**Pyrrolidine-1-carbodithionic acid 4-methoxy-phenyl ester (Table 1, entry 6).** Brown viscous oil; IR (neat) 2952, 2922,

2852, 1712, 1589, 1492, 1427, 1245, 1157, 1026, 1001, 954, 823  $cm^{-1}$ ;  $^1H$  NMR (300 MHz,  $CDCl_3$ )  $\delta$  1.99 (q,  $J = 7.20$  Hz, 2H), 2.11 (q,  $J = 6.81$  Hz, 2H), 3.79 (t,  $J = 6.97$  Hz, 2H), 3.84 (s, 3H), 3.93 (t,  $J = 7.06$  Hz, 2H), 6.96 (d,  $J = 8.66$  Hz, 2H), 7.39 (d,  $J = 8.65$  Hz, 2H);  $^{13}C$  NMR (75 MHz,  $CDCl_3$ )  $\delta$  24.4, 26.4, 51.0, 55.3, 55.4, 114.8 (2C), 122.0, 138.5 (2C), 161.2, 194.3; HRMS Calcd for  $C_{12}H_{15}NOS_2$  [M + Na]<sup>+</sup>: 276.0493; Found: 276.0488.

**Pyrrolidine-1-carbodithionic acid 4-acetyl-phenyl ester (Table 1, entry 7).** White solid (mp 79 °C); IR (KBr) 2923, 2869, 2862, 1683, 1433, 1259, 1159, 1002, 954  $cm^{-1}$ ;  $^1H$  NMR (300 MHz,  $CDCl_3$ )  $\delta$  1.99–2.03 (m, 2H), 2.12–2.16 (m, 2H), 2.62 (s, 3H), 3.80 (broad, 2H), 3.92 (broad, 2H), 7.59 (d,  $J = 8.25$  Hz, 2H), 7.99 (d,  $J = 8.26$  Hz, 2H);  $^{13}C$  NMR (75 MHz,  $CDCl_3$ )  $\delta$  24.5, 26.4, 26.8, 51.3, 55.4, 128.8 (2C), 136.7, 137.0 (2C), 137.8, 197.5; HRMS Calcd for  $C_{13}H_{15}NOS_2$  [M + Na]<sup>+</sup>: 288.0493; Found: 288.0497.

**Dimethyl-dithiocarbamic acid 4-trifluoromethoxy-phenyl ester (Table 1, entry 8).** Pale yellow solid (mp 65 °C); IR (KBr) 2927, 2846, 1487, 1373, 1255, 1215, 1170, 981, 920, 842, 513  $cm^{-1}$ ;  $^1H$  NMR (300 MHz,  $CDCl_3$ )  $\delta$  3.52 (s, 3H), 3.58 (s, 3H), 7.30 (d,  $J = 8.29$  Hz, 2H), 7.53 (d,  $J = 8.65$  Hz, 2H);  $^{13}C$  NMR (75 MHz,  $CDCl_3$ )  $\delta$  42.0, 45.8, 118.7, 121.1 (2C), 130.2, 138.7 (2C), 150.5, 196.6; HRMS Calcd. for  $C_{10}H_{10}F_3NOS_2$  [M + H]<sup>+</sup>: 282.0234; Found: 282.0226.

**Pyrrolidine-1-carbodithionic acid 2-*p*-tolyl vinyl ester (Table 1, entry 11).** White solid (mp 112 °C); IR (KBr) 2966, 2945, 2916, 2868, 1467, 1440, 1330, 1161, 1006, 958, 854, 821, 790, 520  $cm^{-1}$ ;  $^1H$  NMR (300 MHz,  $CDCl_3$ )  $\delta$  1.89 (q,  $J = 6.68$  Hz, 2H), 1.97 (q,  $J = 6.66$  Hz, 2H), 2.25 (s, 3H), 3.63 (t,  $J = 6.41$  Hz, 2H), 3.87 (t,  $J = 6.56$  Hz, 2H), 6.66 (d,  $J = 11.04$  Hz, 1H), 7.07 (d,  $J = 7.89$  Hz, 2H), 7.25 (d,  $J = 7.94$  Hz, 2H), 7.37 (d,  $J = 11.08$  Hz, 1H);  $^{13}C$  NMR (75 MHz,  $CDCl_3$ )  $\delta$  21.3, 24.1, 25.9, 50.8, 55.3, 122.6, 128.1, 128.7 (2C), 129.1 (2C), 133.6, 137.4, 189.0; HRMS Calcd for  $C_{14}H_{17}NS_2$  [M + H]<sup>+</sup>: 264.0881; Found: 264.0872.

**Morpholine-4-carbodithionic acid 2-*p*-tolyl vinyl ester (Table 1, entry 12).** Yellow solid; (mp 118 °C); IR (KBr) 2954, 2920, 2850, 1473, 1425, 1261, 1222, 1110, 1028, 985, 852, 823, 524  $cm^{-1}$ ;  $^1H$  NMR (300 MHz,  $CDCl_3$ )  $\delta$  2.36 (s, 3H), 3.74–3.77 (m, 4H), 4.19 (broad, 4H), 6.83 (d,  $J = 10.97$  Hz, 1H), 7.18 (d,  $J = 7.86$  Hz, 2H), 7.33 (d,  $J = 7.97$  Hz, 2H), 7.41 (d,  $J = 10.97$  Hz, 1H);  $^{13}C$  NMR (75 MHz,  $CDCl_3$ )  $\delta$  21.3, 51.0 (2C), 66.2 (2C), 122.1, 128.7 (2C), 129.1 (2C), 129.2, 133.3, 137.6, 193.9; HRMS Calcd for  $C_{14}H_{17}NOS_2$  [M + H]<sup>+</sup>: 280.0830; Found: 280.0825.

**Diethyl-dithiocarbamic acid 2-*p*-tolyl-vinyl ester (Table 1, entry 13).** Colorless viscous oil; IR (neat) 2977, 2931, 1488, 1417, 1353, 1269, 1205, 1143, 1008, 981, 823  $cm^{-1}$ ;  $^1H$  NMR (300 MHz,  $CDCl_3$ )  $\delta$  1.27–1.35 (m, 6H), 2.36 (s, 3H), 3.79 (q,  $J = 6.94$  Hz, 2H), 4.04 (q,  $J = 6.87$  Hz, 2H), 6.78 (d,  $J = 11.07$  Hz, 1H), 7.18 (d,  $J = 7.92$  Hz, 2H), 7.36 (d,  $J = 7.98$  Hz, 2H), 7.44 (d,  $J = 11.08$  Hz, 1H);  $^{13}C$  NMR (75 MHz,  $CDCl_3$ )  $\delta$  11.5, 12.7, 21.2, 46.8, 49.9, 123.0, 128.2, 128.7 (2C), 129.0 (2C), 133.5, 137.3, 191.9; HRMS Calcd for  $C_{14}H_{19}NS_2$  [M + H]<sup>+</sup>: 266.1037; Found: 266.1030.

**Piperidine-1-carbodithionic acid 2-(4-chloro-phenyl)-vinyl ester (Table 1, entry 14).** Colorless viscous liquid; IR (neat) 2937, 2923, 2854, 1488, 1475, 1427, 1242, 1226, 1089, 1010, 974, 850,

829;  $^1\text{H}$  NMR (300 MHz,  $\text{CDCl}_3$ )  $\delta$  1.70 (broad, 6H), 3.93 (broad, 2H), 4.29 (broad, 2H), 6.73 (d,  $J = 11.10$  Hz, 1H), 7.23–7.35 (m, 4H), 7.50 (d,  $J = 11.10$  Hz, 1H);  $^{13}\text{C}$  NMR (75 MHz,  $\text{CDCl}_3$ )  $\delta$  24.8, 25.9 (2C), 52.1, 53.9, 125.4, 127.5, 128.9 (2C), 130.4 (2C), 133.5, 135.3, 191.8; HRMS Calcd for  $\text{C}_{14}\text{H}_{16}\text{ClNS}_2$   $[\text{M} + \text{H}]^+$ : 298.0491; Found: 298.0483.

**Diethyl-dithiocarbamic acid 2-(4-chloro-phenyl)-vinyl ester (Table 1, entry 15).** Colorless viscous oil; IR (neat) 2977, 2931, 2869, 1488, 1417, 1203, 1091, 1010, 829  $\text{cm}^{-1}$ ;  $^1\text{H}$  NMR (300 MHz,  $\text{CDCl}_3$ )  $\delta$  1.18–1.33 (m, 6H), 3.73 (q,  $J = 6.94$  Hz, 2H), 3.99 (q,  $J = 6.94$  Hz, 2H), 6.67 (d,  $J = 11.11$  Hz, 1H), 7.18–7.31 (m, 4H), 7.42 (d,  $J = 11.10$  Hz, 1H);  $^{13}\text{C}$  NMR (75 MHz,  $\text{CDCl}_3$ )  $\delta$  11.9, 13.2, 47.3, 50.4, 125.4, 127.4, 128.9 (2C), 130.4 (2C), 133.5, 135.3, 191.7; HRMS Calcd for  $\text{C}_{13}\text{H}_{16}\text{ClNS}_2$   $[\text{M} + \text{H}]^+$ : 286.0491; Found: 286.0602.

**Diethyl-dithiocarbamic acid 2-(bromo-phenyl)vinyl ester (Table 1, entry 16).** Viscous yellow liquid; IR (neat) 2976, 2929, 2869, 2852, 1488, 1417, 1354, 1269, 1203, 1143, 1024, 764  $\text{cm}^{-1}$ ;  $^1\text{H}$  NMR (300 MHz,  $\text{CDCl}_3$ )  $\delta$  1.29 (t,  $J = 7.05$  Hz, 6H), 3.74 (q,  $J = 7.05$  Hz, 2H), 4.04 (q,  $J = 7.05$  Hz, 2H), 6.93 (d,  $J = 10.89$  Hz, 1H), 7.13 (t,  $J = 7.58$  Hz, 1H), 7.26–7.34 (m, 1H), 7.53–7.59 (m, 3H);  $^{13}\text{C}$  NMR (75 MHz,  $\text{CDCl}_3$ )  $\delta$  11.6, 12.9, 47.0, 50.0, 124.1, 126.9, 127.1, 127.8, 129.1, 129.9, 132.8, 136.6, 191.6; HRMS Calcd for  $\text{C}_{13}\text{H}_{16}\text{BrNS}_2$   $[\text{M} + \text{H}]^+$ : 329.9986; Found: 329.9813.

**Pyrrolidine-1-carbodithioic acid 2-*p*-tolyl-vinyl ester (Table 1, entry 19).** White solid (mp 113 °C); IR (KBr) 2968, 2948, 2913, 2860, 1462, 1438, 1335, 1168, 1012, 938, 848  $\text{cm}^{-1}$ ;  $^1\text{H}$  NMR (300 MHz,  $\text{CDCl}_3$ )  $\delta$  1.99 (t,  $J = 6.67$  Hz, 2H), 2.10 (t,  $J = 6.75$  Hz, 2H), 2.33 (s, 3H), 3.67 (t,  $J = 6.82$  Hz, 2H), 3.95 (t,  $J = 6.79$  Hz, 2H), 6.73 (d,  $J = 16.05$  Hz, 1H), 7.13 (d,  $J = 7.97$  Hz, 2H), 7.34 (d,  $J = 7.98$  Hz, 2H), 7.47 (d,  $J = 16.03$  Hz, 1H);  $^{13}\text{C}$  NMR (75 MHz,  $\text{CDCl}_3$ )  $\delta$  21.3, 24.4, 26.2, 50.8, 54.8, 121.4, 126.6 (2C), 129.4 (2C), 132.2, 133.6, 138.1, 190.5; HRMS Calcd for  $\text{C}_{14}\text{H}_{17}\text{NS}_2$   $[\text{M} + \text{H}]^+$ : 264.0881; Found: 264.0873.

**Diethyl-dithiocarbamic acid 2-(4-methoxyphenyl)-vinyl ester (Table 1, entry 20).** Brownish viscous liquid; IR (neat) 2976, 2931, 2833, 1606, 1510, 1488, 1417, 1269, 1251, 1031, 833, 785  $\text{cm}^{-1}$ ;  $^1\text{H}$  NMR (300 MHz,  $\text{CDCl}_3$ )  $\delta$  1.25–1.32 (m, 6H), 3.72 (q,  $J = 6.79$  Hz, 2H), 3.78 (s, 3H), 4.01 (q,  $J = 6.73$  Hz, 2H), 6.68 (d,  $J = 15.95$  Hz, 1H), 6.85 (d,  $J = 8.65$  Hz, 2H), 7.25 (d,  $J = 15.88$  Hz, 1H), 7.38 (d,  $J = 8.62$  Hz, 2H);  $^{13}\text{C}$  NMR (75 MHz,  $\text{CDCl}_3$ )  $\delta$  11.5, 12.5, 46.9, 49.2, 55.2, 114.0 (2C), 119.7, 127.9 (2C), 129.1, 132.3, 159.5, 193.5; HRMS Calcd for  $\text{C}_{14}\text{H}_{19}\text{NOS}_2$   $[\text{M} + \text{H}]^+$ : 282.0986; Found: 282.0980.

**Piperidine-1-carbodithioic acid 2-(4-chloro-phenyl)-vinyl ester (Table 1, entry 21).** White solid (mp 122 °C); IR (KBr) 2941, 2925, 2854, 1471, 1488, 1429, 1242, 1232, 1118, 1010, 979, 835, 781  $\text{cm}^{-1}$ ;  $^1\text{H}$  NMR (300 MHz,  $\text{CDCl}_3$ )  $\delta$  1.73 (broad, 6H), 3.88 (broad, 2H), 4.29 (broad, 2H), 6.69 (d,  $J = 15.99$  Hz, 1H), 7.30 (d,  $J = 8.45$  Hz, 2H), 7.38 (d,  $J = 8.43$  Hz, 2H), 7.50 (d,  $J = 16.0$  Hz, 1H);  $^{13}\text{C}$  NMR (75 MHz,  $\text{CDCl}_3$ )  $\delta$  24.5, 25.6 (2C), 51.8, 52.8, 123.8, 127.8 (2C), 128.9 (2C), 130.9, 133.8, 134.9, 192.8; HRMS Calcd for  $\text{C}_{14}\text{H}_{16}\text{ClNS}_2$   $[\text{M} + \text{H}]^+$ : 298.0491; Found: 298.0488.

## 4. Conclusion

The present procedure using copper nanoparticles provides a very efficient and convenient methodology for the synthesis of aryl and styrenyl dithiocarbamates by a one-pot three component condensation of aryl/styrenyl halide, carbon disulfide and amine in water. The advantages offered by this procedure are operational simplicity, general applicability to acyclic and cyclic amines, ligand- and base-free reaction, high yields of products, excellent diastereoselectivity for styrenyl dithiocarbamates, and green protocol providing recyclability of catalyst up to four times without loss of efficiency, and use of water as reaction medium. To the best of our knowledge, condensation of amine, carbon disulfide and aryl/styrenyl halide catalyzed by Cu nanoparticles in water for the synthesis of aryl and styrenyl dithiocarbamates is novel and not reported earlier. Moreover, this methodology further demonstrates the potential of Cu nanoparticles and water in organic reactions.

## Acknowledgements

We are pleased to acknowledge the financial support from DST [Grant No. SR/S5/GC-02/2006] for this investigation. S.B. and A.S. are thankful to CSIR for their fellowships.

## References

- (a) C.-J. Li and T.-H. Chan, in *Organic Reactions in Aqueous Media*, Wiley, New York, 1997; (b) *Organic Synthesis in Water*, ed. P. A. Grieco, Blackie Academic and Professional, London, 1998; (c) U. M. Lindstrom, *Chem. Rev.*, 2002, **102**, 2751; (d) C. J. Li, *Chem. Rev.*, 2005, **105**, 3095.
- (a) N. Azizi and M. R. Saidi, *Org. Lett.*, 2005, **7**, 3649; (b) N. Azizi, F. Aryanasab, L. Torkiyan, A. Ziyaei and M. R. Saidi, *J. Org. Chem.*, 2006, **71**, 3634; (c) G. L. Khatik, R. Kumar and A. K. Chakraborti, *Org. Lett.*, 2006, **8**, 2433; (d) B. C. Ranu and S. Banerjee, *Tetrahedron Lett.*, 2007, **48**, 141; (e) B. C. Ranu and T. Mandal, *Synlett*, 2007, 925.
- (a) A. K. Mukherjee and R. Ashare, *Chem. Rev.*, 1991, **91**, 1; (b) U. Boas, H. Gertz, J. B. Christensen and P. M. H. Heegaard, *Tetrahedron Lett.*, 2004, **45**, 269.
- P. Morf, F. Raimondi, H.-G. Nothofex, B. Schnyder, A. Yasuda, J. M. Wessels and T. A. Jung, *Langmuir*, 2006, **22**, 658.
- (a) M. Dhooghe and N. De Kime, *Tetrahedron*, 2006, **62**, 513; (b) A. W. Drian and S. M. Sherif, *Tetrahedron*, 1999, **55**, 7957.
- C. Rafin, E. Veignie, M. Sancholle, D. Postal, C. Len, P. Villa and G. Ronco, *J. Agric. Food Chem.*, 2000, **48**, 5283.
- (a) L. Ronconi, C. Marzano, P. Zanello, M. Corsini, G. Miolo, C. Macca, A. Trevisan and D. Fregona, *J. Med. Chem.*, 2006, **49**, 1648; (b) G. H. Elgemeie and S. H. Sayed, *Synthesis*, 2001, 1747.
- (a) H. Tilles, *J. Am. Chem. Soc.*, 1959, **81**, 714; (b) W. Chin-Hsien, *Synthesis*, 1981, 622.
- (a) B. C. Ranu, A. Saha and S. Banerjee, *Eur. J. Org. Chem.*, 2008, 519; (b) N. Azizi, F. Aryanasab and M. R. Saidi, *Org. Lett.*, 2006, **8**, 5275; (c) D. Chaturvedi and S. Ray, *Tetrahedron Lett.*, 2006, **47**, 1307; (d) R. N. Salvatore, S. Sahab and K. W. Jung, *Tetrahedron Lett.*, 2001, **42**, 2055.
- Z.-C. Chen, Y. Y. Jin and P. J. Stand, *J. Org. Chem.*, 1987, **52**, 4117.
- Z.-Z. Huang and L. L. Wu, *Synth. Commun.*, 1996, **26**, 509.
- (a) R. Galli, *J. Org. Chem.*, 1987, **52**, 5349; (b) A. Krasovskiy, A. Gavryushin and P. Knochel, *Synlett*, 2005, 2691; (c) K.-Y. Jen and M. P. Cava, *Tetrahedron Lett.*, 1982, **23**, 2001; (d) J. R. Grunwell, *J. Org. Chem.*, 1970, **35**, 1500; (e) P. Giboreau and C. Morin, *J. Org. Chem.*, 1994, **59**, 1205.
- Y. Liu and W. Bao, *Tetrahedron Lett.*, 2007, **48**, 4785.
- (a) D. Astruc, *Inorg. Chem.*, 2007, **46**, 1884; (b) D. Astruc, F. Lu and J. R. Aranzas, *Angew. Chem., Int. Ed.*, 2005, **44**, 7852; (c) I. P. Beletskaya and A. V. Cheprakov, *Chem. Rev.*, 2000, **100**, 3009.



- 15 (a) B. C. Ranu and K. Chattopadhyay, *Org. Lett.*, 2007, **9**, 2409; (b) B. C. Ranu, K. Chattopadhyay and L. Adak, *Org. Lett.*, 2007, **9**, 4595; (c) B. C. Ranu, A. Saha and R. Jana, *Adv. Synth. Catal.*, 2007, **349**, 2690; (d) B. C. Ranu, R. Dey and K. Chattopadhyay, *Tetrahedron Lett.*, 2008, **49**, 3430.
- 16 H. Zhu, C. Zhang and Y. Yin, *Nanotechnology*, 2005, **16**, 3079.
- 17 CCDC no. 684382; single crystal X-ray diffraction: Crystal data for: C<sub>14</sub> H<sub>16</sub> Cl N S<sub>2</sub>, FW = 297.85, monoclinic, P2<sub>1</sub>/c, a = 10.704(3), b = 15.143(4), c = 8.924(2), β = 100.006(3), V = 1424.5(7) Å<sup>3</sup>, D<sub>c</sub> = 1.389 g cm<sup>-3</sup>, F(000) = 624, T = 100(2) K, final residuals (for 227 parameters) were R<sub>1</sub> = 0.0321 for 2229 reflections with I > 2σ(I) and R<sub>1</sub> = 0.0358, wR<sub>2</sub> = 0.0924, GOF = 1.037 for all 2504 reflections. X-ray single crystal data were collected using Mo Kα (λ = 0.7107 Å) radiation on a SMART APEX diffractometer equipped with CCD area detector. The structure was solved by the direct methods and refined in a routine manner.
- 18 Y. H. Kim, B. C. Cheng and H. S. Chang, *Tetrahedron Lett.*, 1985, **26**, 1079.
- 19 I. Shibuya, Y. Taguchi, T. Tsuchiya, A. Oishi and E. Katoh, *Bull. Chem. Soc. Jpn.*, 1994, **67**, 3048.
- 20 N. Pradhan, A. Pal and T. Pal, *Langmuir*, 2001, **17**, 1800.

# Recyclable indium catalysts for additions of 1,3-dicarbonyl compounds to unactivated alkynes affected by structure and acid strength of solid supports†

Kiyotomi Kaneda,<sup>\*a</sup> Ken Motokura,<sup>b</sup> Nobuaki Nakagiri,<sup>b</sup> Tomoo Mizugaki<sup>b</sup> and Koichiro Jitsukawa<sup>b</sup>

Received 20th June 2008, Accepted 6th August 2008

First published as an Advance Article on the web 25th September 2008

DOI: 10.1039/b810490e

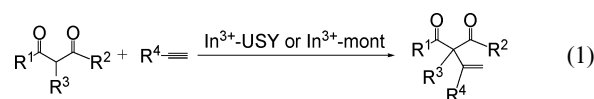
Indium has received much attention as a widely used rare metal, which has led to its consumption and cost increasing dramatically. Development of economical and ecological procedures for indium recycling is highly desired in all fields consuming indium. Here, we propose that indium species can be immobilized on solid acids by ion exchange, which increases their activity and enables the generation of the first recyclable heterogeneous indium catalysts for addition reactions of 1,3-dicarbonyl compounds to unactivated alkynes. This reaction was first reported in 2003, as a typical green protocol using abundant carbon sources for useful fine chemicals. The In<sup>3+</sup>-exchanged ultrastable Y zeolite (In<sup>3+</sup>-USY) and montmorillonite (In<sup>3+</sup>-mont) showed various unique catalyses. For example, the alkenylation reaction proceeded successfully without any additives except for the catalysts.

## Introduction

Indium is a widely used rare metal in semiconductors,<sup>1</sup> liquid crystal displays,<sup>2</sup> solar cells,<sup>3</sup> and light-emitting diodes,<sup>4</sup> which has resulted in a six-fold increase in the amount of indium consumption over the past five years. This rapidly rising demand for indium has led to a dramatic increase in cost and it is estimated that there is only a several decades' supply of indium left at current consumption rates.<sup>5</sup> Therefore, the development of economical and ecological procedures for indium recycling is highly desired in all fields which consume indium.<sup>6</sup>

Since 2000, a sharp and continuing increase in the number of publications reporting indium catalysts in organic synthesis has also been observed. In 2003, Nakamura and co-workers reported the first example for addition reactions of 1,3-dicarbonyl compounds to unactivated alkynes, which can be promoted by Lewis acidic homogeneous indium catalysts.<sup>7</sup> This reaction is regarded as a typical green protocol for the synthesis of useful precursors of functional materials. The utilization of abundant carbon sources, such as unactivated alkenes<sup>8</sup> and alkynes, to synthesize fine chemicals is one of the goals of green chemistry because it reduces and/or eliminates the installation of activating groups on unreactive carbon sources. In the above reaction system, the heterogenization of the indium catalysts for easy recovery and recycling is necessary to realize industrially acceptable processes. Immobilization of metals on typical oxide supports,

such as SiO<sub>2</sub> and Al<sub>2</sub>O<sub>3</sub>, by metal–oxygen covalent bonding or on electron-donating ligands anchored on a support surface can be considered as heterogenization techniques, but such procedures often cause extensive damage to the Lewis acidic sites of the metal centers resulting in a decrease of their intrinsic catalytic functions. To solve this problem, we have focused on the utilization of solid acids, such as montmorillonites and zeolites, as ion-exchangeable supports of Lewis acidic metals.<sup>9</sup> Here, we present indium species immobilized on solid acids by an ion exchange method as a typical procedure to realize both heterogenization and activation of indium. This is the first report on recyclable heterogeneous indium catalysts for addition reactions of 1,3-dicarbonyl compounds to unactivated alkynes (eqn (1)). The alkenylation reaction proceeded successfully without any additives other than the catalysts. In addition, the activities of the catalysts could be controlled by varying acid strengths and pore sizes of the supports, which enabled substrate-selective addition reactions.



## Results and discussion

In<sup>3+</sup>-exchanged ultrastable Y zeolite (In<sup>3+</sup>-USY) was easily prepared by treatment of H-USY (N. E. Chemcat, Si/Al = 10) with an aqueous solution of InCl<sub>3</sub>. X-ray diffraction studies verified the retention of the USY structure, and the In K-edge X-ray absorption near edge structure (XANES) spectrum showed the formation of a trivalent In species. The absence of chloride anion was revealed by X-ray photoelectron spectroscopy (XPS). In the Fourier transform of the *k*<sup>3</sup>-weighted In K-edge extended X-ray absorption fine structure (EXAFS), the lack of peaks

<sup>a</sup>Research Center for Solar Energy Chemistry, Osaka University, 1-3 Machikaneyama, Toyonaka, Osaka, 560-8531, Japan

<sup>b</sup>Department of Materials Engineering Science, Graduate School of Engineering Science, Osaka University, 1-3 Machikaneyama, Toyonaka, Osaka, 560-8531, Japan

† Electronic supplementary information (ESI) available: XRD, XANES, EXAFS, and FT-IR spectra of In<sup>3+</sup>-USY and In<sup>3+</sup>-mont. See DOI: 10.1039/b810490e

**Table 1** Addition of **1** to **2** using various In catalysts<sup>a</sup>

Entry	Catalyst	Conversion of <b>1</b> (%)	Yield of <b>3</b> (%)
1	In <sup>3+</sup> -USY	>99	99
2	In <sup>3+</sup> -USY (Reuse 1)	>99	>99
3	In <sup>3+</sup> -USY (Reuse 2)	>99	>99
4	In <sup>3+</sup> -USY (Reuse 3)	>99	99
5	In <sup>3+</sup> -USY (Reuse 4)	99	99
6	In <sup>3+</sup> -mont	80	68
7	In <sup>3+</sup> -beta	50	37
8	In <sup>3+</sup> -silicaalumina	24	6
9	In <sup>3+</sup> -ZSM-5	Trace	Trace
10	In <sup>3+</sup> -mordenite	Trace	Trace
11	In/SiO <sub>2</sub>	Trace	Trace
12	In/TiO <sub>2</sub>	Trace	Trace
13	In/Al <sub>2</sub> O <sub>3</sub>	Trace	Trace
14	In/MgO	Trace	Trace
15 <sup>b</sup>	In <sub>2</sub> O <sub>3</sub>	Trace	Trace
16 <sup>b</sup>	InCl <sub>3</sub>	44	25
17	H-USY	Trace	Trace

<sup>a</sup> **1** (1.0 mmol), **2** (5.0 mmol), catalyst (0.10 g), 140 °C, 5 h. Conversion and yield were determined by GC with an internal standard. The used catalyst was calcined at 800 °C before the recycle experiment. <sup>b</sup> In (2.4 × 10<sup>-2</sup> mmol).

around 3.6 Å showed that there were no In–In bonds in the In<sup>3+</sup>-USY. Conclusively, a monomeric In<sup>3+</sup> species was introduced into the USY by ion-exchange. In<sup>3+</sup>-montmorillonite (In<sup>3+</sup>-mont) was also prepared in a similar fashion and the presence of monomeric In<sup>3+</sup> species in In<sup>3+</sup>-mont was confirmed.

Results of the addition reaction of 2-methyl acetoacetic acid ethyl ester (**1**) to 1-heptyne (**2**) using various supported and unsupported In catalysts without solvent are summarized in Table 1. Remarkably, In<sup>3+</sup>-USY showed excellent catalytic activity, affording the alkenylation product (**3**) in quantitative yield (entry 1). After the reaction, the catalyst was easily separated from the reaction mixture by simple filtration, and could be reused four times with retention of its high catalytic activity and selectivity (entries 2–5).<sup>10</sup> In<sup>3+</sup>-mont also showed good performance (entry 6). Indium species with other acidic supports, such as ZSM-5 and mordenite, were hardly functional as catalysts (entries 9 and 10) and the reaction scarcely proceeded in the case of neutral and basic oxide-supported In species (entries 11–14). Indium oxide was also inactive (entry 15). The catalyst precursor InCl<sub>3</sub> showed a much lower performance (entry 16), suggesting that the activity of the indium species increased by the ion-exchange with USY and mont. Although excess **2** was used to obtain high yield of **3**, the product selectivities based on **2** (= yield of **3**/conversion of **2** × 100) was 88% and >99% for fresh and reuse In<sup>3+</sup>-USY, respectively.<sup>11</sup> These values are higher than that of the homogeneous In(OTf)<sub>3</sub> (85%) under identical reaction conditions.

The addition reactions of various 1,3-dicarbonyl compounds to **2** with In<sup>3+</sup>-USY or In<sup>3+</sup>-mont are illustrated in Table 2. 1,3-Diketones were found to be good substrates for the In<sup>3+</sup>-USY-catalyzed reaction, and the corresponding 2-alkenylation products were formed in good to excellent yields (entries 1,

**Table 2** Addition of 1,3-dicarbonyl compounds to alkynes with In<sup>3+</sup>-USY and In<sup>3+</sup>-mont<sup>a</sup>

Entry	Dicarbonyl compound	Temperature/°C	Yield (%) (Reaction time/h)	
			In <sup>3+</sup> -USY	In <sup>3+</sup> -mont
1 <sup>b</sup>		100	93(42)	72(42)
2 <sup>b</sup>		100	29(40) <sup>c</sup>	73(40) <sup>c</sup>
3 <sup>b</sup>		100	99(24)	99(24) <sup>d</sup>
4		140	86(8)	17(8)
5 <sup>b</sup>		100	99(6)	66(12)
6		100	99(6)	65(12)
7		140	75(1)	48(5)
8 <sup>d</sup>		140	99(5)	68(5)
9 <sup>d,e</sup>		160	10(14)	89(14) <sup>c</sup>
10 <sup>d,e</sup>		160	11(14)	78(14)

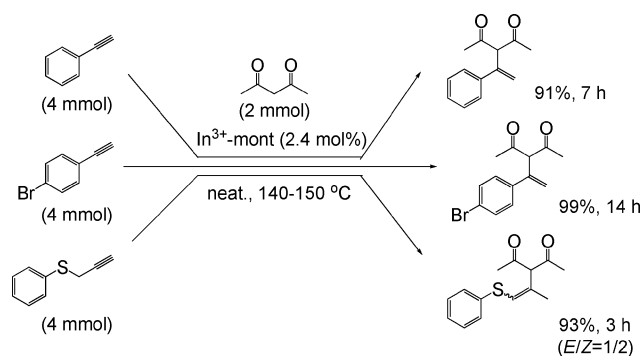
<sup>a</sup> 1,3-Dicarbonyl compound (1.0 mmol), **2** (5.0 mmol), catalyst (0.10 g), toluene (2 mL). Yield was determined by GC with an internal standard.

<sup>b</sup> 1,3-Dicarbonyl compound (2.0 mmol), **2** (4.0 mmol). <sup>c</sup> Isolated yield.

<sup>d</sup> Neat. <sup>e</sup> Reaction with 1-octyne.

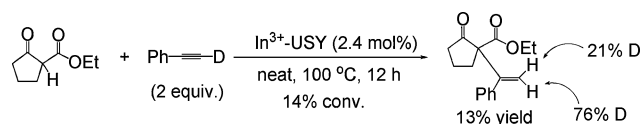
3, and 4) except for dibenzoyl acetone which showed better reactivity with In<sup>3+</sup>-mont (entry 2). Interestingly, these reactions of 1,3-diketones proceeded without any additives, whereas the In(OTf)<sub>3</sub> catalyst system needs triethylamine and BuLi for improvement of product selectivity.<sup>7c</sup> β-Ketoesters also reacted with 1-heptyne using In<sup>3+</sup>-USY or In<sup>3+</sup>-mont catalyst to afford the corresponding products in excellent yields (entries 5–8). The reactions of 1,3-diester with relatively high pK<sub>a</sub> values proceeded successfully with In<sup>3+</sup>-mont, but In<sup>3+</sup>-USY showed low catalytic performances (entries 9 and 10). Other alkynes, such as phenylacetylene and phenyl propynyl thioether, also showed excellent reactivities (Scheme 1).

After the treatment of In<sup>3+</sup>-USY with acetyl acetone, the IR spectrum revealed the formation of an In-enolate species. The presence of a Lewis acidic site was also confirmed by IR analysis of pyridine adsorbed In<sup>3+</sup>-USY. The reaction of ethyl cyclopentanone-2-carboxylate to 1-deuterio-2-phenylethyne afforded the corresponding addition product with 76% deuterium incorporation at the *trans*-position together with 21% deuterium



**Scheme 1** Addition reactions of acetyl acetone to various alkynes.

at the *cis*-position (Scheme 2).<sup>12</sup> From these results, the proposed reaction mechanism is as follows. An indium enolate is first generated by the reaction of the  $\text{In}^{3+}$  species with a 1,3-dicarbonyl compound. This is assisted by a macro-counter anion of the solid surface through proton abstraction.<sup>9</sup> This unusual nucleophilicity of the solid surface affords efficient addition reactions without basic additives. Next, an alkyne also coordinates to the  $\text{In}^{3+}$  species, followed by the formation of the addition product through a transition state of *cis*-carbometalation.<sup>7c</sup> From Table 2,  $\text{In}^{3+}$ -USY surpassed the performance of the  $\text{In}^{3+}$ -mont catalysts except in the cases of large 1,3-dicarbonyl compounds (entry 2) and 1,3-diester (entries 9 and 10). The  $\text{In}^{3+}$ -USY with meso pores ( $7.4 \times 7.4 \text{ \AA}$ ) has potential utility as a size-selective catalyst, and the montmorillonite having a two-dimensional expandable interlayer<sup>13</sup> can allow reactions even on large substrates. The reaction scarcely occurred with In-ZSM-5 as a result of its restricted pore size ( $5.1 \times 5.5 \text{ \AA}$ , Table 1, entry 8). In addition, the higher performances of  $\text{In}^{3+}$ -mont than  $\text{In}^{3+}$ -USY for the reaction of 1,3-diester might originate from the acid strengths of the solid supports ( $\text{H}^+$ -mont:  $\Delta H = 111 \text{ kJ mol}^{-1}$ ;  $\text{H}^+$ -USY:  $122 \text{ kJ mol}^{-1}$ ).<sup>8f</sup> Owing to the weak acidity of the mont, the anionic interlayer of the  $\text{In}^{3+}$ -mont has higher nucleophilicity than that of the  $\text{In}^{3+}$ -USY, which allows the formation of an In-enolate intermediate by proton abstraction from 1,3-diester with higher  $\text{p}K_{\text{a}}$  values than diketones and ketoesters. It can be expected that highly acidic mordenite ( $\Delta H = 160 \text{ kJ mol}^{-1}$ )<sup>8f</sup> cannot abstract protons from 1,3-dicarbonyls due to its low nucleophilicity (Table 1, entry 9). *Utilization of the solid acids as supports for  $\text{In}^{3+}$  species enables not only recycling of the In catalyst but also controls the catalysis of the alkenylation reaction.*



**Scheme 2** Addition of ethyl cyclopentanone-2-carboxylate to D-deuterio-2-phenylethyne.

## Conclusions

Heterogeneous indium catalysts for addition reactions of 1,3-dicarbonyl compounds to unactivated alkynes were developed with the use of solid acids. The indium catalyst can be reused

with retention of its high activity and selectivity. The substrate selectivity strongly depends on the structure and acid strength of the supports. This catalyst system will be applicable to other rare metal recycling methods and contribute highly to green and sustainable chemical processes.

## Experimental

### General

<sup>1</sup>H- and <sup>13</sup>C-NMR spectra were obtained on JEOL GSX-270 or JNM-AL400 spectrometer at 270 or 400 MHz in  $\text{CDCl}_3$  with TMS as an internal standard. Infrared spectra were obtained with a JASCO FTIR-410. Analytical GLC and GLC-mass were performed using a Shimadzu GC-8A PF with flame ionization detector equipped with KOCL 3000T, Silicon SE-30, and OV-17 columns, and a Shimadzu GCMS QP5050A equipped with ULBON HR-1 columns. Powder X-ray diffraction patterns were recorded using Philips X'Pert-MPD with  $\text{Cu K}\alpha$  radiation. XPS were measured on Shimadzu ESCA-KM using  $\text{MgK}\alpha$  radiation. In K-edge X-ray absorption spectra were recorded at the beam line 01B1 station attached to the Si(111) monochromator at SPring-8 for JASRI, Harima, Japan. Fluorescence yield was collected at room temperature. Data analyses were performed with the "REX2000 ver. 2.3" program (RIGAKU).

Unless otherwise noted, materials were purchased from Wako Pure Chemicals, Tokyo Kasei Co., Nacal tesque, and Aldrich Inc. and were used after appropriate purification.  $\text{Na}^+$ -montmorillonite ( $\text{Na}^+$ -mont),  $\text{Na}_{0.66}(\text{OH})_4\text{Si}_8(\text{Al}_{3.34}\text{Mg}_{0.66}\text{Fe}_{0.19})\text{O}_{20}$ , was purchased from Kunimine Industry Co. Ltd., Japan as Kunipia F. H-USY (N. E. Chemcat. Si/Al = 10), H-ZSM-5 (JRC-Z5-25H), and H-Mordenite (JRC-Z-HM20) were used. The identities of products were confirmed by comparison with reported mass and NMR data.

### Preparation of the $\text{In}^{3+}$ -USY

The H-USY (2.0 g) was added to 140 mL of a  $2.3 \times 10^{-4} \text{ M}$  aqueous solution of  $\text{InCl}_3$ . Then the heterogeneous mixture was stirred at  $90 \text{ }^\circ\text{C}$  for 24 h under air. The solid product was separated by centrifugation, washed thoroughly with deionized water and dried at  $110 \text{ }^\circ\text{C}$ , affording In-USY (In content: 2.8 wt%). Various indium supported solid base catalysts, such as  $\text{In}^{3+}$ -mont (In: 5.5 wt%),  $\text{In}^{3+}$ -beta,  $\text{In}^{3+}$ -silicalumina,  $\text{In}^{3+}$ -ZSM-5,  $\text{In}^{3+}$ -mordenite, In/ $\text{SiO}_2$ , In/ $\text{TiO}_2$ , In/ $\text{Al}_2\text{O}_3$ , In/ $\text{MgO}$ , In/hydroxalcite, and In/hydroxyapatite were synthesized by the same procedure.

### A typical example for the $\text{In}^{3+}$ -USY-catalyzed addition of 1,3-dicarbonyl compounds to alkynes

Into a pyrex pressure tube (15 mL) were placed the  $\text{In}^{3+}$ -USY (0.10 g, In:  $2.4 \times 10^{-2} \text{ mmol}$ ), 2-methyl acetoacetic acid ethyl ester (1.0 mmol), and 1-heptyne (5.0 mmol). The resulting mixture was vigorously stirred at  $140 \text{ }^\circ\text{C}$  under Ar. After 5 h, the catalyst was separated by filtration and the GC analysis of the filtrate showed up to 99% yield of ethyl 2-acetyl-2-methyl-3-methyleneoctanoate. The filtrate was purified by column chromatography using silica (hexane/ethyl acetate = 9/1) to afford a pure product (0.21 g, 92% isolated yield). The used



catalyst was calcined at 800 °C for 10 h in the air and then could be reused at least 4 times without appreciable loss of its activity and selectivity.

### Reaction with deuterated phenylacetylene

Into a pyrex pressure tube (15 mL) were placed the In<sup>3+</sup>-USY (5.0 × 10<sup>-2</sup> g, In: 1.2 × 10<sup>-2</sup> mmol), ethyl cyclopentanone-2-carboxylate (1.0 mmol), and 1-deuterio-2-phenylethyne (2.0 mmol). The resulting mixture was vigorously stirred at 100 °C under Ar. After 12 h, the catalyst was separated by filtration and <sup>1</sup>H NMR analysis revealed 14% yield of the addition product. The ratio of deuterium at *cis/trans*-position was also determined by <sup>1</sup>H NMR.

### Acknowledgements

This investigation was supported by a Grant-in-Aid for Scientific Research from the Ministry of Education, Culture, Sports, Science, and Technology of Japan, and also supported by Grant-in-Aid for Scientific Research on Priority Areas (No.18065016, "Chemistry of Concerto Catalysis") from Ministry of Education, Culture, Sports, Science and Technology, Japan.

### References

- 1 A. D. Bianchi, M. Kenzelmann, L. DeBeer-Schmitt, J. S. White, E. M. Forgan, J. Mesot, M. Zolliker, J. Kohlbrecher, R. Movshovich, E. D. Bauer, J. L. Sarrao, Z. Fisk, C. Petrović and M. R. Eskildsen, *Science*, 2008, **319**, 177.
- 2 T. Minami, *Thin Solid Films*, 2008, **516**, 1314.
- 3 N. G. Dhere, *Sol. Energy Mater. Sol. Cells*, 2006, **90**, 2181.
- 4 S. Nakamura, *Science*, 1998, **281**, 956.
- 5 D. Cohen, *New Sci.*, 2007, **26**, 34.
- 6 (a) T. Muratami, T. Honma, T. Maeseto, M. Shimada, PTC Int. Appl. WO2007015392, Feb 08, 2007; (b) A. Wildermann, Y. Foricher, T. Netscher and W. Bonrath, *Pure Appl. Chem.*, 2007, **79**, 1839.
- 7 (a) M. Nakamura, K. Endo and E. Nakamura, *J. Am. Chem. Soc.*, 2003, **125**, 13002; (b) M. Nakamura, K. Endo and E. Nakamura, *Adv. Synth. Catal.*, 2005, **347**, 1681; (c) K. Endo, T. Hatakeyama, M. Nakamura and E. Nakamura, *J. Am. Chem. Soc.*, 2007, **129**, 5264; (d) H. Tsuji, K. Yamagata, Y. Itoh, K. Endo, M. Nakamura and E. Nakamura, *Angew. Chem., Int. Ed.*, 2007, **46**, 8060; (e) H. Tsuji, T. Fujimoto, K. Endo, M. Nakamura and E. Nakamura, *Org. Lett.*, 2008, **10**, 1219; (f) Rhenium-catalyzed reaction was also reported: Y. Kuninobu, A. Kawata and K. Takai, *Org. Lett.*, 2005, **7**, 4823.
- 8 (a) A. L. Rodriguez, T. Bunlaksananusorn and P. Knochel, *Org. Lett.*, 2000, **2**, 3285; (b) T. Pei and R. A. Widenhoefer, *J. Am. Chem. Soc.*, 2001, **123**, 11290; (c) K. Hirase, T. Iwahama, S. Sakaguchi and Y. Ishii, *J. Org. Chem.*, 2002, **67**, 970; (d) M. Nakamura, T. Hatakeyama, K. Hara and E. Nakamura, *J. Am. Chem. Soc.*, 2003, **125**, 6362; (e) D. Yang, J.-H. Li, Q. Gao and Y.-L. Yan, *Org. Lett.*, 2003, **5**, 2869; (f) M. Nakamura, T. Hatakeyama and E. Nakamura, *J. Am. Chem. Soc.*, 2004, **126**, 11820; (g) X. Tao and C.-J. Li, *J. Am. Chem. Soc.*, 2004, **126**, 6884; (h) A. Leitner, J. Larsen, C. Steffens and J. F. Hartwig, *J. Org. Chem.*, 2004, **69**, 7552; (i) K. Motokura, N. Fujita, K. Mori, T. Mizugaki, K. Ebitani and K. Kaneda, *Angew. Chem., Int. Ed.*, 2006, **45**, 2605.
- 9 T. Kawabata, M. Kato, T. Mizugaki, K. Ebitani and K. Kaneda, *Chem.–Eur. J.*, 2005, **11**, 288.
- 10 The In<sup>3+</sup>-USY-catalyzed reaction stopped completely after simple filtration of the catalyst at *ca.* 50% conversion. In addition, the inductive coupled plasma (ICP) analysis of the filtrate after the reaction confirmed the In content was below the detection limit (0.05 ppm). These results rule out any contributions to the reaction by homogeneous indium species.
- 11 After the calcination of the used In<sup>3+</sup>-USY at 800 °C, the *k*<sup>3</sup>-weighted In K-edge EXAFS analysis revealed the formation of a few In–In bonds with retention of almost all the In–O bonds, which suggests that a part of the monomeric indium species was converted to indium clusters. It is likely that a small amount of unselective indium species outside of the USY pores was quenched by the aggregation, and the selectivity of the addition reaction based on the alkyne increased.
- 12 It can be expected that H–D exchange reaction between the 1-deuterio-2-phenylethyne substrate and the addition product occurs competitively during the addition reaction (see ESI†). Such an exchange reaction makes the mechanistic investigation difficult. Since the deuterium distribution of the initial product should be analyzed, the addition reaction has to be stopped at a low conversion (14%) to minimize the influence of this undesired reaction.
- 13 T. J. Pinnavaia, *Science*, 1983, **220**, 365.

## Call for Papers

# Metallomics

## Integrated biometal science

### Launching January 2009

*Metallomics: Integrated biometal science* is a new peer-reviewed journal covering the research fields related to biometals. It is expected to be the core publication for the emerging metallomics community as they strive to fully understand the role of metals in biological, environmental and clinical systems.

The journal will publish a full mix of primary articles, communications and reviews. Papers published in *Metallomics* will benefit from wide exposure, with free online access to all content published during 2009 and 2010 giving maximum visibility to your research. The journal will maintain a strong conference presence, and receive extensive promotion to the wider scientific press.

Contact the Editor, Niamh O'Connor, at [metallomics@rsc.org](mailto:metallomics@rsc.org) or visit the website for more details.



#### International Editorial Board members include:

**Professor Joseph A. Caruso**, University of Cincinnati and Metallomics Center of the Americas, US (Editorial Board Chair)

**Professor Ariel Anbar**, Arizona State University, US

**Professor Emeritus Hiroki Haraguchi**, Nagoya University, Japan

**Professor Gary Hieftje**, University of Indiana, Bloomington, US

**Professor Ryszard Lobinski**, CNRS UMR 5034, France and Warsaw University of Technology, Poland

**Professor David Salt**, Purdue University, US

**Professor Emeritus Bibundhendra Sarkar**, University of Toronto and The Hospital for Sick Children, Canada

**Professor Hongzhe Sun**, University of Hong Kong, Hong Kong

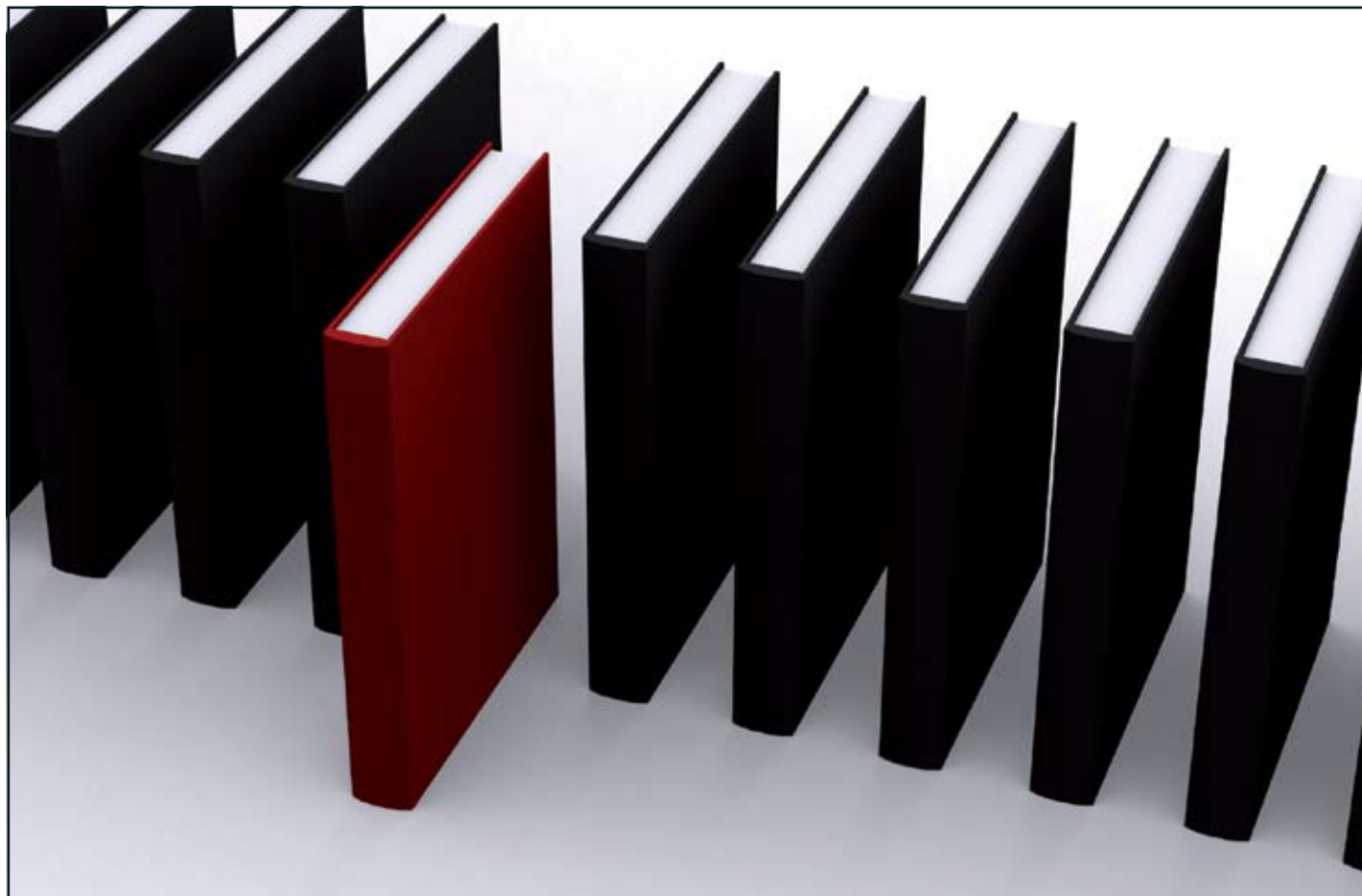
## Submit your work now!

RSC Publishing

Supporting the **iSM**  
International  
Symposium  
on Metallomics

[www.rsc.org/metallomics](http://www.rsc.org/metallomics)

Registered Charity Number 207890



## 'Green Chemistry book of choice'



Why not take advantage of free book chapters from the RSC? Through our 'Green Chemistry book of choice' scheme *Green Chemistry* will regularly highlight a book from the RSC eBook Collection relevant to your research interests. Read the latest chapter today by visiting the *Green Chemistry* website.

The RSC eBook Collection offers:

- Over 900 new and existing books
- Fully searchable
- Unlimited access

Why not take a look today? Go online to find out more!

RSC Publishing

[www.rsc.org/greenchem](http://www.rsc.org/greenchem)

Registered Charity Number 207890